

Assessing the complex nature of behavior:
Sequence-based and transcriptomic analyses
in a mouse model of extremes in trait anxiety

Dissertation

der Fakultät für Biologie
der Ludwig-Maximilians-Universität München

vorgelegt von
Ludwig Czibere

München, 30. September 2008

Erstgutachter: Prof. Dr. Rainer Landgraf

Zweitgutachter: Prof. Dr. Thomas Cremer

Datum der mündlichen Prüfung: 06. Mai 2009

"Nothing in biology makes sense, except in the light of evolution."

Theodosius Grygorovych Dobzhansky, 1973

Meinen lieben Eltern für ihre stetige Unterstützung

Drága szüleimnek állandó támogatásukért

**Abstract**

To unravel the molecular pylons of innate anxiety, a well established animal model has been characterized using transcriptome- and sequence-based analyses. The animal model – hyper (HAB) and hypo (LAB) anxious mice – has been created by selective inbreeding based on outbred CD1 mice using the extreme values the mice spent on the open arm of the elevated plus-maze, a test also used to screen drugs for anxiolytic or anxiogenic effects.

These mice proved a robust phenotypic divergence, also for depression-like behavior and stress-axis reactivity.

In a first assay, brain regions unambiguously involved in regulating anxiety-related behavior were screened for gene expression differences between HAB and LAB animals in a microarray experiment covering the whole genome. This led to the identification of thousands of differentially expressed transcripts. The highest significant results were further validated by quantitative PCR or other techniques focusing either on protein quantification or enzyme activity. Applying this strategy, differential regulation of 15 out of 28 transcripts could be validated: vasopressin, tachykinin 1, transmembrane protein 132D, RIKEN cDNA 2900019G14 gene, ectonucleotide pyrophosphatase/phosphodiesterase 5, cathepsin B, coronin 7, glyoxalase 1, pyruvate dehydrogenase beta, metallothionein 1, matrix metalloproteinase 15, zinc finger protein 672, syntaxin 3, solute carrier family 25 member 17 and ATP-binding cassette, sub-family A member 2. Additionally, analysis of cytochrome c oxidase activity resulted in the identification of differences in long-term activity between HAB and LAB mice in the amygdala and the hypothalamic paraventricular nucleus pointing to an important role of these brain regions in shaping the anxiety-related extremes in these mice.

In a second genome-wide screening approach, 267 single nucleotide polymorphisms were identified to constantly differ between HAB and LAB animals (i.e. to carry the opposite homozygous genotype at these loci) and subsequently genotyped in 520 F2 mice, the offspring of reciprocally mated HABxLAB animals. These F2 mice have been previously phenotyped in a broad variety of behavioral tests and show – as descendants of intermediate heterozygotes for all polymorphic genomic loci between HAB and LAB mice – a free segregation of all alleles, thus allowing genotype-phenotype associations based on whole-genome analysis. Only focusing on the most significant findings, associations have been observed between anxiety-related behavior and loci on mouse chromosomes 5 and 11, between

ATGCTCGCCAGGA
TACGAGCGGTCCT



Abstract

depression-like behavior and chromosome 2 and between stress-axis reactivity and chromosome 3.

The locus on chromosome 11 is marked by a polymorphism located in the 3' untranslated region of zinc finger protein 672, a gene also markedly overexpressed in LAB mice and expressed at lower levels in HAB mice leading to a probable causal involvement in shaping the phenotype. Further associations on chromosome 5 include two functional polymorphisms in enolase phosphatase 1 that result in a different mobility of the enzyme in proteomic assays and with a polymorphism located in the transmembrane protein 132D gene. Furthermore, independently, an association of a polymorphism in this particular gene, together with the resulting gene expression differences has been observed in a group of panic disorder patients, highlighting this gene as a causal factor underlying anxiety-related behavior and disorders in both the HAB/LAB mouse model and human patients.

The combination of expression profiling and confirmation by quantitative PCR, single nucleotide polymorphism analysis and F2 association studies, i.e. unbiased and hypothesis driven approaches were key to the identification and functional characterization of loci, genes and polymorphisms causally involved in shaping anxiety-related behavior. Thus, it provides an overview of some new promising targets for future pharmaceutical treatment and will contribute to a better understanding of the molecular processes that shape anxiety and thereby also animal and human behavior.



	Abstract _____	i
	Table of contents _____	iii
	Table of abbreviations and comments _____	vi
1.	Introduction _____	1
1.1.	The evolution of threat assessment systems _____	1
1.2.	The evolution of neuroactive compounds _____	2
1.3.	Anxiety and depression disorders _____	5
1.4.	Assessing anxiety/depression in mice _____	7
1.5.	The hypothalamo-pituitary-adrenal (HPA) axis, gene expression and translation _____	9
1.6.	The influence of genetic polymorphisms _____	10
1.7.	The HAB/LAB mouse model _____	11
1.7.1.	Phenotypic characteristics of HAB/LAB mice _____	12
1.7.2.	Molecular characteristics of HAB/LAB mice _____	13
1.7.3.	The F2 panel _____	13
2.	Animals, materials and methods _____	15
2.1.	The HAB phenotype reversal by selective breeding _____	15
2.2.	Identification of candidate genes _____	16
2.2.1.	Animals and behavioral tests for the gene expression studies _____	16
2.2.2.	Gene expression profiling on the MPI24K-platform _____	16
2.2.2.1.	Tissue dissection _____	16
2.2.2.2.	Total RNA isolation and amplification _____	18
2.2.2.3.	Array hybridization and quantification _____	19
2.2.2.4.	Statistical analysis _____	20
2.2.3.	Gene expression profiling on the Illumina-platform _____	20
2.2.3.1.	Tissue laser-microdissection _____	20
2.2.3.2.	Total RNA isolation and amplification _____	21
2.2.3.3.	Array hybridization and quantification _____	21
2.2.3.4.	Statistical analysis _____	22
2.2.4.	Analysis of candidate genes by quantitative PCR _____	22
2.2.5.	Assessment of candidate gene functions _____	26
2.2.5.1.	Glyoxalase I (GLO1) and metabolic stimulation _____	27
2.2.5.1.1.	Metabolism and blood plasma parameters _____	27
2.2.5.1.2.	Behavioral manipulation via metabolism _____	27
2.2.5.1.3.	Western Blot analysis of glyoxalase 1 (GLO1) _____	28
2.2.5.2.	Tachykinin 1 (<i>Tac1</i>)-encoded peptide quantification _____	29



2.2.5.3.	Cytochrome c oxidase (COX) activity _____	32
2.3.	Identification of polymorphisms _____	32
2.3.1.	Animals and behavioral tests _____	33
2.3.2.	DNA isolation _____	33
2.3.3.	Prescreening _____	34
2.3.4.	Screening of the F2 panel and CD1 mice _____	35
2.3.5.	Sequencing of candidate genes _____	43
2.3.5.1.	Cloning of fragments _____	43
2.3.5.2.	Cycle sequencing _____	44
2.3.5.3.	Vasopressin (<i>Avp</i>) _____	45
2.3.5.4.	Corticotropin-releasing hormone (<i>Crh</i>) _____	46
2.3.5.5.	Tachykinin 1 (<i>Tac1</i>) _____	47
2.3.5.6.	Cathepsin B (<i>Ctsb</i>) _____	49
2.3.5.7.	Metallothionein 1 (<i>Mt1</i>) _____	51
2.3.5.8.	Transmembrane protein 132D (<i>Tmem132d</i>) _____	52
2.3.6.	Assessing the effects of polymorphisms _____	53
2.3.7.	Allele-specific transcription of vasopressin (<i>Avp</i>) _____	54
2.4.	Association and linkage of SNPs with behavioral parameters _____	54
2.5.	Statistical data analysis _____	54
3.	Results _____	56
3.1.	The HAB phenotype reversal by selective breeding _____	56
3.2.	Identification of candidate genes _____	56
3.2.1.	Animals and behavioral tests _____	56
3.2.2.	Gene expression profiling on the MPI24K-platform _____	59
3.2.2.1.	Tissue dissection _____	59
3.2.2.2.	RNA amplification _____	59
3.2.2.3.	Differential expression data _____	60
3.2.3.	Gene expression profiling on the Illumina-platform _____	61
3.2.3.1.	Tissue laser-microdissection _____	61
3.2.3.2.	Total RNA isolation and amplification _____	62
3.2.3.3.	Differential expression data _____	64
3.2.4.	Validation of results by quantitative PCR _____	65
3.2.5.	Effects of selected candidate genes _____	69
3.2.5.1.	Glyoxalase I (GLO1) and metabolic stimulation _____	70
3.2.5.1.1.	Metabolism and blood plasma parameters _____	70
3.2.5.1.2.	Behavioral manipulation by metabolic stimulation _____	70
3.2.5.1.3.	Western Blot analysis of glyoxalase 1 (GLO1) _____	72



3.2.5.2.	Tachykinin 1 (<i>Tac1</i>) encoded peptides _____	73
3.2.5.3.	Cytochrome c oxidase (COX) activity _____	73
3.3.	Identification of polymorphisms _____	74
3.3.1.	Prescreening _____	74
3.3.2.	Screening of the F2 panel _____	75
3.3.3.	Genotype frequencies in wildtype CD-1 mice _____	76
3.3.4.	Sequencing of candidate genes _____	76
3.3.4.1.	Vasopressin (<i>Avp</i>) _____	76
3.3.4.2.	Corticotroin-releasing hormone (<i>Crh</i>) _____	78
3.3.4.3.	Tachykinin 1 (<i>Tac1</i>) _____	78
3.3.4.4.	Cathepsin B (<i>Ctsb</i>) _____	78
3.3.4.5.	Metallothionein 1 (<i>Mt1</i>) _____	81
3.3.4.6.	Transmembrane protein 132D (<i>Tmem132d</i>) _____	81
3.3.4.7.	Further sequencing results _____	82
3.3.5.	The effects of polymorphisms _____	82
3.3.6.	Allele-specific transcription analyses of vasopressin (<i>Avp</i>) _____	83
3.4.	Association and linkage of SNPs with behavioral parameters _____	84
4.	Discussion _____	88
5.	Perspectives _____	109
6.	Supplementary tables _____	111
7.	References _____	127
8.	Acknowledgements _____	141
9.	<i>Curriculum vitae</i> _____	142
10.	List of publication list other contributions _____	143
11.	Declaration / Erklärung _____	144

Table of abbreviations and comments

ACTH	adrenocorticotropin
aRNA	amplified ribonucleic acid
BLA	basolateral amygdala
BLA/LA	basolateral and lateral amygdala
BNST	bed nucleus of the <i>stria terminalis</i>
bp	basepairs
BSA	bovine serum albumin
CD1	ICR (CD1): outbred mouse strain; Institute of Cancer Research Cesarean derived 1
CeA	central amygdala
Cg	cingulate cortex
chr.	chromosome
CNV	copy number variation
CORT	corticosterone
COX	cytochrome c oxidase
Cp	crossing point
Cy3 / Cy5	cyanine 3 / cyanine 5
DAB	3,3-diaminobenzadine
DER	downstream enhancer region
DG	dentate gyrus
DNA	deoxyribonucleic acid
EDTA	ethylenediaminetetraacetic acid or 2-[2-(bis(carboxymethyl)amino)ethyl-(carboxymethyl)amino]acetic acid
EKA /B /C /D	endokinin A /B /C /D
ELISA	enzyme-linked immunosorbent assay
EPF	elevated platform
EPM	elevated plus-maze
ETAS	evolutionary threat assessment system
F1	offspring of a HABxLAB intercross breeding-pair
F2	offspring of an F1xF1 breeding-pair
FST	forced swim test
HAB	high anxiety-related behavior
HDL	high-density lipoproteins
HK-1	hemokinin 1
HPA	hypothalamic-pituitary-adrenocortical
HPLC	high performance liquid chromatography
IPTG	isopropyl- β -D-thiogalactopyranoside
kbp	Kilobasepairs
KWH	Kruskal-Wallis test
LAB	low anxiety-related behavior
LDL	low-density lipoproteins
Mbp	Megabasepairs
MeA	medial amygdala
MGD	Mouse Genome Database
mRNA	messenger ribonucleic acid
MWU	Mann-Whitney test
NAB	normal (intermediate) anxiety-related behavior
NAc	<i>nucleus accumbens</i>

NCBI	National Center for Biotechnology Information
NF1	Nuclear factor 1
NK _{1/2/3}	neurokinin receptor 1 /2 /3
NKA	neurokinin A
NKB	neurokinin B
NPK	neuropeptide K
NP γ	neuropeptide γ
NSF	N-ethylmaleimide sensitive factor
OF	open field
PBS	phosphate buffered saline
PCR	polymerase chain reaction
PFA	paraformaldehyde
PMSF	phenylmethanesulphonyl-fluoride
pNPP	p-nitrophenyl phosphate
PPT-A ($\alpha, \beta, \gamma, \delta$)	preprotachykinin A ($\alpha, \beta, \gamma, \delta$)
PVDF	polyvinylidene difluoride
PVN	hypothalamic paraventricular nucleus
qPCR	quantitative polymerase chain reaction
QTL	quantitative trait locus
rHAB	reversed high anxiety-related behavior
RNA	ribonucleic acid
rpHPLC	reversed phase high performance liquid chromatography
SDS	sodium dodecyl sulfate
SEC	stimulus evaluation check
SEM	standard error of the mean
SNAP	soluble NSF attachment proteins
SNARE	soluble N-ethylmaleimide sensitive factor attachment protein receptors
SNP	single nucleotide polymorphism
SON	supraoptic nucleus
SP	substance P
SSC	standard saline citrate
TBE	Tris/borate/EDTA
TBS	Tris-buffered saline
TGS	Tris/glycine/SDS
Tris	trisaminomethane or 2-Amino-2-hydroxymethyl-propane-1,3-diol
TST	tail suspension test
UTR	untranslated region
X-Gal	5-bromo-4-chloro-3-indolyl- β -D-galactoside

Please note that all units are indicated as defined by the International System of units (SI) or are SI derived units with the respective prefixes and are therefore not considered in the list of abbreviations (except for the abbreviation of basepairs).

Table of gene symbols

<i>2900019G14Rik</i>	RIKEN cDNA 2900019G14 gene
<i>5230400G24Rik</i>	RIKEN cDNA 5230400G24 gene
<i>Abca2</i>	ATP-binding cassette, sub-family A (ABC1), member 2 gene

<i>Aldh3a2</i>	aldehyde dehydrogenase family 3, subfamily A2 gene
<i>Apbb1</i>	amyloid beta (A4) precursor protein-binding, family B, member 1
<i>Atp2b1</i>	ATPase, Ca ⁺⁺ transporting, plasma membrane 1
<i>Atp5j</i>	ATP synthase, H ⁺ transporting, mitochondrial F0 complex, subunit F
AVP	arginine-vasopressin peptide
<i>Avp</i>	mouse arginine-vasopressin coding gene
<i>Ccdc104</i>	coiled-coil domain containing 104
<i>Coro7</i>	coronin 7
<i>Crh</i>	corticotropin-releasing hormone
<i>Ctsb</i>	cathepsin
<i>Dgkh</i>	diacylglycerol kinase, eta
<i>Dgkq</i>	diacylglycerol kinase, theta
<i>Enpp5</i>	ectonucleotide pyrophosphatase / phosphodiesterase 5
<i>Ep400</i>	E1A binding protein p400
<i>Gapdh</i>	glyceraldehyde-3-phosphate dehydrogenase
<i>Gig1</i>	(<i>Zfp704</i>) zinc finger protein 704
<i>Glo1</i>	glyoxalase 1
<i>Gnaq</i>	guanine nucleotide binding protein, alpha q polypeptide
<i>Hbb-b1</i>	hemoglobin, beta adult major chain
<i>Hmgn3</i>	high mobility group nucleosomal binding domain 3
<i>Hrrr</i>	hornerin
<i>Hprt1</i>	hypoxanthine guanine phosphoribosyl transferase 1
<i>Kcnh1</i>	potassium voltage-gated channel, subfamily H, member 1
<i>Mbnl1</i>	muscleblind-like 1 (Drosophila)
<i>Mmp15</i>	matrix metalloproteinase 15
<i>Msrb2</i>	methionine sulfoxide reductase B2
<i>Mt1</i>	metallothionein 1
<i>Npy</i>	neuropeptide y
OXT	oxytocin peptide
<i>Oxt</i>	mouse oxytocin coding gene
<i>P2rx7</i>	purinergic receptor P2X, ligand-gated ion channel, 7
<i>Pdhb</i>	pyruvate dehydrogenase (lipoamide) beta
<i>Polr2b</i>	polymerase (RNA) II (DNA directed) polypeptide B
<i>Ppp3ca</i>	protein phosphatase 3, catalytic subunit, alpha isoform
<i>Pxk</i>	PX domain containing serine/threonine kinase
<i>Rab6</i>	RAB6, member RAS oncogene family
<i>Rpl13a</i>	ribosomal protein L13a
<i>Slc1a2</i>	solute carrier family 1 (glial high affinity glutamate transporter), member 2
<i>Slc25a17</i>	solute carrier family 25 (mitochondrial carrier, peroxisomal membrane protein), member 17
<i>Smarcd3</i>	SWI/SNF related, matrix associated, actin dependent regulator of chromatin, subfamily d, member 3
<i>Spnb3</i>	spectrin beta 3
<i>Stx3</i>	syntaxin 3
TAC1 /3 /4	human tachykinin 1 /3 /4 gene
<i>Tac1</i> /2 /4	mouse tachykinin 1 /2 /4 gene
<i>Tmem132d</i>	transmembrane protein 132D
<i>Tpd52</i>	tumor protein D52
<i>Trib2</i>	tribbles homolog 2 (Drosophila)

<i>Ttbk1</i>	tau tubulin kinase 1
<i>Ttr</i>	transthyretin
<i>Uros</i>	uroporphyrinogen III synthase
<i>Zfp672</i>	zinc finger protein 672

Please note: murine gene symbols are written in italicized minor letters with the first letter in capital, also if it refers to the respective mRNA. If murine peptides or proteins are referred to corresponding gene or protein symbols are held in capital non-italicized letters. As the same script conventions apply to human gene symbols and murine peptides and proteins, the former are explicitly mentioned in the text. The symbols and gene definitions are based on the information provided by the Mouse Genome Database (MGD, Mouse Genome Informatics, The Jackson Laboratory, Bar Harbor, ME. World Wide Web URL: <http://www.informatics.jax.org>; September, 2008) and are subject to change.

ATGCTCGCCAGGA
TACGAGCGGTCCT



Table of abbreviations and comments



1. Introduction

1.1. The evolution of threat assessment systems

Anxiety and fear are two similar, but nevertheless well distinguishable emotions combined with physical and physiological reactions. Both have a common background and sense at a former evolutionary stage (Flannelly *et al.*, 2007; Rosen and Schulkin, 1998).

Fear itself is an adequate evolutionary adaptation, to prevent being eaten by predators, or to escape from life-threatening situations, that an individual is confronted with suddenly (Belzung and Philippot, 2007). This reaction ability might already play a vital role in organisms that are capable of actively changing their position.

To differentiate between fear and anxiety, fear is the reaction to an acute threat with a defined danger, whereas anxiety is strictly context-based and evokes the impression of a threatening situation without the direct contact with something that would justify the described reaction. This way, to perceive something as anxiogenic, an individual must have the cognitive ability, to (I) perceive a threat *per se*, (II) to learn associations with a specific context and (III) to recall the memory (association). From this point of view fear is a basic prerequisite to any kind of higher emotion related to threat assessment, like anxiety (Belzung and Philippot, 2007).

Belzung and Philippot (2007) indeed summarized these conditions resulting in five distinct stimulus evaluation checks (SEC) in organisms that have to be accomplished in order to provoke an anxiety-related reaction. However, even protozoans or nematodes show the capability to perform at least the first three SECs (“novelty check”, “intrinsic pleasantness check” and “goal/need conduciveness check”) even if a detailed discrimination of these is hard to prove for these organisms. The ability to change morphology and behavior in response to a predator-induced threat has even been demonstrated for protozoans like *Euplotes*. Basically, if these three SECs work, many physiological reactions typical of an acute stressor can be observed, allowing an adequate threat response.

The fourth SEC is proven to function in all vertebrates but also for some insects. In brief, animals able to learn helplessness, i.e. to learn to cope with and not to escape from a hopeless and threatening situation, but as soon as the opportunity is given to do so, are able to perform this fourth SEC. Nevertheless, the fifth SEC (“norm/self compatibility check”) seems to be unique to primates, as it requires cultural transmission (Belzung and Philippot, 2007). This brief description of evaluation circuits, demonstrates the sense of threat assessment, i.e. the decision on a fight or



flight reaction. For individual survival, it might be favorable to overestimate threatening stimuli (i.e. to react, if the organism would not have to, costs less compared to loss of life). These SECs already include a bias towards the interpretation in favor of a defensive behavior, independent of whether this takes place in single cell or more complex organisms.

With differentiation of more complex classes and species, these SECs increasingly require central control. This was taken over quite early in evolutionary terms, by neurons, the cell type most suitable for intercellular communication and coordination. They represent an ancient and vigorously conserved cell type in metazoans, with cnidarians and sponges already bearing neuronal cells (Holland, 2003), able to communicate with each other and coordinate their action. Starting from cnidarians, also a basic epidermal nerve net is present in eumetazoa (Holland, 2003). Emerging complexity gave rise to neuronal agglomerations in these nerve nets, forming ganglia in species like *Caenorhabditis elegans* and other more complex organisms building the core of a central nervous system in all invertebrates, that was also transferred to vertebrates combined with the dorsoventral body axis inversion (Denes *et al.*, 2007).

A broad variety of changes and adaptations has led to the development of the brain, with the hypothalamus and functional equivalents of the hippocampus and amygdala already present in fish (Belzung and Philippot, 2007). Many brain structures and systems have already been attributed to fear and anxiety in vertebrates, with the evolutionary oldest one, the basal ganglia, that already function at a pre-emotional level and the limbic system which also already works at a preconscious level. Most importantly, the prefrontal cortex also plays an important role in mammals as for the modulation of the autonomic nervous system, social cognition and emotional decision making. These three systems can be summarized as evolutionary threat assessment systems (ETAS). It also has been proposed, that many different kinds of threats require different ETAS even at the most rudimentary level of evolution, like for threats originating from predators, conspecifics, height or from insects (Flannelly *et al.*, 2007), thus forming the basis of multiple systems, involved in the anticipation and processing of potentially threatening situations, competing with and complementing each other, resulting in the complex trait called anxiety, which already include a bias towards the overinterpretation of anxiogenic stimuli.

1.2. The evolution of neuroactive compounds

In parallel to the morphologic and organogenic evolution of neurons, ganglia and brains, a high degree of complexity and diversity was established in mammals,



originating from a few neuroactive compounds in the first neurons. First forms of substance P-related tachykinin peptides are known from hydra or vasopressin- and oxytocin-like peptides are already present in the locust (Gwee *et al.*, 2008; Severini *et al.*, 2002). Nevertheless, the basic forms of neuronal communication via molecules do not necessarily require a vast degree of complex substances, as pre-neuronal cell to cell communication might already take place by the release of glutamate, gamma-aminobutyric acid, glycine, acetylcholine, serotonin or any other small neurotransmitter. Additionally, mechanisms of cell to cell communication to convey information also exist for prokaryotes, especially in colony-forming bacteria as *Pseudomonas aeruginosa*. However, most of the best-characterized substances used for 'quorum sensing' in bacteria comprise substances like quinolones, pentandione-based molecules, long fatty acids or short peptides (Williams, 2007). This makes a major difference to eukaryotic cells and organisms, as these substances are hardly applied in signal transduction processes (except for the short peptides).

Interestingly, this suggests that the broad variety of substances used for intercellular communication arose from the same basis of only a few molecules (Landgraf and Holsboer, 2005); especially as bacteria show a variety that uses different substances). Also release mechanisms from vesicles seem to be quite conserved and are not a privilege of neurons. First forms of endo- and exocytosis must have been present in the first cells that required more than the uptake of substances via diffusion. Equivalently, proteins of the superfamily of soluble N-ethylmaleimide sensitive factor attachment protein receptors (SNARE) and their interacting proteins seem to play a pivotal role for the release of substances from vesicles. Whereas SNAREs are required for the fusion of vesicles with a membrane, NSF (N-ethylmaleimide sensitive factor) and soluble NSF attachment proteins (SNAP) are necessary for the regeneration of used (cis-) SNARE complexes. This principle works in all neuronal synapses, but the same way in yeast (Ungar and Hughson, 2003). Complexity and diversity of signaling molecules significantly increased, also displaying a big but not unconservative variety between species. Good examples for this are tachykinin and tachykinin-like peptides. Amphibians and other submammalian representatives display a broad variation of tachykinins. Their exact sequence and of course their function do not completely correspond to that of mammalian tachykinins, but some of them are potent agonists of mammalian tachykinin receptors. They also share a common hydrophobic C-terminal sequence, defined as FXGLM-NH₂, where X stands for any hydrophobic residue. Numerous studies demonstrated the indispensability of this sequence for the interaction with



one of the three known mammalian receptors for tachykinins, NK₁, NK₂ and NK₃. Nevertheless it took about 70 years of intense research from the first identification of substance P (SP) by von Euler and Gaddum in 1931 over neurokinin A (NKA) and neurokinin B (NKB) in mammals to the discovery of more tachykinins that has only reached the current state in the last years (Page, 2004; Severini *et al.*, 2002).

Three genes are known in mammals that encode for tachykinins, that have most probably arose from two genome duplications which took place during vertebrate and mammalian development. In humans TAC1, TAC3 and TAC4, in rodents (mouse and rat) *Tac1*, *Tac2* and *Tac4*, with *Tac2* of mice and rats displaying high homology to the human TAC3 gene and both encoding NKB (Duarte *et al.*, 2006). The two other genes, *Tac1* and *Tac4* are similar concerning their structure both expressing at least four different splicing variants.

Tac1 transcripts (i.e. splicing variants) produce the following peptides: SP, NKA, neuropeptide K (NPK) and neuropeptide γ (NP γ), with all of these peptides representing tachykinin peptide family members (Fig. 1). In contrast, *Tac4* transcript variants encode the peptides hemokinin 1 (HK-1) and the endokinins A, B, C and D (EKA, EKB, EKC, EKD) with the EKC and EKD representing only tachykinin-like peptides as their C-terminal sequence bears two significant modifications replacing the tachykinin motif FXGLM to FQGLL that also decreases its hydrophobicity. Another specialty of *Tac4* gene products is represented by the fact that these endokinins are only specific to human cells and have not been described to be expressed or synthesized in rodents. Nevertheless recent studies indicate that similar endokinins might be encoded by *Tac4* in rabbits (Page, 2004).

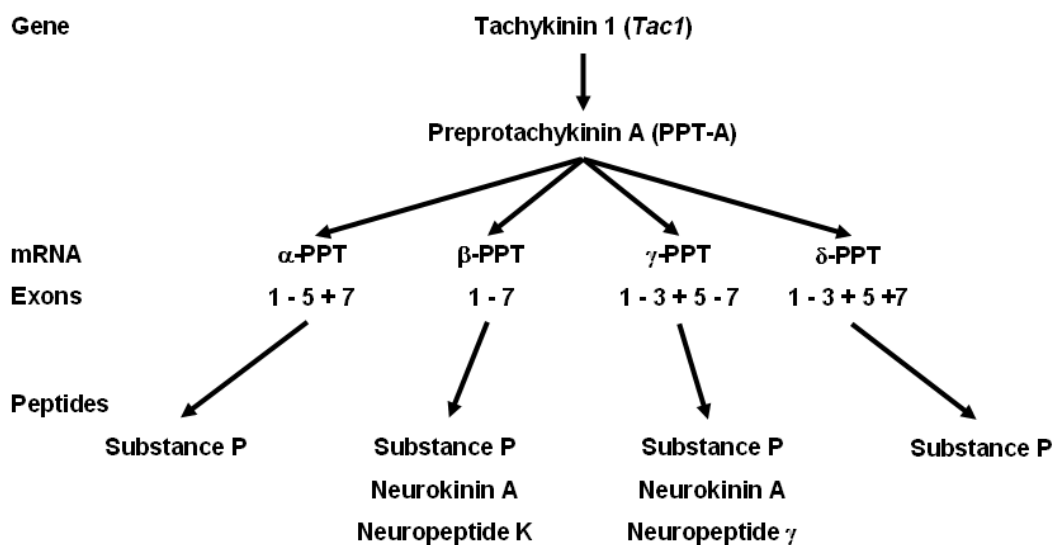


Figure 1: Gene, mRNA with splicing variants and peptides encoded by tachykinin 1 (*Tac1*).



Three different receptors are described, all classified as neurokinin receptors and consequently named NK₁, NK₂ and NK₃. All tachykinins displaying the FXGLM peptide motif bind to all NK receptors differing only in their binding affinity. The distribution of receptors is to a certain extent tissue specific. Although mammalian tachykinins are the natural ligands of the receptors, other – non-mammalian but vertebrate - tachykinins, like uperolein (from *Uperuleia marmorata*), physalaemin (from *Physalaemus biligonigerus*), kassinin (from *Kassina senegalensis*) or phyllomedusin (from *Phyllomedusa bicolor*), can bind to the respective receptors with fairly high affinity. Beside other tachykinin-like peptides (the locustatachykinins) that only differ in their last amino acid residue, concerning the specific five amino acid motif, even some authentic tachykinins were isolated from invertebrate species like eleidosin (from *Eledone aldovrandi*) or sialokinin I and II (from *Aedes aegypti*) which display similar receptor binding effects in mammals, thereby representing potent agonists NK receptor (Severini *et al.*, 2002).

Another result of a single gene duplication event is the evolution of arginine-vasopressin (*Avp*) and oxytocin (*Oxt*) gene loci from one single progenitor, vasotocin. Beside the high sequence homology of the peptides and also the genes in nearly all mammals, the two genes are located on the same chromosome in close vicinity with each other, placed on the opposite DNA strands. Although they share a big part of their sequence and function as in the body, their function is quite different. In the brain they also act as neuromodulators on similar brain systems and regions but with different function (Fields *et al.*, 2003; Gwee *et al.*, 2008; Landgraf and Neumann, 2004).

1.3. Anxiety and depression disorders

Arising from the threat assessment systems, there is already a bias towards interpreting harmless stimuli as being rather dangerous (Kim and Gorman, 2005). As mentioned before, there are many behavioral and physiological consequences of confrontations with stressful situations. If now the systems regulating these stress responses do not fully return to their former homeostatic state because of the repeated confrontation with a small or due to the confrontation with one strong stressor, the state of heightened alertness might never recover to basal level anymore, or can be triggered by much smaller events to the same strong reactions. This is the state, anxiety disorder patients have to cope with. As one can imagine, there is a smooth transition along a continuum between normal and pathological anxiety. The patients' genetic predisposition, their nurturing and education, their experiences and their environment shape their overall predisposition and likelihood



of being affected by any kind of these disorders. The overall lifetime-prevalence in industrialized countries for anxiety disorders is above 25% and patients suffering from one of these disorders are also prone to develop a second or third kind of anxiety disorder (Bittner *et al.*, 2004; Hettema *et al.*, 2004; Hettema *et al.*, 2005; Jacobi *et al.*, 2004; Kim and Gorman, 2005) The co-occurrence of multiple anxiety disorders clearly points to a kind of stress-dosage effect and the reduced ability of the stress-regulation systems to recover to a homeostatic state. These clear-cut effects of genetic predisposition, the effects of maternal care and nurturing have also been demonstrated for animals and animal models (Caldji *et al.*, 1998; Francis and Meaney, 1999; Wilkins and Haig, 2003a).

Anxiety disorder patients are also highly in danger to develop a depression disorder during their later life which is well described as comorbidity of these two disorders. The rate of comorbidity is fairly between 50-60% (Landgraf, 2001a). Depression disorders – similarly to anxiety disorders – pose a huge burden for affected persons, their close environment and also for economy. But whereas anxiety disorders might only slightly affect one patient's life, as is the case with specific phobias, where patients do not face the threat in everyday situations, in depression persons might be disabled for months or years, not taken into account that depressive episodes might return repeatedly.

Also the currently available pharmaceutical treatment for both, anxiety disorders and depression, is still far away from an optimal state. Best recovery can be reached utilizing a combination of pharmaceutical and behavioral (cognitive) therapy. Nevertheless, treatment response takes weeks or months, only one third of patients show a treatment response for the commonly used substances. As anxiolytics, benzodiazepines are widely used, although antidepressants like selective serotonin reuptake inhibitors, tricyclics and monoamine oxidase inhibitors are also prescribed often (Nutt, 2005). However, all of them might cause side effects, like analgesic or sedative ones. As the systems that are blocked do not exclusively exert functions in the central nervous system, side effects can also affect muscle function, the gut, skin, kidney or the complete hormone system (Simon *et al.*, 2008).

Therefore, many efforts are undertaken to identify new targets for pharmaceutical treatment, bearing with higher efficacy and selectivity. A new possible target – the neurokinin receptors – were found and analyzed during the last ten years, also reaching the clinical trial phase with saredutant. Although the results obtained were similar to the treatment with antidepressants, in one study the placebo control group was even more effective, so the drug failed (Czeh *et al.*, 2006). With more efforts



aimed at the characterization of the underlying mechanisms, new and more specific targets can be identified in the near future.

Furthermore, many studies underline the complex genetics behind anxiety and depression and support the consideration of data obtained from linkage and association studies in humans and animal models as well as the investigation of single specific molecular circuits. Further emphasis is on the fact most analysis from patients point to: genetic variation contributing to behavioral effects is not simply multifactorial, but each genetic locus contributing to these behavioral effects is expected to cause a variance of not more than 3% in the respective phenotype (Conti *et al.*, 2004; Hovatta and Barlow, 2008; Peters *et al.*, 2007; Schadt *et al.*, 2005; Smoller *et al.*, 2000). This increases the importance of quantitative trait locus (QTL) analysis (i.e. the identification of loci, contributing to multiple traits to a tiny percentage) and also makes the need for an integrative research combining the analysis of genetic predisposition (using polymorphisms as genomic markers) with gene and peptide expression profiles obvious (Schadt *et al.*, 2005).

Applying this strategy, new systems can be targeted, where the currently available high-throughput genome, transcriptome and proteome analysis systems might be of valuable help. Genome analysis systems reveal differences in the genetic sequence and can be directed at single nucleotide polymorphisms (SNP), copy number or any other kind of polymorphic structure. Transcriptome analysis systems assess the gene expression rate on a whole genome basis and proteomic assays can also detect quantitative and qualitative differences in proteins and peptides. They might provide the basis of a personalized therapy by (I) delivering the necessary biomarkers for a detailed molecular diagnosis and (II) the treatment targets for anxiety disorders, depression and many more complex diseases including some autoimmune syndromes or cancer.

1.4. Assessing anxiety/depression in mice

Unfortunately, the assessment of the systems involved – especially the central nervous system – is rather problematic in humans – not exclusively because of ethical concerns – so model organisms have to be studied and can even reveal more in some cases, as researchers can follow the line from less to more complex nervous systems, from simple to complex behaviors and from metabolic products to complex biosynthetic enzymes and enzyme complexes.

In some cases even invertebrate species can be used to study specific behavioral aspects, like aggression in *Drosophila* sp. (Dierick and Greenspan, 2006).



During the 70-ies and 80-ies of the last century a lot of effort has been undertaken to assess anxiety-related and depression-like behaviors in rodents, particularly in rats. The elevated plus-maze (EPM) test for anxiety-related behavior by Lister and the Porsolt forced swim test (FST) for depression-like behavior are the most prominent examples that have also been validated with antidepressant and anxiolytic drug treatment in countless studies. Later on, these tests have been adapted for mice as genetic manipulation found its way into mammalian research (Cryan and Holmes, 2005).

On the EPM, as in most other anxiety-related behavioral tests, the rodents' innate anxiety of open and brightly lit spaces is challenged versus the – also innate – exploratory drive to investigate unknown terrain. The animals may choose between exploring a dark and closed (with walls) or an open and brightly lit compartment, where the total amount of time spent in each one is indicative of the individuals' anxiety-related behavior (Bourin *et al.*, 2007; File, 2001). However, this anxiety-related behavior might be contaminated with locomotor hyperdrive or deficits. To exclude this bias, the open field (OF) test may be applied, to receive locomotor activity unaffected by anxiety-related behavior by measuring the distance traveled, if only moderate illumination is applied in the test. Still, anxiety-related behavior can be scored by measuring the time spent near the walls (more protected) against the central region, that is less protected (Cryan and Holmes, 2005; Holmes *et al.*, 2002). However, also the total number of arm entries on the EPM can be regarded as a valid parameter measuring locomotor activity (Ramos *et al.*, 2008).

Another possibility to assess anxiety-related behavior independent of locomotion is the elevated platform (EPF) test where the animals are placed on a round platform that is quite big enough, to turn around. Although this test is most commonly used as a mild stressor (Ebner *et al.*, 2004; Kavushansky and Richter-Levin, 2006), the amount of explorative head dips (going over the edge of the platform) is indicative of the animals' anxiety-related behavior (Kessler, 2007).

In the FST, depression-like behavior is assessed by challenging the animal in an inescapable, desperate situation (a glass cylinder filled with water, but the edge out of reach for the animal). The parameter measured is the total time the animal tries to escape (active coping) or just floats (passive coping) in the cylinder. Similarly, but only working for mice, a test paradigm has been developed that does not require the water as a surplus stressor to the inescapable situation, the so-called the tail suspension test (TST), where mice are hung up by their tail tip to a bar, some centimeters above the ground (Cryan and Mombereau, 2004).



Of course these tests do not reflect the full spectrum of anxiety- and stress-related phenotypes, as they only work with innate stressors. In other tests, cognitive abilities in regard of associative learning, fear-conditioning or social defeat and social recognition abilities can be assessed (Bunck, 2008; Frank *et al.*, 2006; Frank and Landgraf, 2008).

1.5. The hypothalamo-pituitary-adrenal (HPA) axis, gene expression and translation

For stress responses and the following reestablishment of the homeostatic state, the hypothalamo-pituitary-adrenal (HPA) axis is the pivotal contributor. In the hypothalamic paraventricular nucleus (PVN) input signals from amygdala nuclei, the bed nucleus of the *stria terminalis* (BNST), the pons or the *locus coeruleus* ransom the release of peptide hormones like corticotrophin-releasing hormone (CRH) and vasopressin (AVP). Once released, these neuropeptides trigger the stimulation of the pituitary to secrete adrenocorticotropin (ACTH) into the peripheral blood vessels (Lang *et al.*, 2000) acting on the adrenal cortex to secrete cortisol or corticosterone (CORT) to suppress stress-related reactions of the PVN and other brain nuclei (Herman and Cullinan, 1997; Tsigos and Chrousos, 2002). If now either the expression or translation of AVP, CRH, ACTH, or CORT is inhibited, the system can not work efficiently enough. Interestingly, not only an increased cortisol or CORT response has been observed in anxiety-related disorders (Strohle and Holsboer, 2003), but also hypocortisolism has been reported in many cases of stress-related disorders, among others like in post traumatic stress disorder (Frank *et al.*, 2006; Raison and Miller, 2003).

Furthermore, as mentioned before, a big and well-coordinated orchestra of molecular signaling molecules has to be available to mediate any stress response. Therefore, not only the transmitter molecules have to be available, but the synthesizing enzymes and also receptors have to be expressed and translated in the cells, where they are required. With respect to the HPA axis, the roles of CRH or NK₁ receptors are well-described (Ebner and Singewald, 2006; Muller *et al.*, 2001; Saria, 1999). The same applies to the respective neuropeptide ligands. Anything that might interfere with a correctly operating sequence might lead to severe consequences in the required behavioral and physiological responses. As the “orchestra” is quite big, the “drop out” of one violin player will not cause the failure of the whole concert (especially, as there are many mechanisms which are meant to compensate for the failure of single mechanisms). To mention just some of the active compounds and peptides: γ -aminobutyric acid, glutamate, glycine,



epinephrine, norepinephrine, substance P, glucagon-like peptide 1, serotonin, oxytocin, prolactin or urocortin (Herman and Cullinan, 1997; Landgraf, 2001b; Zafra and Gimenez, 2008).

But if more systems are affected and disturb fine-coordination or cause a total failure it may lead to serious consequences for the whole system.

Tissue and especially brain area-specific gene expression therefore is a prerequisite to a well-functioning organism. To reveal the specific mechanisms leading e.g. to a specific but complex phenotype, examining gene expression is an especially helpful tool (Green *et al.*, 2004; Hovatta and Barlow, 2008).

1.6. The influence of genetic polymorphisms

Besides physical and physiological disturbances that lead to the loss of the homeostatic state, genetic polymorphisms play a vital role, first of all for the evolution *per se*, but genetic polymorphisms can enhance or limit individual capacities and capabilities in everyday life.

Genetic polymorphisms arise from mutations, irrespective of their genomic position. They can lead to both, loss and gain of function, if they cause a change in the genetic triplets (missense mutation) for amino acids in protein-coding genomic regions (Lewin, 2004). Polymorphisms may even affect mRNA stability, if they cause synonymous mutations at the third 'degenerate' base position (Shabalina *et al.*, 2006). Furthermore they influence mRNA transcription rates, if they are located in genomic regions near genes where transcription factors and cofactors can be recruited to (cis-regulatory effect). This applies to at least 20% of polymorphisms found in promoter regions and even to gene introns (Buckland *et al.*, 2004; Hubler and Scammell, 2004; Levine and Tjian, 2003). Trans-regulatory effects on gene expression may also come to effect, if a regulatory region is in close spherical proximity to the regulated gene but on the physical genomic map would be located thousands or millions of basepairs (bp) away from the respective gene. Some studies highlight that due to the close and dense package of DNA in cell nuclei such interactions are possible (if not even the main mechanism for transcriptional regulation) and play a pivotal role in tissue-specific gene expression (Engel *et al.*, 1992; Yvert *et al.*, 2003).

The most common class of genetic polymorphisms are SNPs, as they can arise from the most simple kind of error that might occur during replication. So far, 30 million SNPs have been identified in humans that would mean one SNP per 1kbp of total DNA. Although other mutations might occur as well, as transitions, deletions or duplications of single fragments of different size, and might have a major impact on



the individual's viability, they occur less often and are therefore less well documented in different species and also harder to compare in inter-species approaches. Nevertheless, recent advances in genotyping large amount of loci, also facilitate the discovery and mapping of inter-individual copy number variations (Feuk *et al.*, 2006).

Popular examples for gain-of-function by mutations is the protective mutation in hemoglobin that causes sickle-cell anemia, but protects from malaria infection, or a polymorphism that has been described to protect from both the bubonic plague epidemic known from the Middle Ages and HIV infection (Altschuler, 2000; Ayi *et al.*, 2004).

As another example for complex traits, scientists recently succeeded in identifying genomic loci, highly associated with the restless-legs syndrome by screening for SNPs in a large group of patients vs. unaffected controls (Schormair *et al.*, 2008; Winkelmann *et al.*, 2007; Winkelmann *et al.*, 2008).

The same way, researchers have to search for mutations, involved in anxiety disorders and depression to elucidate new ways for more effective and personalized treatments (Holsboer, 2008).

1.7. The HAB/LAB mouse model

For the analysis of any biological mechanism in humans, it is not only because of ethical considerations impossible to make these assessments in humans. In service of the modular understanding of the existing circuitries, the best possible approach is to put emphasis on model organisms that are on one hand simple enough to keep, breed and raise them for long-term experiments but are, on the other hand, complex enough to reflect complex traits, like anxiety or depression-like behavior in a way that can be applied analogously or extrapolated to primates. In this respect, rodents play a major role for psychiatric research, although some aspects of the respective phenotypes in humans won't be reflected at all by any model, such as feeling of worthlessness.

Following a breeding strategy that was also successfully applied to rats (Landgraf and Wigger, 2002; Liebsch *et al.*, 1998a; Liebsch *et al.*, 1998b) before, a mouse model has been established in the same manner, i.e. starting from the CD1 outbred mouse strain animals displaying high anxiety-related behavior (HAB) in the EPM test have been selected to form the basis of the HAB mouse line. HAB mice usually spend less than 10% of the total test time on the open arm of the EPM. Accordingly, animals showing low anxiety-related behavior (LAB) were selected and bred to generate the LAB mouse line, spending more than 50% on the open arm of the EPM



(Kessler *et al.*, 2007; Kromer *et al.*, 2005; Landgraf *et al.*, 2007). During the first seven generations, an outbreeding protocol was applied to warrant for the equal distribution of anxiety-related susceptibility genes and starting from generation 10 switched to a strict inbreeding (brother-sister) protocol. This was to ensure the fixation of loci critically involved in producing the phenotype in a homozygous state. Additionally, a normal anxiety-related (NAB) mouse line has been added two years ago, where the animals should spend around 30% of the total test time on the open arm of the EPM (Landgraf and Kessler, personal communication), which also reflects the mean value of outbred CD1 mice (Bunck *et al.*, submitted; Touma *et al.*, 2008). Nevertheless, during the last 30 generations, numerous different endophenotypes have been assessed in HAB, NAB and LAB mouse lines, also involving outbred CD1 (referred to as CD1) in some cases.

1.7.1. Phenotypic characteristics of HAB/LAB mice

HAB and LAB mice do not only differ in their anxiety-related behavior as measured on the EPM, but their divergence in anxiety-related test parameters can also be detected and quantified in the dark/light box, OF and EPF tests (Kromer *et al.*, 2005); Keßler *et al.*, in preparation). Importantly, the difference in the EPM has been verified under independent, but similar testing conditions at the University of Regensburg and Innsbruck (Bosch *et al.* and Sartori *et al.*, in preparation). Furthermore, HAB and LAB mice show differences in depression-like behavior measures as assessed by the TST and FST, with HABs displaying significantly more passive, LABs a more active coping strategy in those desperate test situations (Kromer *et al.*, 2005). A further interesting finding is the differential HPA axis regulation in HAB vs. LAB mice. While neither line shows differences in basal levels of CORT or ACTH, HAB mice exhibit a significantly flattened CORT response in blood plasma upon a strong physical stressor (restraint stress or stress reactivity test) relative to LAB mice (Kessler *et al.*, in preparation).

Also cognitive differences were observed between the two mouse lines, with HABs being able to discriminate for a longer time-interval between a novel and a familiar ovariectomized female as compared to LAB mice in the social discrimination test. These cognitive differences also apply to the performance in the Morris water maze, the Y-maze or fear conditioning related measures (Bunck, 2008).

Importantly, the mouse lines do not differ in body weight, locomotor activity, locomotor capability or their ability to hear, smell or see (Zurmuehlen, 2007).



1.7.2. Molecular characteristics of HAB/LAB mice

A pronounced deficit in AVP peptide and the *Avp*-coding mRNA has been demonstrated in LAB mice in various brain regions, as compared to CD1 or HAB mice (Bunck *et al.*, submitted), which is in close association with a polymorphism in the AVP preprohormone-coding mRNA and anxiety-related behavior and signs of central diabetes insipidus (Kessler *et al.*, 2007).

Similarly HAB, but not LAB or CD1, mice exhibit an overexpression of *Crh* in multiple regions, linked to depression-like behavior (Bunck *et al.*, in preparation).

Not much is known about the genetic background of HAB/LAB mice, as both are derived from CD1 mice. Up to date there is no information available on genetic polymorphisms or their allelic frequency, although the latter might even vary from supplier to supplier. The most closely related inbred strains often used in animal models are FVB/J and NOD/J (Beck *et al.*, 2000).

1.7.3. The F2 panel

To test hypothesis in behavioral biology, one can either apply substances to block enzymes, hormones, receptors or to enhance them and then take a look at behavioral consequences. The other possibility is, but this only applies to model systems which are based on the same species with definite (if possible, not too many) differences, to take the two lines – in our case HAB and LAB mice, mate them reciprocally to create a genetically completely heterozygous F1 generation (in all alleles differing between HAB and LAB mice) and to mate these F1 mice to each other again to establish the F2 generation, where each genotype and phenotype has the possibility to segregate freely, if they are not linked to each other (Henderson *et al.*, 2004; Turri *et al.*, 1999; Valdar *et al.*, 2006). So far, the breeding has been completed, all HABxLAB F2 intercross mice (N = 521) tested for a number of behavioral (EPM, OF, EPF, FST, TST and stress reactivity) and physiological (body weight, water consumption) parameters (Kessler *et al.*, in preparation).

The aim of this thesis was to shed some light on the molecular mechanisms underlying trait anxiety and depression-like behavior as modeled in HAB and LAB mice.

Therefore, phenotypic stability of HAB mice was addressed by a selective breeding approach first, to drive them towards less anxious behavior.

Then, to screen for gene products differing between HAB and LAB mice, gene expression profiles in various brain regions involved in the regulation of anxiety-



related behavior were generated by using two different microarray platforms. The most significant findings were reanalyzed in an independent approach by quantitative PCR (qPCR) and could be partially confirmed. Other assays tried to assess the effects of differential regulation, based on enzyme-activity or measurements of protein levels.

In another unbiased whole-genome assay, SNPs were identified that constantly differed between HAB and LAB animals (i.e. both lines carried the opposite alleles homozygously), thus allowing the genotyping of F2 and CD1 mice and helping to gain some insight into the genetic variability available in outbred CD1 mice. Further, sequencing of candidate genes helped to reveal differences, the observed gene expression differences might be related to.

Finally, to reveal functional associations of genomic loci with behavior, the genotyping information on SNPs in F2 mice made the analysis of genotype/phenotype associations possible, highlighting the role of single genomic regions in actively influencing anxiety-related behavior. In this whole study, the focus is on selected, highly significant results, while other findings also of potential interest are neglected at this stage.

Further this thesis represents the first approach to integrate data obtained in gene expression analyses and genotyping for a large number of polymorphic loci to identify genes causally involved in shaping the anxiety-related and depression-like behaviors in HAB vs. LAB mice. These results could partially be extrapolated to other animal and – last but not least – to human studies, dealing with anxiety disorders and depression. Further this study contributes to the analysis of the genetic background in outbred CD1 mice.



2. Animals, materials and methods

All animal experiments were carried out with the approval of local authorities and conducted according to current regulations for animal experimentation in Germany and the European Union (European Communities Council Directive 86/609/EEC). All animals were kept in the animal facility of the Max Planck Institute of Psychiatry under standard housing conditions (room temperature $23\pm 2^{\circ}\text{C}$, relative air humidity $60\pm 5\%$, 12h/12h dark/light cycle with lights on at 7 a.m) in groups of two to four animals per cage. If animals were ordered from a supplier, they were granted at least one week of habituation before starting with any behavioral study. Animal numbers, the respective generation of animals and the mouse lines used for each experiment are indicated each. Behavioral experiments were carried out under standard housing conditions and were always performed between 8 a.m. and 1 p.m. All animals were tested in a randomized order, blind to the mouse line. This also applies to the processing of individual samples from animals.

All mice used were either HAB, LAB, HABxLAB F1 intercross, HABxLAB F2 intercross, NAB or CD1 mice. NAB mice are inbred mice, selectively inbred for displaying an intermediate phenotype (i.e. spending around 30% of the total EPM test time on the open arms). Inbreeding NAB mice, only started by the end of the year 2006. Outbred CD1 mice are referred to as CD1 only.

Except where indicated, all chemicals were purchased from Sigma-Aldrich (Taufkirchen b. München, Germany); centrifugations of volumes smaller 2ml were done in a Hermle Z 233 MK centrifuge (Hermle Labortechnik, Wehingen, Germany). For pipetting volumes up to 1ml, pipets by Gilson (Pipetman, Gilson, Middleton, WI) were used with pipet tips manufactured by Sarstedt (Nürnbrecht, Germany). For all experimental steps involving handling of RNA filter pipet tips were used.

2.1. The HAB phenotype reversal by selective breeding

To assess the phenotypic stability of HAB mice and estimate the remaining genetic variability in HAB mice after more than 20 generation of bidirectional and more than 12 generations of strict inbreeding, the selection criterion of HAB mice (high anxiety-related behavior – as reflected by the EPM test) was intended to be reversed (i.e. to selectively breed HAB mice for a less anxious phenotype). Therefore three HAB sib pairs were selected of generation 23, which were most non-anxious in the EPM test with spending more than 10% of the total test time on one of the open arms, and mated to each other, following the standard breeding procedure as already described (Kromer *et al.*, 2005). Descendants of six consecutive generations were all tested on the EPM, always applying the reversed HAB (rHAB) criterion (reduced



anxiety-related behavior) for breeding. Additionally, 14 male mice of the 5th rHAB generation (G5) were tested in the TST. Throughout all seven generations two to four families were run in parallel. HAB mice descending from the rHAB parental mice served as reference.

2.2. Identification of candidate genes

For the identification of candidate genes relevant to anxiety-related and depression-like behavior, gene expression profiling was carried out on two different microarray platforms, the MPI24K – the 2nd generation microarray platform of the Max Planck Institute of Psychiatry – and on a commercially available platform of Illumina (San Diego, CA).

2.2.1. Animals and behavioral tests for the gene expression studies

Mice for microarray analyses on both the MPI24K and Illumina platform were tested in both the EPM test and the TST. Only mice were selected for gene expression profiling that did not deviate more than 5% from their group means in any measure. HAB mice, displaying nearly no locomotion on the EPM were excluded from further analysis. For the MPI24K platform based microarray, mouse pools consisting of six HAB and six LAB mice each (G16) were compared. For the Illumina platform based experiment eight HAB, eight LAB (G25) and seven NAB mice (G3) were selected. Animals for the validation of microarray-based gene expression analyses were HAB and LAB mice from G22 - G27, unselected CD1 mice as well as NAB animals of G4. Both male and female mice were tested on the EPM. Male mice were additionally tested in the TST.

2.2.2. Gene expression profiling on the MPI24K-platform

The gene expression profiling system of the MPI24K array, which is an upgrade of the MPI17K microarray platform (Deussing *et al.*, 2007), is based on dual color direct comparison experimental protocol using indirect labeling.

2.2.2.1. Tissue dissection

Anaesthetized animals aged ten weeks were killed by decapitation 3d after the TST. Brains were collected, dissected in slices of 200µm and mounted to Superfrost microscope slides (Menzel, Braunschweig, Germany) in a cryostat (Microm MH50, Microm, Walldorf, Germany) from rostral to caudal. From these frozen slices the brain areas of interest were acquired by micropuncture as described before (Palkovits, 1973) utilizing punchers with a diameter of 0.5 or 1mm (Fine Science



Tools, Heidelberg, Germany). The brain regions collected included the anterior part of the cingulate cortex (Cg), the *nucleus accumbens* core and shell (NAc), the PVN, the supraoptic nucleus (SON) and the basolateral/lateral (BLA/LA), central (CeA) and medial (MeA) amygdala. Punches of 1mm diameter were collected from Bregma +1.3mm to +0.9mm, twice sampling the tissue medially about 0.5mm from the dorsal tissue border to receive the Cg and bilaterally sampling the NAc core and unpreventably a minor part of its shell around the anterior commissure (Fig. 2A). Further tissue was collected medially 0.8mm above the ventral tissue limit ($\varnothing=1$ mm) and bilaterally from the optic tract ($\varnothing=0.5$ mm) to acquire tissue from the PVN and SON, from Bregma -0.56mm to -0.96mm (Fig. 2B). Amygdala tissue samples were collected bilaterally from two slides for each region acquiring punches of 1mm diameter. CeA was collected from Bregma -0.96mm to -1.36mm dorsomedially from the ventral end of the external capsule (Fig. 2C), MeA from -1.16mm to -1.56mm dorsolaterally from the optic tract and BLA/LA was collected from Bregma -1.36mm to -1.76mm from in between the bifurcation of the external capsule (Fig. 2D).

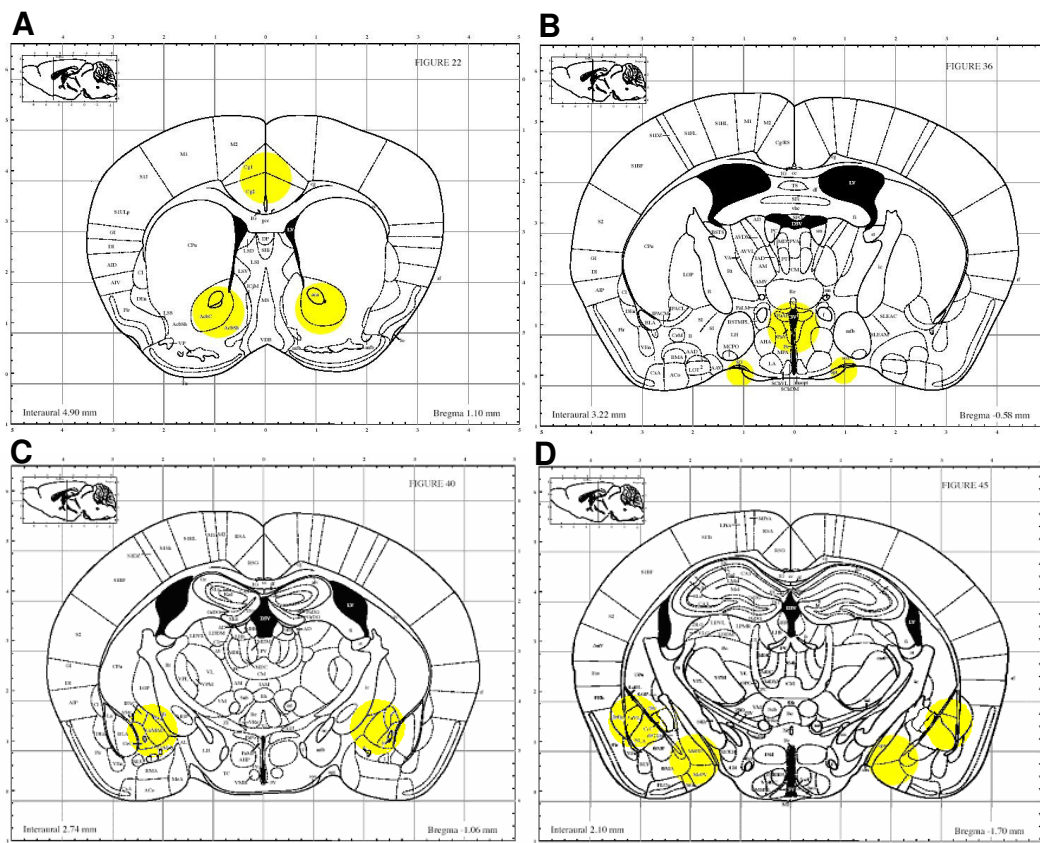


Figure 2: Approximate locations in mouse coronal brain sections to acquire the (A) cingulate cortex and nucleus accumbens, (B) hypothalamic paraventricular nucleus and supraoptic nucleus, (C) central amygdala and (D) basolateral/lateral and medial amygdala. Pictures are based on the Mouse Brain Atlas (Paxinos and Franklin, 2001).

Coordinates were selected according to the mouse brain atlas (Paxinos and Franklin, 2001) and are subject to vary ± 0.05 mm.



2.2.2.2. Total RNA isolation and amplification

Total RNA was extracted in presterilized 1.5ml Safelock tubes (Eppendorf, Hamburg, Germany) using a TRIzol (Invitrogen, Karlsruhe, Germany) chloroform standard protocol. After tissue homogenization in 300µl of TRIzol by pipetting, 1µl linear acrylamide (5mg/ml, Ambion, Austin, TX) and 60µl of chloroform (Carl Roth, Karlsruhe, Germany) were added and the samples vortexed. Centrifugation for 5min at 18°C and 13,000rpm followed, then RNA was precipitated with 180µl isopropanol (Carl Roth) overnight at -20°C, centrifuged at 4°C and 13,000rpm for 30min and washed twice in 500µl 70% ethanol (Carl Roth) with centrifugation steps at 4°C and 13,000rpm of 10min in between. Following the last centrifugation step, all remaining liquid was removed with a pipet, pellets were dried in an incubator for 15min at 45°C and resolved in 13µl of autoclaved bidistilled water.

Extracted total RNA was amplified and dye coupled in two rounds with Ambion's Amino Allyl MessageAmp aRNA kit (Ambion) according to the manufacturer's protocol using T7 oligo(dT) primers for the first round to select specifically for mRNA for reverse transcription and random hexamer primers for the second round of reverse transcription. The procedure included the synthesis of a first then a second strand of cDNA and an *in vitro* transcription step overnight. cDNA synthesis was carried out in PCR tubes (Abgene, Hamburg, Germany) using a thermal cycler (GeneAmp PCR System 9700, PE Applied Biosystems, Foster City, CA). For *in vitro* transcription, the tubes provided by the kit's manufacturer were used, after pipetting all reagents, tubes were sealed with parafilm (American National Can, Neenah, WI) and incubated at 37°C in a warm room constantly heated. In the second round of *in vitro* transcription, an amino allyl extension to every second uracyl base was incorporated to receive the amino allyl RNA (aRNA) for the following indirect dye coupling reaction. Before aRNA purification the filters were equilibrated with 100µl aRNA binding buffer and incubated for 5min. All samples were pooled to one sample per line and brain region. The dye swapped experimental design required coupling of one half of each pooled sample to cyanine 3 (Cy3, Amersham Biosciences, Buckinghamshire, UK) the other half to cyanine 5 (Cy5, Amersham Biosciences). Correct quantification of aRNA was ensured by photometric assessment of the optic density in a photometer (Ultrospec II, Pharmacia LKB Biochrom, Cambridge, United Kingdom) and additional analysis on agarose gel.



2.2.2.3. Array hybridization and quantification

Prehybridization buffer:

125ml	formamide
62.5ml	20xSSC
2.5ml	10% SDS
2.5ml	BSA (10mg/ml)
57.5ml	water

Hybridization buffer:

500µl	formamide
250µl	20xSSC
10µl	10% SDS
5µl	mouse-COT1-DNA (20mg/ml, Invitrogen)
40µl	poly adenylic acid (2.5µg/µl, Amersham Biosciences)

Ten array slides per brain region (MPI24K Arrays, MPI of Psychiatry, Munich, Germany) – serving as technical replicates - were prehybridized prior to the experiment in the prehybridization buffer for 1h at 42°C, then washed in water and isopropanol and dried by centrifugation (Megafuge 1.0R, Heraeus, Hanau, Germany) at 1500g for 3min in 50ml tubes (Sarstedt). Dye coupled aRNA samples were mixed with the contrary dye coupled sample from the other mouse line of the specific regions and loaded with a hybridization buffer to five arrays each under m-Series LifterSlips (Menzel). All arrays were hybridized at 50°C over 16-17h in separate hybridization chambers. Then arrays were washed in 2xSSC and 0.1% SDS for 5min at 42°C, 10min room temperature in 0.1xSSC and 0.1% SDS, four times in 0.1xSSC for 1min and finally for 20s in 0.01xSSC solutions. Slides were dried by centrifugation at 1,500rpm for 3min. Then, arrays were scanned on a PerkinElmer ScanArray 4000 (PerkinElmer Life and Analytical Sciences, Shelton, CT) laser scanner using automatic focusing and adapting laser power between 60 and 80 for Cy3 and 40 and 70 for Cy5. This ensured that for both dyes - in average - the same fluorescence intensities were reached and that not more than 1-2% of spots showed fluorescence intensities over the point of saturation. Quantification of all arrays was performed with QuantArray-software (GSI Lumonics, Billerica, MA) applying a fixed-circle quantification protocol and manual positioning of all grids over the hybridized spots. To provide a negative control for the hybridization and evaluation procedure, excess aRNA was used for an additional hybridization in both Cy3 and Cy5 combinations.



2.2.2.4. Statistical analysis

For statistical evaluation, analytic methods were applied as previously described (Dudoit *et al.*, 2002; Yang *et al.*, 2002). In brief, first an MA-plot was generated to display raw fluorescence intensities of Cy5 (R) and Cy3 (G) with $M = \log_2 R/G$ and $A = \log_2 \sqrt{RG}$. Data were normalized to exclude systematic and technical errors. For two normalization steps, a function c was subtracted from the logarithmized fluorescence intensities ($\log_2 R$ and $\log_2 G$). First a global normalization was performed, based on the assumption that R and G correlate:

$$\log_2 \frac{R}{G} \Rightarrow \log_2 \frac{R}{G} - c = \log_2 \frac{R}{kG}.$$

In a second normalization step, an intensity-dependent normalization was added, which was performed applying a LOESS smooth, as it is implied in the R software package (<http://www.r-project.org>). This is calculated from:

$$\log_2 \frac{R}{G} \Rightarrow \log_2 \frac{R}{G} - c(A) = \log_2 \frac{R}{k(A)G},$$

where $c(A)$ stands for the LOESS smooth of the MA-plot. From the MA-plot, 40% of values were used to calculate the smooth. In several other normalization steps, differences were minimized that resulted from unequal distribution of probes from the array production or from unbalanced fluorescence intensities within one array slide. All data were merged in a matrix, p-values for multiple testing were calculated by permutation and are therefore called adjusted p-values.

2.2.3. Gene expression profiling on the Illumina-platform

The MouseWG-6 v1.1 Expression BeadChip-system by Illumina (Illumina, San Diego, CA), provided a gene expression screening platform that could identify 46,000 individual gene transcripts that were represented on each array (for each sample) between 10 to 30 times. This technology made the manual setup of technical replicates (as has been done with the MPI24K platform) obsolete and provided the opportunity of measuring individual samples combined with a single color labeling protocol that eliminated problems arising from basal differences in signal intensity due to different dyes.

2.2.3.1. Tissue laser-microdissection

Animals and the according brains were treated as described in 2.2.2.1. with the difference that 25 μ m slices were acquired in the cryostat (Microm). Only brain slices containing the brain areas of interest were sampled, including the anterior part of the Cg, the PVN, the SON, the anterior dentate gyrus (DG), the CeA and the basolateral



amygdala (BLA). For the DG, the same coordinates as for the PVN and SON were applied. To cover the whole area of interest an overall depth of 400µm per region was chosen. While sampling the CG, BLA and CeA four brain slices were mounted onto an LMD6000 metallic frame slide covered with a membrane of polyethylene terephthalate (Leica Microsystems Deutschland, Bensheim, Germany), the following four to Superfrost slides (Menzel). This procedure was repeated for the next eight slices. For the region containing the PVN, SON and DG only two slices were mounted to one slide always alternating the LMD6000 frame and the Superfrost microscope slides. Only the LMD6000 slides were used for further processing and stored at -80°C. Right before laser-microdissection, brain slices on the LMD6000 frame slides were stained with cresyl violet applying a modified staining protocol that included 1.5min staining in cresyl violet, followed by washing in 70% and 96% ethanol for 20s each and in isopropanol for 5min. The slides were refrozen and processed at the laser-microdissection microscope (AS LMD, Leica, kindly provided by PD Dr. Gabriele Rieder at the Max von Pettenkofer Institute of the Medical Faculty of the Ludwig Maximilians University in Munich). For the dissection procedure of the required brain areas, a magnification of 100x was chosen with laser power between 80-100% and speed varying between 1 and 4. Cut-out brain areas were captured in the caps of 0.2ml PCR soft tubes (Biozym Scientific, Hessisch Oldendorf, Germany) and cooled on dry ice immediately after completion of one brain region. Pictures of the processed brain slices were acquired by means of the IM1000 software (Leica, see Fig. 14).

2.2.3.2. Total RNA isolation and amplification

From all samples, total RNA was extracted individually (one sample per mouse and brain region) as described in chapter 2.2.2.2. RNA was amplified and labeled using the Illumina TotalPrep RNA Amplification kit (Ambion) with only one round of in vitro transcription, where biotinylated uracyl bases were built in to the newly synthesized aRNA. 5µg per sample were required for loading to the microarray slides. Correct quantification was ensured by measurement of optic density in a NanoPhotometer (Implen, Munich, Germany) and additional analysis on agarose gel. Samples not fulfilling all criteria of homogeneity (inadequate concentrations, too many small but few larger aRNA fragments) were excluded from further analysis.

2.2.3.3. Array hybridization and quantification

Each microarray slide had the capacity for six samples, same brain regions were hybridized in the same batch comparing a maximum of six individual mice of each



breeding line. Reagents and material were provided by Illumina, the procedure was strictly conducted according to the manufacturer's protocol. In brief, each sample was mixed with hybridization buffer, loaded onto the designated array field and the slides were put into hybridization chambers and incubated for 17h in incubation chambers provided by Illumina. Arrays were washed in several steps, incubated with Cy3, washed several times again and dried by centrifugation. Finally, fluorescence signals were detected on a BeadStation scanner (Illumina) and analyzed by the BeadStudio (Illumina) software. The manufacturer's built-in controls have been analyzed including hybridization controls and sample dependent parameters. Only microarrays fulfilling Illumina's recommendations for quality control have been used for further evaluation.

2.2.3.4. Statistical analysis

Illumina BeadStudio gene expression results were further analyzed similar to the statistical analysis as described in 2.2.2.4. All analyses have been performed using R-packages, based on 'beadarray' system as described by Dunning et al. (2007), which simplifies the comparison between a high number of arrays. First, pair wise box plots were generated to compare mean expression within each line and brain region. Normalization for expression values has been applied to all samples with the 'QSpline' function. Each sample has been clustered to ensure that each brain region per line shows similar expression patterns using the 'hclust' function. Three samples from different brain regions have been identified as inadequate during the scan process and have therefore been excluded from further analysis. For differential expression analysis, functions of the 'LIMMA' package have been applied on \log_2 -transformed values. The resulting matrix has been used for all subsequent analyses. Significantly regulated genes were ranked using an empirical BAYES method implemented in the LIMMA R-package (Lonnstedt and Speed, 2002; Smyth, 2004).

2.2.4. Analysis of candidate genes by quantitative PCR

Candidate genes for anxiety-related behavior and for further characterization were picked from the gene expression screening analyses according to their p-values ($p < 0.1$) and relative expression. Gene transcripts showing high (around 2-fold) expression differences in all brain regions between HAB and LAB mice were selected, as well as some other transcripts that were already described in connection to anxiety-related behavior, but were only detected as significantly regulated in only two or three brain regions. For analysis by qPCR, tissue samples for the Cg, PVN, SON, CeA and BLA/LA were acquired by micropuncture as



described in chapter 2.2.2.1. For whole brain analyses, three coronal sections of 200µm were taken at different brain levels. Total RNA extraction from both, micropunches or representative whole brain material was performed as described in chapter 2.2.2.2. before, but using TRI-Reagent (Sigma-Aldrich) instead of TRIzol. The yield of total RNA was between 0.3 and 1.5µg. A maximum of 1µg of total RNA was reverse transcribed with Superscript II (Invitrogen, Karlsruhe, Germany) after DNase treatment according to the manufacturer's protocol. For quality control, a small aliquot of each cDNA was analyzed on an agarose gel. For expression analysis of unspliced *Avp*, primers were designed to detect a sequence from the first intron and RNA was reverse transcribed using random hexamer primers and three samples of HAB and LAB aRNA each from the experiment described in 2.2.2.2. cDNA of male or female HAB, unselected CD1 mice, or LAB mice was analyzed by qPCR, using the QuantiFast SYBR Green PCR Kit (Qiagen GmbH, Hilden, Germany) according to the manufacturer's instructions, the respective oligonucleotide primers were designed based on Primer3 (Rozen and Skaletsky, 2000) and purchased from Sigma-Aldrich. The same applies to primers for the detection of specific splicing variants of *Tac1*. For this, primers had to hybridize to half of one and half of the following exon. Amplificates from the *Tac1* splicing variant and intronal *Avp* detection were additionally sequenced. The procedure is described in the following chapter 2.3.5. Gene products to be quantified by qPCR were selected by the following criteria: significant expression differences between HAB and LAB mice (adj. p-value < 0.10, fold regulation at least 1.3 fold and differential expression in the microarray experiment (in most cases) for all or some (at least three) analyzed regions. All primers for qPCR are listed in table 1. Experiments were performed in duplicates on the Lightcycler®2.0 instrument (Roche Diagnostics, Mannheim, Germany) under the following PCR conditions: Initial denaturation at 95°C for 10min, followed by 40 cycles of denaturation (95°C for 10s) and a combined annealing and extension phase (60°C for 30s). At the end of every run, a melting curve (50-95°C with 0.1°C/s) was generated to ensure the quality of the PCR product. Crossing points (Cp) were calculated by the LightCycler®Software 4.0 (Roche Diagnostics) using the absolute quantification fit points method. Threshold and noise band were set to the same level in all compared runs. Relative gene expression was determined by the $2^{-\Delta\Delta CT}$ method (Livak and Schmittgen, 2001) using the real PCR efficiency calculated from an external standard curve. Cp were normalized to the housekeeping genes *Gapdh*, *Hprt1*, *Atp2b1*, *Rpl13a* and *Polr2b* or any combination of two of the mentioned genes. Fold regulation values were



calculated relative to the expression mean of the group displaying the lowest expression.

Table 1: List of primers for qPCR with chromosomes and exons the primers hybridized to. In-1 refers to the first intron. List is sorted alphabetically according to the gene symbols. A clear exon definition was not possible for the first two genes.

Chr.	Gene symbol	Orient-ation	Exon	Primer sequence 5'→3'	Prod. size
2	<i>2900019</i> <i>G14Rik</i>	forward		TTG GAA ACC TTC CTT TGC AG	175bp
		reverse		AAA CAC ATT CAC CCC CAT TC	
1	<i>5230400</i> <i>G24Rik</i>	forward		TAT GAA ATG GAA TAC ACC GAA GG	210bp
		reverse		ATC TGC TGG TCT TGA AAA TGA AA	
2	<i>Abca2</i>	forward	47	CAT CAG CTT CGA GGA AGA GC	206bp
		reverse	48	CAT TCG GGG AGG ATG GTA G	
11	<i>Aldh3a2</i>	forward	9	TCC TGC TGA AGC AGT TCA AC	157bp
		reverse	10	ACA GGG AAG TCC ACC AGA TC	
7	<i>Apbb1</i>	forward	13	TTC TCT CCT TCC TGG CTG TG	162bp
		reverse	14	GAC ACT TCT GGT AGC GGA GC	
10	<i>Atp2b1</i>	forward	1	CAT TAC GGA AAA TAC AGG AGA GC	182bp
		reverse	2	TGC TTC CCA GAC TAA CTG AAG AA	
16	<i>Atp5j</i>	forward	4	TAT TGG CCC AGA GTA TCA GCA	134bp
		reverse	5	GGG GTT TGT CGA TGA CTT CAA AT	
2	<i>Avp</i>	forward	In-1	TTC CTT ATG ACT GGG CTT GG	170bp
		reverse	In-1	GCA CTG CTG GCT AGA AAA GG	
2	<i>Avp</i>	forward	1	TCG CCA GGA TGC TCA ACA C	164bp
		reverse	2	TTG GTC CGA AGC AGC GTC	
11	<i>Ccdc104</i>	forward	1	AAG AAG AGG ACG AAG TGG AAT G	180bp
		reverse	2	TCT TGA TGG ATT TCT GTG TAG G	
16	<i>Coro7</i>	forward	1	AGG TGT CCA AGT TTC GGC ATA	113bp
		reverse	2	GCA GCT TGA TTT GAT GTG GTT	
14	<i>Ctsb</i>	forward	1	CTG CGC GGG TAC TTA GGA GT	148bp
		reverse	2	CAG GCA AGA AAG AAG GAT CAA G	
14	<i>Dgkh</i>	forward	27	GGA GCC TCC TCT GGA TTG TA	211bp
		reverse	29	AGT GTG ACC ACC CCT CAG AC	
5	<i>Dgkq</i>	forward	22	TAC AAG GTG GGC TAC GCT CT	188bp
		reverse	23	CAA GGT GTC CAC TCG GGT AT	
17	<i>Enpp5</i>	forward	3	TGC CCA TCC TAA TCT AAC GG	186bp
		reverse	4	GGA TGC ATT TCT GCT AAT GC	
5	<i>Ep400</i>	forward	1	GGT GCA AGC GAA CGG GAT AG	202bp
		reverse	2	GAC TGG CTG ATG GAG CGA AAG	
6	<i>Gapdh</i>	forward	3	CCA TCA CCA TCT TCC AGG AGC GAG	227bp
		reverse	4.5	GAT GGC ATG GAC TGT GGT CAT GAG	
3	<i>Gig1</i>	forward	8	CAG GAG AGC AGA GAC AGC AC	185bp
		reverse	9	AAT GGC TCA GTC AAT GAA CC	
19	<i>Gnaq</i>	forward	6	CAT GGA GGA GAG CAA AGC AC	178bp
		reverse	7	GGT TCA GGT CCA CGA ACA TT	
7	<i>Hbb-b1</i>	forward	1	CCT GTG GGG AAA GGT GAA C	148bp
		reverse	2	GGC CTT CAC TTT GGC ATT AC	
9	<i>Hmgn3</i>	forward	5	AGG TGC TAA GGG GAA GAA GG	171bp
		reverse	6	GTC CCG AGA GGT ACG TGA AA	



Chr.	Gene symbol	Orientation	Exon	Primer sequence 5'→3'	Prod. size
X	<i>Hprt1</i>	forward	8	GTC AAG GGC ATA TCC AAC AAC AAA C	240bp
		reverse	3	CCT GCT GGA TTA CAT TAA AGC ACT G	
1	<i>Kcnh1</i>	forward	10	ACG CCC TTC AGA AAG TGC TA	182bp
		reverse	11	GTG GTC AGG AGG CAG GAT AA	
3	<i>Mbn1</i>	forward	1	ACG ACC AGA CAC GGA ATG TAA	168bp
		reverse	2	CGC CCA TTT ATC TCT AAC TGT GT	
8	<i>Mmp15</i>	forward	1	CCG AGA TGC AGA GTT TCT ATG G	189bp
		reverse	2	TGA AGG TCA GGT GGT AAT TGT TC	
8	<i>Mt1</i>	forward	1	CTA AGC GTC ACC ACG ACT TC	157bp
		reverse	2	GCA CTT GCA GTT CTT GCA G	
6	<i>Npy</i>	forward	1	GCT CTA TCT CTG CTC GTG TGT TT	175bp
		reverse	2	GTG TCT CAG GGC TGG ATC TCT	
14	<i>Pdhb</i>	forward	9	TCG AAG CCA TAG AAG CCA GT	173bp
		reverse	10	AGG CAT AGG GAC ATC AGC AC	
5	<i>Polr2b</i>	forward	9	CAA GAC AAG GAT CAT ATC TGA TGG	157bp
		reverse	7	AGA GTT TAG ACG ACG CAG GTG	
3	<i>Ppp3ca</i>	forward	1	ATA ACA GAG GGT GCT TCG ATT CT	158bp
		reverse	2	ACA CAC ACC ACC GAC AAG AG	
14	<i>Pxk</i>	forward	16	AAC AGT GAG GAG CAG CCA GT	161bp
		reverse	19	GGT AAT GCT GAA GAC AGT CC	
7	<i>Rab6</i>	forward	8	GCC TTT CTT GCC TCT TCC TTT	244bp
		reverse	8	GCT CAT AGC CTG GAG CTG TC	
7	<i>Rpl13a</i>	forward	8	CAC TCT GGA GGA GAA ACG GAA GG	181bp
		reverse	10	GCA GGC ATG AGG CAA ACA GTC	
2	<i>Slc1a2</i>	forward	9	ACC GAA TGC AGG AAG ACA TC	221bp
		reverse	10	AAT TGG CTG AGA ATC GGG TC	
15	<i>Slc25a17</i>	forward	1	CAT GGC CTC TGT GCT GTC CTA C	139bp
		reverse	2	GAA GCC GAA GTC TAG CAG TAT CCA	
5	<i>Smarcd3</i>	forward	1	CAA TAC TTT TAA CCC TGC GAA GC	154bp
		reverse	2	GTC CAA CTC AAT GAC CAA ACT CT	
19	<i>Spnb3</i>	forward	24	GCC CAG ACC ATC AAA CAA CT	221bp
		reverse	25	TCA CGC TCC TGT ATC CAC TG	
19	<i>Stx3</i>	forward	10	CTT CTA CCA TTG GGG GCA TA	145bp
		reverse	11	TGC CCT GTG TTG TGA GTT TC	
6	<i>Tac1</i> unspecific	forward	1	GGC CAA GGA GAG CAA AGA G	127bp
		reverse	2	ACA GTT GAG TGG AAA CGA GAA	
5	<i>Tmem132d</i>	forward	1	CAT CCC TTC TTC AGC CAG AG	187bp
		reverse	2	AGT GAG AAC CGC TGA ATG CT	
3	<i>Tpd52</i>	forward	3	AGT ATT GGC CGC AAA AGA GA	194bp
		reverse	4	CTG AGC CAA CCG ATG AAA AT	
12	<i>Trib2</i>	forward	1	TCG GGA AAT ACT TAC TGT TGG AG	219bp
		reverse	2	AGC TTC GCT CAA AGA ACA CAT AG	
17	<i>Ttbk1</i>	forward	13	ATC AGT GTG TCC ATG CCT GT	148bp
		reverse	14	ACT GTT TGG GAC GGA GGT C	
18	<i>Ttr</i>	forward	1	CCT CGC TGG ACT GGT ATT TG	121bp
		reverse	2	TTA CAG CCA CGT CTA CAG CAG	
7	<i>Uros</i>	forward	5	TCT GAA AGA CAG ATG GAA TGC C	174bp
		reverse	7	CCA CAC GGA AAG AGA AGA GGC	



Chr.	Gene symbol	Orientation	Exon	Primer sequence 5'→3'	Prod. size
11	<i>Zfp672</i>	forward	1	GTC CTC AAG GTC ACA CAA TTA GTC	207bp
		reverse	2	CAG ACA TGA GTG TAG GGT GCA AG	
6	<i>Tac1</i> specific to splicing variants	forward	3/4	CAA GCG GGA TGC TGA TTC	
		forward	3/5	AAG CGG GAT GCT GGA CAT	
		reverse	5/7	GCC ATT TTG TGA GAG ATC TGG	
		reverse	6/7	CGC TTC TTT CAT AAG CCA CAG	

2.2.5. Assessment of candidate gene functions

Similarly to the candidate genes analyzed by qPCR, for some genes the protein or peptide level, its activity or capability for manipulation was assessed. Also basic metabolic parameters were analyzed in HAB and LAB mice, as many of the ostentatious candidate genes were part of metabolic pathways (many kinase, phosphatase and carrier-coding proteins).

Glyoxalase I (GLO1), as an example was identified to be expressed at different levels between HAB, CD1 and LAB mice, with HAB animals displaying the lowest and LAB mice the highest concentration of the protein, not only in the brain, but even in red blood cells (Kromer *et al.*, 2005; Landgraf *et al.*, 2007). As the present study revealed that this is also true for mRNA expression (not exclusively to the protein), together with the ubiquitous expression differences of some other proteins connected to metabolism, first blood plasma concentrations of lactate and other blood plasma parameters related to metabolism were assessed, followed by a metabolism challenging behavioral manipulation study using CD1 mice to examine the effects of higher calorie intake.

As also different transcript variants for tachykinin 1 (*Tac1*) are known and have been investigated using qPCR, also a subsequent detection and quantification of the peptides encoded by these transcript variants has been performed to investigate how gene expression differences translate into peptide levels.

Furthermore, as many subunits of cytochrome c oxidase (COX) were differentially expressed between HAB and LAB mice in a variety of brain regions, the complete enzyme's activity has been measured in HAB vs. LAB brains to elucidate the effects of differential expression of COX-subunits on overall COX activity. Moreover COX activity also serves as a long-term cellular activity marker as it's a vital part of the enzymatic system forming ATP. Additionally, it has also been demonstrated that a decrease in COX activity is associated with reduced mRNA expression (Christen, 2000; Simonian and Hyman, 1993).



2.2.5.1. Glyoxalase I (GLO1) and metabolic stimulation

As metabolic factors seemed to show differences, first some metabolic and metabolism-related blood plasma parameters were investigated followed by a metabolic manipulation experiment. *Glo1* encodes for a detoxifying enzyme, that eliminates methylglyoxal, a destructive byproduct from the citrate cycle. As reported by a previous study (Kromer *et al.*, 2005) and confirmed in this study, the enzyme is ubiquitously overexpressed in LAB mice, whereas HAB mice rather show a deficit of this enzyme. So, if basic metabolic processes are involved in shaping the anxiety-related phenotype, an artificial imbalance in the metabolic system should influence the behavioral phenotype.

2.2.5.1.1. Metabolism and blood plasma parameters

Characterizing the metabolic system of HAB and LAB mice, first food intake was monitored in single-housed HAB, LAB and CD1 mice aged nine weeks (ten per line), measuring the amount of food in gram (standard diet, Altromin, Lage, Germany), that was consumed over a period of six days.

Blood plasma analysis of ten HAB and nine LAB animals (aged ten weeks each) was performed from trunk blood. Blood was sampled via decapitation of the animals after anesthesia in isoflurane (Forene, Abbott, Wiesbaden, Germany) into EDTA-coated tubes (KABE Labortechnik, Nürnberg-Elsenroth) and immediately centrifuged at 4°C and 400rpm for 10min. Plasma was separated and kept on ice. Blood plasma concentrations of L-lactate, cholesterol, triglycerides, high- (HDL) and low- (LDL) density lipoproteins were assessed using commercially available kits (Roche Diagnostics) according to the manufacturer's instructions.

2.2.5.1.2. Behavioral manipulation via metabolism

44 CD1 mice were purchased from Charles River (Sulzfeld, Germany) aged four weeks and single-housed upon arrival. Bodyweight, food and water consumption were measured every two to three days. After one week habituation time to the new location and housing conditions, water was replaced by an 0.5M saccharose solution for every second mouse, with changing to a fresh saccharose solution every second time of measurement. EPM and OF testing was carried out in these animals aged ten weeks. Three days after testing, six mice per group (treatment vs. control) were sacrificed for blood plasma and urine osmolality analysis with an osmometer (Vogel, Gießen, Germany) as well as for GLO1 protein concentration measurement. Saccharose feeding was continued until all mice were aged 14 weeks with a



repetition of the EPM and OF testing. Then all animals were sacrificed for the analysis of GLO1 protein concentration by Western blot from red blood cells.

2.2.5.1.3. Western Blot analysis of glyoxalase 1 (GLO1)

Required solutions:

4x sample buffer for protein gels

1.25ml	1M Tris; pH = 6.8
4.6ml	20% SDS
0.6g	dithiothreitol DTT
4ml	glycerol (100%)
0.001%	bromphenol blue

Mix and add H₂O to 10ml.

Transfer buffer without SDS

12g	Tris
60g	glycine
800ml	methanol

Mix and add H₂O to 4000ml.

1x TBS

8g	NaCl
2.43g	Tris
0.05ml	Tween 20

Mix and add H₂O to 1000ml.

100µl of red blood cells, settling at the bottom of EDTA-coated tubes after centrifugation, have been transferred to 15ml tubes and washed three times in 1xPBS (phosphate buffered saline). After centrifugation at 2,500rpm at 4°C for 5min, the supernatant was removed. Then samples were kept at -80°C until further processing. Pellets were then transferred to 1.5ml tubes and 400µl of cold water containing 1mM PMSF (phenylmethanesulphonyl-fluoride) as a protease inhibitor were added. After centrifugation, the supernatant was transferred to a fresh tube. For protein quantification by Bradford protein assay 1:100 dilutions were prepared. Concentrations were assessed by calculation to a standard curve based on bovine serum albumin (BSA). Concentrations (i.e. optic density) were assessed in 96-well microtiter plates in an ELISA reader *Dynatech MR5000* (Dynatech Laboratories, Denckendorf, Germany) at 595nm wavelength.

100µg of total protein mixed with 5µl of 4x sample buffer and the volume filled up to 25µl with water were loaded to a combined stacking and separating polyacrylamide gel that was prepared in a gel pouring frame by Bio-Rad (Bio-Rad, Hercules, CA).



Gels were electrophorized at 150V for 45min in 1xTGS (Tris/glycine/SDS) buffer (Stock 10xTGS, Bio-Rad). Before blotting to the polyvinylidene difluoride (PVDF) membrane, the membrane was briefly incubated in methanol and in water then the transfer chambers were laid into transfer buffer. On layers of sponges and filter paper, first the polyacrylamide gel was placed onto the black side (negative pole) and covered with the PVDF membrane. Transfer to PVDF membrane was performed in the blotting apparatus (Criterion blotter, Bio-Rad) at 100V for 1h with water cooling and changing of cooling packs after 30min). Membranes were blocked with 5% milkblock (2.5g milk powder + 50ml TBS-T) at 4°C overnight on a shaker. After rinsing them in TBS-T, they were incubated with an anti-glyoxalase-I antibody (10µl/30ml TBS-T plus 5% milk powder; the antibody was kindly provided by Dr. Kenneth Tew, Fox Chase Cancer Center, Philadelphia, PA) for 2h at room temperature on a shaker. The membranes were washed five times with water, then about three times for 15min with TBS-T followed by the incubation with the secondary antibody protein A horseradish peroxidase from Amersham Biosciences (1µl/10ml TBS-T) for about 40min and shaken at room temperature. Again membranes were washed five times in water, then for 1h in TBS-T with changing to a fresh solution every ten minutes. Finally the membranes were incubated in ECL+ solution (Amersham Biosciences) for 5min and fixed in a film cassette. Before developing, the film (ECL Film, Amersham Biosciences) was placed in ruby light on the membranes for 5min. Films were scanned, signal intensity of the GLO1 bands was determined using the Scion Image software (Alpha 4.0.3.2; Scion, Frederick, MD).

2.2.5.2. Tachykinin 1 (*Tac1*) encoded peptide quantification

Required solutions (all data on percentage is volume-based):

Solvent A:

100% 50mM potassium phosphate buffer, pH=2.5

Solvent B:

70% acetonitril

30% 37mM potassium phosphate buffer, pH=2.5

PBS-T:

99.05% 1x phosphate buffered saline (PBS), pH=7.2

0.05% TWEEN 20

Blocking buffer:

3% BSA

96.98% PBS-T



0.02% sodium azide

Based on the qPCR results, the following question was how the differential expression of single splicing variants translates into peptide levels. Therefore high performance liquid chromatography (HPLC) was applied to first separate fractions with the respective peptides and then to identify them in an enzyme-linked immunosorbent assay (ELISA) with an antibody specific for the last five amino acids of tachykinin peptides.

Brains of female HAB, CD1 and LAB mice (twelve each) were harvested, the PVN and BLA/LA were dissected as described in chapter 2.2.2.1. For peptide extraction, tissue punches were lysed in 50µl of boiling 5% acetic acid by gentle shaking at 95°C for 30min in a thermomixer (5436, Eppendorf, Hamburg, Germany). After chilling the samples on ice for 10min, samples were sonified (Sonifier Cell Disruptor B15, Branson Ultrasonics, Danbury, CT) using 15 impulses twice and frozen at -80°C overnight. Then, lysed tissue was centrifuged at 4,000rpm and 4°C for 20min after thawing on ice, the supernatant was separated and centrifuged again under the same conditions for 10 min. Again only the supernatant was kept and concentrated to a volume of 12µl at 45°C (Concentrator 5301, Eppendorf). For reversed phase HPLC (rpHPLC), all instruments (HPLC Series 1100) were manufactured by Agilent Technologies (Böblingen, Germany) and used with C-18 columns (EC550/2 Nucleosil 300-5 C18, Macherey-Nagel). For fractioning of the samples a gradient protocol was applied (see table 2). Specific elution time for each peptide was determined by analysis of 5µg of each peptide and a mixture of 0.2µg of each peptide (SP, NKA, NKB, NPK and NPγ) in a solution of 12µl 5% acetic acid. Details of the elution protocol are documented in table 3 with the respective fractions sampled.

Table 2: The gradient protocol of solvents for rpHPLC fractioning of peptide extractions from the BLA/LA and the PVN.

Step	Time [min]	Solvent A	Solvent B	Flow rate µl/min
1	0	100%	0%	200
2	10	72%	28%	200
3	70	43%	57%	200
4	75	0%	100%	200
5	76	100%	0%	200
6	96	100%	0%	50



Table 3: Elution protocol of tachykinin peptides during rpHPLC. Not further required fractions, like from steps 2 or 8 were discarded later.

Step	Time [min]	Elution period [min]	Total elution volume [μ l]	Peptide
1	18.5	3	600	NP γ
2	21.5	2	400	
3	23.5	3	600	NKA
4	26.5			
5	29	6	1200	SP
6	35			
7	40	5	1000	NPK
8	45	2	400	
9	47	5	1000	NKB
10	52	4	1200	X

Further processed samples were transferred from U96 MicroWell plates (Nunc, Wiesbaden, Germany) to 1.5ml tubes and concentrated to a volume of 5 μ l.

ELISA was prepared and performed on F96 Immobilizer Amino plates (Nunc), with measuring one standard curve for each peptide in eleven concentrations from 2 to 400 pg/ μ l. Samples were diluted to a total volume of 100 μ l in sodium carbonate buffer (100mM, pH=9.6), sealed and incubated overnight at 4°C under gentle shaking (Polymax 1040, Heidolph Instruments, Schwabach, Germany). After washing all wells three times with 200 μ l PBS-T, plates were sealed and incubated for 5h at 4°C on a shaker with 300 μ l blocking buffer in each well. After incubation, samples were washed with 200 μ l PBS-T each and incubated overnight at 4°C on a shaker with 100 μ l of a 1:700 dilution of the primary antibody (rat monoclonal [NC1/34 HL] to substance P, Abcam, Cambridge, UK) in blocking buffer. Samples were subsequently washed four times in 200 μ l PBS-T and incubated in 100 μ l of a 1:1000 dilution of the secondary antibody (goat polyclonal to rat IgG – H&L AP; Abcam) in blocking buffer for 4h at 4°C on a shaker. Washing was repeated four times and incubation with 100 μ l of an alkaline phosphatase chromogen, p-nitrophenyl phosphate (pNPP, 1 μ g/ μ l) followed. Optic density was assessed after 20, 30, 40 and 60min after addition of pNPP in the Dynatech MR5000 ELISA reader. Blank value means were subtracted from each individual value per plate, individual values per plate were normalized based on control measurements on each plate. Based on the standard curves for each peptide, absolute quantity of material [mol] could be calculated.



2.2.5.3. Cytochrome c oxidase (COX) activity

Required solutions:

0.1M phosphate buffer pH 7.4:

22.8g NaH₂PO₄

115g Na₂HPO₄

add H₂O to 2000ml.

4% PFA (paraformaldehyde):

Dilute 20% paraformaldehyde to 4% with 0.1M phosphate buffer

Cytochrome c / DAB solution:

140mg 3,3-diaminobenzadine (DAB)

50mg cytochrome c

11.11g saccharose

50mg nickel ammonium sulfate

50ml 0.1M phosphate buffer

Brains of six basal HAB and LAB mice each were prepared as described before in 2.2.2.1. Brains were sectioned to 40µm slices, with keeping the same sections as in 2.2.2.1. Microscope slides containing the brain sections were stained during incubation for 2h at 37°C in the cytochrome c / DAB solution, protected from light and under mild shaking. Brains were then washed for 10min in 0.1M phosphate buffer on ice, followed by fixation for 30min in 4% PFA. Then washing was continued by washing the slides twice in 0.1M phosphate buffer for 5min, in 50% ethanol for 1min, in 70% ethanol for 1min, in 96% ethanol for 1min followed by 5min in isopropanol and finally by 10min in Roti-Histol (Roth). Slices were embedded in Roti-Histokitt (Roth) and covered by cover slips. Slides were captured using a binocular camera system with the same settings for all slides (Leica). Quantification of each slide was performed using Scion Image.

2.3. Identification of polymorphisms

Most studies on mouse genetics focus on mice from inbred strains. They are supposed to have the same genetic configuration and the only thing differing between individuals is probably their hierarchical status, if they are not single-housed. Nevertheless, even these mice acquire different experiences during their development and interpret similar stimuli as more or less pleasant or harmful. The other advantage of studying inbred mice is that there is a lot known about variations occurring in the genes of these mouse strains. About 25,000 SNPs are known to exist if a variety of inbred strains is compared only on a middle-sized chromosome like chromosome 10 (MGD).



Unfortunately less is known about the occurrence of polymorphisms and other variations in outbred mouse strains. Although their frequency would be lower, as compared to wild mice, up to date, nearly no information about their genetic variability is available (Chia *et al.*, 2005). Therefore, a better genetic characterization of outbred stocks is urgently needed, with the following experiments contributing to this issue. However, as the focus of the present experiments lies on the genetic background of anxiety-related behavior, the main interest was to identify genetic polymorphisms in a variety of candidate genes that are associated with the anxiety-related phenotype.

2.3.1. Animals and behavioral tests

For SNP screenings, i.e. the determination of the frequency of polymorphisms, animals used were unselected male (N = 77) and female CD1 (N = 165) mice, 16 male and female HAB and LAB mice (the grandparental generation of the HABxLAB F2 intercross mice), 18 male and female heterozygous HABxLAB F1 intercross mice (referred to as F1) and 521 male HABxLAB F2 intercross mice (referred to as F2). These mice have been phenotyped (except for the female CD1 mice) in a broad test battery, including EPM and TST.

DNA samples from two HAB and LAB mice from G18 or higher were used for the detection of polymorphisms by sequencing, as they don't show all the variation in CD1 mice, but represent the variation responsible for the phenotypic variance. For most genomic variations, they should have a homozygous state and are therefore easy to detect.

2.3.2. DNA isolation

required reagents:

Tail buffer:

20ml	20xTris; pH = 8
80ml	0.5M EDTA
8ml	5M NaCl
20ml	20% SDS
Mix and add H ₂ O to 400ml.	

TE buffer:

1.21g	Tris; pH = 8
0.37g	EDTA
Mix and add H ₂ O to 1000ml.	



DNA was isolated from mouse tail tips (about 6mm) were sampled after euthanasia of the animals. Tail tips were kept on -20°C until DNA isolation. For DNA isolation the NucleoSpin Tissue (Macherey-Nagel) kit was applied according to the manufacturer's instructions. Alternatively, for smaller sample amounts (e.g. for sequencing), DNA was isolated from the tail tips by starting with a digestion by adding 10µl of proteinase K (20mg/ml) and 700µl of tail buffer to the tail tips and incubating them at 56°C in a thermo-shaker (Eppendorf) for 3h. After vortexing, 300µl of a saturated NaCl solution (7M) were added to the samples that were vigorously shaken afterwards and centrifuged at 13,000rpm for 10min. 750µl of supernatant were transferred to fresh tubes and 500µl of isopropanol were added. Then samples were mixed again manually and centrifuged for 5min at 13,000rpm followed by one wash step with 500µl of 70% ethanol. After a final centrifugation step at 13,000rpm for 5min, all liquid was removed and the pellets were dried at 65°C for 5-10min. Then pellets were dissolved in 100µl of TE buffer and DNA quantity and quality were assessed by photometric measurement (Nanophotometer, Implen or Ultrospec II, Pharmacia LKB Biochrom, Cambridge, United Kingdom).

2.3.3. Prescreening

To receive an overview of SNPs available as specific markers for HAB and LAB mice that would further provide the basis of genotype-phenotype associations in F2 mice, 16 male and female HAB and LAB mice, 18 F1 and 34 F2 mice were genotyped. For SNPs, where HAB and LAB mice would show the opposite genotype homozygously (AA vs. BB), F1 mice should show only a heterozygous genotype (AB), for biallelic markers. To assess a large number of SNPs, the Mouse Medium Density Linkage Panel (Illumina) was chosen to allow the determination of 1449 genotypes simultaneously. DNA samples were all prepared in 96 well plates (Nunc) and diluted to a concentration of 50ng/µl. Random inspection of every tenth sample on agarose gel was performed to ensure DNA quality and quantity. Samples were processed according to the manufacturer's instructions as described in the Illumina Golden Gate Assay for Sentrix Array Matrix workflow sheets. After purification and sequence amplification, samples were hybridized from a 96-well plate to probes placed on top of fiber bundles (Fig. 3).

ATGCTCGCCAGGA
TACGAGCGGTCCT

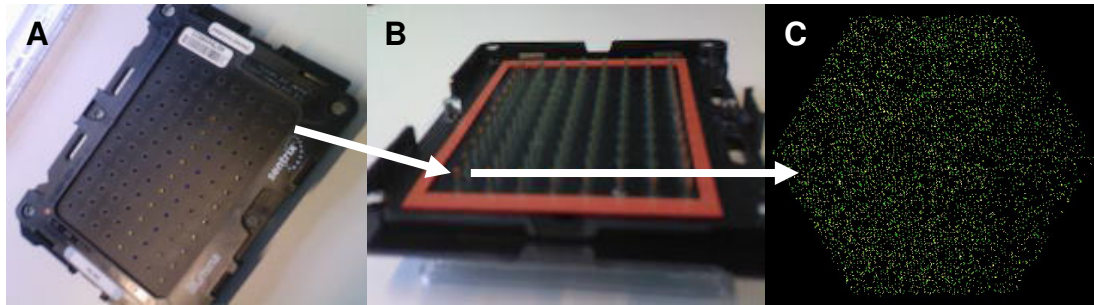


Figure 3: Illumina Sentrix Array Matrix (for GoldenGate Assay). **(A)** The upper side of the array matrix, this side is scanned. **(B)** Bottom side of the array matrix, probes were fixed here and the samples hybridized. **(C)** Scan picture of one fiber bundle.

Fluorescence signals of hybridized samples were captured in the Illumina BeadStation, genotypes were called from fluorescence intensity clusters using the Illumina BeadStudio software Ver. 3.1.0.0, with the genotyping module Ver. 3.1.12. All intensity clusters were inspected individually and adjusted manually, if necessary. Analysis of genotypes focused on the detection of valid genotypic SNP markers to distinguish between HAB and LAB mice.

2.3.4. Screening of the F2 panel and CD1 mice

Based on the prescreening experiment (as described in chapter 2.3.3.) a custom designed oligo pool (384 SNPs) was set up for genotyping all 521 F2 mice, 32 HAB and LAB mice as well as 77 CD1 mice, to receive further insight into the distribution of genotypes in unselected outbred CD1 mice, i.e. the progenitors of the HAB and LAB lines. The custom designed oligo pool was designed to work on the Illumina GoldenGate Assay-based Sentrix Array Matrix 250 SNPs were added, which were identified in the screening from the previous chapter (table 2). Two further polymorphisms have been identified between HAB and LAB mice, resulting in qualitative differences in the enzyme enolase-phosphatase 1 (coding gene is referred to as *Enoph1*) by 2D-gel electrophoresis (Ditzen *et al.*, submitted). Furthermore, two polymorphic loci around the *Avp* locus (see chapter 2.5.2.3 and the results) were added for detection by the customer designed oligo pool. As about 130 slots were still available for SNPs, the loci to analyze were recruited from 10kbp around candidate genes from the MPI24K gene expression analyses or from other research groups of the Max Planck Institute of Psychiatry focusing on human anxiety and depression patients (Ising, Erhardt and Binder, personal communication). Putative SNPs were selected from MGD and are also displayed in table 4. All samples were processed and analyzed as described in chapter 2.3.3.



Table 4: Single nucleotide polymorphisms (SNP) to test with the custom designed oligo pool. Source (1) refers to SNPs, taken from the Medium Density Linkage Panel, (2) described added SNPs based on genes known from gene expression studies or from research groups of the Max Planck Institute of Psychiatry focusing on human anxiety and depression patients. Gene association is assumed, if a SNP is located 10kbp around a gene locus.

Source	SNP identifier	Chr.	Position [bp]	Associated gene
1	mCV23695025	1	22,398,088	-
1	mCV24784983	1	25,476,000	<i>Bai3</i>
1	rs3677683	1	27,321,156	-
1	rs4137502	1	30,887,618	<i>Phf3</i>
1	rs3707642	1	32,568,345	<i>Khdrbs2</i>
1	rs3683997	1	35,935,818	-
1	rs13475827	1	40,990,938	-
1	CEL-1_44668113	1	44,620,787	-
1	rs13475881	1	58,439,402	-
1	rs13475919	1	73,020,555	-
2	Rs30238170	1	82,719,300	-
2	rs30238169	1	82,720,355	<i>5230400G24Rik</i>
2	rs30238168	1	82,720,980	<i>5230400G24Rik</i>
2	rs30237262	1	82,722,282	<i>5230400G24Rik</i>
2	rs30236408	1	82,726,579	<i>5230400G24Rik</i>
2	rs30242174	1	82,749,582	-
1	UT_1_89.100476	1	87,014,950	<i>Chrnd</i>
1	rs13476012	1	101,,801,487	<i>Cntnap5b</i>
1	CEL-1_103251925	1	103,228,922	-
1	rs3685919	1	111,528,321	-
1	rs13476050	1	112,508,292	-
1	rs3699561	1	132,988,758	<i>Mapkapk2</i>
1	rs3672697	1	147,028,489	-
1	rs13476163	1	148,717,645	<i>B830045N13Rik</i>
1	rs6393307	1	152,872,095	-
1	rs13476187	1	156,052,564	<i>ENSMUSG00000066797</i>
1	rs6157620	1	185,385,733	-
1	rs3667164	1	190,511,531	<i>Ush2a</i>
1	rs6240512	2	10,900,065	<i>100040690</i>
1	CZECH-2_15618849	2	15,594,129	-
1	rs13476366	2	19,320,592	-
1	rs13476503	2	53,042,643	<i>Prpf40a</i>
1	rs4223189	2	61,638,140	<i>Psmc14</i>
1	rs3664661	2	71,436,620	-
1	CEL-2_73370728	2	73,174,311	-
1	rs13476639	2	92,666,968	-
1	rs6406705	2	100,200,136	-
1	rs13476666	2	101,163,197	-
1	rs13476689	2	107,305,294	-
1	rs13476723	2	117,118,533	<i>Rasgrp1</i>
2	chlcdelavp2	2	130,273,975	<i>Avp</i>
2	cmlicsnpavp1	2	130,276,153	<i>Avp</i>
1	rs13476783	2	133,686,867	-
1	rs3664408	2	161,205,958	-
1	CEL-2_168586738	2	168,032,354	<i>Nfatc2</i>
2	rs31438972	3	19,586,067	<i>Trim55</i>
2	rs31145247	3	19,586,366	<i>Trim55</i>
2	rs30796162	3	19,597,491	-



Source	SNP identifier	Chr.	Position [bp]	Associated gene
2	rs31286319	3	19,598,902	-
1	rs13477043	3	31,379,500	-
1	gnf03.030.222	3	32,722,005	-
1	rs6376008	3	86,465,169	<i>Lrba</i>
1	rs6211610	3	90,025,782	<i>Rab13</i>
1	rs13477268	3	93,138,727	-
1	rs4138887	3	102,493,088	-
1	CEL-3_120379605	3	118,794,515	-
1	rs13477379	3	122,540,626	<i>Pde5a</i>
1	rs3671119	3	126,116,580	<i>Arsj</i>
2	rs13477411	3	131,922,067	-
2	rs6166189	3	132,079,726	-
2	rs31556559	3	132,298,496	<i>EG433653</i>
2	rs30263909	3	132,299,981	<i>EG433653</i>
1	rs3676039	3	135,880,574	<i>Bank1</i>
1	rs6407142	3	142,720,843	-
1	gnf03.160.599	3	156,149,851	<i>Negr1</i>
2	rs3022975	4	8,073,046	<i>Car8</i>
1	CEL-4_30653207	4	30,606,147	-
2	rs3090720	4	57,221,105	<i>Ptpn3</i>
1	rs3708471	4	76,516,632	<i>Ptprd</i>
1	rs13477873	4	101,102,850	<i>Ak3l1</i>
2	rs3022996	4	111,044,395	<i>4931433A01Rik</i>
1	rs3023025	4	142,772,319	<i>Prdm2</i>
1	rs13478110	5	9,741,228	-
1	rs3714258	5	12,371,157	-
1	rs6341620	5	37,492,799	<i>Jakmip1</i>
1	CEL-5_45872918	5	46,008,170	-
1	rs3664008	5	54,048,319	<i>Rbpj</i>
1	mCV23386455	5	62,987,260	<i>Tbcd1d</i>
1	rs3667334	5	83,471,068	-
1	rs13459087	5	87,521,105	<i>Ugt2b36</i>
1	CEL-5_87173557	5	88,825,844	<i>Amtn</i>
1	gnf05.084.686	5	89,982,732	<i>Npffr2</i>
1	rs3673049	5	90,116,719	<i>Adamts3</i>
2	rs31780700	5	92,889,948	<i>Scarb2</i>
2	rs29583970	5	92,983,999	-
2	rs31786987	5	93,102,064	<i>4932413O14Rik</i>
1	rs3661241	5	98,266,375	-
2	rs13460000	5	100,488,240	<i>Enoph1</i>
2	rs13460001	5	100,490,027	<i>Enoph1</i>
1	rs13478433	5	104,357,982	-
1	rs13459186	5	110,534,259	<i>Gtpbp6 / Plcx1d</i>
1	rs13478483	5	118,405,617	<i>Nos1</i>
1	rs13478518	5	128,264,975	<i>Tmem132d</i>
2	rs33711358	5	128,515,999	<i>Tmem132d</i>
2	rs13478520	5	128,616,797	<i>Tmem132d</i>
1	rs6298689	5	140,240,607	<i>Ints1</i>
2	rs36247439	5	149,857,285	<i>Hmgb1</i>
2	rs29781244	5	149,862,877	<i>Hmgb1</i>
2	rs33343556	5	149,865,874	-
2	rs36309698	5	149,868,499	-
2	rs37452785	5	149,868,789	-



Source	SNP identifier	Chr.	Position [bp]	Associated gene
2	rs30116240	6	7,499,262	-
2	rs30221186	6	7,503,288	<i>Tac1</i>
2	rs30206506	6	7,512,626	<i>Tac1</i>
2	rs30771076	6	7,512,775	<i>Tac1</i>
1	rs3655269	6	17,922,618	-
1	rs13478649	6	18,518,251	-
1	rs13478656	6	21,893,927	-
1	rs3684494	6	24,365,693	-
1	rs13478697	6	32,800,650	<i>Chchd3</i>
1	rs4139698	6	49,819,544	-
2	rs13478762	6	54,175,671	<i>Chn2</i>
2	rs30228387	6	54,224,143	<i>Chn2</i>
1	rs3672029	6	75,345,665	-
1	rs6285738	6	93,485,969	-
1	rs6239023	6	94,005,991	<i>Magi1</i>
1	rs6349084	6	96,697,598	-
1	rs6339546	6	133,917,751	-
1	rs13479053	6	134,201,252	<i>Etv6</i>
1	rs3672808	6	139,805,730	<i>Pik3c2g</i>
1	rs3711088	6	148,260,469	<i>Tmtc1</i>
1	rs3659551	7	6,909,503	<i>Usp29</i>
1	mCV23738426	7	8,465,811	<i>Vmn2r52</i>
1	CEL-7_5627457	7	12,296,204	-
2	rs32116079	7	19,147,099	<i>Psg27</i>
2	rs13461382	7	19,591,025	<i>Irf2bp1</i>
2	rs31505570	7	19,721,049	<i>Fbxo46</i>
1	CEL-7_36725559	7	43,396,959	-
1	rs4232449	7	48,581,740	-
2	rs31525495	7	53,894,287	<i>Sergef</i>
2	rs31708001	7	53,903,710	<i>Tph1</i>
2	rs32373825	7	53,904,154	<i>Tph1</i>
2	rs6279417	7	53,931,049	-
2	rs6279463	7	53,931,082	-
2	rs6281625	7	53,931,473	-
1	rs6160140	7	73,426,174	<i>Lrrk1</i>
1	rs3705155	7	75,667,606	-
1	rs13479347	7	83,432,559	-
1	rs13479355	7	85,431,231	<i>Ntrk3</i>
1	rs13479358	7	86,843,104	<i>5730590G19Rik</i>
2	rs31060727	7	107,753,415	<i>Mrpl48</i>
2	rs32330100	7	107,755,420	<i>Mrpl48 / Rab6</i>
2	rs32034601	7	107,756,141	<i>Mrpl48 / Rab6</i>
2	rs31746209	7	107,758,176	<i>Rab6</i>
2	rs31908266	7	107,771,055	<i>Rab6</i>
2	rs32020539	7	107,791,025	<i>Plekhh1</i>
1	rs3713052	7	108,918,190	<i>Clpb</i>
1	rs6357312	7	109,389,815	<i>Rhog</i>
2	rs13479460	7	118,818,343	<i>Galnt14</i>
1	rs6194926	7	121,509,575	<i>4933406I18Rik</i>
1	CEL-7_115892950	7	122,464,255	<i>Rgs10</i>
1	CEL-7_122752866	7	129,495,978	<i>Dock1</i>
1	rs13479506	7	131,822,778	<i>3100003L05Rik</i>
1	rs3682038	7	133,483,665	-



Source	SNP identifier	Chr.	Position [bp]	Associated gene
1	rs13479535	7	138,763,317	-
1	rs3663988	7	146,505,067	-
1	CEL-8_33812776	8	33,652,415	<i>Tnks</i>
2	rs33319598	8	54,406,484	-
2	rs32893761	8	54,441,823	-
2	rs32900718	8	54,584,421	-
2	rs37502172	8	54,664,031	-
1	rs3707439	8	61,429,008	-
1	rs13479807	8	68,141,750	<i>Mar1</i>
1	rs13479811	8	69,577,205	-
1	rs13479871	8	87,590,219	<i>Fbxw9</i>
1	rs6257357	8	88,071,460	<i>Dnaja2</i>
1	rs13479880	8	89,271,028	<i>ENSMUSG00000074178</i>
1	rs13479884	8	90,183,245	-
1	gnf08.108.032	8	106,104,093	<i>Tmco7</i>
1	gnf08.118.027	8	116,136,203	-
1	rs6400423	8	129,106,325	-
2	rs3697596	8	130,354,209	-
1	mCV25073238	9	10,596,883	-
1	gnf09.012.310	9	17,874,218	-
1	rs13480092	9	18,926,807	<i>Olfr836</i>
1	rs3088801	9	24,802,456	-
1	rs4135590	9	42,796,186	<i>Arhgef12</i>
1	rs13480173	9	46,336,655	-
1	rs3676124	9	83,013,939	<i>Hmgn3</i>
1	rs3669564	9	87,780,386	-
1	rs3711089	9	105,393,993	<i>Atp2c1</i>
1	rs13480421	9	111,761,261	-
1	rs6320810	9	115,065,092	<i>Osbpl10</i>
1	rs3669563	9	117,827,882	-
1	rs13459114	9	121,825,029	<i>Cyp8b1</i>
1	rs13459119	10	20,045,489	<i>Bclaf1</i>
1	rs3679120	10	22,641,085	-
1	rs13480581	10	38,685,357	<i>Lama4</i>
2	rs3090642	10	44,860,993	<i>Prep</i>
1	rs13480630	10	67,283,841	-
1	rs13480638	10	68,907,415	-
2	rs29326309	10	95,590,622	-
2	rs13480738	10	102,999,447	-
2	rs13480739	10	103,185,336	-
1	rs13480740	10	103,515,832	-
2	rs6282517	10	103,725,176	-
1	rs3688351	10	103,953,112	-
2	rs13480742	10	103,966,226	-
2	rs13480743	10	104,097,543	-
2	rs13480744	10	104,441,816	<i>100042383</i>
2	rs13480749	10	105,437,651	-
1	rs6243755	10	108,174,849	<i>Syt1</i>
1	rs13480773	10	114,179,165	<i>Trhde</i>
2	rs6350239	10	114,513,832	<i>Tph2</i>
2	rs4228474	10	114,515,997	<i>Tph2</i>
2	rs29341895	10	114,624,510	-
2	rs29354500	10	114,624,607	-



Source	SNP identifier	Chr.	Position [bp]	Associated gene
2	rs29327697	10	114,625,405	-
1	mCV24217147	10	117,503,347	<i>Smgp21b</i>
1	rs13480803	10	122,568,425	<i>Usp15</i>
1	mCV22832306	10	125,997,604	-
2	rs3697243	10	126,250,067	-
1	rs13480836	11	3,454,200	-
1	rs6190775	11	6,312,209	-
1	gnf11.017.294	11	18,007,065	-
1	rs3723987	11	19,368,928	-
2	rs13480933	11	29,118,539	<i>Smek2</i>
2	rs26822202	11	29,122,316	<i>Ccdc104</i>
2	rs29469152	11	29,122,634	<i>Ccdc104</i>
2	rs29473241	11	29,147,356	<i>Ccdc104</i>
2	rs26822189	11	29,147,449	<i>Ccdc104</i>
2	rs29410558	11	29,149,274	-
1	rs13459123	11	30,958,902	<i>Asb3</i>
2	rs26950069	11	58,126,592	<i>Zfp692</i>
2	rs29402173	11	58,128,820	<i>Zfp672</i>
2	rs29406291	11	58,129,646	<i>Zfp672</i>
2	rs29387701	11	58,138,073	<i>1700047K16Rik</i>
2	rs29427167	11	58,138,512	-
2	rs29397704	11	58,140,748	-
1	rs3697686	11	58,381,052	<i>Olfr327-ps1</i>
1	rs3711357	11	61,266,066	<i>Zfp179</i>
1	rs13481061	11	62,806,119	<i>Cdrt4</i>
1	rs13481071	11	65,014,320	<i>Myocd</i>
2	rs26888740	11	74,739,049	<i>Smg6 / Srr</i>
2	rs26888739	11	74,739,210	<i>Smg6 / Srr</i>
2	rs26888734	11	74,740,289	<i>Smg6</i>
2	rs6192434	11	74,745,116	<i>Smg6</i>
2	rs29479272	11	74,978,579	<i>Hic1</i>
2	rs6155957	11	74,978,877	<i>Hic1</i>
2	rs28226774	11	76,806,816	-
2	rs28226773	11	76,806,890	-
2	rs28226748	11	76,840,125	<i>Slc6a4</i>
2	rs28226747	11	76,840,970	<i>Slc6a4</i>
2	rs28226743	11	76,841,856	<i>Slc6a4</i>
2	rs28226734	11	76,846,429	-
1	rs13481119	11	79,360,701	<i>Nf1</i>
1	rs13481161	11	92,322,572	-
1	rs13481313	12	14,876,064	-
1	rs13481321	12	16,687,164	<i>Greb1</i>
1	rs13481371	12	30,883,465	<i>Sntg2</i>
1	rs6223000	12	34,867,610	-
1	rs13481445	12	51,443,486	<i>Prkd1</i>
1	rs3677344	12	65,698,044	-
1	rs13481541	12	77,479,299	<i>Zbtb1</i>
1	rs3662628	12	80,362,465	<i>Zfyve26</i>
1	rs13481556	12	81,763,540	<i>Slc39a9</i>
1	rs13481588	12	93,207,169	<i>EG667589</i>
1	rs3023711	12	117,417,767	-
2	rs3692361	12	118,957,587	<i>Rapgef5</i>
1	rs13481673	13	5,584,894	-



Source	SNP identifier	Chr.	Position [bp]	Associated gene
1	rs6348604	13	15,502,938	-
1	rs13481706	13	16,432,650	-
1	rs3710348	13	31,365,187	-
1	rs3688207	13	45,454,657	-
2	rs13462828	13	62,915,954	-
2	rs30073403	13	63,213,965	<i>2010111101Rik</i>
2	rs29584318	13	63,383,551	<i>2010111101Rik</i>
2	rs29636134	13	63,405,500	<i>Fancc</i>
1	rs13481871	13	71,432,597	-
1	rs3686443	13	86,662,750	-
1	rs3655061	13	89,723,142	<i>Hapln1</i>
1	rs13481961	13	98,040,192	-
1	rs4230144	14	8,924,022	<i>Rpp14</i>
1	rs6322899	14	10,651,880	<i>Fhit</i>
1	rs6290836	14	13,378,532	<i>Cadps</i>
2	rs3696385	14	18,195,504	-
1	rs13482104	14	27,163,606	-
1	rs6396829	14	28,814,149	<i>Erc2</i>
1	gnf14.055.608	14	55,370,255	<i>Mipep</i>
2	rs3703075	14	63,543,436	<i>Wdfy2</i>
2	rs13459144	14	76,317,480	<i>Gtf2f2</i>
1	rs13482327	14	97,600,347	-
2	rs3692362	14	100,175,288	-
1	rs6191117	14	100,606,904	-
1	rs3708779	14	111,167,655	<i>EG668772</i>
1	rs13482375	14	112,079,790	<i>Slitrk5</i>
1	rs6169105	14	117,657,346	<i>Gpc6</i>
1	rs13459176	15	3,229,130	<i>Sepp1</i>
1	CEL-15_9687257	15	9,601,488	-
1	rs13482431	15	11,241,219	<i>Adamts12</i>
1	rs3715857	15	19,181,733	-
1	rs13482509	15	31,971,924	-
2	rs32005588	15	32,841,248	-
2	rs31983176	15	32,849,387	<i>Sdc2</i>
2	rs32228111	15	32,858,088	<i>Sdc2</i>
2	rs32250555	15	32,874,418	<i>Sdc2</i>
2	rs4230687	15	32,964,635	<i>Sdc2</i>
2	rs3695416	15	38,414,152	-
1	rs3683326	15	41,219,409	-
1	rs6400804	15	56,637,987	-
2	rs36320059	15	81,147,953	<i>Slc25a17</i>
2	rs37939180	15	81,148,568	<i>Slc25a17</i>
2	rs37394767	15	81,148,663	<i>Slc25a17</i>
2	rs38717462	15	81,151,100	<i>Slc25a17</i>
2	rs36586819	15	81,167,126	<i>Slc25a17</i>
2	rs36346494	15	81,192,154	-
2	rs32320164	15	83,392,328	<i>Tspo</i>
2	rs31717709	15	83,393,007	<i>Tspo</i>
2	rs32046139	15	83,399,802	<i>Tspo</i>
2	rs31565634	15	83,400,032	<i>Tspo</i>
2	rs31717505	15	83,406,204	<i>Till12</i>
1	rs13482712	15	92,076,446	<i>Cntn1</i>
1	rs4152638	16	4,326,609	<i>Adcy9</i>



Source	SNP identifier	Chr.	Position [bp]	Associated gene
1	rs4152790	16	4,850,158	<i>4930562C15Rik</i>
1	rs4173902	16	37,352,904	<i>Stxbp5l</i>
1	rs4177651	16	40,683,387	-
2	rs3696661	16	51,676,815	-
1	rs4197150	16	66,296,803	-
1	rs3718160	16	76,867,900	-
1	rs6317052	16	79,493,030	-
1	rs4211364	16	80,830,317	-
1	rs3672065	17	14,336,401	<i>Dact2</i>
1	rs3726555	17	16,539,606	-
1	rs13482899	17	17,761,307	<i>Lnpep</i>
1	rs13482914	17	20,982,760	<i>V1re8</i>
2	rs3696835	17	22,818,022	<i>ENSMUSG00000046088</i>
2	rs3693494	17	29,917,069	-
2	rs33798776	17	30,661,307	<i>Btbd9</i>
2	rs33800126	17	30,695,419	-
2	rs33798569	17	30,702,010	-
2	rs33797503	17	30,703,669	-
2	rs30778922	17	30,809,092	<i>Dnahc8</i>
2	rs3145477	17	30,814,214	<i>Dnahc8</i>
1	rs6298471	17	36,684,410	<i>H2-M11</i>
1	rs6272475	17	53,622,040	<i>Rab5a</i>
1	rs3714226	17	55,409,410	-
1	rs3715723	17	58,810,428	-
1	rs3675634	17	71,590,806	<i>Lpin2</i>
2	rs33372832	17	74,733,598	-
2	rs33595841	17	74,733,692	-
2	rs33340320	17	74,733,758	-
2	rs13465627	17	74,787,631	<i>Spast</i>
2	rs33394982	17	74,790,564	-
1	rs6229946	17	75,590,536	<i>Ltbp1</i>
1	rs13483157	17	89,287,847	-
1	rs6397044	17	93,594,172	-
1	rs13483183	18	3,516,539	<i>Bambi</i>
1	gnf18.001.688	18	4,647,835	-
2	rs30263474	18	20,822,913	<i>Ttr</i>
2	rs31313820	18	20,822,943	<i>Ttr</i>
2	rs6273344	18	20,825,921	<i>Ttr</i>
2	rs31315882	18	20,830,086	<i>Ttr</i>
1	rs13483271	18	29,116,312	-
2	rs29540760	18	31,595,494	<i>Syt4</i>
2	rs29551386	18	31,598,369	<i>Syt4</i>
2	rs30031611	18	31,600,912	<i>Syt4</i>
2	rs30133602	18	31,683,612	<i>EG383420</i>
2	rs29823717	18	31,699,317	-
2	rs30303190	18	31,703,097	-
1	rs3718586	18	33,291,841	<i>Camk4</i>
1	rs3658163	18	68,820,968	-
1	rs6161154	18	71,609,676	<i>Dcc</i>
1	rs4137441	18	88,803,388	-
1	rs13483525	19	10,518,533	<i>Syt7</i>
1	rs6316813	19	11,396,714	<i>Ms4a7</i>
2	rs38304960	19	12,859,265	<i>Zfp91</i>



Source	SNP identifier	Chr.	Position [bp]	Associated gene
2	rs31193418	19	12,862,342	<i>Zfp91</i>
1	rs6372656	19	21,917,692	<i>Tmem2</i>
1	rs13483643	19	45,386,221	-
1	rs6194426	19	50,203,520	-
1	mCV23069572	19	52,369,475	-
1	rs6304326	19	53,512,609	-
1	rs6191324	19	59,396,320	<i>Pdzd8</i>
1	gnfX.026.801	X	36,745,486	<i>Stag2</i>
1	rs13483765	X	54,787,689	-
1	gnfX.080.189	X	90,784,538	-
1	rs13483894	X	93,694,393	<i>Heph</i>
1	rs6182892	X	94,171,734	-
1	rs6221690	X	127,572,284	-
1	rs13483997	X	128,648,050	-
1	rs13484004	X	130,310,074	-
2	rs3697198	X	132,751,198	<i>Tceal7</i>
1	rs13484043	X	139,242,663	<i>Tmem164</i>
1	gnfX.148.995	X	162,427,214	<i>Arhgap6</i>

2.3.5. Sequencing of candidate genes

To identify polymorphic sites between HAB and LAB mice, the *Avp*, corticotropin-releasing hormone (*Crh*), *Tac1*, cathepsin B (*Ctsb*), metallothionein 1 (*Mt1*) and the transmembrane protein 132D (*Tmem132d*) coding genes were sequenced. In all cases, except for *Tmem132d*, about 2,500bp of the gene promoter, the complete exons and introns and about 2,000bp of the downstream enhancer regions (DER) were sequenced. For *Tmem132d*, only 1,500bp of the promoter, the exons, conserved sequences from intron 3 and intron 4 and 1,000bp from the DER were analyzed, as the first three introns together are spanning more than 500kbp. Sequencing primers were designed to cover between 500-600bp.

Sequencing was also applied to verify qPCR reaction products. This was done for the intronal *Avp* and for the *Tac1* splicing variants. In this case, fragments were between 100 and 250bp.

2900019G14Rik was sequenced to explain for differences in the melting curves observed during qPCR (see results). qPCR fragments of *Tac1* and PCR fragments of *Avp* for polymorphism detection were cloned into a vector prior to sequencing.

2.3.5.1. Cloning of fragments

If cloning of DNA fragments was required before sequencing (this is indicated for fragments cloned prior to sequencing), the PCR product was purified from the PCR reaction mix with the NucleoSpin Extract II kit (Macherey-Nagel). For this, 8.5µl of the PCR reaction were diluted with 91.5µl water and 200µl of the NT buffer were



added. Otherwise, purification was performed according to the manufacturer's instructions. Then 4.2µl of each purified PCR product were incubated with 5µl ligation buffer, 0.3µl pGEM-T vector and 0.5µl T4-DNA ligase (pGEM-T Easy Vector System, Promega, Madison, WI) for 1h at room temperature. After incubation, 1µl of 3M sodium acetate, 20µl 99% ethanol and 1µl glycogen (10mg/ml) were added to each sample and vigorously mixed. Samples were shock-frozen in liquid nitrogen and centrifuged for 30min at 13,000rpm and 4°C, the supernatant was discarded and pellets washed in 300µl 70% ethanol. After centrifugation under the same conditions for 5min and removal of the remaining liquid, pellets were dried at 65°C and resuspended in 5µl water.

45µl of competent *Escherichia coli* DH5α cells were added to each sample and transferred into pre-cooled electroporation cuvettes (Bio-Rad). To permeabilize the cell membranes for the vector a voltage of 1.5kV was applied (GenePulser, Bio-Rad) to all cuvettes containing the vector / *E. coli* suspension. Transformed bacteria were collected in 1ml SOB medium and incubated for 1h at 37°C. 150µl of the suspension were incubated overnight at 37°C on lysogeny broth/ampicillin agar plates inoculated with 5-bromo-4-chloro-3-indolyl-β-D-galactoside (X-Gal: 25µl; 10%, Fermentas, St. Leon-Rot, Germany) and isopropyl-β-D-thiogalactopyranoside (IPTG: 30µl; 0.1M, Fermentas) dissolved in dimethyl sulfoxide. Colonies were picked according to blue / white selection and their plasmid inserts amplified using T7 and SP6 primers and *Taq* polymerase (Fermentas) for 25-µl reactions under the following conditions: initial denaturation at 94°C for 4min, 35 cycles of denaturation (94°C for 1min), annealing (49°C for 1min), extension (72°C for 1min) and a final extension of 10min at 72°C. 5µl of each PCR product were analyzed on a 1.5% agarose gel, fragments with proper insert were required to have the expected sequence length plus 143bp. 2µl of the PCR reaction were used for further analysis.

2.3.5.2. Cycle sequencing

2µl of PCR or qPCR product were purified by washing twice with nuclease-free water using the NucleoFast 96 PCR Clean-up kit (Macherey-Nagel). Clean-up plates were centrifuged at 9°C and 4,500xg for 10min (Heraeus Multifuge 4KR, Thermo Fisher Scientific, Waltham, MA) and resolved during 10 more minutes in 25µl water on a shaker (Eppendorf). 2.4µl of cleaned up PCR product were used for the sequencing reaction (BigDye Terminator Kit, Applied Biosystems, Foster City, CA) by using 1.2µl sequencing buffer, 0.4µl BigDye reagent and 1µl of the forward primer per sample. If sequencing reaction results were unclear or unreadable, sequencing reaction was also performed with the reverse primer. Sequencing



reactions were performed in ThermoFast 96 PCR plates (ABgene, Hamburg, Germany) using a PTC-225 Gradient MultiCycler (MJ Research, Miami, FL) under the following conditions: initial denaturation at 96°C for 1min, 35 cycles of denaturation (96°C for 10s), annealing (50°C for 5s), extension (60°C for 4min). Sequencing reaction products were purified by washing them twice in 20µl injection solution using Montage SEQ96 plates (Millipore, Billerica, MA) on a vacuum pump (Biomek 2000 Laboratory Automation Workstation, Beckman Coulter, Fullerton, CA) and transferred to 96 well plates. Sequences were resolved by capillary electrophoresis on a 3730 DNA Analyzer (Applied Biosystems) at the HelmholtzZentrum's Institute of Human Genetics (Neuherberg, Germany). Sequence analysis and comparison were performed using FinchTV Ver. 1.2 (Geospiza, Seattle, WA) and BioEdit Ver. 7.0.2 (Tom Hall, Ibis Biosciences, Carlsbad, CA) software programs.

2.3.5.3. Vasopressin (*Avp*)

For sequencing *Avp* (Fig. 4), all 1,944 bp of the unspliced transcript, 3,258bp of the promoter and 3,012bp of the DER were analyzed. The respective primers are described in table 5. All amplified sequences were cloned into the pGEM-T vector. The sequencing reaction was run with T7 and SP6 primers.

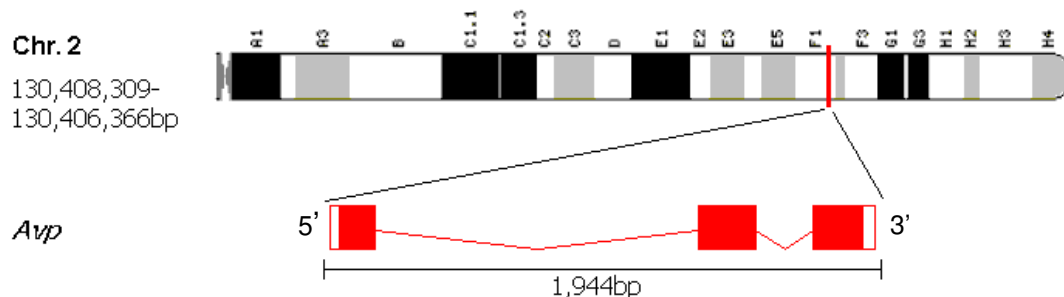


Figure 4: The vasopressin (*Avp*) gene's physical position on mouse chromosome 2. Exons are shown as red boxes, filled parts refer to translated, unfilled to untranslated regions. Spliced introns are indicated. As the gene is encoded on the minus strand, the start position has a higher value as the end position. Figure is based on data from Ensembl (www.ensembl.org, 08.01.2008).

Table 5: Primer sequences used for sequencing of the vasopressin (*Avp*) gene including the PCR fragment length resulting from each reaction.

Gene symbol and primer number	Orientation	Primer sequence 5'→3'	Product size [bp]
<i>Avp</i> 1	forward	GAC ACA GTG TGC CTC TAT G	784
	reverse	GCT CTC CTG GAC CTT CTG	
<i>Avp</i> 2	forward	AAT ACT CTA GGA AGA AGA CAA	731
	reverse	GAA ACA GCT TCC TGG TCA	
<i>Avp</i> 3	forward	GGA CAT GCC ACT CAA GGG	701
	reverse	TAC AGG CGT GCA TCA CGG	



Gene symbol and primer number	Orientation	Primer sequence 5'→3'	Product size [bp]
<i>Avp 4</i>	forward	CTA GAA GCC GTG GGC TAG GT	798
	reverse	GGG GGT GGG AGA GCT GGG AAT AGT	
<i>Avp 5</i>	forward	CAT TGC CAC CAT AGC TTT CC	805
	reverse	CTC TTG GGC AGT TCT GGA G	
<i>Avp 6</i>	forward	GAG CAG AGC CTG AGC TGC ACA CAG T	673
	reverse	ACA TAC AAT ACA ACA GAT CTG	
<i>Avp 7</i>	forward	CCA TGC CCA AGT GGA GC	682
	reverse	GCT GGA ACG AGG CCA AG	
<i>Avp 8</i>	forward	AAA GCA GCA GGT GAC ACT AGG	829
	reverse	CTA TGC ACG ACT TCG GGT GTG	
<i>Avp 9</i>	forward	ACT CCG TGG ATT CTG CCA AGC	793
	reverse	GAT GCC TTC TGC TCC TGA GAC	
<i>Avp 10</i>	forward	GCA CGG AAA TAG ACA AGA TAG	815
	reverse	AAC TGA CCA TCC TGA GCC ACC	
<i>Avp 11</i>	forward	AGA GAT TAG TCT CAG TGA CCT G	817
	reverse	CTG GAG TTG TGA GGT GGT TGT G	
<i>Avp 12</i>	forward	ACG GCT CAA GGA GGT AGG CG	830
	reverse	AAG TGA CCA CAA AGC ACG GAG	

2.3.5.4. Corticotropin-releasing hormone (*Crh*)

To analyze *Crh* (Fig. 5) for sequence variations, all 1,916 bp of the unspliced transcript, 3,028bp of the promoter and 2,197bp of the DER were sequenced. The respective primers are described in table 6. All amplified sequences were analyzed in the sequencing reaction using the indicated primers in a nested PCR reaction.

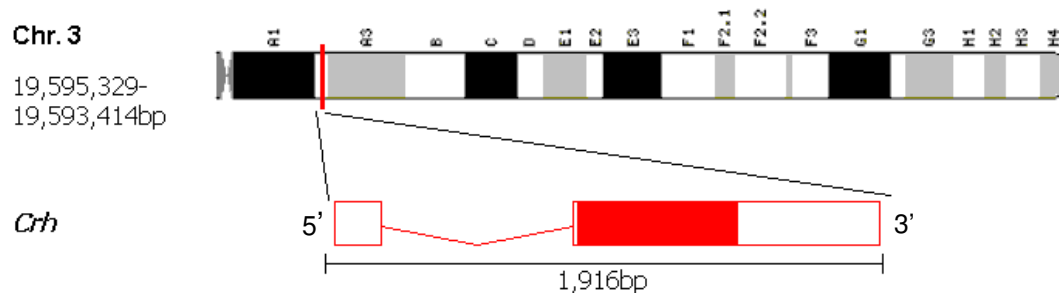


Figure 5: The corticotropin-releasing hormone (*Crh*) gene's physical position on mouse chromosome 3. Exons are shown as red boxes, filled parts refer to translated, unfilled to untranslated regions. Spliced introns are indicated. As the gene is encoded on the minus strand, the start position has a higher value as the end position. Figure is based on data from Ensembl (www.ensembl.org, 08.01.2008).

Table 6: Primer sequences used for sequencing of the corticotropin-releasing hormone (*Crh*) gene including the PCR fragment length resulting from each reaction.

Gene symbol and primer number	Orientation	Primer sequence 5'→3'	Product size [bp]
<i>Crh 1</i>	forward	AAA GTG CAA AGA GAT GCA G	508
	reverse	TCT ATT ACA AGA CTC ACA CCA AGA G	
<i>Crh 2</i>	forward	CTT GGT GCC CAT ATT TCT TGA	538
	reverse	TTA CAC AGC ATC ACG GCA TC	



Gene symbol and primer number	Orientation	Primer sequence 5'→3'	Product size [bp]
<i>Crh 3</i>	forward	GCT GAT ATG TGT GTT GCT CCA	590
	reverse	TTC ACC TCA GTG TTT GGG ATT	
<i>Crh 4</i>	forward	GAA TTG GTC AGG AAT GAA AG	464
	reverse	GTC TGG GAT TCG CTT CAG	
<i>Crh 5</i>	forward	CCA GAA ACA GGG AAC AGG AA	592
	reverse	CGA GGA AGG CCA TAA ACA AA	
<i>Crh 6</i>	forward	GGG AAC AGT CCT GAT TAA CTT T	614
	reverse	ATA TTT ATC GCC TCC TTG GTG A	
<i>Crh 7</i>	forward	CCA CAC TTG GAT AGT CTC ATT	599
	reverse	TTA AGG CAC AGT TAG CGA CA	
<i>Crh 8</i>	forward	CTG GAA TGC CTG TGC CTA TG	597
	reverse	CTC TGA AGC ACC GAG GTT G	
<i>Crh 9</i>	forward	AAG CCT AGA GCC TGT CTT GTC	616
	reverse	GAA GGT GAG ATC CAG AGA GATG	
<i>Crh 10</i>	forward	CGC CCA TCT CTC TGG ATC T	501
	reverse	CTA GCC ACC CCT CAA GAA TG	
<i>Crh 11</i>	forward	GCA GAT GGG AGT CAT CCA GT	561
	reverse	TCT GAC CTT CTC CAG TTG TCC	
<i>Crh 12</i>	forward	CTG AGG ACC GAG GAA GTG TG	525
	reverse	CAG TCT CCC AGC AAT TTA TTC A	
<i>Crh 13</i>	forward	GCC CTG GAA ATA TGC TTG AT	496
	reverse	GGC CAC ACG TCC ATA GTC C	
<i>Crh 14</i>	forward	TGT CAA AAG AGT TGC CCT AGA	577
	reverse	CAC ATA GGC AGC AGG AAA CA	
<i>Crh 15</i>	forward	AGA AAT CCT GTC CAG AGG TC	514
	reverse	GAA AGC CAA GCA GGG AAC	

2.3.5.5. Tachykinin 1 (*Tac1*)

For sequencing *Tac1* (Fig. 6) all 7,903 bp of the unspliced transcript, 2,935bp of the promoter and 2,773bp of the DER were analyzed. The respective primers are described in table 7. All amplified sequences were analyzed in the sequencing reaction using the indicated primers in a nested PCR reaction.

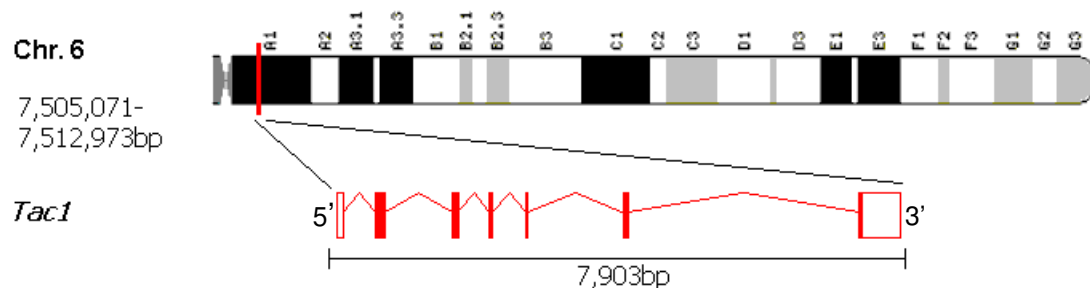


Figure 6: The tachykinin 1 (*Tac1*) gene's physical position on mouse chromosome 6. Exons are shown as red boxes, filled parts refer to translated, unfilled to untranslated regions. Spliced introns are indicated. The gene is encoded on the plus strand. Figure is based on data from Ensembl (www.ensembl.org, 08.01.2008).



Table 7: Primer sequences used for sequencing of the tachykinin 1 (*Tac1*) gene including the PCR fragment length resulting from each reaction.

Gene symbol and primer number	Orientation	Primer sequence 5'→3'	Product size [bp]
<i>Tac1</i> 1	forward	GTA CGA AAT GGA TGG TGA CTG	529
	reverse	GGT TTG GTG GCT GAT TAT AGG	
<i>Tac1</i> 2	forward	AGC TAA GTC GAA AGG ATG GAC	619
	reverse	GGT AAG TAG AGA CCA CAA TCC AG	
<i>Tac1</i> 3	forward	ATG AAG TGG GAA TGG GTG TTA G	576
	reverse	TCA TGC CTC CGC TTA TGT AG	
<i>Tac1</i> 4	forward	GCT TAA ATC TGT GAG GTC TTT G	552
	reverse	GAT GAA GTA AAC GAT GTT GCA G	
<i>Tac1</i> 5	forward	AGG CTG AGT TAG GAG AAT ACC C	572
	reverse	CTA GAG GAG GAA AGC AGA CTT G	
<i>Tac1</i> 6	forward	TAC GTT CCA CAT GCT GTT CTA C	490
	reverse	CCA TCC AAT CCA GAG AGA CC	
<i>Tac1</i> 7	forward	CTC AAG ATT CCC TGA CTC CTC	621
	reverse	GGT ATT TGC ACA CTT TCT CTC C	
<i>Tac1</i> 8	forward	TCT GCT CCC ACT CCA TTC TC	591
	reverse	TTA TAT TCC AGT GCG CCT CTC	
<i>Tac1</i> 9	forward	AGA TCA AGG TGA GTC CCA AAC	611
	reverse	GTG AAC AGT AGG GTG GAT GAA G	
<i>Tac1</i> 10	forward	CAT TCA GTG CTC CAA GTT TCC	599
	reverse	TAT TGC TCA TCT CAC CAG CAT C	
<i>Tac1</i> 11	forward	GAG CCC TTT GAG CAT CTT C	501
	reverse	CAT TAA CTC TTC ACA AGC TCC AC	
<i>Tac1</i> 12	forward	CCA GGC TCA GGT GAA AGA TG	459
	reverse	AAG GTA GAA CTG TGG GAC TCT TG	
<i>Tac1</i> 13	forward	CGC GTG TAT TTT AAG CTC CTG	650
	reverse	CAG ACA TGA GTG CTT GTG AGG	
<i>Tac1</i> 14	forward	AGC AGA ACA TAG AGC CCA ATA G	650
	reverse	GTT ACC AGT TTG GAG TTT ACC C	
<i>Tac1</i> 15	forward	ATC CAG AGG TGA CAG GAA GTC	583
	reverse	GCT GAA ACC CAT ATT GTG AGC	
<i>Tac1</i> 16	forward	TCC CAC ACA CAA ATG TAT AAC C	630
	reverse	CCA AAG ACT CAG GGT ATG TAA TG	
<i>Tac1</i> 17	forward	CAA ATG TTC ATA GTG TCT GTA GCC	570
	reverse	CCT GTG GCG TTT ATG TAG AAA G	
<i>Tac1</i> 18	forward	GAT TGT CCT TGA CCC AAA GC	552
	reverse	TGT GAG CAC TGA TAA ATC TGG AG	
<i>Tac1</i> 19	forward	CCA GCC TTG AGA GAT GGA ATA TAG	627
	reverse	AAT GTC TAC CAG CTT CTG TGT CC	
<i>Tac1</i> 20	forward	AGC CAC CTG ATC CCT ACT GTC	626
	reverse	GAG GGT ATT TCG TCA TCT CAG C	
<i>Tac1</i> 21	forward	GGG CAA CTA TTT ACA GGA GCA C	468
	reverse	TCT CTT CTC TCT TGG ACA CCT TC	
<i>Tac1</i> 22	forward	AAT ATC GGT CTC AAG GGC AAT C	514
	reverse	TCC TAG TTT CTT TGG GCA TCT G	
<i>Tac1</i> 23	forward	TGT GGT AGG TAT GGT CCT TTC TC	612
	reverse	ACT AAT TTC TAC TTC TGG GGA GGT C	
<i>Tac1</i> 24	forward	ATG TGC GCT ATG AGG AAT G	535
	reverse	GAA GAA AGG CTG TTG ATT TGA C	



Gene symbol and primer number	Orientation	Primer sequence 5'→3'	Product size [bp]
<i>Tac1 25</i>	forward	TCA ATG TAA TTC TCT GGT CTT CAG	643
	reverse	CCC ATT CCT TTC AGT GTT ATG	
<i>Tac1 26</i>	forward	TTG CTG ACA CCC ATA ATC TTC	602
	reverse	GCT CCT TTG TAA TCC ACA CTT ATC	
<i>Tac1 27</i>	forward	CGT TTT ACA GAT GGG GAA AGA G	617
	reverse	CAC CAA TGT GCC TAT GAA AAT C	
<i>Tac1 28</i>	forward	ATG CAC AGG GTA TGT TTT ATG G	508
	reverse	TTA TAT GGC CTG ATC TTT GTG G	
<i>Tac1 29</i>	forward	GTG ACT AGG GCA ATG GAA AGA G	485
	reverse	GGG AGG AGA GCA GAG TTA TGT G	
<i>Tac1 30</i>	forward	CTA GGC TCA AGA ATG AAC ACA GG	612
	reverse	GCT TTA TGT AGG AGT TTG GAG CAG	

2.3.5.6. Cathepsin B (*Ctsb*)

To screen for sequence variations between HAB and LAB mice in *Ctsb* (Fig. 7), 8,045bp of the unspliced transcript, 2,441bp of the promoter and 1,797bp of the DER were analyzed. Due to the size of the unspliced transcript (20,619bp), 10,278bp from intron 1 and 2,266bp from intron 8 were ignored in the sequencing reaction. The respective primers are described in table 8. All amplified sequences were analyzed in the sequencing reaction using the indicated primers in a nested PCR reaction.

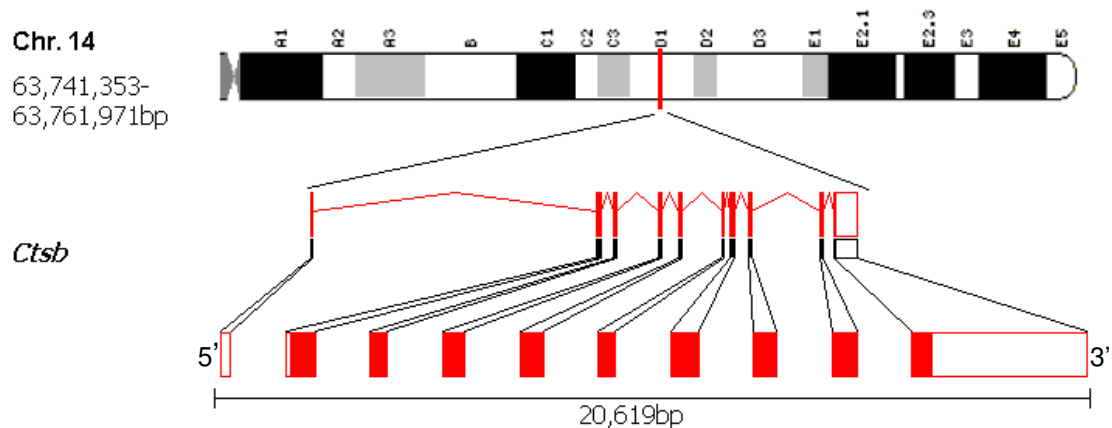


Figure 7: The cathepsin B (*Ctsb*) gene's physical position on mouse chromosome 14. Exons are shown as red boxes, filled parts refer to translated, unfilled to untranslated regions. Spliced introns are indicated. The gene is encoded on the plus strand. Figure is based on data from Ensembl (www.ensembl.org, 08.01.2008).



Table 8: Primer sequences used for sequencing of the cathepsin B (*Ctsb*) gene including the PCR fragment length resulting from each reaction.

Gene symbol and primer number	Orientation	Primer sequence 5'→3'	Product size [bp]
<i>Ctsb</i> 1	forward	ACA GCA AGG AAC AAC ATA GCA C	502
	reverse	GAT GGA AGC AGA AAG GTC AAA G	
<i>Ctsb</i> 2	forward	ATA GGT CAT TGG GCT GTG TAG G	621
	reverse	GAG AGA CAA GAA CCC AGA AGT ACC	
<i>Ctsb</i> 3	forward	GTG AGC AGG CAG TGA TAT GG	554
	reverse	AAA TGA GCA GCC TTT CTT GG	
<i>Ctsb</i> 4	forward	GCA GCC AGA GAC ACT TTT GG	591
	reverse	CCC ATG AAT TTT GTC CAA GG	
<i>Ctsb</i> 5	forward	AGA TCA ACT AGG TCA GCC AGC TTC	540
	reverse	AAC TGG TGG TTT GTC TGC TCT CT	
<i>Ctsb</i> 6	forward	TGC ATG TCA CGA AGA TGT TG	562
	reverse	ACT GGA AAG AAG CCG ATC AC	
Intron 1: 10,278bp not sequenced			
<i>Ctsb</i> 7	forward	TCC ACC TTA ACG CTG ACT CTT C	603
	reverse	CTC GCT CCA AAG CTC ACT TAT C	
<i>Ctsb</i> 8	forward	ATT GCT CTC CAG TCT CCA TGT T	529
	reverse	TCC CTA CAC TCC AAC ACT AGC A	
<i>Ctsb</i> 9	forward	AGG CTG GAC GCA ACT TCT AC	516
	reverse	CAA TCT TCT CCC ACC TTT CTT G	
<i>Ctsb</i> 10	forward	TCA AAT CAG GCA AGG CAT AG	532
	reverse	CGG AGG TCA GAG GGA TTA TTA G	
<i>Ctsb</i> 11	forward	CTG GAG AGA TGG CTA AGT GGT T	606
	reverse	GCA CTG GCT CTA TGC TCA TTT A	
<i>Ctsb</i> 12	forward	AGG AAG GAA GGA AGG AAG GAA C	581
	reverse	ACA GTG ATG GGA AGA AAT GGA C	
<i>Ctsb</i> 13	forward	GCA TAT CTA GGG AGG GAC CAG	575
	reverse	AGA GCC TTC AAC CTT CTG AGT G	
<i>Ctsb</i> 14	forward	ATC TGC CTT GGA ATT TGC TC	537
	reverse	TTG GAG ACG ACA GTT CTT TCT G	
<i>Ctsb</i> 15	forward	AGA TGG AGC TTG GTT GAG TCC	531
	reverse	AGG GAT GGT GTA TGG TAA GCA G	
<i>Ctsb</i> 16	forward	CCT CAA TAC AGG AGC TGA CC	545
	reverse	TGA GAC AAG ACA GAG TGT GGA C	
<i>Ctsb</i> 17	forward	AAA CAG GAG CAG TAA GGA GGA G	573
	reverse	GAA GAG AGC AGA AGG GAG ACT G	
Intron 8: 2,266bp not sequenced			
<i>Ctsb</i> 18	forward	AAA GAC TAT GGG TGC TGG AGA C	515
	reverse	AGT TCT CGT CAC ATG CTG CTC	
<i>Ctsb</i> 19	forward	CCC CTC CTC AAA CTA CAT AAG C	537
	reverse	CTC CCC TGT CTA CCT CAT TCC	
<i>Ctsb</i> 20	forward	CTG CTT TGA CTT CAT TGT CCA G	515
	reverse	AAT GTC GAT GGA TGC AGA TG	
<i>Ctsb</i> 21	forward	ACT TCA CGA GAG GAC AAA TGC	545
	reverse	GTG TGA GCA GTT ACA GGT ACG G	
<i>Ctsb</i> 22	forward	GGA ATG TCT GTG CCA ATA AAC C	533
	reverse	GCC TCA AAC CGA GTT ACA CTT C	
<i>Ctsb</i> 23	forward	TGT AAC TCG GTT TGA GGC AAC	526
	reverse	GAG GAC CAC ACA AAG AAC ACA C	
<i>Ctsb</i> 24	forward	CCA TGT CGG CAA TCA GAA C	581
	reverse	ACC ACA CAA AGA ACA CAC AAC G	



Gene symbol and primer number	Orientation	Primer sequence 5'→3'	Product size [bp]
<i>Ctsb</i> 25	forward	CCG ATC TCT GGG AGT TTG AG	488
	reverse	GAT GTG CTT GCT ACC TTC CTC T	
<i>Ctsb</i> 26	forward	CGC TCT CAC TTC CAC TAC CAC	591
	reverse	CTA AGT TCA ATT CCC AGC AAC C	

2.3.5.7. Metallothionein 1 (*Mt1*)

For sequencing *Mt1* (Fig. 8), all 1,085bp of the unspliced transcript, 2,187bp of the promoter and 1,878bp of the DER were analyzed. The respective primers are described in table 9. All amplified sequences were analyzed in the sequencing reaction using the indicated primers in a nested PCR reaction.

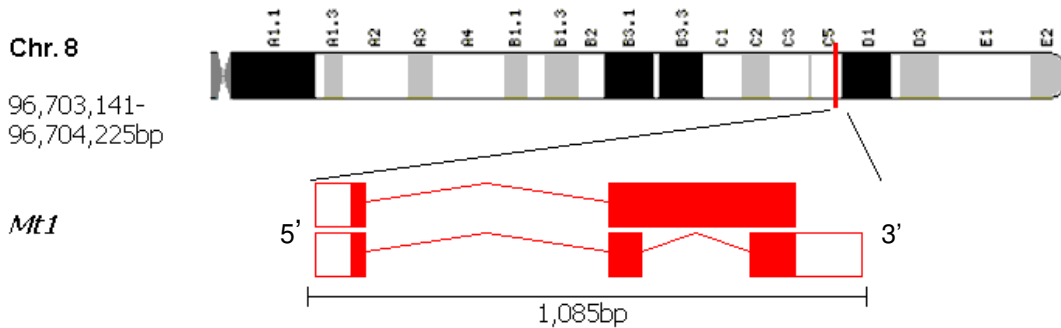


Figure 8: The metallothionein 1 (*Mt1*) gene's physical position on mouse chromosome 8. Exons are shown as red boxes, filled parts refer to translated, unfilled to untranslated regions. Spliced introns are indicated. The gene is encoded on the plus strand. Figure is based on data from Ensembl (www.ensembl.org, 08.01.2008).

Table 9: Primer sequences used for sequencing of the metallothionein 1 (*Mt1*) gene including the PCR fragment length resulting from each reaction.

Gene symbol and primer number	Orientation	Primer sequence 5'→3'	Product size [bp]
<i>Mt1</i> 1	forward	CAA GAG GTC TAA AGG CCC AAG	511
	reverse	TGG TCA ACA AAG TGA GTT CCA G	
<i>Mt1</i> 2	forward	GAT CTG GAG AGA ACT GAC CAA C	564
	reverse	TTC ATG GTG GTT TAG ATA CAA GTG	
<i>Mt1</i> 3	forward	GCT GTG TTG TCT CCT CCA AG	601
	reverse	TGC ATA CCA TCA CTT CTG AGC	
<i>Mt1</i> 4	forward	CTG AAT CCT CTG TCC TTG TGT G	535
	reverse	CTC TCT CTG GAT CGA AGC TAG G	
<i>Mt1</i> 5	forward	AGC AGA TGG GTT AAG GTG AGT G	546
	reverse	CTG CCC TCT TTA TAG TCG TTG G	
<i>Mt1</i> 6	forward	TGA CTA TGC GTG GGC TGG AG	659
	reverse	CAT GAG GGA GGC AGC ATT ACA G	
<i>Mt1</i> 7	forward	CCC TGA CTT AAC CTG TGA GGA G	585
	reverse	GGG TGG AAC TGT ATA GGA GAC G	
<i>Mt1</i> 8	forward	TCC TTT CTA GGC TGC TGG CTC	562
	reverse	TAC CCA CCT CCT TAT ACC CAA C	
<i>Mt1</i> 9	forward	TGG TCA GGT CTT GTG TTA GGG	642
	reverse	GGC CAT CTT CTG CTA CAT ACG	



Gene symbol and primer number	Orientation	Primer sequence 5'→3'	Product size [bp]
<i>Mt1</i> 10	forward	TCA GCT ATT GGA TGG AAC ACA G	629
	reverse	GAG ATG GCT CAG TGG GTA AGA G	
<i>Mt1</i> 11	forward	ATT TGA ACT CCT GAC CTT CG	640
	reverse	ACG TCT CAC GGG CTA GAG	

2.3.5.8. Transmembrane protein 132D (*Tmem132d*)

To identify SNPs in *Tmem132d* (Fig. 9), 8,339bp of the unspliced transcript, 1,132bp of the promoter and 103bp of the DER were analyzed. Due to the size of the unspliced transcript (675,077bp), only exons, fragments of 100-500 bp around exons, furthermore two rather conserved intronal sequences from intron 3 (717bp and 389bp) and 839bp from intron 4 were considered for sequencing of the whole unspliced transcript. The respective primers are described in table 10. All amplified sequences were analyzed in the sequencing reaction using the indicated primers in a nested PCR reaction.

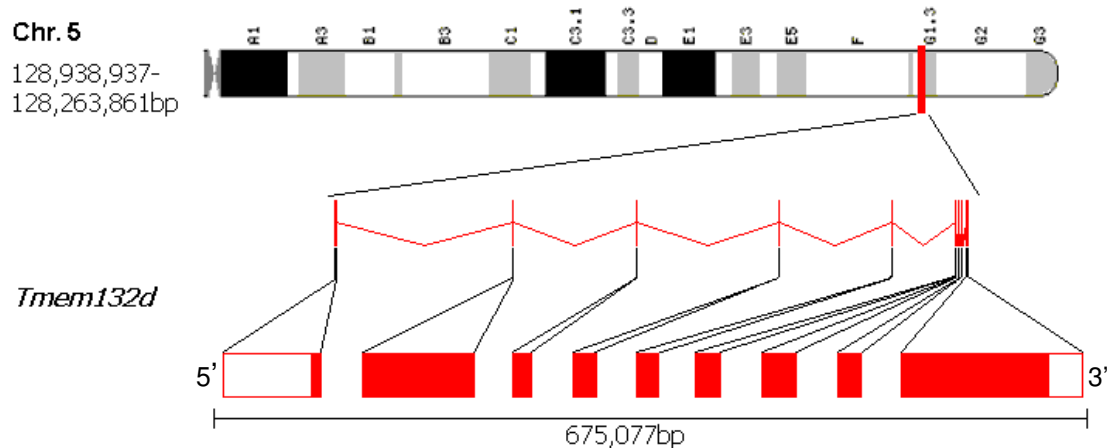


Figure 9: The transmembrane protein 132D (*Tmem132d*) gene's physical position on mouse chromosome 5. Exons are shown as red boxes, filled parts refer to translated, unfilled to untranslated regions. Spliced introns are indicated. As the gene is encoded on the minus strand, the start position has a higher value as the end position. Figure is based on data from Ensembl (www.ensembl.org, 08.01.2008).

Table 10: Primer sequences used for sequencing of the transmembrane protein 132D (*Tmem132d*) gene including the PCR fragment length resulting from each reaction.

Gene symbol and primer number	Orientation	Primer sequence 5'→3'	Product size [bp]
<i>Tmem132d</i> 1	forward	TGC TGC CAA GCT GTG ATA AA	483
	reverse	TGC GGA TAA AAA TGG ACT GG	
<i>Tmem132d</i> 2	forward	AGC CCA AAA CGG ACT CTC TT	460
	reverse	GGA CAG TTC AGG AAC CCC TA	
<i>Tmem132d</i> 3	forward	TCA GGG ACA GGA ATT TGA GG	367
	reverse	TTT TTA AGC CCC ACC CTT CT	



Gene symbol and primer number	Orientation	Primer sequence 5'→3'	Product size [bp]
<i>Tmem132d 4</i>	forward	CCA GGA AGG TGG GAC CTA CT	582
	reverse	CTG AGG ACT GGC TCG TGA AT	
<i>Tmem132d 5</i>	forward	CCA GCC GGA GTC CTC AGA	476
	reverse	CCA CCC ACA TCC ACA TCT ACT	
<i>Tmem132d 6</i>	forward	AAA GTG AGG CTG TGG GTA GC	505
	reverse	GTT CTC GTC CCT GTG GTC AT	
<i>Tmem132d 7</i>	Forward	CCA ACC CAT TTG GAT TCA CT	504
	reverse	TCC TTC AAA GGT GGA CTG CT	
<i>Tmem132d 8</i>	forward	AGG AGG ATT CGA GGA AGA GC	317
	reverse	TCT GCA GAC AGT TCC ACA GC	
<i>Tmem132d 9</i>	forward	TAA ACC TGA TTC CCC GTG AG	460
	reverse	GCC CTG TGT GGG TTC ACT AT	
<i>Tmem132d 10</i>	forward	CTT CCT CAA GCT CCT TCT GG	457
	reverse	GGC TAC CCT TGG GAT ATG GT	
<i>Tmem132d 11</i>	forward	ACA GGT TAA TGC CCT GTT GC	413
	reverse	AGC TTT GCA CAC TGC ACT TC	
<i>Tmem132d 12</i>	forward	GGA CTG GGA AAG ATG TGG AC	439
	reverse	GGT CTG GAG AGT GTG GGA AC	
<i>Tmem132d 13</i>	forward	GAG ACG TGA TAG GCC CAT GT	601
	reverse	CCT TTT ACA GGG GTC GCA TA	
<i>Tmem132d 14</i>	forward	TTG TGG ATG GTG GTC AGT CC	424
	reverse	CCA TTT TTG TCC CCA TTT TG	
<i>Tmem132d 15</i>	forward	TGT TGC ACC AGC GTT GTA C	412
	reverse	ATC TGG CGT CGC TAT TAT TAG	
<i>Tmem132d 16</i>	forward	GAA GCA CCG TGT GTC TAA GG	554
	reverse	CCT GGA GCT TGC TGG TCT AC	
<i>Tmem132d 17</i>	forward	ACA TTT GGC TTC CTG TGA CC	451
	reverse	CCA GGC ATG GGT TAT AGC AG	
<i>Tmem132d 18</i>	forward	ATT CCC TGG TCT GTG GAC TG	482
	reverse	GGC AGA GTC TAG GCA CTT GG	
<i>Tmem132d 19</i>	forward	AAC CAC CTG TCA TGC CTC TC	624
	reverse	CCC TGT GTC TCC CAT GTA TC	
<i>Tmem132d 20</i>	forward	TTA TAA CAT GGG ATG GCT GG	432
	reverse	GGG ATA GAA ACC CCT GAT GG	
<i>Tmem132d 21</i>	forward	ACC CAA TTC TTT TCC TCG AC	436
	reverse	TCC ACT CTC ACT GCT GTT GG	
<i>Tmem132d 22</i>	forward	TCT CCC TGA TGG CTA CAT CC	420
	reverse	AAC AGG TTT TCC TGG CCT TC	
<i>Tmem132d 23</i>	forward	TGA CAG GAG GTC CAA AAA GC	520
	reverse	AGT CCA GAC CCC TGT CAA TG	
<i>Tmem132d 24</i>	forward	TCA CTC TCA CGA CTG GGT TG	372
	reverse	GTG TCC CCG TTA TAC GTG CT	
<i>Tmem132d 25</i>	forward	TCA GAC GAT GGG TGT CCT TC	532
	reverse	CTG ACC CAC ACA TGC TCA AC	

2.3.6. Assessing the effects of polymorphisms

All SNPs and other polymorphisms identified by sequencing were analyzed if they are located in the exons or at exon borders, if they influence the amino acid sequence or if they are located in the promoter or DER. *Avp* and *Tmem132d* were



additionally screened for transcription factor binding motifs via the the Transcription Element Search System (TESS, <http://www.cbil.upenn.edu/cgi-bin/tess/tess>). Putative binding sites of transcription factors were additionally checked for their function and occurrence within the brain according to the NCBI database (<http://www.ncbi.nlm.nih.gov/>).

2.3.7. Allele-specific transcription analyses of vasopressin (*Avp*)

For *Avp*, in addition to the validation of gene expression differences, an allele-specific transcription analysis has been performed based on the identified polymorphisms, to analyze the effects of the identified polymorphisms on the gene's expression.

Therefore, PVN and SON were dissected from the hypothalamus of four female F1 mice that were heterozygous for the recently described C(40)T (rs50049109) single nucleotide polymorphism (SNP). Total RNA was extracted using a TRIzol chloroform extraction protocol and reverse transcribed with Omniscript (Qiagen, Hilden, Germany) according to the manufacturer's instructions. 208bp of the *Avp* transcript containing the SNP at position C(40)T were amplified by PCR in 40 identical cycles of denaturation at 94°C for 1min, annealing at 56°C for 1min and elongation at 72°C for 1min using Taq polymerase (Fermentas, St. Leon-Roth, Germany) and 5' gagcagagcctgagctgcacacagt 3' as forward and 5' agcagatgcttggtccgaagcagc 3' as reverse primers (MWG Biotech, Ebersberg, München). Amplified fragments were ligated into a vector and transfected into competent *Escherichia coli* cells that were grown overnight as described above.

From each agar plate, 25 colonies with proper insert (according to white/blue selection) were picked and sequenced. The specific alleles from each transcript were determined by the C(40)T polymorphism.

2.4. Association and linkage of SNPs with behavioral parameters

For the F2 panel, statistical analysis was performed using WG-Permer (www.mpipsykl.mpg.de/wg-permer). Trait values were rank-transformed to protect against artifacts. Analysis was done using a genotypic model, i.e. the three genotypic classes possible for each of the phenotypes were treated as a separate class each and global test on equality of the three means was performed.

2.5. Statistical data analysis

All data, except for data from high throughput gene expression profiling and genotyping were analyzed using SPSS Ver. 16.0.1 (Chicago, IL), applying the

ATGCTCGCCAGGA
TACGAGCGGTCCT



Animals, materials and methods

Kruskal-Wallis test (KWH) for comparisons over more than two groups with subsequent Mann-Whitney tests (MWU) and sequential Bonferroni correction for multiple testing, if applicable. For allele-specific expression analysis of *Avp*, χ^2 test was applied (Preacher, 2001: Calculation for the chi-square test: An interactive calculation tool for chi-square tests of goodness of fit and independence [Computer software], available from <http://www.quantpsy.org>).



3. Results

3.1. The HAB phenotype reversal by selective breeding

Continuous breeding of rHAB mice towards a less anxious phenotype resulted in elevated group means for the percentage of time that these mice spent on the open arms of the EPM (less anxiety) although this effect was only significant for rHAB males (MWU: $p = 0.04$), not for females (MWU: $p = 0.14$; Fig. 10A). For females, only the number of full open arm entries was elevated significantly (MWU: $p = 0.04$; Fig. 10B), whereas for males in addition to the percentage of time, the latency time to the first entry was decreased (MWU: $p = 0.03$; Fig. 10C). There was no significant difference in body weight or any parameter assessing locomotion on the EPM, independent of gender. In the TST, no significant difference could be observed in any parameter (Fig. 10D and E).

3.2. Identification of candidate genes

3.2.1. Animals and behavioral tests

At any time, HAB and LAB mice displayed the trait-specific differences, in the EPM and TST irrespective of gender. HAB and LAB mice never displayed significant differences concerning body weight or locomotion on the EPM. CD1 and NAB showed elevated body weight in comparison to HAB and LAB mice (data not shown, example for CD1 in Fig. 11F).

For the MPI24K platform-based gene expression analyses, HAB and LAB mice were used that displayed significant differences regarding the percentaged time spent on the open arms of the EPM (MWU: $p = 3.95 \times 10^{-3}$; Fig. 11A) and in the total test time spent immobile in the TST (MWU: $p = 3.88 \times 10^{-3}$; Fig. 11B).

HAB, NAB and LAB mice used for the Illumina-based gene expression profiling displayed significant differences in the time spent on the open arms of the EPM (KWH: $p = 8.80 \times 10^{-5}$; MWU: HAB and NAB vs. LAB $p = 3.58 \times 10^{-3}$; HAB vs. NAB $p = 1.75 \times 10^{-3}$; Fig. 11C).

HAB and NAB vs. LAB mice also showed significant differences in the total time spent immobile in the TST (KWH: $p = 6.65 \times 10^{-4}$; MWU: HAB and NAB vs. LAB $p = 3.55 \times 10^{-3}$; HAB vs. NAB $p = 0.84$; Fig 11D). Only HAB and LAB vs. NAB mice showed significant differences regarding body weight (KWH: $p = 3.45 \times 10^{-3}$; MWU: HAB vs. NAB: 9.62×10^{-3} ; LAB vs. NAB $p = 0.01$; HAB vs. LAB $p = 0.46$) with a mean difference of 3.52g, with NAB mice having an increased body weight at the age of seven weeks. NAB mice also exhibited increased locomotion compared to both HAB



and LAB mice, as reflected by the number of closed arm entries on the EPM (data not shown).

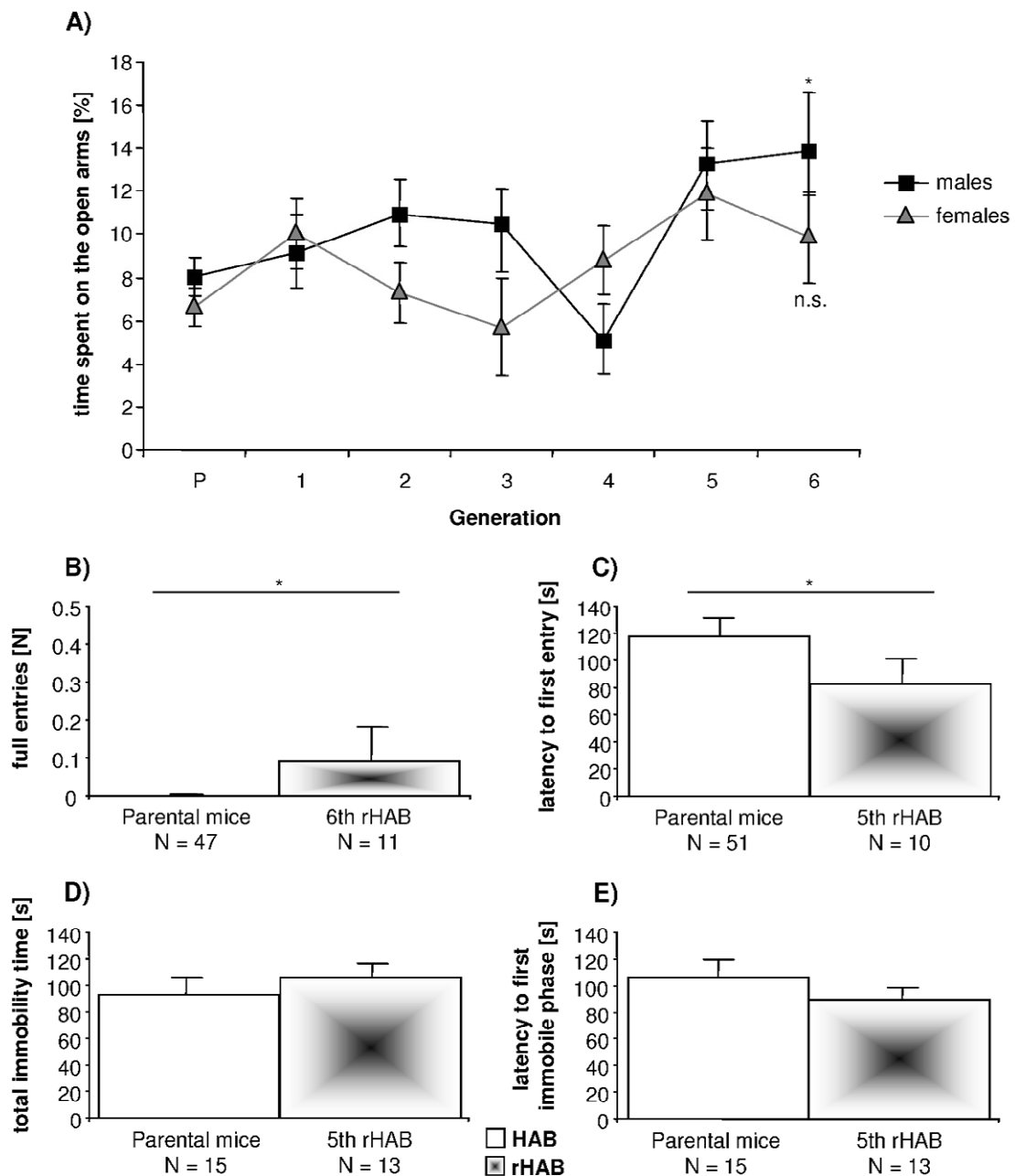


Figure 10: Behavioral assessment of reversed HAB (rHAB – in **B-E**: black) mice vs. HAB (in **B-E**: white) mice with **(A)** the development of the percentaged time spent on the open arms of the elevated plus-maze (EPM) in rHAB mice in the course of breeding generations; **(B)** number of full open arm entries on the EPM for rHAB females; **(C)** latency time of rHAB males to their first open arm entry; The depression-like behavior of rHAB vs. HAB males as measured by the **(D)** total immobility time in the tail suspension test and **(E)** the latency to the first immobility. Statistical significance calculated against parental generation HAB mice. Data are displayed as means \pm SEM in **(A)** and + SEM in **(B-E)**; * $p < 0.05$.

Similarly, in female HAB, CD1 and LAB and male HAB, NAB and LAB mice the differences for the percentaged time spent on the open arms of the EPM were highly significant in females (KWH: $p = 1.73 \times 10^{-4}$; MWU: HAB vs. LAB $p = 2.39 \times 10^{-3}$; HAB



vs. CD1 $p = 2.33 \times 10^{-3}$; CD1 vs. LAB $p = 0.02$; Fig. 11E). CD1 mice showed significantly increased locomotion and body weight compared to HAB and LAB mice (data not shown, body weight in Fig. 11F).

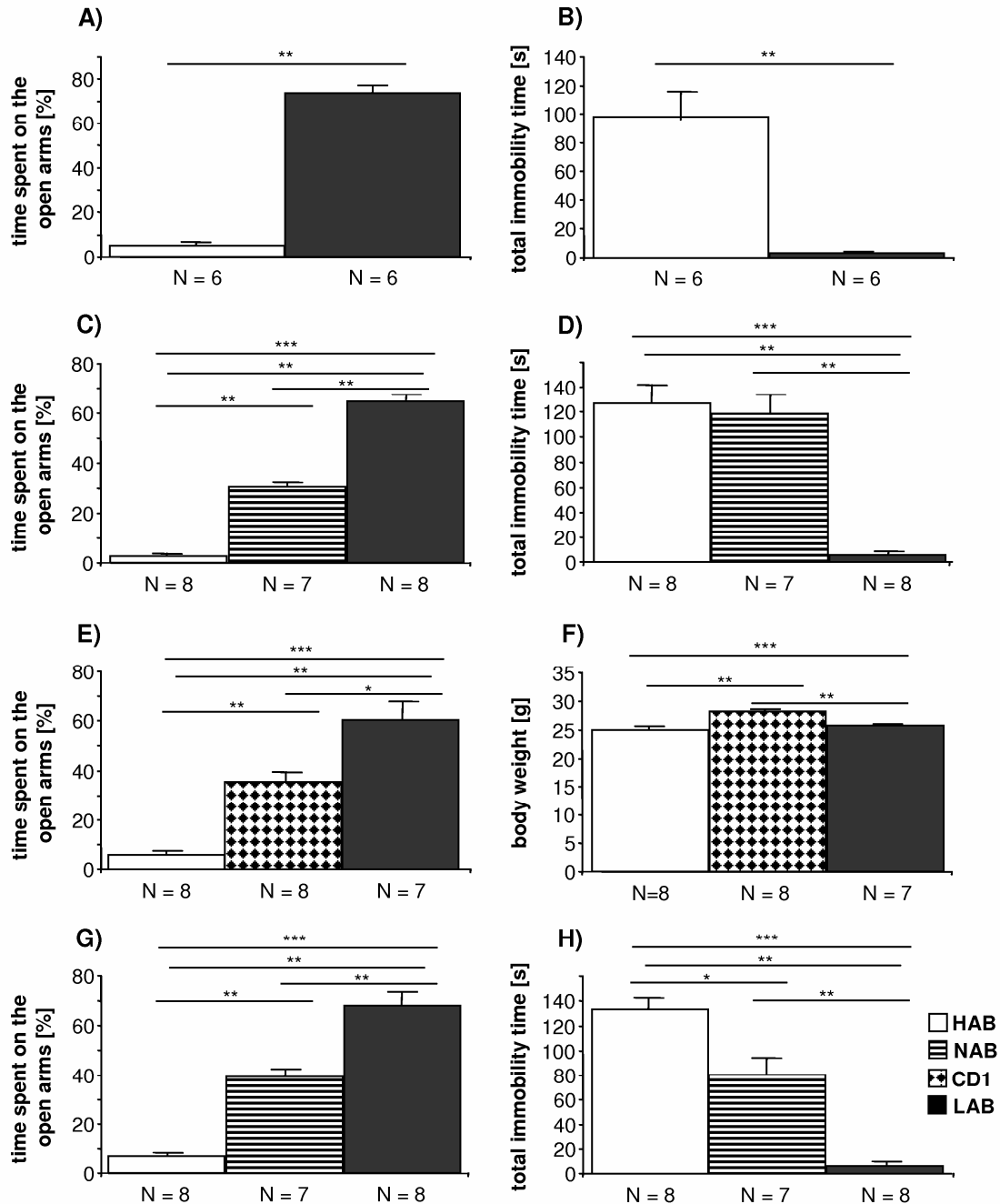


Figure 11: Behavioral assessment of mice used for gene expression profiling. (A-B) Male mice used in the MPI24K-based gene expression analyses; (C-D) male mice used in the Illumina platform-based gene expression profiling; (E-F) Female and (G-H) male mice used for validation via qPCR. (A, C, E, G) The mice's anxiety-related behavior as assessed by the time they spent on the open arms of the elevated plus-maze and (B, D, H) their depression-like behavior as reflected by the total immobility time in the tail suspension test. (F) Displays the body weight of female mice aged seven weeks. Data are displayed as means + SEM; * $p < 0.05$; ** $p < 0.01$; *** $p < 0.001$.

3.2.2. Gene expression profiling on the MPI24K platform



3.2.2.1. Tissue dissection

Micropunching of brain tissue achieved an accuracy of 0.1-0.2mm deviation in any direction relative to the expected coordinates as described in the Mouse Brain Atlas (Fig. 12).

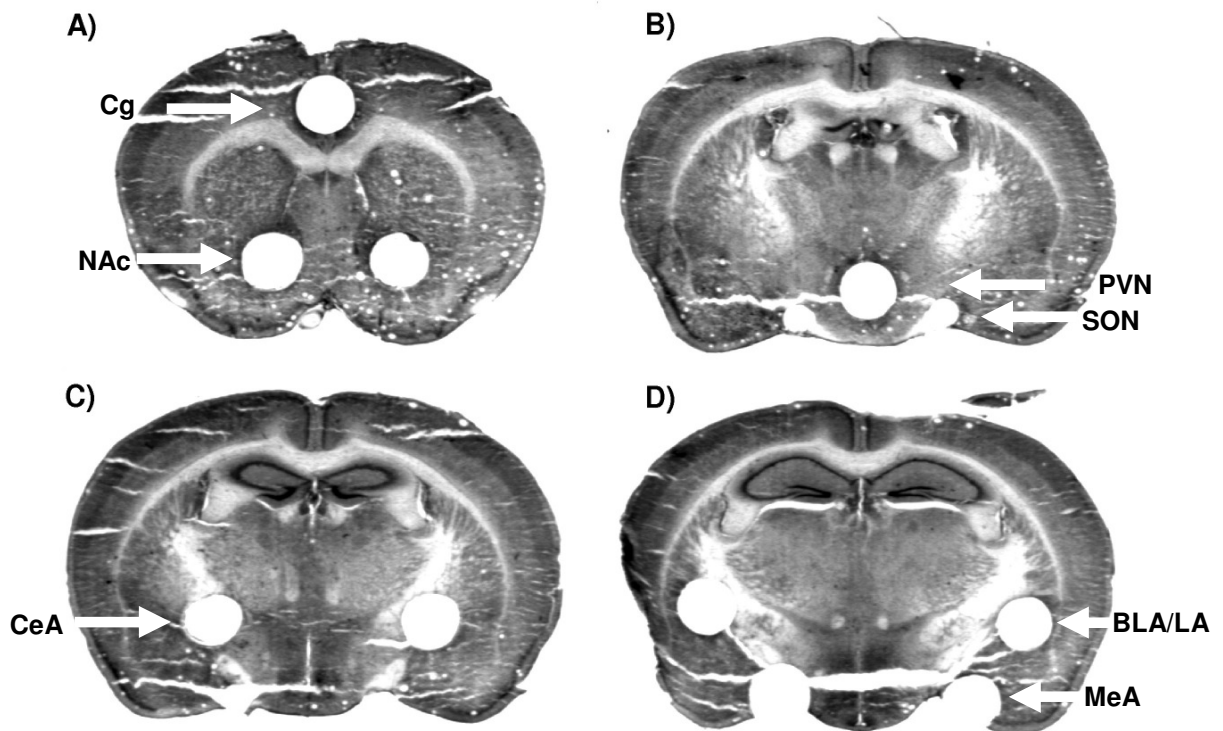


Figure 12: Brain regions acquired by micropuncture from 200 μ m slices. The (A) cingulate cortex (Cg) and *nucleus accumbens* (NAc) from both sides, (B) paraventricular nucleus (PVN) and supraoptic nuclei (SON), (C) central (CeA), (D) basolateral/lateral (BLA/LA) and medial amygdala (MeA).

3.2.2.2. RNA amplification

Amplification of pooled total RNA samples yielded 50-100 μ g of aRNA. The agarose gels revealed similar fragment sizes of aRNA mainly ranging from 500 to 1,500bp in size (Fig. 13).

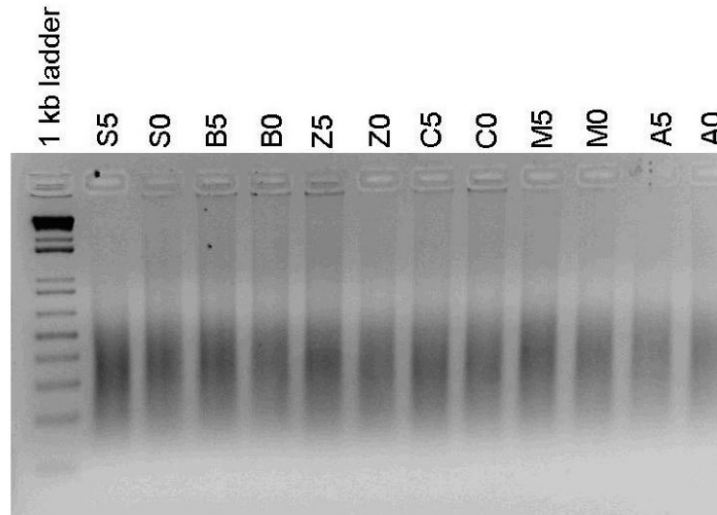


Figure 13: Amplified RNA samples from different brain regions including the supraoptic nuclei (S), basolateral/lateral (B), central amygdala (Z), cingulate cortex (C), medial amygdala (M) and *nucleus accumbens* (A).

3.2.2.3. Differential expression data

The gene expression analyses based on the MPI24K platform resulted in the identification of 30 to 450 genes per brain region that were significantly ($p < 0.05$) differentially regulated between HAB and LAB mice. If the threshold was set to detect genes potentially regulated ($p < 0.1$), seven transcripts were identified to be regulated in all analyzed brain regions, two genes in only six, 23 in five, 74 in four, 204 in three, 545 in two and 1,651 specifically in one brain region, giving a total of 2,507 differentially expressed sequences (excerpt of the list in supplementary table 1). The 19 highest ranking differentially expressed sequences (according to their p-value and number of brain regions, they were found to be differentially expressed in) were selected for further investigation. Additionally, three neuropeptide coding genes were further analyzed that were differentially expressed in at least two brain regions and one gene was extremely differentially expressed (14-fold expression difference in the BLA/LA; Table 11).

Table 11: Gene transcripts selected for further investigation including their fold regulation, the respective p-value and the brain regions, where they were identified. Negative fold regulation values refer to an increased expression in LAB compared to HAB mice, whereas positive values to an increased expression in HAB compared to LAB mice. Cytochrome c oxidase subunits are summarized, as some subunits were higher expressed in HAB and others in LAB mice in at least two brain regions.

Fold regulation	p-value	Brain regions	Gene symbol	Gene name
-8.81	2.00×10^{-4}	BLA/LA	<i>Ttr</i>	transthyretin
-3.47	5.86×10^{-3}	all	<i>Slc25a17</i>	solute carrier family 25, member 17
-2.26	0.02	all \MeA	<i>Ctsb</i>	cathepsin B
-2.26	0.02	all \MeA	<i>Mmp15</i>	matrix metalloproteinase 15



Fold regulation	p-value	Brain regions	Gene symbol	Gene name
-2.00	0.01	all	<i>Zfp672</i>	zinc finger protein 672
-1.89	0.02	all	<i>Glo1</i>	glyoxalase 1
-1.88	0.01	all	<i>5230400G24Rik</i>	RIKEN cDNA 5230400G24 gene
-1.71	0.02	all \BLA/LA and SON	<i>Coro7</i>	coronin 7
-1.66	0.02	all \BLA/LA and SON	<i>Ccdc104</i>	coiled-coil domain containing 104
-1.56	0.03	all \BLA/LA and SON	<i>Ep400</i>	E1A binding protein p400
-1.53	0.01	Cg MeA NAc PVN	<i>Mt1</i>	metallothionein 1
-1.44	0.10	CeA BLA/LA	<i>Npy</i>	neuropeptide Y
-1.42	0.03	MeA PVN SON	<i>Tac1</i>	tachykinin 1
1.74	0.02	all \CeA	<i>Hmgn3</i>	high mobility group nucleosomal binding domain 3
1.80	0.05	PVN SON	<i>Avp</i>	arginine vasopressin
4.36	2.28×10^{-3}	all	<i>Rab6</i>	RAB6, member RAS oncogene family
1.72 or -1.50	0.03	all	<i>Cox6b</i> <i>Cox6c</i> <i>Cox7b</i> <i>Cox8a</i> <i>Cox17</i>	cytochrome c oxidase, subunit VIb1 cytochrome c oxidase, subunit VIc cytochrome c oxidase, subunit VIIb cytochrome c oxidase, subunit VIIla cytochrome c oxidase, subunit XVII

3.2.3. Gene expression profiling on the Illumina platform

3.2.3.1. Tissue laser-microdissection

Laser-microdissection of brain tissue delivered much more accurate results compared to micropuncture (Fig. 12), as the outline of each brain region could be well adapted due to the staining of brain slices (Fig. 14)

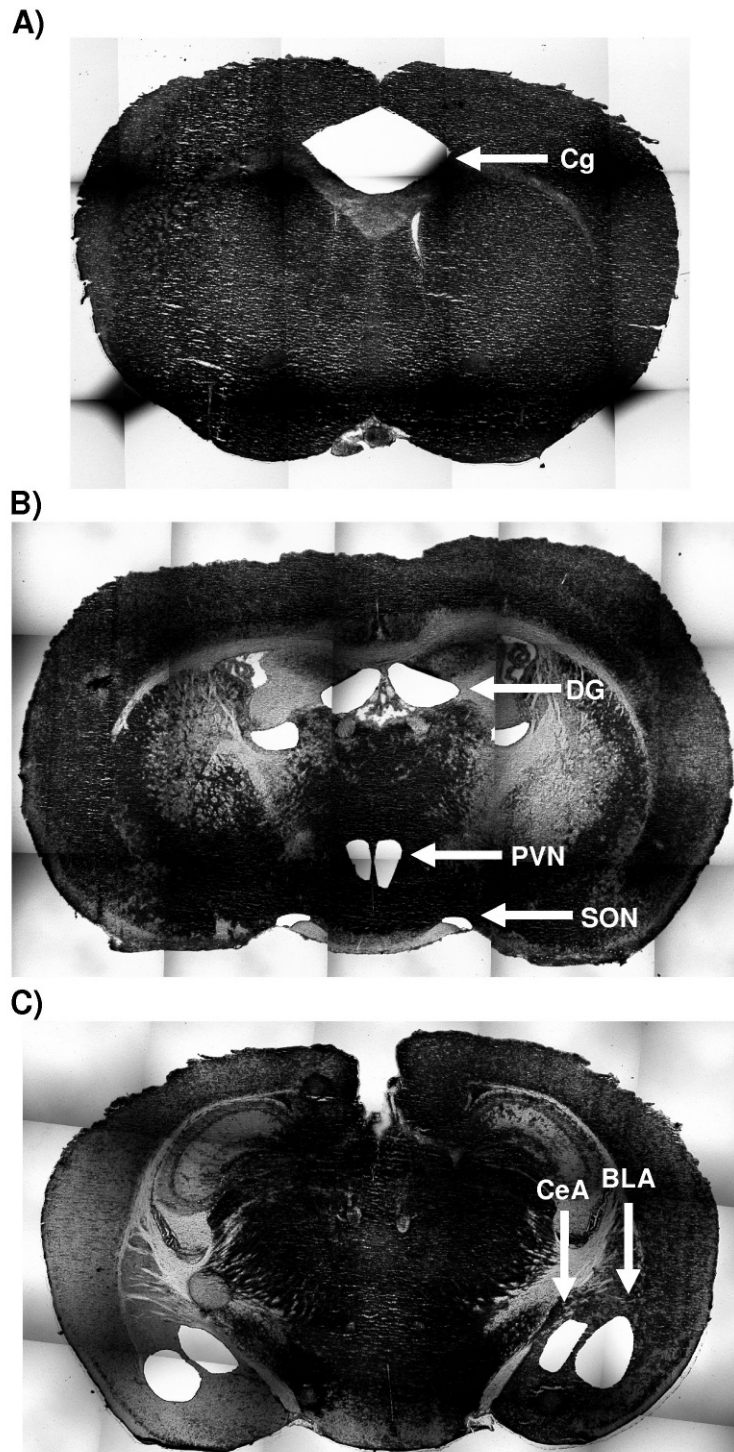


Figure 14: Brain regions acquired by laser-microdissection with the (A) cingulate cortex (Cg), (B) dentate gyrus (DG), hypothalamic paraventricular nucleus (PVN) and supraoptic nucleus (SON) and (C) central (CeA) and basolateral amygdala (BLA).

3.2.3.2. Total RNA isolation and amplification

RNA isolation from the laser-microdissected tissue yielded in average 580ng of total RNA, with the highest amounts isolated from the BLA ($\varnothing = 1,574\text{ng}$) and the lowest from the SON ($\varnothing = 92\text{ng}$). After individual amplification of all samples, only one sample from the SON yielded enough aRNA to process it on the microarray for gene

ATGCTCGCCAGGA
TACGAGCGGTCCT



Results

expression profiling. Therefore, all samples from the SON were excluded from further processing. Some more samples were excluded from a variety of brain regions based on the agarose gel picture of the samples (Fig. 15).

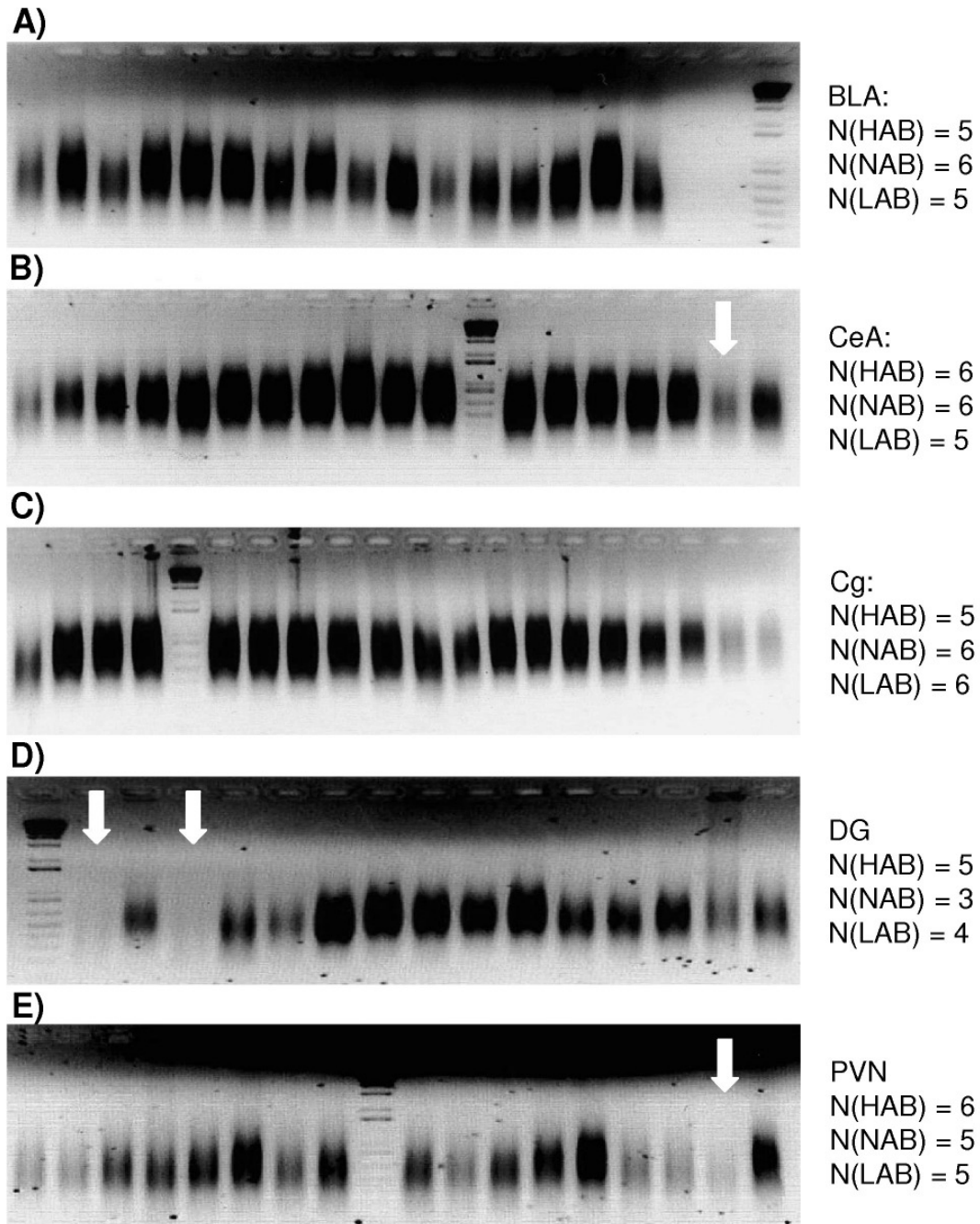


Figure 15: Color inverted agarose gel pictures of all aRNA samples with the respective number of samples per line from the **(A)** basolateral (BLA), **(B)** central amygdala (CeA), **(C)** cingulate cortex (Cg), **(D)** dentate gyrus (DG) and **(E)** hypothalamic paraventricular nucleus (PVN). White arrows indicate samples excluded from further processing.



3.2.3.3. Differential expression data

In the second gene expression analysis experiment based on the Illumina platform, 2770 transcripts were identified to be differentially expressed between HAB and LAB mice (excerpt of the list in supplementary table 2). For about 90% of these transcripts, NAB mice displayed an intermediate expression level or were expressing the transcripts at the same level as HAB or LAB animals. In less than 4% of transcripts, NAB mice showed an increased or decreased expression as compared to both HAB and LAB mice. Additionally, about 959 transcripts could be identified, where only NAB animals showed deviation from the expression levels of HAB and LAB mice. Out of these transcripts, 231 were found to be differentially regulated in all regions, 99 in only four, 125 in three, 296 in two and 2019 specifically in only one brain region. 22 transcripts were further characterized, with 20 found regulated in nearly all regions and a further two regulated rather less strong but specifically in one single brain region (Table 12).

Table 12: Gene transcripts selected for further investigation identified in the Illumina platform-based gene expression profiling including their fold regulation (HAB vs. LAB column), the respective p-value and the brain regions, where they were identified. Negative fold regulation values refer to an increased expression in LAB compared to HAB mice, whereas positive values indicate an increased expression HAB compared to LAB mice. The last column refers to the fold regulation of HAB vs. NAB mice analogous to the first column. Genes identified also on the MPI24K platform are indicated in bold letters.

HAB vs. LAB	p-value	Brain regions	Gene symbol	Gene name	HAB vs. NAB
-14.15	1.33x10 ⁻⁹	all	<i>Enpp5</i>	ectonucleotide pyrophosphatase/ phosphodiesterase 5	-5.05
-12.29	4.88x10⁻³¹	all	<i>Ctsb</i>	cathepsin B	-13.61
-3.58	1.41x10 ⁻⁷	all	<i>Kcnh1</i>	potassium voltage-gated channel 1	-2.59
-2.61	1.95x10⁻⁹	all	<i>Glo1</i>	glyoxalase 1	-1.69
-2.15	4.53x10 ⁻²¹	all	<i>Apbb1</i>	amyloid beta (A4) precursor protein-binding 1	-2.07
-2.03	7.19x10⁻¹²	all	<i>Slc25a17</i>	solute carrier family 25, member 17	-1.92
1.34	0.02	DG	<i>Pxk</i>	PX domain containing serine/threonine kinase	1.43
1.34	0.09	Cg	<i>Tmem132d</i>	transmembrane protein 132D	1.00
1.62	1.89x10 ⁻⁶	all \Cg	<i>Slc1a2</i>	solute carrier family 1, member 2	1.57
1.93	4.34x10 ⁻¹²	all	<i>Dgkq</i>	diacylglycerol kinase, theta	1.00
2.05	1.52x10⁻¹⁶	all	<i>Hmgn3</i>	high mobility group nucleosomal binding domain 3	2.08
2.14	4.38x10⁻²³	all	<i>Pdhb</i>	pyruvate dehydrogenase beta	-1.58
2.14	4.17x10⁻⁸	all	<i>Cox6a2</i>	cytochrome c oxidase	1.23



HAB vs. LAB	p-value	Brain regions	Gene symbol	Gene name	HAB vs. NAB
2.21	3.15x10 ⁻¹²	all	<i>Dgkh</i>	diacylglycerol kinase, eta	2.58
2.57	1.26x10 ⁻¹³	all	<i>Abca2</i>	ATP-binding cassette, sub-family A (ABC1), member 2	1.03
3.46	2.23x10 ⁻¹⁹	all	<i>Aldh3a2</i>	aldehyde dehydrogenase family 3, subfamily A2	1.48
3.60	1.02x10 ⁻²²	all	<i>Gnaq</i>	guanine nucleotide binding protein	3.72
4.05	1.75x10 ⁻¹⁰	all	<i>Hbb-b1</i>	hemoglobin beta adult major chain	3.41
4.05	1.29x10 ⁻³⁷	all	<i>Stx3</i>	syntaxin 3	4.25
4.54	1.23x10 ⁻¹³	all	<i>Gig1</i>	glucocorticoid induced gene 1	1.56
5.23	4.47x10 ⁻⁶	all	<i>2900019G14Rik</i>	RIKEN cDNA 2900019G14 gene	2.16
6.12	1.07x10 ⁻⁹	all	<i>Ttbk1</i>	tau tubulin kinase 1	1.73

3.2.4. Validation of results by quantitative PCR

In whole brain material of female mice, expression differences for six genes from the MPI24K platform array could be confirmed (*Coro7*, *Ctsb*, *Mmp15*, *Mt1*, *Slc25a17*, and *Zfp672*) delivering significant results over all three mouse lines and displaying an overall 2-fold increased expression in LAB compared to HAB mice (Table 13). For two other genes (*Trib2* and *Mbnl1*), originally tested as potential housekeeping genes, significant expression differences were found, too. In genes that were expressed region specifically, no significant differences have been observed in the analysis of whole brain tissue.

Table 13: Gene transcripts analyzed in whole brain tissue from female mice with the relative (rel.) fold expression in HAB, NAB and LAB mice ±SEM, followed by the p-values of the Kruskal-Wallis (KWH) and Mann-Whitney tests (MWU) for HAB vs. LAB, HAB vs. NAB and NAB vs. LAB mice. Statistically significant results are indicated in bold letters.

Gene symbol	Rel. expression HAB ±SEM	Rel. expression NAB ±SEM	Rel. expression LAB ±SEM	KWH	MWU HAB vs. LAB	MWU HAB vs. NAB	MWU NAB vs. LAB
<i>Ccdc104</i>	1.00±0.16	1.06±0.19	1.05±0.12	0.77			
<i>Coro7</i>	1.00±0.19	1.41±0.26	1.79±0.10	0.02	0.01	0.22	0.25
<i>Ctsb</i>	1.00±0.13	1.59±0.31	2.03±0.31	0.03	0.03	0.11	0.36
<i>Ep400</i>	1.00±0.26	1.17±0.25	1.24±0.47	0.71			
<i>5230400G24Rik</i>	1.00±0.13	1.11±0.17	1.26±0.20	0.69			
<i>Mbnl1</i>	1.00±0.23	1.36±0.30	2.05±0.22	0.04	0.03	0.34	0.17
<i>Mmp15</i>	1.00±0.27	2.03±0.45	2.34±0.36	0.03	0.03	0.10	1.00
<i>Mt1</i>	1.00±0.06	2.16±0.66	1.87±0.21	0.01	3.51 x10⁻³	0.11	0.30
<i>Npy</i>	1.00±0.10	1.81±0.54	1.32±0.14	0.35			
<i>Rab6</i>	1.38±0.16	1.12±0.07	1.00±0.20	0.39			
<i>Slc25a17</i>	1.00±0.09	1.47±0.21	1.73±0.15	0.01	0.02	0.11	0.11
<i>Tac1</i>	1.21±0.27	1.43±0.15	1.00±0.17	0.12			



Gene symbol	Rel. expression HAB \pm SEM	Rel. expression NAB \pm SEM	Rel. expression LAB \pm SEM	KWH	MWU HAB vs. LAB	MWU HAB vs. NAB	MWU NAB vs. LAB
<i>Tmem132d</i>	1.00 \pm 0.24	1.16 \pm 0.23	1.26 \pm 0.16	0.68			
<i>Trib2</i>	1.00\pm0.27	2.57\pm0.45	3.06\pm0.49	4.36 $\times 10^{-3}$	0.01	0.02	0.75
<i>Zfp672</i>	1.00\pm0.23	2.23\pm0.32	1.97\pm0.21	0.02	0.05	0.03	0.77

Additionally, in whole brain material from male mice, differential expression of six more genes could be confirmed with remarkably high expression differences between HAB and LAB mice for syntaxin 3 (*Stx3*; 2.26-fold in LAB) ATP-binding cassette, sub-family A (ABC1), member 2 (*Abca2*; 6.16-fold in HAB) and for the RIKEN cDNA 2900019G14 gene (*2900019G14Rik*; 15.90-fold in HAB; Tables 14 and 15). Although differences for some transcripts reached similar tendencies as in the microarray experiment, the differences did not reach statistical significance.

Table 14: Gene transcripts analyzed in whole brain tissue from male mice with the relative (rel.) fold expression in HAB, NAB and LAB mice \pm SEM, followed by the p-values of the Kruskal-Wallis (KWH) and Mann-Whitney tests (MWU) for HAB vs. LAB, HAB vs. NAB and NAB vs. LAB mice. Statistically significant results are given in bold letters.

Gene symbol	Rel. expression HAB \pm SEM	Rel. expression NAB \pm SEM	Rel. expression LAB \pm SEM	KWH	MWU HAB vs. LAB	MWU HAB vs. NAB	MWU NAB vs. LAB
<i>Apbb1</i>	1.00 \pm 0.11	1.05 \pm 0.15	1.28 \pm 0.17	0.21			
<i>Hbb-b1</i>	1.34 \pm 0.16	1.62 \pm 0.27	1.00 \pm 0.15	0.11			
<i>Kcnh1</i>	1.00 \pm 0.11	1.16 \pm 0.20	1.15 \pm 0.15	0.83			
<i>Scl1a2</i>	1.12 \pm 0.14	1.21 \pm 0.23	1.00 \pm 0.14	0.98			
<i>Stx3</i>	1.00\pm0.31	1.34\pm0.07	2.26\pm0.27	0.01	0.08	0.09	0.01

Table 15: Gene transcripts analyzed in whole brain tissue from male mice with the relative (rel.) fold expression in HAB and LAB mice \pm SEM, followed by the p-values of the Mann-Whitney tests (MWU) for HAB vs. LAB mice. Statistically significant results are given in bold letters.

Gene symbol	Rel. expression in HAB \pm SEM	Rel. expression in LAB \pm SEM	MWU HAB vs. LAB
<i>2900019G14Rik</i>	15.90\pm1.70	1.00\pm0.09	4.48$\times 10^{-3}$
<i>Abca2</i>	6.16\pm0.80	1.00\pm0.22	2.70$\times 10^{-3}$
<i>Dgkh</i>	2.01 \pm 0.56	1.00 \pm 0.12	0.29
<i>Dgkq</i>	1.61 \pm 0.59	1.00 \pm 0.18	0.36
<i>Enpp5</i>	2.14\pm0.55	1.00\pm0.03	0.01
<i>Gig1</i>	1.00 \pm 0.12	1.04 \pm 0.13	0.72
<i>Gnaq</i>	1.00 \pm 0.21	1.15 \pm 0.31	0.67
<i>Hmgn3</i>	2.08\pm0.39	1.00\pm0.16	0.03
<i>Pdhb</i>	1.60\pm0.28	1.00\pm0.12	0.06
<i>Pxk</i>	1.31 \pm 0.22	1.00 \pm 0.14	0.27
<i>Tbkl1</i>	1.14 \pm 0.21	1.00 \pm 0.21	0.94



Altogether, the expression differences of twelve genes could be confirmed by qPCR out of the 28 transcripts analyzed irrespective of specific brain regions.

Vasopressin (*Avp*)

Investigation of the *Avp* transcript in the PVN and SON of female HAB, CD1 and LAB mice revealed reduced *Avp* expression in the PVN (Fig. 16A) and SON (Fig. 16B) in LAB compared to HAB or CD1 animals (PVN KWH: $p = 0.03$; MWU: HAB vs. LAB $p = 0.01$, HAB vs. CD1 $p = 0.20$, CD1 vs. LAB $p = 0.57$; SON KWH: $p = 3.89 \times 10^{-3}$; MWU: HAB and CD1 vs. LAB $p = 0.01$, HAB vs. CD1 $p = 0.55$).

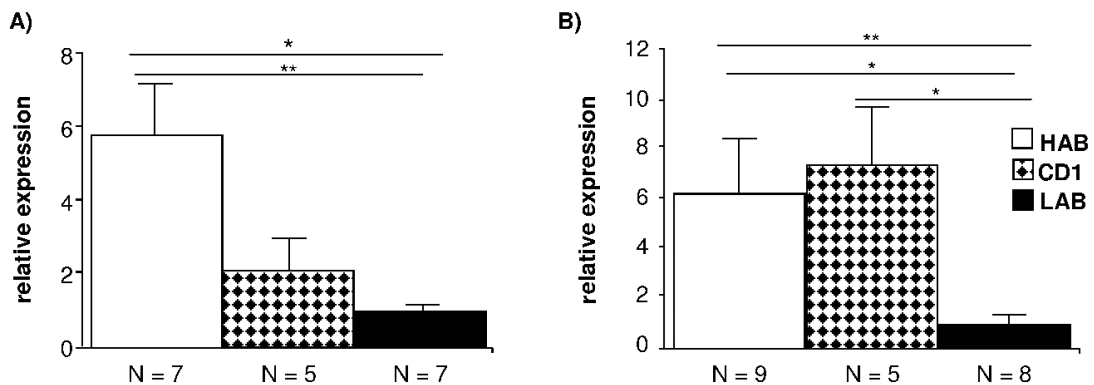


Figure 16: Vasopressin (*Avp*) expression patterns as measured by quantitative PCR in the (A) hypothalamic paraventricular nucleus and (B) supraoptic nucleus of female mice. Data are presented as means +SEM; ** $p < 0.01$; * $p < 0.05$.

qPCR measurements also revealed slightly elevated concentrations of unspliced *Avp* in HAB compared to LAB that, however, failed to reach significance. Correct sequence of the *Avp* intron-specific amplicates was confirmed by sequencing (data not shown).

Tachykinin 1 (*Tac1*)

Not completely in line with the results from the gene expression screening, for *Tac1* transcripts a higher expression could be observed by qPCR in all female mice, but only the results for the basolateral/lateral amygdala and the supraoptic nucleus reached statistical significance (BLA/LA KWH: $p = 0.03$; MWU: HAB vs. LAB $p = 0.03$, HAB vs. CD1 $p = 0.05$, CD1 vs. LAB $p = 0.72$; SON KWH: $p = 6.16 \times 10^{-3}$; MWU: HAB vs. LAB $p = 0.02$, HAB vs. CD1 $p = 0.35$, CD1 vs. LAB $p = 0.02$; PVN KWH: $p = 0.07$; MWU: HAB vs. LAB $p = 0.06$, HAB vs. CD1 $p = 0.25$, CD1 vs. LAB $p = 0.37$; Fig. 16).

ATGCTCGCCAGGA
TACGAGCGGTCT



Results

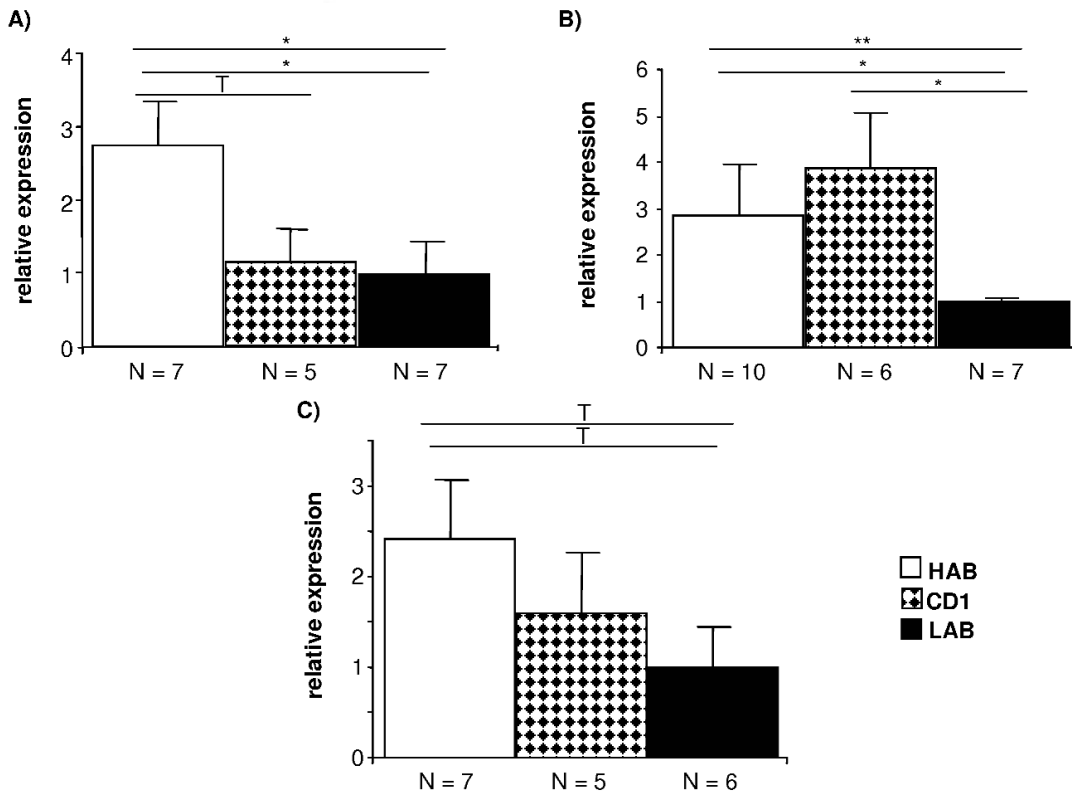


Figure 17: Tachykinin 1 (*Tac1*) expression patterns as measured by quantitative PCR in the (A) basolateral/lateral amygdala, (B) supraoptic nucleus and (C) hypothalamic paraventricular nucleus of female mice. Data are presented as means +SEM; T $p < 0.1$; * $p < 0.05$; ** $p < 0.01$.

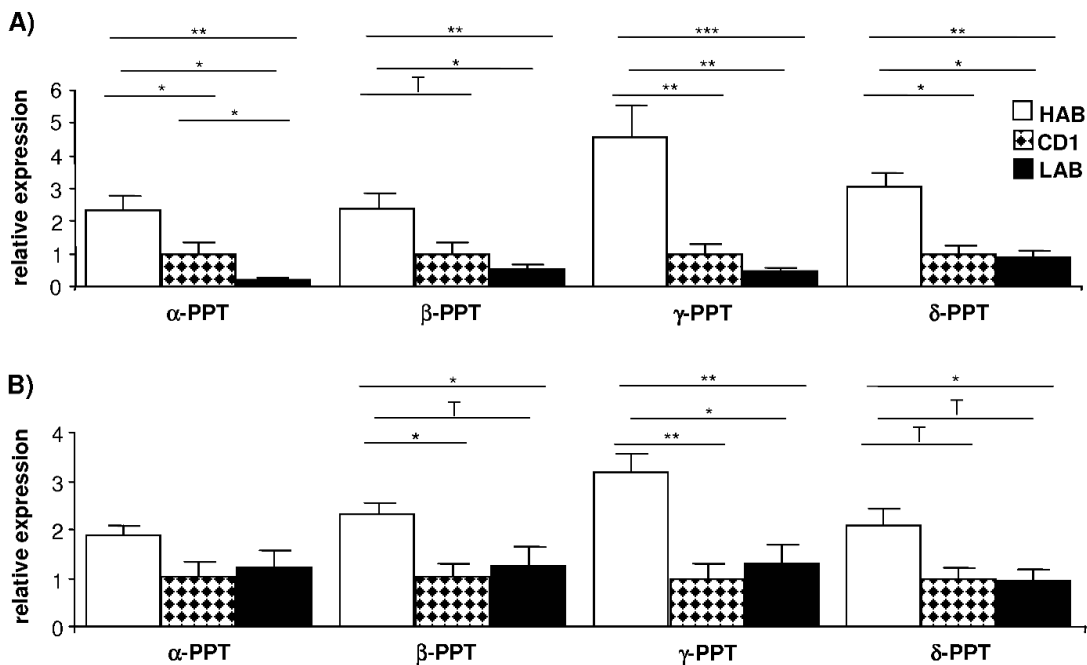


Figure 18: Gene expression levels of tachykinin 1 (*Tac1*) transcript variants (α -, β -, γ - and δ -PPT) in female HAB, CD1 and LAB mice (eight each) in (A) the basolateral/lateral amygdala and (B) the hypothalamic paraventricular nucleus. Data are presented as means +SEM; *** $p < 0.001$; ** $p < 0.01$; * $p < 0.05$; T $p < 0.1$.



Also for the detailed analysis of *Tac1* splicing variants, no significant differences could be observed in the PVN for all transcripts variants. However, in the BLA/LA all four known splicing variants were significantly higher expressed in HAB compared to CD1 and LAB mice (Fig. 18). Especially for the \square -PPT and \square -PPT fragments HAB animals exhibited a 10-fold increased expression compared to LAB mice. Neither for the SON nor for the CeA a differential expression of single transcript variants could be confirmed.

Transmembrane protein 132D (*Tmem132d*)

qPCR analysis further confirmed the significantly increased expression of *Tmem132d* in the cingulate cortex of HAB compared to LAB mice with CD1 animals displaying an intermediate expression level (KWH: $p = 0.02$; MWU: HAB vs. LAB $p = 0.03$, HAB vs. CD1 $p = 0.13$; CD1 vs. LAB $p = 0.14$; Fig. 19).

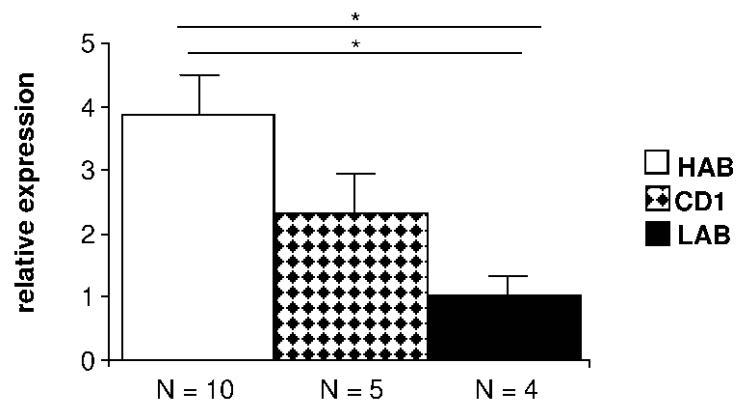


Figure 19: Gene expression levels of the transmembrane protein 132D gene (*Tmem132d*) as confirmed in tissue punches from the cingulate cortex of female HAB, CD1 and LAB mice. Data are presented as means +SEM; * $p < 0.05$.

Transthyretin (*Ttr*)

Gene expression analysis of *Ttr* by qPCR failed to reveal any differences in the BLA/LA between HAB and LAB mice. Although there were two LAB mice that expressed the *Ttr* transcript in excess, in other mice of the LAB group expression levels were under the detection threshold (data not shown).

3.2.5. Effects of selected candidate genes

Further investigation of candidate gene-related phenomena revealed new and significant physiological differences between HAB and LAB mice.



3.2.5.1. Glyoxalase I (GLO1) and metabolic stimulation

3.2.5.1.1. Metabolism and blood plasma parameters

Measurement of food intake over six days in single housed HAB, CD1 and LAB mice demonstrated significantly elevated food intake by 25% in LAB mice compared to both, HAB and CD1 animals (KWH: $p = 2.28 \times 10^{-3}$; MWU: HAB vs. LAB $p = 7.49 \times 10^{-3}$, HAB vs. CD1 $p = 0.56$, CD1 vs. LAB $p = 9.31 \times 10^{-3}$; Fig. 20). However, no significant differences between HAB and LAB mice could be observed, when tested for blood plasma concentrations of lactate, triglycerides, cholesterol, HDL and LDL.

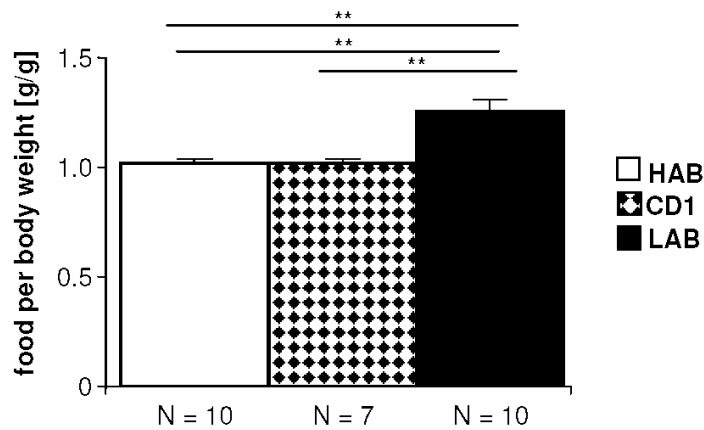


Figure 20: Food consumption of male HAB, CD1 and LAB mice per day and per gram of body weight. Data are presented as means +SEM; ** $p < 0.01$.

3.2.5.1.2. Behavioral manipulation by metabolic stimulation

Control measurements conducted throughout the complete experiment (15 weeks) confirmed that mice fed with 0.5M saccharose showed a significant increase in calorie uptake and likewise increased water consumption. Interestingly, they exhibited decreased food consumption. There was no significant difference detectable between saccharose-soaked and control mice regarding their body weight at any time-point of the experiment (Fig. 21).

As a control parameter of physiological stress caused by dehydration, urine osmolality was assessed and revealed a significant decrease in the 0.5M saccharose-soaked group, with no difference in blood plasma osmolality was (Fig. 22).

The first testing of treated vs. control mice on the EPM revealed a significant increase of the latency to first enter into the open arm (KWH: $p = 0.03$; Fig. 23 C) combined with a decrease in the total time spent on the open arms (KWH: $p = 0.09$; Fig. 23 B).



Treated mice also exhibited a decrease in the percentaged time spent on the open arms, but the difference for this parameter failed to reach significance ($\Delta = 9\%$; KWH: $p = 0.12$; Fig. 23A). The second EPM test showed similar results with only the latency still being slightly reduced in treated mice (KWH: $p = 0.08$; Fig. 23D, E). Locomotion did not differ between the treated and control group as measured by the total distance traveled in the OF (Fig. 23F).

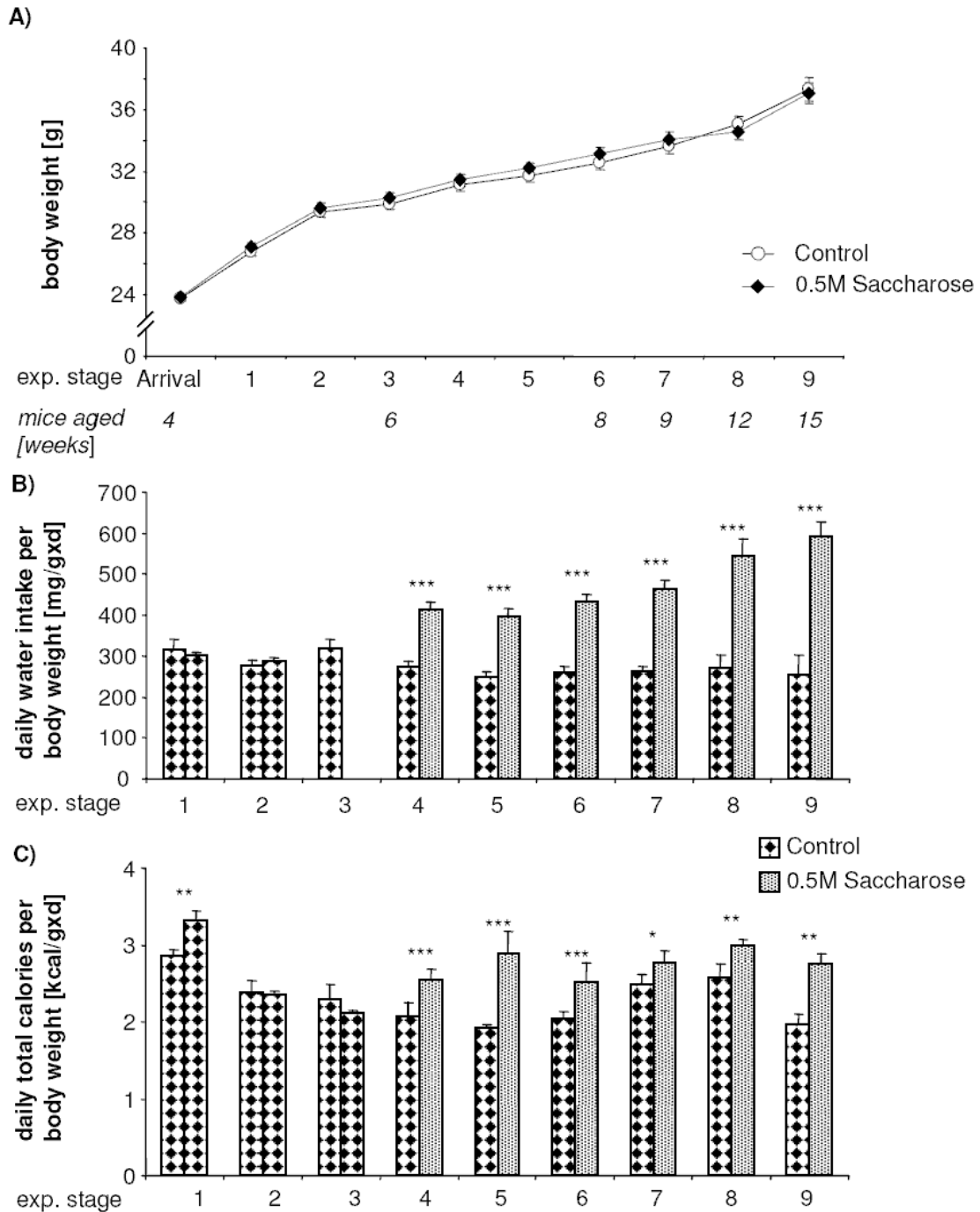


Figure 21: Body weight and metabolic indicators of CD1 mice drinking 0.5M saccharose and controls in the experimental time course. **(A)** The animals' body weight at different experimental stages and their corresponding age in weeks. **(B)** Daily water consumption of the mice at all stages and **(C)** the calculated daily total calorie uptake. Data are presented as means +SEM; *** $p < 0.001$; ** $p < 0.01$; * $p < 0.05$.

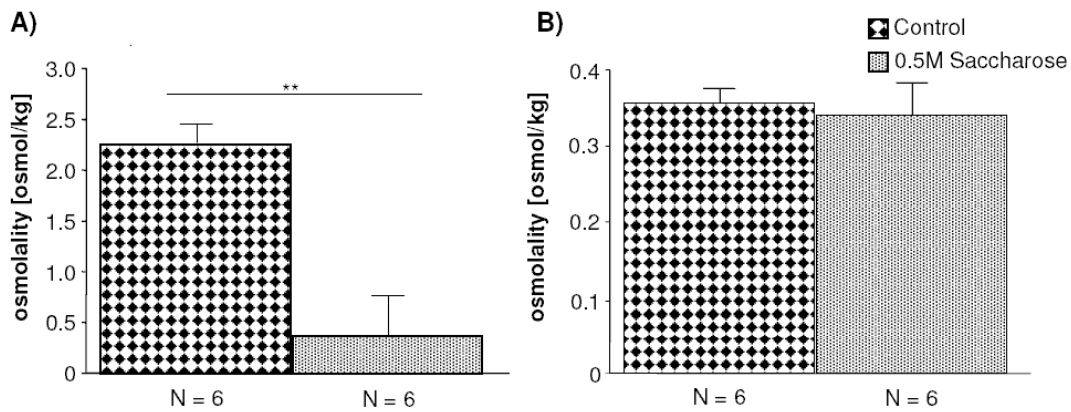


Figure 22: (A) Urine and (B) blood plasma osmolality in CD1 mice soaked with 0.5M saccharose (aq) vs. controls. Data are presented as means +SEM; ** $p < 0.01$.

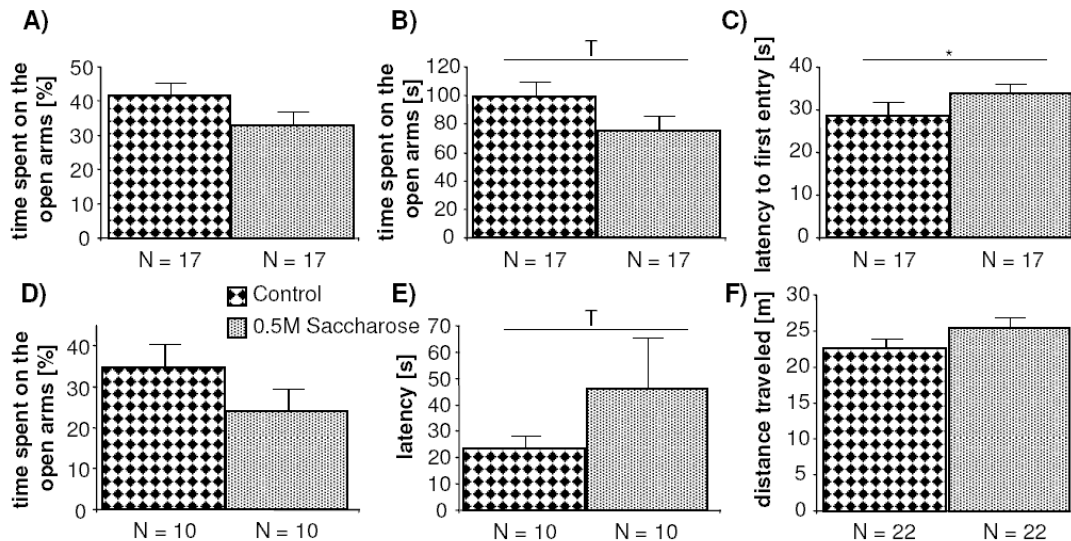


Figure 23: Assessment of anxiety-related behavior and locomotion in CD1 mice soaked with 0.5M saccharose (aq). (A) Anxiety-related behavior as reflected by the percentaged time spent on the open arms of the elevated plus-maze (EPM), mice tested for the first time; (B) Total time spent the open arms of the EPM in mice tested for the first time; (C) Latency time to first enter one open arm of the EPM in mice tested for the first time; (D) Percentaged time spent on the open arms of the EPM, mice tested for the second time; (E) Latency time to first enter one open arm of the EPM in mice tested for the second time; (F) Total distance traveled in the open field as a measure of locomotion. Data are presented as means +SEM; * $p < 0.05$; T $p < 0.10$.

3.2.5.1.3. Western Blot analysis of glyoxalase 1 (GLO1)

The first time point of GLO1 measurement from red blood cells pointed to a decreased expression in the 0.5M saccharose-treated group, failing to show statistical significance but still reaching a trend four weeks after the start of treatment (MWU: $p = 0.08$; Fig. 24A). Interestingly, an effect in the other direction (i.e. an increase in the treated group) was observed in red blood cell extracts taken nine weeks after treatment's start (MWU: $p = 0.09$; Fig. 24B).

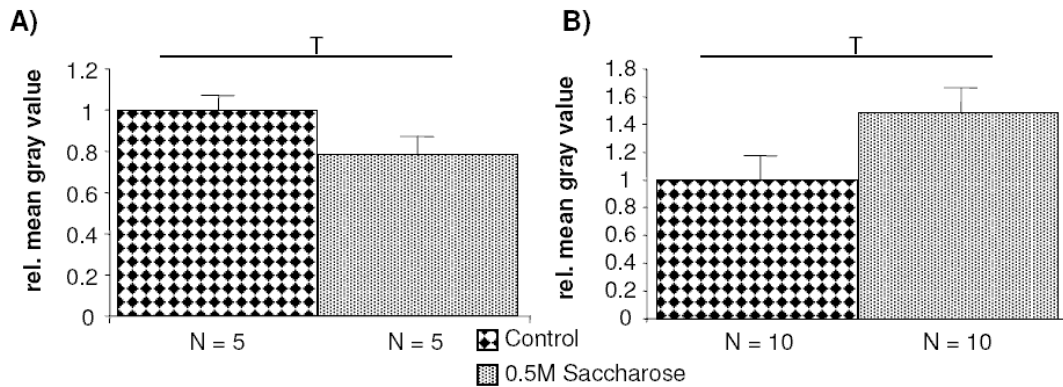


Figure 24: Measurement of glyoxalase I protein from red blood cells by Western Blot of CD1 mice soaked with 0.5M saccharose (aq) **(A)** from five animals after four weeks of elevated calorie uptake and **(B)** of ten mice per group after nine weeks of elevated calorie uptake. Data are presented as means +SEM; T p < 0.10.

3.2.5.2. Tachykinin 1 (*Tac1*) encoded peptides

All measured values for NKB were below the detection limit, but all other peptides could be quantified by ELISA. No significant differences in peptide levels could be identified between HAB, CD1 and LAB mice, neither in the BLA/LA nor in the PVN. The quantity of substances ranged from 100-1,600fmol with the lowest concentrations measured for NPK and the highest for SP. While, in the basolateral/lateral amygdale, SP exhibited the highest level of all peptides ranging from 1,000 to 1,600fmol and all other peptides were present below a level of 500fmol, in the PVN NP γ also reached concentrations of approximately 800 to 1,200fmol for all tested mouse lines. Another interesting result is that in contrast to the BLA/LA, where NKA was found at a level between 200 and 800fmol and NPK only at 100fmol, this proportion was inverted for these two peptides in the PVN (data not shown).

3.2.5.3. Cytochrome c oxidase (COX) activity

Assessing the enzyme activity of the cytochrome c oxidase, significant differences were identified in the BLA and CeA, where HAB displayed increased enzyme activity compared to LAB mice (BLA and CeA MWU: p = 0.02; Fig. 25A, B). A similar tendency was observed for the shell of the NAc (MWU: p = 0.07; Fig. 25C), whereas a decreased activity of cytochrome c oxidase was observed in HAB compared to LAB animals in the PVN (MWU: p = 0.04; Fig. 25D). No difference in enzyme activity was detected in the Cg, the complete NAc or hippocampal regions between HAB and LAB mice.

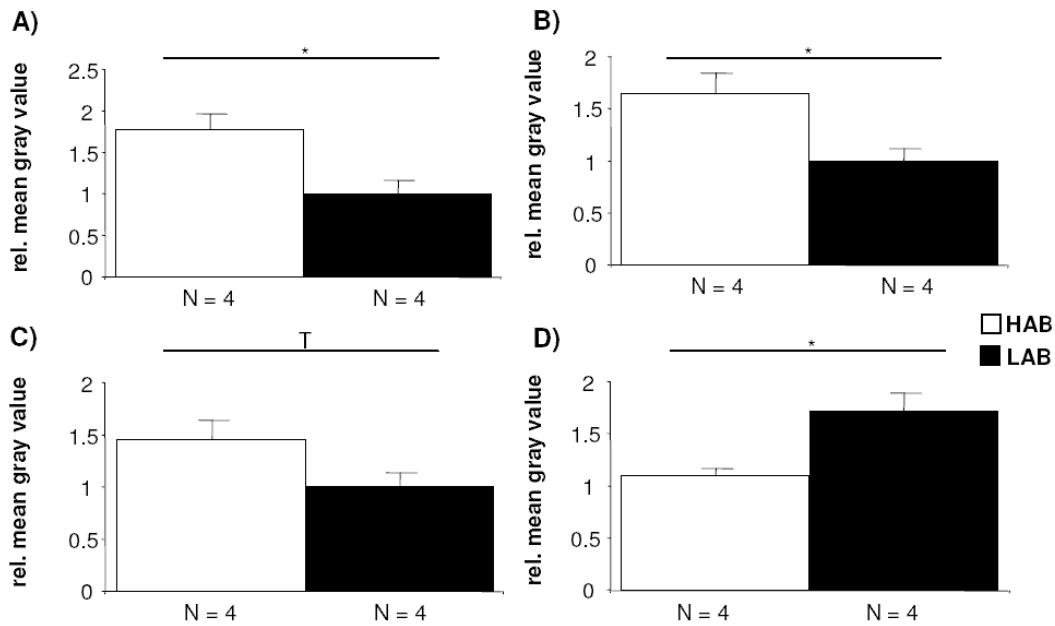


Figure 25: Measurement of cytochrome c oxidase activity in diverse brains regions of HAB and LAB mice in the (A) basolateral amygdala, (B) central amygdala, (C) shell of the *nucleus accumbens* and (D) hypothalamic paraventricular nucleus. Data are presented as means +SEM; * $p < 0.05$; T $p < 0.10$.

3.3. Identification of polymorphisms

3.3.1. Prescreening

Prescreening on the Illumina Mouse Medium Density Linkage Panel resulted in the identification of 235 individual SNPs (Table 4, SNPs with the source code '1') that were found to display opposite homozygous genotypes in HAB vs. LAB mice (i.e. if all HAB mice showed the genotype 'AA', all LAB mice displayed the genotype 'BB'). In detail, 301 autosomal SNPs were identified as having homozygous state in both HAB and LAB animals, but showing an inconsistent state in LAB mice (most SNPs with the same homozygous genotype in LABs, but some showing the opposite genotype). Therefore, when focusing on LAB mice, two well-defined subgroups could be identified, where one subgroup carried the opposite homozygous genotype to HAB mice at 275 loci and the other one at 277. If referred to one of the LAB subgroups, they are termed LAB-A and LAB-B mice. The genotypic difference between the two LAB mouse subgroups included 76 SNPs that left a total of 225 autosomal SNPs as useful markers differing between the HAB and the complete LAB group (Fig. 26A; made up of both subgroups). Additionally, 20 HABxLAB F1 intercross animals also consistently showed a strictly heterozygous genotype for the 225 autosomal SNPs, identified in HAB vs. LAB animals. Results for X-chromosomal markers were analogous.



Further 41 SNPs were identified, where some animals were either hetero- or homozygous, without displaying any consistency between lines or families within these lines. In average, all mice carried about ten SNPs (of the above mentioned 41) heterozygously, displaying no significant difference between the mouse lines (Fig. 26). 30 SNPs were excluded from the analysis as they displayed fluorescence rates below the threshold, over which they can be reassigned reliably (call rate).

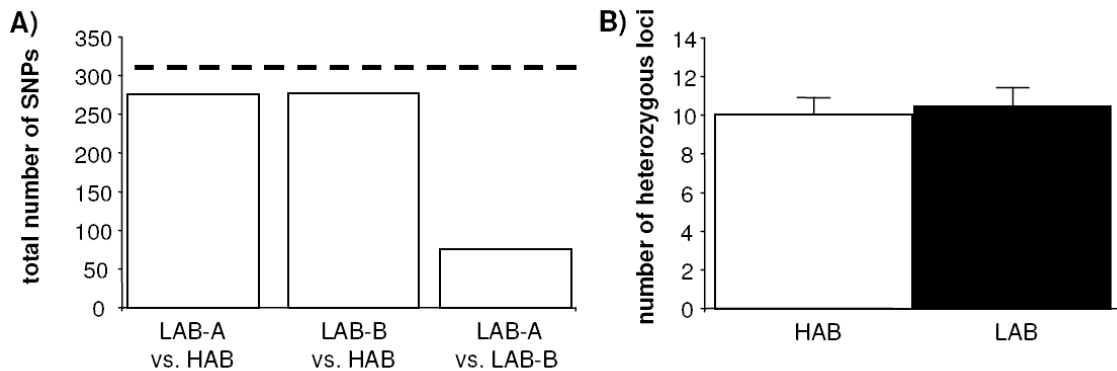


Figure 26: Characterization of HAB and LAB mice based on the screening for 1449 single nucleotide polymorphisms (SNPs). **(A)** The number of SNPs detected as exclusively opposite homozygous between HAB and LAB mice. The dashed line indicates the total number of SNPs, bars show the number of SNPs for comparisons of HAB mice versus both LAB subgroups (LAB-A and LAB-B) and between the two LAB subgroups only. **(B)** The total number of heterozygous SNP loci detected in individual HAB and LAB mice. Data are presented as means +SEM.

3.3.2. Screening of the F2 panel

For 26 SNPs, genotypes could not be reassigned as they displayed low call rates. Thereof 13 SNPs were identified in the prescreening experiment (gnf05.084.686, CEL-7_5627457, CEL-5_87173557, rs13482712, rs13481706, rs13481161, rs13480092, rs13476503, rs3664408, rs3688351, rs3692362, rs4232449, rs6239023), 13 further loci were added to this genotyping-assay (rs30263474, rs3022996, rs30228387, rs29327697, rs26888739, rs13480933, rs32005588, rs31193418, rs31983176, rs32034601, rs32900718, rs33319598, rs29469152).

From the added SNPs to this genotyping-assay (not included in the prescreening experiment), 35 loci delivered genotypes bearing with informative value, i.e. they were showing opposite homozygous genotypes in HAB vs. LAB mice. This includes two SNPs that were identified to be typical for LAB-A mice only. In F2 mice, the distribution of genotypes was not deviating significantly from the expected 1:2:1 ratio for any allele.

Additionally, an X-chromosomal-like distribution of alleles was observed for eleven SNPs (rs6221690, rs6182892, rs3697198, rs13484043, rs13484004, rs13483997,



rs13483894, rs13483765, gnfX.148.995, gnfX.080.189, gnfX.026.801). Examination of their actual genomic position confirmed this hypothesis.

All independent control samples (one HAB and LAB sample each, run once each on every plate), delivered concordant results throughout all assays. 12 control samples from plates 1-6 run on the 8th plate also delivered the same genotypes as before. Altogether, only 89 SNPs showed no informative value concerning the F2 panel, leaving a total of 267 SNPs as valid and stable markers.

Additionally, all HAB and LAB animals could be reassigned to their line based on the distribution of genotypes, also confirming the results of genotyping from the pre-screening experiment.

3.3.3. Genotype frequencies in wildtype CD-1 mice

In contrast to HAB, LAB, F1 and F2 mice, only for 46 loci no variation was detectable at all. For 21 SNPs, the minor allele had a frequency under 10%, for 130 SNPs (42% of all SNPs showing variations) allele frequencies were between 35 and 65%. Significant deviation from Hardy-Weinberg equilibrium was obtained for 13 SNPs in CD1 animals. For 42 SNPs, sequence variation was unique to CD1, but not for any HAB and LAB or HABxLAB F1 intercross mouse. Not one single SNP was detected, where any HAB or LAB breeding-derived animal showed a new variation that has not been found in unselected CD1 mice.

3.3.4. Sequencing of candidate genes

To investigate whether differences in gene expression originated from differences in the sequences of HAB-and LAB-specific alleles, differentially expressed genes were sequenced. In about 50% of genes sequenced, variations between HAB and LAB mice were found in and around the gene loci.

3.3.4.1. Vasopressin (*Avp*)

Sequencing of the *Avp* gene resulted in the identification of nine polymorphic sites, of which eight correspond to SNPs and one comprises a 12bp deletion (Fig. 27).

The upstream promoter region contains two SNPs: T(-2521)C with HABs carrying thymine and LABs cytosine and C(-1422)T with HABs carrying cytosine and LABs thymine. Furthermore, LAB mice miss a 12bp segment mapping to Δ (-2180-2191). The gene-coding locus contains three SNPs: position C(40)T with HABs carrying cytosine and LABs thymine, A(1431)G with HABs carrying adenine and LABs guanine, and T(1527)C with HABs carrying thymine and LABs cytosine. The downstream enhancer region, also referred to as intergenic region between *Avp* and

ATGCTCGCCAGGA
TACGAGCGGTCCT



Results

Oxt, contains three SNPs: A(+399)G with HABs carrying adenine and LABs carrying guanine, T(+476)G with HABs carrying thymine and LABs carrying guanine, and C(+2444)A with HABs carrying cytosine and LABs carrying adenine.

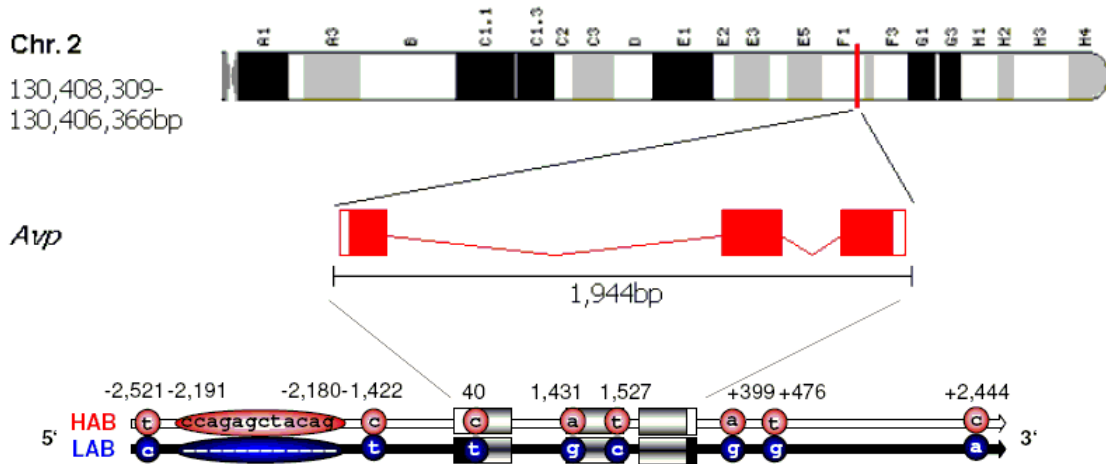


Figure 27: Vasopressin (*Avp*) gene sequence of HAB vs. LAB mice. Polymorphic sites are indicated with positions from transcription start (-1 to -2600bp) in the promoter region (two SNPs and deletion in LABs), within the *Avp* coding sequence from transcription start (1 to 1944bp; three SNPs) and in the downstream enhancer region (+1 to +2600bp; three SNPs). Exons with untranslated regions (UTRs) are indicated by boxes (exons shaded, UTRs completely filled black or white).

For both the C(40)T SNP and the 12bp deletion, NAB and F2 mice always showed the same linkage consisting of three variations: the homozygous HAB-specific combination of alleles (CC) at the 40 locus polymorphism, which appears always associated with the presence of the intact 12bp region of the promoter in both alleles (+/+) the homozygous LAB-specific combination (TT and -/-) or a heterozygous combination (CT and +/-). The most frequent genotype combination in NAB mice was the HAB-specific one (Table 16).

Table 16: Genotype frequencies in a CD1 population (n = 165) for the SNP in the *Avp* signal peptide and the strictly linked promoter deletion. The same strict linkage was obvious in a freely-segregating F2 panel (HABxLAB intercross offspring, n = 508).

Locus (40)	CD1 mice			F2 mice		
	Genotype frequency	Δ (-2191-2180)	Locus (40)	Genotype frequency	Δ (-2191-2180)	Locus (40)
CC	73.30%	+/+	CC	25.90%	+/+	CC
CT	26.10%	+/-	CT	51.90%	+/-	CT
TT	0.60%	-/-	TT	23.20%	-/-	TT



3.3.4.2. Corticotropin-releasing hormone (*Crh*)

No sequence variations have been identified at the *Crh* locus differing between HAB and LAB mice. Only some variations differing between HAB and LAB mice and the reference sequence, that was based on mice from the C57BL/6J strain could be identified (data not shown).

3.3.4.3. Tachykinin 1 (*Tac1*)

Also for the *Tac1* locus, no sequence variations could be identified, that would allow for the discrimination of a HAB vs. LAB mouse line-specific allele.

3.3.4.4. Cathepsin B (*Ctsb*)

In contrast to *Tac1* or *Crh*, many polymorphic loci were identified at the *Ctsb* locus. Altogether, 76 SNPs, eight insertions and nine deletions were found in HAB vs. LAB mice. The definition of insertion or deletion was made in reference to the sequence of the mouse strain C57BL/6J. In the promoter region, ten SNPs and two insertions were found. In the ten exons, eight polymorphic sites (all SNPs) were identified (Fig. 28).

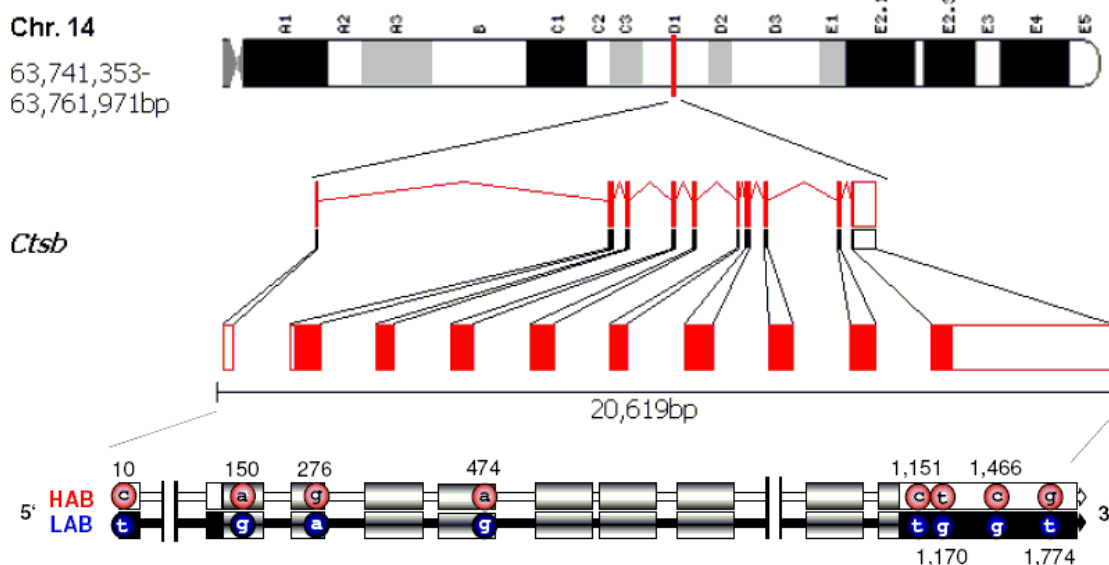


Figure 28: Cathepsin B (*Ctsb*) gene sequence of HAB vs. LAB mice. Polymorphic sites are indicated with positions in the coding sequence from transcription start in the spliced mRNA. Exons and untranslated regions (UTRs) are indicated by boxes (exons shaded, UTRs completely filled black or white).

The vast majority of variations was identified in the introns and the DER (Table 17). Interestingly, in the promoter about six variations are located within 230bp between -2,269 and -2,045bp. Similar proximity of polymorphic sites was found in the third and fourth intron, where also within 550 and 400bp 18 and twelve variations were in



close neighborhood. Additionally, condensation of twelve variable sites could be identified in the DER (at a length of 350bp).

Table 17: Variations identified in the cathepsin B (*Ctsb*) gene. Variation type refers to single nucleotide polymorphisms (SNPs), deletions or insertions, the genomic position to the physical position on chromosome 14, HAB and LAB to their line specific allele, location in the gene to the functional structure of the variation locus (downstream enhancer region: DER), relative (rel.) position to the *Ctsb* locus, position in mRNA to the spliced mRNA and SNP identifier to already described polymorphisms. Functional structures are indicated by horizontal disjunctions.

Variation type	Genomic position	HAB	LAB	Location in the gene	Rel. position	Pos. in mRNA	SNP identifier
SNP	63,739,084	C	T	Promoter	-2,269		
SNP	63,739,124	C	G	Promoter	-2,229		
Insertion	63,739,210	GAGA	-	Promoter	-2,143		
SNP	63,739,257	C	T	Promoter	-2,096		
SNP	63,739,273	C	T	Promoter	-2,080		
SNP	63,739,308	G	A	Promoter	-2,045		
Insertion	63,739,394	C	-	Promoter	-1,959		
SNP	63,739,609	G	A	Promoter	-1,744		
SNP	63,740,071	G	C	Promoter	-1,282		
SNP	63,740,540	C	A	Promoter	-826		rs30963834
SNP	63,740,968	T	C	Promoter	-398		rs30962992
SNP	63,741,271	G	T	Promoter	-95		
SNP	63,741,362	C	T	Exon 1	10	10	rs30962990
SNP	63,741,423	A	G	Intron1	71		rs30962988
SNP	63,752,252	A	G	Exon 2	10,900	150	
SNP	63,752,362	T	C	Intron 2	11,010		
SNP	63,752,540	A	G	Intron 2	11,188		
SNP	63,752,557	C	T	Intron 2	11,205		rs30973898
SNP	63,752,683	C	T	Intron 2	11,331		rs16791841
SNP	63,752,876	G	A	Exon 3	11,524	276	rs16791842
SNP	63,753,119	C	T	Intron 3	11,767		rs16791844
SNP	63,753,163	A	G	Intron 3	11,811		
SNP	63,753,224	A	G	Intron 3	11,872		rs30972751
SNP	63,753,468	T	C	Intron 3	12,116		
SNP	63,753,529	C	T	Intron 3	12,177		
SNP	63,753,684	T	A	Intron 3	12,332		
SNP	63,753,699	C	G	Intron 3	12,347		
SNP	63,753,705	C	T	Intron 3	12,353		
Insertion	63,753,712	A	-	Intron 3	12,360		
SNP	63,753,733	T	A	Intron 3	12,381		
SNP	63,753,745	C	T	Intron 3	12,393		
SNP	63,753,778	C	T	Intron 3	12,426		
Deletion	63,753,885	-	AATAAAT CTAAGAG AAGGATG AGTCACT	Intron 3	12,533		
SNP	63,753,914	G	A	Intron 3	12,562		



Variation type	Genomic position	HAB	LAB	Location in the gene	Rel. position	Pos. in mRNA	SNP identifier
SNP	63,753,930	T	G	Intron 3	12,578		
Deletion	63,753,945	-	TAAAAATAA GCCTGAAG	Intron 3	12,593		
SNP	63,754,102	A	G	Intron 3	12,750		
SNP	63,754,112	C	A	Intron 3	12,760		
Deletion	63,754,125	-	GGAA	Intron 3	12,773		
Insertion	63,754,163	ACA	-	Intron 3	12,811		
SNP	63,754,221	T	C	Intron 3	12,869		
SNP	63,754,227	C	T	Intron 3	12,875		rs30972744
SNP	63,754,228	G	A	Intron 3	12,876		
SNP	63,754,279	C	T	Intron 3	12,927		rs30971633
SNP	63,754,724	G	A	Intron 4	13,372		
Deletion	63,754,741	-	G	Intron 4	13,389		
SNP	63,754,763	T	C	Intron 4	13,411		
SNP	63,754,764	G	C	Intron 4	13,412		
SNP	63,754,866	A	G	Intron 4	13,514		
SNP	63,754,907	A	C	Intron 4	13,555		
SNP	63,754,931	A	T	Intron 4	13,579		
SNP	63,754,948	C	T	Intron 4	13,596		rs30971631
SNP	63,755,037	C	T	Intron 4	13,685		
SNP	63,755,050	C	G	Intron 4	13,698		
SNP	63,755,110	C	G	Intron 4	13,758		
SNP	63,755,122	C	A	Intron 4	13,770		rs30971628
SNP	63,755,186	C	T	Intron 4	13,834		
SNP	63,755,315	A	G	Exon 5	13,963	474	rs13462712
SNP	63,755,474	G	A	Intron 5	14,122		
Deletion	63,755,498	-	T	Intron 5	14,146		
SNP	63,755,500	G	T	Intron 5	14,148		
Deletion	63,756,855	-	AA	Intron 5	15,503		
SNP	63,757,503	T	C	Intron 7	16,151		
SNP	63,758,010	A	G	Intron 8	16,658		
SNP	63,760,454	G	A	Intron 8	19,102		rs30969648
SNP	63,760,495	G	A	Intron 8	19,143		rs30969646
Insertion	63,760,849	CACATGG TTTTGTAG ACAGTTC	-	Intron 9	19,497		
SNP	63,761,222	C	T	Exon 10	19,870	1,151	rs13462709
SNP	63,761,241	T	G	Exon 10	19,889	1,170	
SNP	63,761,536	C	G	Exon 10	20,184	1,466	
SNP	63,761,844	G	T	Exon 10	20,492	1,774	rs13462707
SNP	63,762,117	C	G	DER	+144		
SNP	63,762,512	T	C	DER	+539		
SNP	63,762,597	A	C	DER	+624		
SNP	63,762,653	A	G	DER	+680		rs30967661
SNP	63,762,668	A	C	DER	+695		
SNP	63,762,783	T	A	DER	+810		rs30967657
SNP	63,763,038	C	A	DER	+1,065		



Variation type	Genomic position	HAB	LAB	Location in the gene	Rel. position	Pos. in mRNA	SNP identifier
SNP	63,763,124	C	T	DER	+1,151		rs30967655
SNP	63,763,140	C	T	DER	+1,167		rs30966673
Insertion	63,763,172	CA	-	DER	+1,199		
Deletion	63,763,184	-	TC	DER	+1,211		
SNP	63,763,230	A	C	DER	+1,257		
Deletion	63,763,303	-	TTA	DER	+1,330		
SNP	63,763,356	C	T	DER	+1,383		
Insertion	63,763,385	CC	-	DER	+1,412		
Deletion	63,763,400	-	GTTT	DER	+1,427		
SNP	63,763,441	C	G	DER	+1,468		
SNP	63,763,452	A	C	DER	+1,479		
SNP	63,763,470	A	G	DER	+1,497		
SNP	63,763,474	A	G	DER	+1,501		
Insertion	63,763,662	ATA	-	DER	+1,689		
SNP	63,763,715	A	G	DER	+1,742		

3.3.4.5. Metallothionein 1 (*Mt1*)

Comparison of the HAB and LAB mouse sequences at the *Mt1* locus failed to reveal any differences.

3.3.4.6. Transmembrane protein 132D (*Tmem132d*)

By sequencing *Tmem132d*, several polymorphic loci could be identified, among them, two SNPs in the promoter of the gene at positions A(-519)G and A(-310)G.

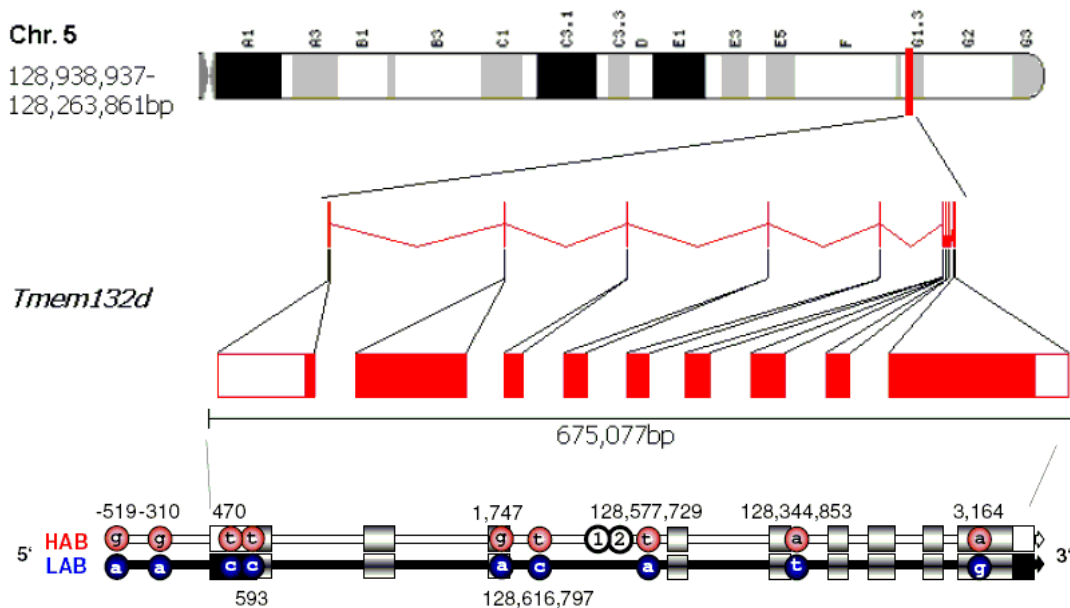


Figure 29: Transmembrane protein 132D (*Tmem132d*) gene sequence of HAB vs. LAB mice. Polymorphic sites are indicated with minus sign for promoter positions in bp, with positions in the coding sequence from transcription start in the spliced mRNA (in bp) or with chromosomal positions for single nucleotide polymorphisms in introns (in bp). Exons and untranslated regions (UTRs) are indicated by boxes (exons shaded, UTRs completely filled)



black or white). Unfilled circles with numbers '1' and '2' refer to two deletions in HAB mice. For '1' at position 128,577,978bp (deletion of CAAA) and '2' at position 128,577,906 (deletion of ACA).

Four further SNPs were identified located in exons, with C(470)T and C(573)T in the untranslated region and A(1,747)G in exon 3 (also known as rs36596918) and A(3,164)G in exon 9 (rs13478518) as part of the protein coding sequence. Furthermore, three SNPs and 2 deletions were discovered in introns, among them C(128,616,797)T (rs13478520), A(128,577,729)T, Δ (128,577,906-128,577,903) and Δ (128,577,978-128,577,974) in the third and T(128,344,853)A in the fifth intron (Fig. 29).

3.3.4.7. Further sequencing results

2900019G14Rik amplicates from qPCR were also sequenced, as qPCR resulted in well detectable products. All products showed slightly shifted melting peaks, when analyzing the melting curves, with HAB animals displaying a slightly decreased melting peak temperature. Sequencing of the 137bp-sized amplicate resulted in the identification of two SNPs, C(90)A and C(110)T (positions relative to the amplicon's sequence; Fig. 30).

```
AGAGTATTTTC      TCGTTTCAT  GTGACCTGAG  TGAAGAACTT      AACCTAGAAA
CCCCTGTACT       CATTATTGTT TGCAAATCTC  TGAGTCCAG[C/A]  ACCTTTGTAA
ATACAGCCC[C/T]  GAGGAGGAAT GGGGGTGAAT  GTGTTTA
```

Figure 30: Sequence of the RIKEN cDNA 2900019G14 gene amplicate generated by quantitative PCR.

3.3.5. The effects of polymorphisms

Analysis of the identified SNPs of sequenced genes in the coding sequence revealed that most SNPs in *Ctsb*, *Tmem132d* and *Avp* were synonymous mutations at the third (degenerate) codon. The only exceptions to that are C(40)T and G(1747)A. Whereas C(40)T is located in the coding sequence of the AVP signal peptide, resulting in the change of the amino acid residue from alanine to valine and G(1747)A in *Tmem132d* causing the substitution of an arginine residue by lysine.

A detailed *in silico* search for potential transcription factor binding sites at the polymorphic loci at the *Avp* locus led to the identification of a number of candidates that are summarized in Table 18.

For the polymorphisms in *Tmem132d*, TGA[A/G]CT was identified as a possible binding site for the glucocorticoid receptor (locus referred to as glucocorticoid response element – GRE). The mentioned polymorphism is the A(-310)G, with LAB



animals carrying the A, HAB mice the G allele homozygously. Additionally, at the A(-519)G locus, where also LAB mice carry the A and HAB animals the G allele homozygously, the LAB-specific sequence creates a binding site for a repressor (E12), whereas the HAB-specific site for a transcription factor (NF1).

In *Ctsb* at position A(-2045)G a binding site for CBF1 was predicted that would increase binding in in LAB, but not in HAB mice. Same applies to T(-95)G, where binding of WT1 would be possible in LAB but only at decreased efficiency in HAB mice.

Table 18: Polymorphisms in the promoter and downstream enhancer region of *Avp* between the HAB and LAB specific sequence, with probable binding factors.

Polymorphism	1 st binding factor	2 nd binding factor	Reference
T(-2521)C	NF-1	C/EBPalpha	Kraus <i>et al.</i> , 2001
Δ(-2180-2191)	NF-1	C/EBPbeta	Ji <i>et al.</i> , 1999
C(-1422)T	---	---	---
A(+399)G	c-Ets-2	C/EBPbeta	Chakrabarty and Roberts, 2007
T(+476)G	AP-1 / GATA-1	---	---
C(+2444)A	---	---	---

3.3.6. Allele-specific transcription analyses of vasopressin (*Avp*)

To obtain evidence for a functional role of the polymorphisms in *Avp* contributing to different levels of expression in LAB versus HAB mice, the activity of each allele was studied in an F1 cross between these two lines. Under this condition, both alleles were contained in the same cellular background, thus eliminating differential synaptic input as a confounding factor. Assessing the allele-specific transcription rate, the LAB-specific allele displayed a significantly decreased expression relative to the HAB-specific one in the PVN and SON ($p=1.4 \times 10^{-4}$; Fig. 31). This is consistent with *Avp* mRNA expression data of LAB versus HAB mice (see Fig. 16).

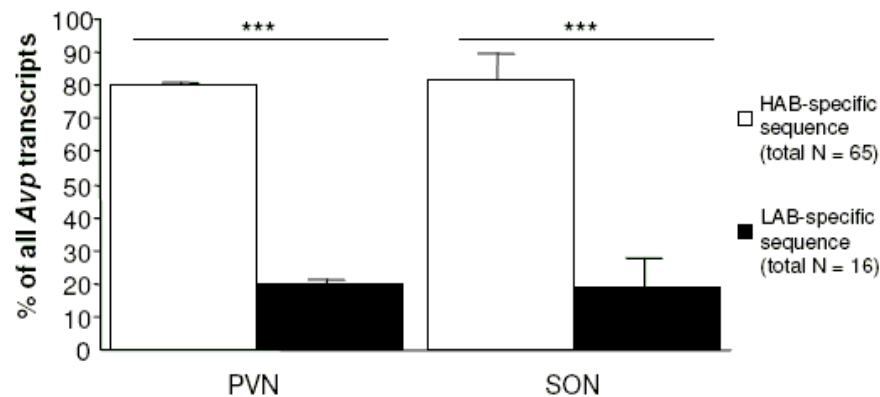


Figure 31: Proportion of HAB vs. LAB allele-specific vasopressin (*Avp*) transcripts from heterozygous F1 (HABxLAB intercross) mice in the paraventricular nucleus (PVN; $\chi^2=14.4$) and the supraoptic nucleus (SON; $\chi^2=15.2$). Data are shown as means +SEM; *** $p < 0.001$.



3.4. Association and linkage of SNPs with behavioral parameters

To further test the functional involvement of the identified SNPs, all SNP loci from the Illumina experiment with the custom-designed oligo pool were associated with a variety of behavioral parameters (excerpt in supplementary table 3).

Most significant and interesting results were obtained for SNPs in *Enoph1*, *Tmem132d*, *Zfp672*, near methionine sulfoxide reductase B2 (*Msrb2*), in *Avp* and hornerin (*Hnrn*).

For *Enoph1*, SNPs in a total of 514 male mice, 111 animals were identified as carrying the HAB-typical SNPs rs13460000 and rs13460001 (GG and CC), 116 animals the LAB-typical AA and TT, and 287 animals the heterozygous AG and CT genotypes. If these SNPs impact on anxiety-related behavior, homozygous GG and CC F2 animals should behave more anxious than their AA and TT counterparts. Indeed, a co-segregation could be detected with AA and TT mice being less anxious on the EPM ($p = 1.05 \times 10^{-6}$) and tending to show reduced depression-like behavior in the tail suspension test, although failing to reach statistical significance ($p = 0.23$; Fig. 32).

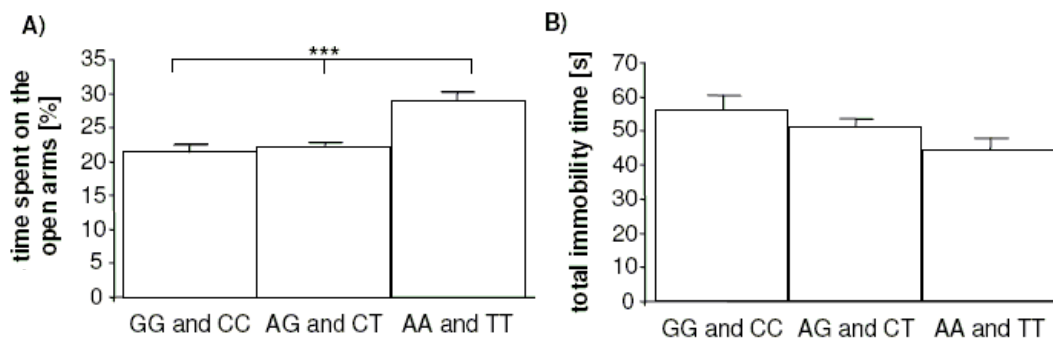


Figure 32: Association between anxiety-related and depression-like behavior and enolase-phosphatase 1 (*Enoph1*) genotypes in the freely-segregating F2 panel. Phenotypic indices of male F2 mice with HAB-specific *Enoph1* genotypes GG and CC (HAB-specific homozygotes, N = 113), AG and CT (heterozygotes, N = 292), or AA and TT (LAB-specific homozygotes, N = 117). **(A)** Percentaged time spent on the open arms of the elevated plus-maze (EPM) and **(B)** total immobility time in the tail suspension test. LAB-specific homozygotes were less anxious and also displayed less immobility, although failing to reach statistical significance. Data are presented as means +SEM; *** $p < 0.001$.

The functional impact of *Tmem132d* was substantiated by the association analysis, where rs13478518 located in exon 9 of *Tmem132d* was found to be associated with anxiety-related behavior on the EPM ($p = 9.80 \times 10^{-4}$), with less anxious animals carrying the LAB-specific (i.e. GG) and more anxious ones the HAB-specific (i.e. AA) genotype (Fig. 33). Both depression-like behavior and locomotor activity failed to show an association (data not shown).

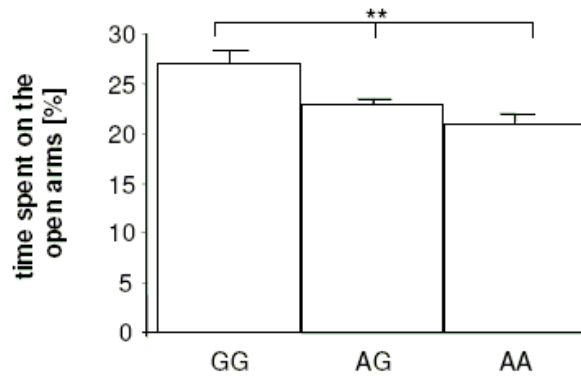


Figure 33: Association between anxiety-related behavior and the transmembrane protein 132D (*Tmem132d*) genotypes in the freely-segregating F2 panel. Phenotypic indices of male F2 mice with LAB-specific *Tmem132d* genotypes GG (LAB-specific homozygotes, N = 128), AG (heterozygotes, N = 276) or AA (HAB-specific homozygotes, N = 118). Percentaged time spent on the open arms of the elevated plus-maze (EPM). LAB-specific homozygotes were less anxious. Data are presented as means +SEM; ** p < 0.01.

Anxiety-related behavior as reflected by the percentaged time spent on the open arms of the EPM also delivered a significant linkage with a SNP (rs29402173) in the 3' UTR of *Zfp672*. Whereas animals bearing the HAB-specific variant (GG) displayed high anxiety-like behavior, mice with the LAB-specific genotype (AA) were less anxious (p = 1.18x10⁻⁹; Fig. 34). Also in this case locomotor activity and depression-like behavior did not reveal any significant differences between animals bearing different genotypes (data not shown). *Zfp672* was identified in the microarray and qPCR analyses as differentially regulated between HAB and LAB mice.

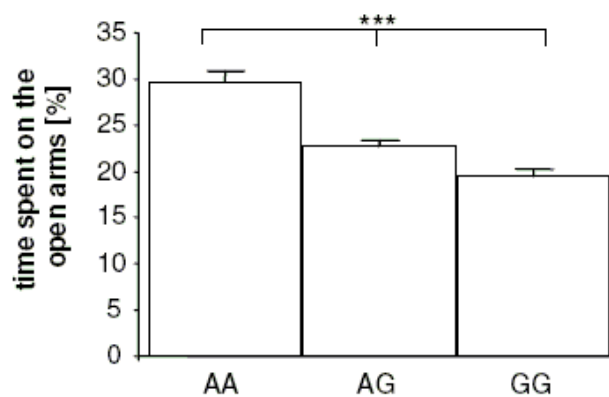


Figure 34: Association between anxiety-related behavior and the zinc finger protein 672 (*Zfp672*) genotypes in the freely-segregating F2 panel. Phenotypic indices of male F2 mice with LAB-specific *Zfp672* genotypes AA (LAB-specific homozygotes, N = 117), AG (heterozygotes, N = 271), or GG (HAB-specific homozygotes, N = 134). Percentaged time spent on the open arms of the elevated plus-maze (EPM). LAB-specific homozygotes were less anxious. Data are presented as means +SEM; *** p < 0.001.

A polymorphism, rs13476366, near (approximately 1,500bp downstream) *Msrb2*, exhibited very high association with depression-like behavior as reflected in both,



the TST ($p = 4.66 \times 10^{-19}$; Fig. 35A) and the FST ($p = 1.23 \times 10^{-37}$; data not shown). F2 mice carrying the HAB-specific (CC) genotype homozygously, spent significantly more time immobile or floating as their counterparts carrying TT. Interestingly, locomotor activity was significantly elevated in the CC carrying group by 25% compared to the TT carrying group ($p = 3.38 \times 10^{-7}$; data not shown). Also anxiety-related behavior was attenuated, but in the group carrying the HAB-specific CC genotype ($p = 3.73 \times 10^{-4}$; Fig. 35B). This polymorphism maps to a location, where also another gene, *Abca2*, is in close neighborhood (and in the SNP screening with the Illumina custom designed oligo pool, this SNP was the closest to *Abca2*) that was also detected in the microarray and qPCR analysis as differentially regulated.

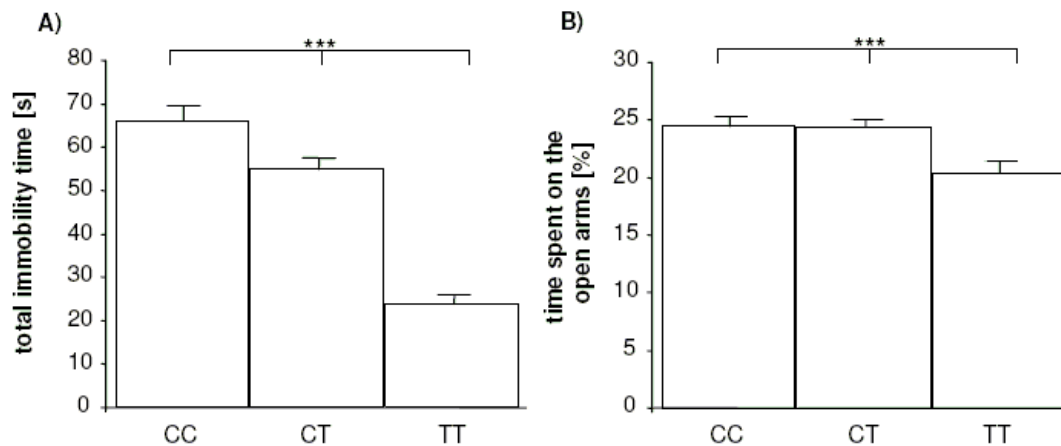


Figure 35: Association between depression-like, anxiety-related behavior and rs13476366 genotypes in the freely-segregating F2 panel. Phenotypic indices of male F2 mice with LAB-specific TT genotypes (LAB-specific homozygotes, N = 121), CT (heterozygotes, N = 249), or CC (HAB-specific homozygotes, N = 152). **(A)** Total immobility time in the tail suspension test of F2 mice with the respective genotypes and **(B)** percentaged time spent on the open arms of the elevated plus-maze (EPM). LAB-specific homozygotes were more anxious, but displayed attenuated depression-like behavior. Data are presented as means +SEM; *** $p < 0.001$.

The *Avp*-related polymorphisms were also assessed in a total of 258 male mice with HAB grandmothers, 67 animals were identified as carrying the HAB-typical polymorphisms positive for the 12bp deletion and C(40)T (+/+ and CC), 49 animals the LAB-typical -/- and TT, and 142 animals the heterozygous +/- and CT genotypes. If these polymorphisms impact on anxiety-related behavior, homozygous -/- and TT F2 animals should behave less anxious than their +/+ and CC counterparts. Indeed, a co-segregation could be detected with -/- and TT mice being significantly less anxious on the EPM ($p = 0.01$; Fig. 36A). Importantly, this association between genetic polymorphisms and anxiety levels was independent of locomotor activity, as measured in the open field (Fig. 36B). In the remaining 250 F2 male mice with LAB grandmothers no association was detectable (data not shown). The allele frequency in the F2 panel roughly reflects a 1:2:1 distribution (Table 16).

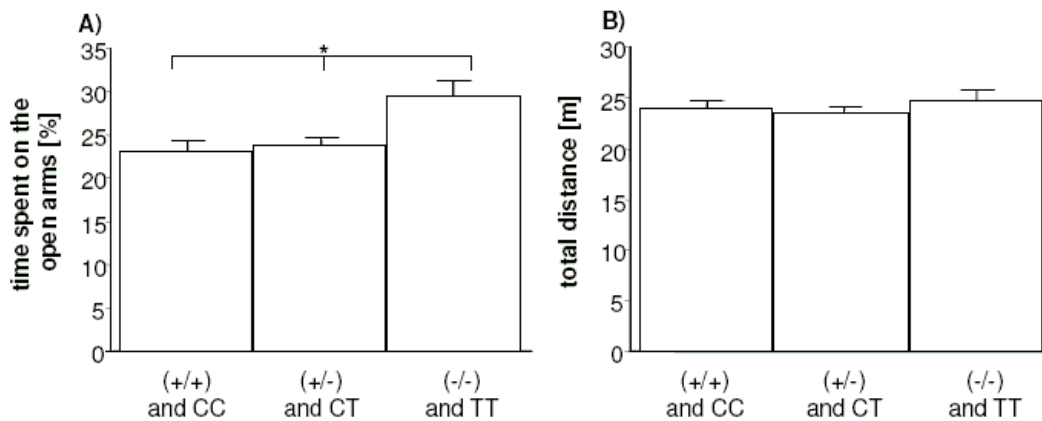


Figure 36: Association between anxiety-related behavior and the vasopressin (*Avp*)-related genotypes in the freely-segregating F2 panel. Phenotypic indices of male F2 mice with HAB grandmothers and *Avp*-related genotypes (+/+) and CC (HAB-typical homozygotes, n = 67), (+/-) and CT (heterozygotes, n = 142), or (-/-) and TT (LAB-typical homozygotes, n = 49). **(A)** Percentaged time spent on the open arms of the elevated plus-maze (EPM) and **(B)** total distance traveled in the open field (OF). LAB-typical homozygotes were less anxious, independent of locomotor activity. Data are presented as means +SEM; * p < 0.05.

Genotype-phenotype association also revealed a significant linkage of a SNP (rs13477268) located 1,500bp downstream hornerin (*Hrrr*) with CORT response to a stressor as measured from the blood plasma. F2 mice carrying the HAB-specific AA genotypes displayed a strongly attenuated increase in blood plasma CORT concentrations, in contrast to their counterparts bearing the LAB-specific GG genotype ($p = 1.20 \times 10^{-50}$; Fig. 37).

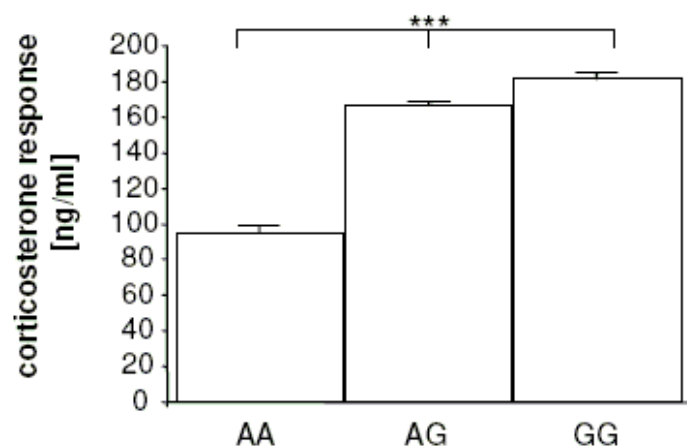


Figure 37: Association between corticosterone increase in blood plasma after restraint stress and rs13477268 genotypes in the freely-segregating F2 panel. Phenotypic indices of male F2 mice with LAB-specific GG genotypes (LAB-specific homozygotes, N = 128), AG (heterozygotes, N = 274), or AA (HAB-specific homozygotes, N = 120). Data are presented as means +SEM; *** p < 0.001.



4. Discussion

In the present study, it has been shown that anxiety-related and depression-like behaviors are adequately mirrored in the HAB/LAB mouse model on a complex multigenic basis. A quite solid genetic background underlying the behavioral trait can be testified for HAB and assumed for LAB mice, as the results of the rHAB-breeding suggests.

Furthermore, 30 candidate genes for anxiety-related (and depression-like) behavior have been identified and elaborated using microarray-based gene expression profiling and further validation either by qPCR or by testing peptide levels, enzyme activity or the influence of gene products on further physiological parameters. Thereby, 14 gene transcripts weathered all tests as possible candidates for anxiety. Among them, *Slc25a17*, *Stx3*, *Abca2*, *Avp*, *Zfp672*, *Tac1* and *Ctsb* exhibited the most convincing effects and are already described (not necessarily in connection to psychiatric disorders), whereas others like *2900019G14Rik* or *Tmem132d* are not described at all yet.

Although many gene products were found to be regulated in metabolic pathways, their regulation in the brain failed to affect the whole organism's physiology, as – except for the higher amount of food consumption in LAB compared to HAB or CD1 mice – many metabolism-related parameters in the blood plasma did not reflect any differences between HAB and LAB mice. Additionally, an approach to influence behavior by a forced enhancement of metabolism via feeding with 0.5M saccharose solution only showed very moderate effects on the animals' anxiety-related behavior. This might be also attributed to the multifactorial nature of behavioral regulation.

Basic analysis of CD1 mice revealed a predictability for SNPs based on inbred strain comparisons, but also showed that HAB and LAB mice have lost more than 70% of the variability in CD1.

Additionally, sequencing of candidate genes mentioned above, shed light on variations in the genome that might influence gene expression, by either enhancing or repressing gene expression, affecting mRNA stability, translation efficiency or enzyme activity.

Screening for variations in the DNA sequences of HAB and LAB mice that would allow for a causal association of single chromosomal regions with selected phenotypes, resulted in the identification of 267 SNPs as viable markers for this purpose. These associations in F2 mice revealed among others a high influence of regions on chromosomes 5 and 11 on anxiety-related behavior, as reflected by the EPM, with genes involved, that have been either characterized by qPCR before



(*Zfp672* and *Tmem132d*), or were highlighted in other studies assessing qualitative differences (*Enoph1*). Further causal associations of single chromosomal regions were detected for depression-like behavior (chromosome 2) and the level of CORT increase in blood plasma in response to a stressor (chromosome 3).

Reversing the HAB phenotype

With the HAB and LAB mouse lines, an animal model has been established, that reflects anxiety-related behavior in a number of behavioral paradigms, including the EPM (selection criterion) and additionally depression-like behavior as reflected by the TST or FST (Kessler *et al.*, 2007; Kromer *et al.*, 2005; Landgraf *et al.*, 2007). As breeding of these mice has now been performed for more than 20 generations with the inbreeding starting as of G8, with G28 a complete inbred status would have been achieved by definition. Therefore, mice of G23 were selected to serve as the basis of rHAB mice, to analyze, if the remaining genetic variance in HAB mice would still be enough to reverse the highly anxious towards a less anxious phenotype. The results suggest on the one hand, that still prevailing variability in HAB mice would be enough to shift the phenotype towards a less anxious behavioral range as reflected by EPM data. On the other hand, behavioral effects on the rHAB-breeding only reached statistical significance with the 7th generation of the reversal of the selection criterion and only in male but not in female mice. However, the level of anxiety was still in a range, which is still considered as high anxiety-related behavior, as even in the HAB/LAB breeding, average anxiety in HAB mice only developed below 15% starting at the 6th generation (Kromer *et al.*, 2005). Also in a recently finished study dealing with the reproduction of the HAB/LAB lines starting from new independent CD1 animals, which was planned and performed as a short-term breeding, the mean value of the percentaged time spent on the open arms of the EPM firstly reached a range around 15% in the 6th and 7th generation (Salvamoser, 2008). As most studies dealing with short-term selective breeding consider the 4th or 5th generation of offspring already as individuals with fully developed phenotype (Belknap *et al.*, 1997; Hitzemann *et al.*, 2008; Palmer *et al.*, 2005; Ponder *et al.*, 2007; Wilhelm *et al.*, 2007), if the phenotype that is selected for is not significantly deviating from the original one, there is probably not enough variability left, to allow for more variability regarding that specific phenotype. Furthermore, many studies suggest an anxiolytic effect by raising mice under non-standard enriched environment (Fox *et al.*, 2006), or an effect of more or less intensive maternal care on the developing mice (Weaver *et al.*, 2006). To dissect genetic effects from effects mediated by maternal care, cross-fostering paradigms are usually applied, where pups of one mother (e.g. HAB animals) are replaced by pups of the other line



(Wigger *et al.*, 2001). Both possibilities have already been investigated in HAB and LAB mice, with environmental enrichment causing significant decrease in anxiety-related behavior in HAB mice (Baier and Bunck, unpublished) and cross-fostering only exerting minor anxiolytic effects on HAB mice with the mean still remaining in a HAB-typical range (Kessler *et al.*, in preparation). Thus, while changes in anxiety-related behavior seem to be possible by applying different approaches, HAB mice do not escape the frame typical of this line (0 - 15% of total test time spent on the open arms of the EPM; except for the enriched environment paradigm, with the values between 20 and 25%).

Genotypes in HAB LAB and CD1 mice

As the present study provided the opportunity to investigate the poorly described genetic background of outbred mouse strains (Chia *et al.*, 2005), the current study allows for an estimation of variability in CD1 mice. As 42 SNPs were identified uniquely in CD1 mice, additional 31 SNPs were also identified displaying variation also in HAB vs. LAB mice giving a total of 73 SNPs. Given the total number of previously (prior to the custom-designed oligo pool genotyping) uncharacterized polymorphisms, 149 SNPs were included to the new assay. Hence, 49% of all tested genotypes showed variability in CD1 mice, in contrast to only 21% being also applicable to HAB vs. LAB mice. This would allow the conclusion that nearly 50% of all already described sequence variations in the MGD would be identifiable in CD1 mice, whereas only about 20% would represent genotypic markers applicable to the HAB and LAB mouse lines. It is important to mention, that most of the currently known polymorphisms rely on comparisons of inbred strains (Bult *et al.*, 2008).

In so far, it's not surprising that results of single gene locus sequencing suggest that overall variation in CD1, HAB and LAB mice would by far exceed the variation known from the database, as for *Tmem132d*, only three of ten identified SNPs were listed there. Similarly, for *Avp* only three of the eight SNPs and for *Ctsb*, 22 out of 76 SNPs were listed in the MGD. Altogether, half of the SNPs known from the MGD are probably identifiable as variable site in CD1 mice, but approximately twice the number of polymorphic sites is not even described at the moment. The discrepancy of genotypes as identified in LAB mice that resulted in the identification of the genetically distinct LAB-A and LAB-B subgroups could be traced back and verified according to a pedigree of LAB mice (Fig. 38). The genealogy of LAB mice makes it obvious that offspring of all LAB animals can be tracked back to common ancestor in the G10. At that point, inbreeding only started two generations earlier, so genetic variability was still nearly unaffected. But if so, why were no HAB sublines



identifiable? Obviously, the HAB mouse line went through a genetic bottle neck quite late in G16, what also makes the smaller variability in the HAB group alleageable.

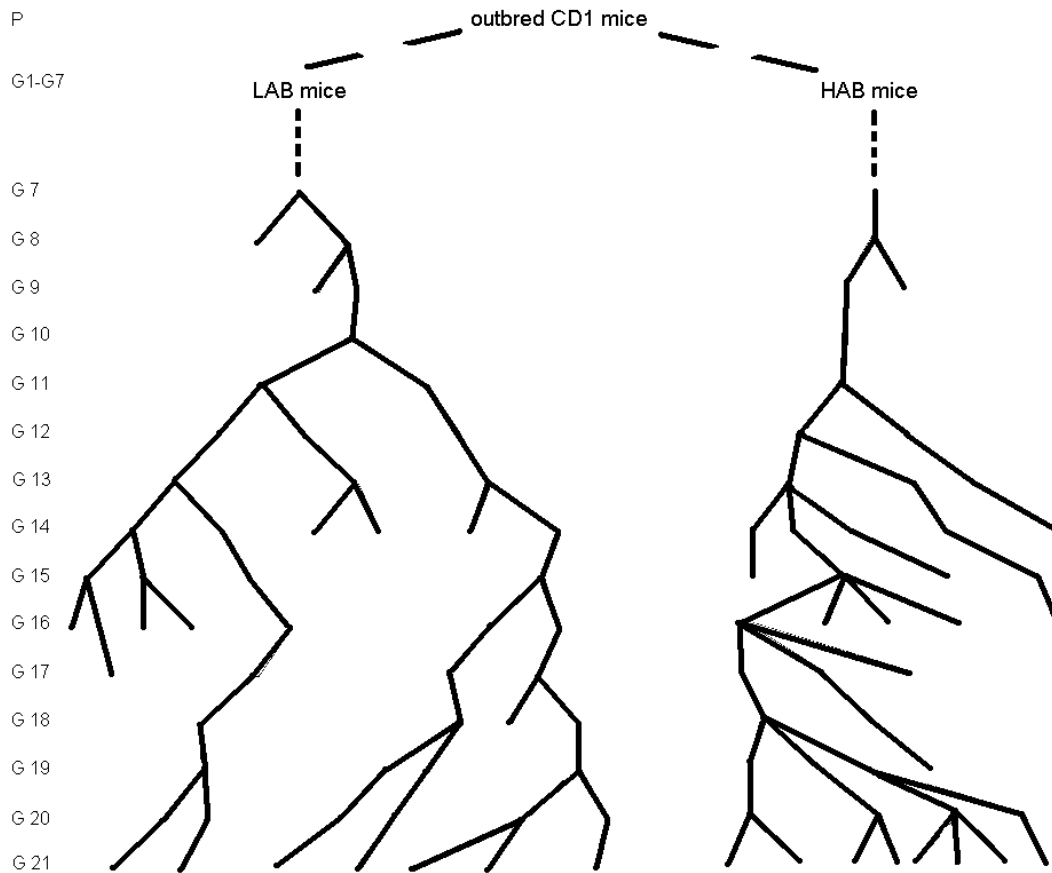


Figure 38: Genealogy of HAB and LAB mice from outbred CD1 progenitors until the parental generation of F2 mice (G21). Each point at each generation represents one breeding pair of mice.

Gene expression analyses and genotype-phenotype associations

Many gene products were characterized in detail, as far as their confirmation of differential expression between HAB and LAB mice or their genetic sequence is concerned. For about 13 of those gene products identified in microarray gene expression profiling analyses, no significant difference in regulation could be verified in HAB vs. LAB mice using qPCR. This can be attributed to multiple causes. First of all, some of the identified gene transcripts might have been differentially expressed between the mouse lines only in that specific generation or at that specific time of the year. Independent observations suggest that annual seasons affect litter sizes even under standardized laboratory conditions, what implicates the possibility on other physiological parameters and especially consequences on the neurochemistry and neurogenetics of the brain (Chesler *et al.*, 2002). Nevertheless, this also implicates, that if these changes in gene expression between the mouse lines is not constant over the year, or even within two distinct generations, their effect on the



phenotypes of interest (anxiety) is negligible. Further, some technical aspects might come into consideration like the non-exclusion of probes in the assay that show only low fluorescence values (Yauk and Berndt, 2007) has been mentioned, but also the selection of housekeeping genes affects the outcome of validation by qPCR (Coulson *et al.*, 2008; Nygard *et al.*, 2007). Furthermore, as the probes used for hybridization using the Illumina platform have a length of 50bp, polymorphisms in the sequence might severely impair the binding capacity of aRNA bearing SNPs. This might also be the reason for a measured 12-fold upregulation of *Ctsb* in LAB mice in the Illumina experiment, although only a 2-fold overexpression could be confirmed (Tables 11-13).

Nevertheless, the differential expression of 15 genes could be confirmed, partially even independent of gender. This increases the value of the corresponding candidate genes for anxiety, as both, males and females of each mouse line always display the line-specific phenotypes. The confirmed candidate genes are: *Coro7*, *Mmp15*, *Slc25a17*, *Zfp672*, *2900019G14Rik*, *Abca2*, *Enpp5*, *Hmgn3*, *Pdhb*, *Ctsb*, *Mt1* and *Stx3* as whole brain tissue is concerned, whereas *Mbnl1* and *Trib2* (Tables 13-15) can be added to the list of candidate genes as based on qPCR. *Tac1*, *Tmem132d* and *Avp* (Fig. 16-19) are also part of the genes confirmed by qPCR, even if their differential expression is restricted to specific brain areas. This results in an overall reproducibility of over 50%, which seems to be acceptable.

Coro7

As *Coro7* is concerned, this gene transcript and its protein have been shown to be important in brain development. Although it is present in most organs of the adult organism, the highest amounts can be found in the brain, kidneys, thymus and spleen. The protein has been identified in the cytosol and as a membrane-bound protein as well. Although not many studies have been dealing with this gene product, they suggest a function in the membrane of the Golgi apparatus and in vesicle trafficking (Rybakin *et al.*, 2004; Rybakin *et al.*, 2006). Elevated expression of this gene in LAB compared to HAB animals, with CD1 mice displaying an intermediate expression level, might contribute to differences at the behavioral level as well as general protein levels would be affected or their homeostatic state disturbed or the transport of vesicles within neurons could be more or less effective between the mouse lines. These effects have not been assessed in HAB and LAB mice yet, but would be an interesting target for further studies.

Mmp15*, *Slc25a17* and *2900019G14Rik

Mmp15 or its gene product is not well-characterized, as far as brain function is concerned, but it seems to bear a role in inflammation- and oncogenesis-related



processes (Do *et al.*, 2006; Wang *et al.*, 2008). Also *Slc25a17* is poorly described, except for its function as peroxisomal ATP transporter (Visser *et al.*, 2002), what makes this candidate gene interesting as a player involved in neurometabolism. For *2900019G14Rik* no description is available at all, although some connection to *Slc1a2* might be assumed, as the physical proximity is below 10kbp (NCBI). It is nevertheless important to mention that this gene exhibited the highest expression difference that could be confirmed in HAB vs. LAB mice (16-fold). Unfortunately, the two polymorphisms identified in the analyzed part of the gene transcript can't reveal any further insight into their functionality at this stage.

Further investigations are required to elucidate possible effects of these four genes on anxiety or any other phenotypic correlate in HAB and LAB mice.

Zfp672

The zinc finger protein, *Zfp672* is a putative transcription factor (NCBI) that has been identified as differentially expressed between HAB and LAB mice. What makes this gene even more important as a candidate gene for anxiety, is the association between one SNP in the 3' UTR and anxiety-related behavior as measured on the EPM in F2 mice (Fig. 34). Importantly, in this case, no significant association has been found with locomotor activity or depression-like behavior.

Hmgn3

This gene was found to be 2-fold overexpressed in HAB vs. LAB mice. HMGN family proteins were identified to promote chromatin unfolding, to enhance accessibility of nucleosomes and to regulate transcription. Especially *Hmgn3* was displaying a significant upregulation of a glycine transporter (*Slc6a9* / GLYT1), a protein that modulates glycine concentration in the synaptic cleft. Furthermore, transcriptional regulation of 0.8% of all genes in a microarray experiment could be attributed to *Hmgn3* (West *et al.*, 2004). So, by altering this gene's expression, the expression of many other gene products is changed that directly affect the capacities required for maintaining synaptic activity (including *Slc6a9*), what can have a major impact on shaping the behavioral phenotypes characteristic of HAB and LAB mice.

Pdhb

Mutations in *Pdhd* have been found to cause severe symptoms in humans, if they lead to a deficiency in that enzyme (Okajima *et al.*, 2008). Its deficiency is especially severe, as the enzyme plays a vital role in alanine and aspartate metabolism, butanoate metabolism, in valine, leucine and isoleucine biosynthesis and in the citric acid cycle. Therefore, if LAB mice would show global signs of PDHB deficiency (gene expression or protein levels have not yet been assessed outside the brain), this could contribute to their elevated food consumption (Fig. 20), without leading to



increased body weight within this line compared to HAB mice. But this deficiency affects definitely the brain, so minor modifications of behavior by deficiency of amino acids can be expected in LAB mice, as many disorders connected with anxiety, hyperactivity, attention deficit or aggression are known to be in direct association with neurometabolic changes or deficiency (Knerr *et al.*, 2008).

Ctsb

Also *Ctsb* is well known to play an important role to assure regular brain development, as neuronal loss and brain atrophy were found to be characteristic to *Ctsb* and cathepsin L (*Ctsl*) knockout mice. These knockout mice also exhibited deficiency in locomotor abilities (Felbor *et al.*, 2002; Stahl *et al.*, 2007), although behavioral alterations have never been screened in knockout mice for *Ctsb* only until now. This would make a great addition to the gene expression data obtained in this work, as a strongly increased expression could be verified for LAB mice, compared to HAB animals, with CD1 mice expressing this gene at intermediate levels. Furthermore a large number of genetic polymorphisms at this gene locus has been identified in sequencing HAB vs. LAB mice (Table 17), where the identified polymorphisms don't affect protein structure, but could definitely affect either mRNA stability (Shabalina *et al.*, 2006) or the recruitability of transcription enhancing or repressing factors.

Mt1

It has been demonstrated for *Mt1* that neurodegenerative diseases as well as metabolic stress enhances its expression in perivascular regions of the cerebral cortex predominantly in astrocytes (Vorbrodt *et al.*, 2006). Further experiments highlighted a connection of physical stress with increased *Mt1* expression in a variety of brain regions and also increased expression has been observed upon subcutaneous administration of steroid hormones (Beltramini *et al.*, 2004a; Beltramini *et al.*, 2004b). High expression of *Mt1* also has been proven to decrease the concentrations of zinc that is required to maintain efficient functioning of immune responses and might contribute to the effects of age-related degenerative diseases (Cipriano *et al.*, 2003). According to all these indices, *Mt1* might play a key role for the HAB/LAB mouse model, where besides the differential expression of *Mt1*, an increased stress response of CORT-release to physical stressors in LAB mice has been demonstrated (Keßler *et al.*, in preparation). Most interestingly, the higher release of CORT in LAB mice upon a stressor could also be shown in an independent short-term breeding approach for trait anxiety (Salvamoser, 2008; Czibere, unpublished), connecting the higher stress response in LAB mice to the anxiety-related phenotype and excluding a co-selection of this trait or artifacts



related to genetic drift. Furthermore, no genetic polymorphisms have been identified in HAB vs. LAB mice that might underlie differential expression. Except of that, only epigenetic factors that affect regulation might play a role in the described expression differences (Majumder *et al.*, 2006).

Stx3

Darios and Davletov (2006) described the importance of *Stx3* that encodes a membrane protein required for neurite growth and neural development as an activator of SNARE complexes. Also arachidonic acid plays an important role for STX3 action, highlighting the impact of metabolism as a potential cofactor fundamental to neurometabolism and thereby brain function (Darios and Davletov, 2006). In HAB vs. LAB mice expression differences in *Stx3* have been identified with NAB mice expressing intermediate levels of that gene. Differential expression of this candidate gene points again to basic differences between HAB and LAB mice regarding neuronal function that has the potential to shape the phenotypic differences.

Abca2

Recently, a research group from Japan created a knockout mouse model for *Abca2*, showing a decrease in body weight and decreased locomotor abilities. Furthermore, the knockout mice displayed an increased susceptibility to environmental stress (Sakai *et al.*, 2007). Especially the last point vindicates to draw parallels to LAB mice, as qPCR also confirmed that LAB only expressed 1/6th of the *Abca2* mRNA as compared to HAB mice indicating a defined deficiency in LAB mice. Also, the results of the phenotype-genotype association in the F2 panel proved a highly significant association of the genomic location of *Abca2* with locomotor activity that was also significantly associated with anxiety-related behavior, but to a lower extent (larger p-value, absolute difference in locomotor activity difference (OF-based): 25%, absolute difference in anxiety-related behavior (EPM-based): 20%). In addition, F2 mice carrying the HAB-specific genotype showed increased depression-like behavior spending much more time immobile in the TST and FST as their counterparts bearing the LAB-specific genotype. Taken together, this makes the genomic locus around *Abca2* a valuable marker for locomotor activity as well as depression-like behavior, as the mice displaying increased locomotor activity were simultaneously displaying increased depression-like behavior. A possible role for other gene products in that region cannot be excluded, as the SNP (rs13476366 – a genomic marker for the region around it) covers a genomic region of more than 5Mbp. Similarly strong associations might be given for any other gene locus around that marker which is also near *Msrb2*. The latter is described to possess cell-



protective function in case of oxidative stress (Cabreiro *et al.*, 2008). Differences regarding gene expression between HAB and LAB mice have also been identified in the microarray analyses for *Msrb2* but have not been confirmed up to date.

Enpp5

This gene is encoding a nucleotide-metabolizing ecto-enzyme, a class of enzymes that is required to regulate the availability of extracellular nucleotides, thereby controlling the signaling through purinoceptors, like the P2X ion channels. Interestingly, especially one P2X ion channel, the P2RX7, has been identified by a number of studies as bearing polymorphic sites (SNPs) that are significantly associated with major depressive disorder in a large number of patients (Barden *et al.*, 2006; Erhardt *et al.*, 2007; Hejjas *et al.*, 2008; Lucae *et al.*, 2006). Further, in knockout mice it has been demonstrated that P2RX7 locates predominantly in the synaptic cleft that would make it interesting for neuronal transmission (Marin-Garcia *et al.*, 2008). If thus a variant of *Enpp5* is higher expressed in HAB compared to LAB, this gene becomes a major candidate gene bearing a high potential to contribute to the behavioral phenotype of our mice making this gene interesting for clinical treatment. Furthermore, the *Enpp5* locus did not show any associations with anxiety or depression-like behavior, in contrast to the loci around *P2rx7* (Supplementary table 3). This gene is located on chromosome 5 in a region that also displayed highly significant association with anxiety-related behavior ($p < 10^{-7}$). Thus, by the expression differences observed for *Enpp5*, the association in the F2 panel can be directly observed as a highly significant effect on the respective behavior at the *P2rx7* locus.

Tac1

As far as *Tac1* expression is concerned, this study revealed quite discrepant results, if compared to the results of the microarray analysis. Indeed, an overexpression has been revealed in the PVN and BLA/LA of HAB mice (Fig. 17) that is the result of elevated levels of all splicing variants and especially γ -PPT in these brain regions. These differences were not confirmable regarding the tachykinin-derived peptides, but a different distribution of peptide expression patterns was revealed in the PVN and BLA/LA. Altogether, the discrepancies are most likely to be caused by differences in the sensitivity of the techniques applied. Gene expression differences between male and female mice for *Tac1* might be explained by a sequence in its promoter that displays a homology of 85% to an estrogen-response element (Carter and Krause, 1990). Indeed, in many brain regions, among others the amygdala, differences for tachykinins between male and female animals were observed (Otsuka and Yoshioka, 1993). As the amygdala is considered essential for



processing emotions, whereas the PVN initiates the reaction to stressors (Herman and Cullinan, 1997), the expression differences of *Tac1* might play a role at multiple levels of anxiety in males and females. As for all brain regions and genders a similar expression pattern of all splicing variants has been observed (Fig. 18), differential expression is unlikely to be caused by the increased or decreased expression of one single splicing variant. The cause for differential expression cannot be traced back to polymorphisms in the gene sequence, since at the whole *Tac1* locus, no single polymorphic site has been identified in HAB vs. LAB mice. Alternatively, differences in promoter methylation could be an underlying cause of differential expression (Bock and Lengauer, 2008). For the quantification of tachykinin-peptides, no differences between the analyzed mouse lines could be detected. This might be due to technical reasons, as during the ELISA experiment, the measured optical density was highly variable within each peptide. Furthermore, even the quantified standards using the same amount of purified peptides showed variances that reached the variance reflected by inter-individual samples. Hence, even if different levels of peptides would be detectable, they might have been masked by the technical variance of the ELISA quantifying the small peptide amounts contained in brain tissue micropunches. Nevertheless, the result that *Tac1* and its splicing variants are expressed at increased rates in highly vs. less anxious mice, is in one line with other studies, confirming the anxiogenic effect of *Tac1* derived peptides and the anxiolytic effects of NK₁ antagonist (Bilkei-Gorzo *et al.*, 2002; Ebner and Singewald, 2006; Quinn *et al.*, 2000; Saria, 1999). Importantly, NK₁ antagonists have also been demonstrated to exert an anxiolytic effect in HAB mice (Sartori, unpublished).

Glo1

As revealed by all gene expression profiling assays, *Glo1* was found to be overexpressed in all brain nuclei investigated in LAB compared to CD1 and HAB mice. As the overexpression in LAB mice was confirmed at peptide level using Western Blot analysis from the brain and even red blood cells (Kromer *et al.*, 2005; Landgraf *et al.*, 2007), confirmation of differential expression of *Glo1* between the mouse lines by qPCR was waived. Overall effects of *Glo1* overexpression in LAB mice were found to be negligible on lactate concentrations, as no differences could be detected between HAB and LAB mice. No differences could be detected between HAB and LAB mice regarding further metabolic parameters assessed from blood plasma samples. This is also important in respect to the function of the previously described *Abca2*, *Pdhb*, *Stx3* or *Enoph1*.

Interestingly, CD1 mice that were saccharose-soaked over ten weeks did not show any increase in body weight compared to control mice (Fig.21). This is remarkable,



as most studies on human health consider soft drinks as one of the main causes together with increased food consumption as the leading causes for increasing obesity in the general population, especially in adolescents (Harrington, 2008). If now considered together with food consumption, the effect of elevated water consumption (with saccharose solution) could not reach levels as expected, because increased water intake in those animals was accompanied by a significant decrease in food consumption. This is mirrored by the lower extent of total calorie intake compared to the clearly higher amount of water consumption. Decreased food intake in combination with elevated water intake, if the latter one was drugged with saccharose, has already been reported in other cases (Scalera and Tarozzi, 2001). This only slight elevation of total caloric intake is probably the reason for the minor behavioral and molecular effects measured in the mice. The effects on physiology might be better mirrored by the measured osmolalities of urine and blood plasma. The clear effect on urine osmolality that was decreased by nearly 80% in the treated group was not accompanied by a decreased plasma osmolality (Fig. 22), so a dehydration effect that could have affected the test animals' behavior can be excluded as a cause (Scalera and Tarozzi, 2001).

Interestingly, saccharose-soaked mice were slightly more anxious as the results on the EPM suggested, although many parameters taken failed to show significant differences. Whereas the effects on anxiety-related behavior were significant in the first EPM test, even the latency time to the first entry onto an open arm failed to reach statistical significance in the second test, only reaching a statistical trend (Fig. 23). Furthermore, a slight decrease in the percentaged time spent on the open arms of the EPM in both the treated and control group could be observed from the first to the second testing. This is not unusual, as this effect has been described for repeated testing on the EPM before (Stern *et al.*, 2008).

In line with our previous findings (Ditzen *et al.*, 2006; Kromer *et al.*, 2005), mice that were more anxious in the EPM test (saccharose-soaked mice) also displayed lower levels of GLO1 protein in their red blood cells after the first test (Fig. 24). In contrast to that, mice tested for GLO1 expression after the second EPM exhibited higher levels of the protein while still being anxious, what would be contrary to our findings and in one line with the findings published by another research group (Hovatta *et al.*, 2005). It is important to mention that in both cases of GLO1 measurement, the effects only reached a statistical trend, so in either way the effect of the saccharose treatment on GLO1 expression is marginal. Second, as the effects on the EPM were less divergent between the control and treatment group, probably first a direct effect of saccharose treatment was observed and by depletion of food intake a negative



regulation of GLO1 expression might have predominated. Longer treatment, over six weeks, could have elevated the protein levels and also caused the behavior to be less divergent between the treated and control group. Additional analysis of the brains of treated and control animals could reveal the causes for the difference, although another kind of treatment such as direct injection of methylglyoxal or a GLO1 inhibitor would be more promising to reveal the inducibility of this protein and demonstrate a behavioral effect, as there would be less enzymatic steps to be considered for their action (Kuhla *et al.*, 2006; Thornalley, 2006).

COX

As cytochrome c oxidase activity is valid marker for long-term cellular activity and also mRNA expression (Christen, 2000; Simonian and Hyman, 1993), this enzyme activity-assessing assay revealed basal differences in long-term activity. Interestingly, in the PVN, HAB showed a decreased activity in comparison to LAB mice, whereas for both amygdala nuclei (the CeA and the BLA) HAB showed an increased activity compared to LAB mice. Thus, the results suggest that for the behavioral trait of high anxiety, a higher activity of the amygdala (i.e. for the processing of emotions) seems to be more important than an increased activity of the PVN. This is also supported by a number of other studies describing the amygdala as a key processor of anxiogenic stimuli and the PVN as the center to control the adequate stress response (Bishop *et al.*, 2004; Bishop, 2008; Herman *et al.*, 2003). Probably this holds also true for the analogous conclusion for LAB mice that a decreased long-term activity in the amygdala is necessary to allow for a low anxiety trait. On the other hand, a higher activity of the PVN in LAB mice explains the higher reactivity of the HPA axis in terms of higher CORT concentrations in response to a physical stressor, as already mentioned before. Although, generally, high levels of CORT response are described to be associated with high anxiety states (Maccari *et al.*, 2003; Wigger *et al.*, 2004), in HAB vs. LAB mice this seems to be the other way round. This finding was even replicated in a short-term breeding experiment (Salvamoser, 2008) and also in CD1 mice, bred for differences in CORT response to a stressor, mice exhibiting lower CORT reactivity tended to be more anxious (Touma *et al.*, 2008). Additionally, even in the HAB/LAB rat model, a strong increase of CORT has been demonstrated after social defeat (strong social stressor) in LAB, but a less strong increase in HAB rats. This might be attributed to a more passive coping style in HAB animals in response to any kind of stressors (Frank *et al.*, 2006). Analogously, the passive coping style of HAB mice in various tests for depression-like behavior might also be the reason for the observed decreased stress reactivity.



Taken together, these findings reveal that high anxiety can be accompanied by lower responsiveness concerning CORT release and suggest that the major effect on anxiety in CD1 mice is probably exerted by mechanisms largely independent of HPA axis function or the decreased responsiveness is connected to the passive coping strategy found in HAB mice.

Further, the results reveal that no direct conclusions from the gene expression pattern of individual COX subunits can be drawn on overall COX activity, as *Cox8a* is similarly higher expressed in the PVN, BLA/LA and Cg of HAB mice, or the regulation in the same direction was found for *Cox6a2* in all brain regions.

Examining the effect of differential gene expression in HAB vs. LAB mice on the phenotype, the characteristics have been best evaluated in this study concerning *Tmem132d*, *Avp* and *Enoph1*.

Avp

Also for *Avp*, decreased expression of *Avp* mRNA in the hypothalamus of LAB animals under basal conditions compared to HAB and CD1 mice could be identified in combination with genetic polymorphisms underlying these *Avp* expression differences. Additional studies underline these findings by extending them to male mice and also including HABxLAB F1 intercross animals (Bunck *et al.*, submitted). Correlative and causative evidence indicates that reduced *Avp* expression contributes to locomotion-independent reduction of anxiety, confirming corresponding results in HAB/LAB rats (Murgatroyd *et al.*, 2004). Sequencing of the *Avp* gene, including the upstream promoter and the downstream enhancer region, resulted in the identification of nine polymorphic loci reliably differing between the HAB and LAB line (Fig. 27). These loci comprised eight SNPs and a 12bp deletion in LAB mice. Additionally, the allele frequency of the $\Delta(-2180-2191)$ deletion and the strictly linked C(40)T SNP was determined in CD1 and F2 populations (Table 16). Both polymorphic sites are likely to be involved in the regulation of gene expression and the processing of the AVP precursor (Kessler *et al.*, 2007), respectively. While there were no polymorphisms identified in the noncoding (untranslated region and intronic) sequences, all three SNPs in the gene locus were located in the coding sequence. Two of these are silent mutations A(1431)G and T(1527)C and the third one C(40)T causes a substitution of alanine to valine in the third amino acid of the AVP signal peptide. As already reported (Kessler *et al.*, 2007), this genetic marker co-segregated in an F2 panel with symptoms of central diabetes insipidus in LAB mice and, partially, with anxiety-related behavior, further confirming the strict linkage between the promoter deletion $\Delta(-2180-2191)$ and C(40)T. This linkage, also detected in 258 mice of a freely-segregating F2 panel, suggests an association of



specific polymorphisms in the *Avp* gene and its expression with the corresponding phenotype.

The individual phenotype is known to be shaped by phenomena that are or are not mediated by sequence variations in DNA, i.e. inheritance is both genetic and behavioral (epigenetic), with the latter primarily relying on the quality of mother-infant interaction (Champagne, 2008). To eliminate possible influences of different epigenetic effects, deriving from the fact that half of the F2 had HAB and the other half LAB grandmothers, split calculations according to the grandmaternal background were performed for associations. Indeed, in addition to correlative evidence, a moderate, though significant association between the promoter deletion and the C(40)T SNP and locomotion-independent anxiety-related behavior was demonstrated in a freely segregating F2 panel (Fig. 36). Thus, while the polymorphisms identified in the *Avp* gene are unlikely to generally cause hypo-anxiety, their variation might contribute to the severity of the phenotype, further supporting the estimate that several dozen quantitative trait loci may be involved in anxiety regulation (Turri *et al.*, 2004). Further studies have to focus on the importance of the (grand)parental background for anxiety-related behavior, as genes regulated by (grand)parent-specific epigenetic modifications can lead to monoallelic gene expression (Delaval and Feil, 2004; Wilkins and Haig, 2003a; Wilkins and Haig, 2003b) or are simply X-linked.

Another explanation might be, based on the higher prevalence of anxiety and depression in women than in men (Jacobi *et al.*, 2004), the (grand)parental influence on anxiety-related behavior, as revealed in our F2 panel, due to a modulating effect of a sex-specific locus. HAB/LAB mice might thus represent a model to further investigate the complex pattern of genetic vs. epigenetic inheritance.

As LAB mice exhibit a deficit not only in AVP precursor processing and neuropeptide release from both dendrites and axon terminals (Kessler *et al.*, 2007), but also in *Avp* expression, additive effects at multiple levels are likely to produce a “global” deficit in bioactive AVP. Remarkably, recent studies in Brattleboro rats and humans confirmed that an AVP deficit may be accompanied by symptoms of central diabetes insipidus, reduced anxiety-related or attenuated depression-like behavior (Mlynarik *et al.*, 2007) and signs of diminished agoraphobia and impaired memory processing (Bruins *et al.*, 2006), respectively, suggesting complementary inter-species genetics. It is of note in this context that impaired social discrimination abilities in LAB mice have also been observed recently (Bunck, unpublished). Still, to make sure that *Avp* under-expression in LAB mice is definitely due to the described genetic polymorphisms rather than to differences in other variables



including epistatic gene-gene interactions or synaptic input to the hypothalamic nuclei an allele-specific transcription analysis was performed, which had already been successfully applied in HAB/LAB rats (Murgatroyd *et al.*, 2004). By breeding HABxLAB F1 intercross animals that host both HAB and LAB line-specific alleles in each cell. Indeed, allele-specific transcription analysis of heterozygous F1 animals revealed a 75% reduced expression of the LAB-specific compared to the HAB-specific allele (Fig. 31), suggesting a causal role of this hypomorphic allele in exerting a reduced drive on *Avp* expression and hypo-anxiety.

Importantly, differences in *Avp* expression were not associated with changes in V1a receptors that could confound the analysis of the behavioral involvement of AVP in these lines (Bunck *et al.*, submitted) Several groups independently reported an association of the V1a receptor with anxiety-related behavior. V1a receptor knockout mice, although at times providing inconsistent results, showed impaired social interaction, social recognition and reduced anxiety-related behavior (Bielsky *et al.*, 2004; Bielsky *et al.*, 2005; Egashira *et al.*, 2007). Furthermore, V1a antisense RNA, targeting the septum, made rats less anxious (Landgraf *et al.*, 1995). In HAB vs. LAB mice, V1a receptor autoradiography revealed no differences in a variety of anxiety-associated brain regions, suggesting that line-specific divergences in behavior are due to events upstream of the receptor, i.e. differential expression and release of AVP, rather than to differences in V1a receptor binding (Bunck *et al.*, submitted). The functional relevance of central AVP and its V1a receptor subtype is underlined by anxiogenic effects of centrally administered AVP in LAB mice (Bosch, unpublished).

How may the identified polymorphisms in the promoter region translate into different expression profiles and phenotypes? While the C(-1422)T SNP is not located in a transcription factor binding site, the T(-2521)C SNP and the Δ (-2180-2191) deletion are located directly in the center of a binding site for nuclear factor 1 (NF-1), a well-known transcription factor in the brain that promotes transcription in combination with C/EBPalpha or C/EBPbeta (Ji *et al.*, 1999). Impaired binding of NF-1, here driven by both polymorphisms, the T(-2521)C SNP and the Δ (-2180-2191) deletion, has recently been demonstrated to result in decreased gene transcription (Alikhani-Koupaei *et al.*, 2007). Both polymorphic sites are also in the proximity of a C/EBP binding site, but only the Δ (-2180-2191) site flanks a C/EBPbeta binding site. Even the T(-2521)C SNP might have a minor effect on reduced *Avp* expression in LABs, though it creates a binding site for NF-1 in LABs, but NF-1 might act as a repressor (Kraus *et al.*, 2001) if a neighboring C/EBP binding site is lacking. Although there is a C/EBPalpha binding site, C/EBPalpha expression is much lower than that of



C/EBPbeta (Horvath, unpublished). Also SNPs in the DER can have an impact on expression, as recently described. There is a repetition of motifs from that 178-bp region mentioned in the publication on the *Avp* DER (Fields *et al.*, 2003) between +370bp and +480bp, where two HAB- and LAB-specific SNPs have been identified. Analysis of this region resulted in the identification of a binding site for c-Ets-2 near to a binding site of C/EBPbeta (Chakrabarty and Roberts, 2007). In the center of the c-Ets-2 binding site, the A(+399)G polymorphism would allow for an enhanced transcription rate in the HAB-specific but not the LAB-specific DNA sequence. Finally, even polymorphisms in the coding region are likely to contribute to lower *Avp* mRNA content by negatively influencing mRNA secondary structure and stability (Shabalina *et al.*, 2006). Determining the most common genotypes in CD1 mice revealed that the HAB-specific polymorphisms represent the most common genetic variant (Table 16). More than 70% of the CD1 mice were found to be homozygous for the HAB-specific sequence, whereas less than 1% carried the LAB-specific allele homozygously. Nevertheless, the respective distribution is in Hardy-Weinberg equilibrium, although with the LAB-specific allele at a decreased frequency.

Despite the higher long-term activity of the PVN in LAB as revealed by the COX activity measurement, *Avp* was found to be expressed at lower level in the PVN as compared to HABs. As mentioned before, probably mechanisms independent of HPA axis function might be involved in mediating the HAB and LAB mouse line-specific effects. Anxiolytic activity of decreased AVP concentrations in LAB and a more anxiogenic activity of AVP in HAB mice might thus be mediated by intracerebral axonal or dendritic release e.g. in the amygdala (Caldwell *et al.*, 2008; Landgraf and Neumann, 2004; Wotjak *et al.*, 1994), rather than by differential activation of the HPA axis. Interestingly, gene expression of *Avp* was significantly elevated in LAB but not in HAB mice 3h after a stressor (TST; Bunck, unpublished), although this might be an effect caused by a more severe shortage of AVP in LAB mice. Nevertheless, this phenomenon requires further investigation, probably AVP localization in different stages after a stressor and electrophysiological studies conducted in the PVN and amygdala might shed light on mechanisms underlying this phenomenon.

Hnrn

Highest association was detected for *Hnrn* regarding the whole genotype-phenotype association study in F2 mice with CORT response to a physical stressor (Fig. 37). No other phenotype showed association with that locus and altogether the differences between the HAB- and LAB-specific homozygous genotypes in CORT-



mirrored stress responsiveness reached nearly 50% of the complete difference that is reachable by selective breeding for that phenotype (Touma *et al.*, 2008). The gene seems to play a role for keratinization, but a function in the central nervous function is not described yet. As one domain (S100B) of the protein putatively has the capacity of binding calcium ions (NCBI), a concentration dependant influence of HRNR on neuronal cells in the brain (Sorci *et al.*, 2003) has to be investigated in detail.

Enoph1

Two different isoforms of the E-1 enzyme (encoded by *Enoph1*) could be detected in the HAB and LAB mouse lines (Ditzen *et al.*, 2006). As the HAB isoform displayed decreased mobility in SDS gels, sequencing of the underlying gene revealed two SNPs that result in two amino acid changes in the protein's sequence. The altered mobility is likely due to a slightly different structure of the HAB vs. LAB E-1 enzyme isoforms, since the two amino acid differences only result in a minor change in molecular weight between the two proteins. Another consequence of the altered HAB E-1 enzyme sequence is a lower enzymatic activity compared to the LAB isoform (Ditzen *et al.*, submitted). The activity difference can have consequences for the methionine salvage pathway, of which E-1 enzyme is a member. However, S-adenosyl-L-methionine is one of the major methylating agents in the cell and hence a necessary compound for epigenetic mechanisms, which are receiving increased attention in the affective disorder field (Mill and Petronis, 2007). S-adenosyl-L-methionine is also known to be involved in the biosynthesis of the polyamines that exert potent effects on neurotransmission due to their modulation of different types of ion channels (Williams, 1997) creating a direct link to affective disorders (Skolnick, 1999). Furthermore, significantly increased amounts of two polyamines were found in HAB relative to LAB mice. Although the evidence is still lacking yet, one can speculate that the reduced E-1 enzyme activity affects the synthesis of the polyamines in HAB mice. As a consequence, a differential modulation of glutamate receptors may result in altered channel properties known to play a role in behavioral phenotypes related to anxiety and depression (Ditzen *et al.*, submitted; Skolnick, 1999). Due to the comorbidity of anxiety and depression and the high probability of shared underlying neuronal circuits (Levine *et al.*, 2001), the lower enzymatic activity of the HAB E-1 enzyme isoform is likely involved in the pathophysiology of the HAB phenotype. Yet, this hypothesis remains to be tested in further experiments.

In F2 mice it was demonstrated that the two SNPs in *Enoph1* likely contribute to both enzymatic activity and phenotype. Indeed, AA and TT mice spent significantly more time on the open arms of the EPM than their GG and CC counterparts (Fig.



32), thus confirming the hypothesized association between the SNPs and also the E-1 enzyme isoform enzymatic activity, metabolic consequences and their functional contribution to the phenotype. Importantly, it was also demonstrated that the co-segregation of genotype and phenotype is independent of locomotor activity, which often contaminates anxiety-related behavior (Kromer *et al.*, 2005). The latter is a polygenic, multifactorial trait presumed to have a complex inheritance and to involve the interaction of multiple genes with epigenetic and environmental factors (Henderson *et al.*, 2004; Landgraf *et al.*, 2007; Turri *et al.*, 2004). It is therefore quite remarkable that F2 animals adopt an anxiety-related behavior if their genetic constellation at the E-1 enzyme locus is HAB-like, i.e. homozygous GG and CC.

Tmem132d

A first genome-wide association study of panic disorder has detected and replicated evidence for association with the gene TMEM132D in samples collected from three independent studies with a combined number of 876 cases and 915 controls (Erhardt *et al.*, submitted). A haplotype consisting of two SNP remained significant after genome-wide correction for multiple testing in the combined sample. Although the size of the discovery sample (216 cases) was modest, the study had adequate power to detect an effect size of odds ratio 1.4 in the combined sample of 876 cases. Genetic effect sizes of this magnitude are probably the exception in complex psychiatric disorders and thus very likely important genes of more modest effects in panic disorder were missed. In addition, the Illumina HumanHap300 chip is providing good but not complete coverage of the European genome so that some susceptibility loci might have been missed due to insufficient marker density (Baum *et al.*, 2008; Consortium, 2007; Erhardt *et al.*, submitted). The top SNPs were retested in two additional samples, where a haplotype association with genome-wide significance in the combined sample (despite the lack of genome-wide significance in the discovery sample) could be confirmed.

In the initial sample, only non-comorbid panic disorder patients were analyzed against “super-healthy” controls, whereas in the second sample panic patients were compared to blood donor controls and in the third sample comorbid panic and anxiety patients were compared to controls screened with a brief questionnaire. The additional evidence from associations with dimensional anxiety measures, as well as human gene expression provided strong support for a role of TMEM132D in anxiety-related disorders. Two SNPs in this gene were associated with anticipatory anxiety in patients with panic disorder as well as the severity of anxiety symptoms in patients with major depression and a population-based cohort but not the severity of depressive symptoms. This pointed towards the possibility that these genetic effects



are specific for anxiety-related symptoms but not restricted to a certain disorder, which is further supported by the fact that the case-control associations could be replicated in a sample containing panic disorder patients comorbid with major depression, bipolar disorder and schizophrenia. The two associated loci were located in intron 3 and 4 of *TMEM132D*, respectively. The linkage disequilibrium structure of both regions suggested that the potential functional variants tagged by these associations do not likely lie in exonic or classic 5' regulatory regions. (Erhardt *et al.*, submitted). Regulatory regions, however, have also been described for introns (Hubler and Scammell, 2004).

In HAB vs. LAB mice, it could be shown that *Tmem132d* mRNA expression in the cingulate cortex was increased with CD1 mice displaying intermediate levels (Fig. 19). This observation was consistent in both microarray and qPCR experiments in male and female HAB, CD1 and LAB animals, suggesting a relationship of *Tmem132d* with anxiety-related behavior independent of gender. The correlation of higher *Tmem132d* expression with extreme anxiety-related behaviors in this animal model is consistent with the finding that the risk genotype AA of rs11060369, over-represented in panic disorder patients, was also associated with increased *TMEM132D* expression in the frontal cortex. Importantly, this anxiety-dependent difference in HAB vs. LAB mice was specific for the Cg. Only the Cg but not the BLA, CeA, DG and PVN showed an upregulation of *Tmem132d* in HAB animals in the microarray experiment. The cingulate cortex is closely connected to the amygdala, the brain region central to the generation of fear and anxiety and its activation seems to modulate the response of the amygdala to anxiety-evoking stimuli and expression of fear in humans (Coplan and Lydiard, 1998; Milad *et al.*, 2007; Milad and Rauch, 2007; Ohman, 2005). A series of functional imaging studies have implicated activity changes in the anterior cingulate cortex not only in fear but also in pathological anxiety states in humans such as phobic fear, panic disorder, generalized anxiety disorder, social anxiety disorder and post traumatic stress disorder studies (Etkin and Wager, 2007; Hasler *et al.*, 2007; Mobbs *et al.*, 2007; Straube *et al.*, 2007). Given the fact that anxiety-related brain circuits seem to be strongly conserved across species, these results could suggest that an altered expression of *Tmem132d* in the Cg may contribute to an altered activation profile of this brain region in the presence of anxiogenic stimuli and thus to a predisposition to pathological states of anxiety.

In addition to differences in expression, an exonic *Tmem132d* SNP was found to co-segregate with anxiety-related behavior in an F2 panel independent of both depression-like behavior and locomotor activity (Fig. 33), thus suggesting an



evolutionary conserved, causal involvement of this gene in anxiety-related phenomena. The molecular function of the gene product, also called transmembrane protein 132D, KIAA1944 and MOLT, is still unclear. TMEM132D is predicted as a single pass type I membrane protein. The predicted 1,099-amino acid protein has a calculated molecular mass of about 130kDa and contains an N-terminal hydrophobic signal peptide, 7 predicted N-glycosylation sites, 2 predicted O-glycosylation sites, a number of phosphorylation sites, and a C-terminal transmembrane domain (NCBI). Immunohistochemical studies showed a 5:1 ratio of TMEM132D expression in white matter compared to gray matter in the cerebral cortex (Nagase *et al.*, 2001). TMEM132D was also detected in *corpus callosum* and in white matter in the spinal cord and optic nerve. Using cultured rat oligodendrocyte lineage cells and stage-specific markers, they showed that TMEM132D was expressed by mature oligodendrocytes but not by oligodendrocyte precursor cells. The conclusion was that oligodendrocytes start expressing TMEM132D in the course of maturation and that this protein could be involved in the neural interconnection and also signaling (Nomoto *et al.*, 2003). Its involvement in oligodendrocyte maturation may be relevant for the efficient connection of the Cg to other anxiety-related brain regions.

Furthermore, sequencing revealed ten more polymorphic sites in and around the *Tmem132d* locus differing between HAB and LAB mice. As the complete gene covers a genomic distance of more than half a million bp, a complete linkage of all variable *Tmem132d* loci in all F2 mice is not expected. Furthermore, a glucocorticoid response element has been identified in the gene with one SNP located directly in its center, what could be the reason of differential expression but its functionality remains to be elucidated.

Altogether, this study demonstrates the strength of combined sequence-, transcriptome- and proteome-based analyses best in further combination with cross-species studies. Using a robust and valid animal model resulted in the identification of candidate genes that are part of neuronal and metabolic pathways pertinent to the disease phenotype.

By genotype-phenotype association analyses in F2 mice, strong evidence for the involvement of specific genomic loci, selected candidate genes and polymorphisms in shaping the anxiety-related, depression-like and stress responsiveness phenotypes could be validated. Although the role of specific mechanisms contributing to the respective phenotypes remains still elusive, a definite involvement can be assured for *Enpp5* (via P2RX7), *Abca2* or *Msrb2*, *Zfp672*,



Enoph1 and *Hrrnr*. Additionally, cross-species approaches further highlight the causal role of *Tmem132d* (in HAB/LAB mice and in panic disorder patients) and of *Avp* (HAB/LAB mice, HAB/LAB rats and patients) in direct connection to the anxiety-related phenotype (Erhardt *et al.*, submitted; Frank and Landgraf, 2008; Murgatroyd *et al.*, 2004; Scott and Dinan, 2002).

Also other gene transcripts identified by gene expression profiling but showing no direct association within the F2 study, can be defined as valuable candidate genes for the respective traits. These include *2900019G14Rik*, *Tac1*, *Mmp15*, *Mt1*, *Coro7*, *Ctsb* and *Slc25a17*, as they all show robust and reproducible expression differences between HAB and LAB mice. Nevertheless, possible interactions of these genes with loci highly associated in the F2 mice are possible, however due to the lack of obvious connections like for *Enpp5* they require further investigation. But already today, all of these candidate genes may serve as valuable targets for further molecular characterization of anxiety- and depression-related phenotypes, not restricted to mice. Furthermore, they might also play a vital role for the development of novel therapeutics, facilitating the treatment of anxiety disorders and depression.



5. Perspectives

Having identified some important molecular players that shape anxiety and emotionality in mice and humans, one major focus in future studies should be the development and testing of substances that are capable of inhibiting or activating the described proteins, thus allowing for the development of novel therapeutics. Therefore, as a first step, targeted overexpression of some gene products might be the tool of choice, as this in general creates less problems as compared to knockout of the respective genes, where the total loss might even cause lethality of the animals. Furthermore, the influence on other genes around the targeted location might be less pronounced than in knockout mice. Also a further functional characterization of some genes and their products is required, as hardly anything is known about the molecular functionality of *Tmem132d* or *Zfp672*, to name just few. Enzyme binding assays, localization in the brain and the identification of further polymorphisms that might interfere with enzyme or protein activity are required for most of the described genes and gene products. For *2900019G14Rik*, absolutely nothing is known, so first of all an identification of the complete gene structure is required.

Testing of already existing knockout mice for some of the described genes might be a complementary approach to investigate gene products that were identified in the gene expression analyses but show no obvious association in the F2 panel, like *Ctsb*. Also siRNA, antisense targeting and other methods directly acting on the transcripts might be the method of choice for further investigations. Similarly, the functional relevance of other gene products not yet mentioned or characterized in the literature published up to date, should be investigated especially with the focus on connections to other phenotypes associated with anxiety, e.g. cognitive abilities. Furthermore, whole-genome sequencing (as it is now available with the “Genome Analyzer II” technique and provided by Illumina based on the Solexa system) of HAB vs. LAB mice would be necessary to receive a complete picture of genetic diversity in these animals, thus providing the basis for a comprehensive overview on genomic interactions.

Furthermore, this study highlighted the genetically stable predisposition of HAB and LAB mice for their line-typical traits. The association of *Avp* with anxiety-related behavior points to an additional effect of inheritable epigenetic factors directly connected to the described phenotypes. Therefore special emphasis is required to unveil the epigenetic factors contributing to this complex trait.

ATGCTCGCCAGGA
TACGAGCGGTCCT



Perspectives

Thus, HAB and LAB mice are a valuable animal model for the future testing some of the hypotheses arising from this study with the potential to provide promising targets for psychiatric and pharmacopsychiatric research, independent of their usage in basic research on mechanisms influencing behavior or as model to test anxiolytic and antidepressant compounds. Considering the genome itself as a target for pharmacological intervention may be a first step in the development of a new generation of anxiolytic drugs.



6. Supplementary tables

Supplementary table 1: Excerpt of transcripts identified on the MPI24K gene expression screening platform, with positive fold regulation values meaning an overexpression in HAB compared to LAB and negative an overexpression of LAB compared to HAB mice. P-values are adjusted to multiple testing. Number of brain regions for significant regulation differences between HAB and LAB mice. Data are presented as means. Most transcripts are at least differentially regulated in three brain regions.

Fold regulation	p-value	# of regions	Gene symbol	Gene name
-8.81	0.0002	1	<i>Ttr</i>	Transthyretin
-3.47	0.0059	7	<i>Slc25a17</i>	Solute carrier family 25, member 17
-2.29	0.0016	3	<i>A430106J12Rik</i>	RIKEN cDNA A430106J12 gene
-2.26	0.0147	6	<i>Ctsb</i>	Cathepsin B
-2.26	0.0147	6	<i>Mmp15</i>	Matrix metalloproteinase 15
-2.09	0.0020	3	<i>Gnao1</i>	Guanine nucleotide binding protein, alpha o
-2.09	0.0123	3	<i>Tbl3</i>	Transducin (beta)-like 3
-2.06	0.0002	3	<i>Lox13</i>	Lysyl oxidase-like 3
-2.02	0.0004	3	<i>AI854703</i>	Expressed sequence AI854703
-2.00	0.0100	7	<i>Zfp672</i>	Zinc finger protein 672
-1.96	0.0011	3	<i>Chtf18</i>	CTF18, chromosome transmission fidelity factor 18
-1.95	0.0003	3	<i>B930037P14Rik</i>	RIKEN cDNA B930037P14 gene
-1.93	0.0001	3	<i>Gpx4</i>	Glutathione peroxidase 4
-1.89	0.0197	7	<i>Glo1</i>	Glyoxalase 1
-1.88	0.0082	7	<i>5230400G24Rik</i>	RIKEN cDNA 5230400G24 gene
-1.85	0.0087	3	<i>Spata2</i>	Spermatogenesis associated 2
-1.81	0.0094	3	<i>9030612M13Rik</i>	RIKEN cDNA 9030612M13 gene
-1.75	0.0235	3	<i>Il1b</i>	Interleukin 1 beta
-1.71	0.0230	5	<i>Coro7</i>	Coronin 7
-1.71	0.0334	4	<i>Pias4</i>	Protein inhibitor of activated STAT, 4
-1.66	0.0005	3	<i>Spnb3</i>	Spectrin beta 3

Fold regulation	p-value	# of regions	Gene symbol	Gene name
-1.66	0.0023	3	<i>Tebp</i>	Prostaglandin E synthase 3
-1.66	0.0244	5	<i>Ccdc104</i>	Coiled-coil domain containing 104
-1.66	0.0244	5	<i>4931428D14Rik</i>	RIKEN cDNA 4931428D14 gene
-1.64	0.0010	3	<i>Sparcl1</i>	SPARC-like 1 (mast9, hevin)
-1.64	0.0073	4	<i>4930438D12Rik</i>	RIKEN cDNA 4930438D12 gene
-1.63	0.0317	4	<i>Sdc2</i>	Syndecan 2
-1.62	0.0014	3	<i>Adpn</i>	Adiponutrin
-1.62	0.0019	3	<i>4933427L07Rik</i>	Dymeclin
-1.61	0.0016	3	<i>Slc1a3</i>	solute carrier family 1, member 3
-1.60	0.0578	3	<i>Mocs2</i>	Molybdenum cofactor synthesis 2
-1.58	0.0002	3	<i>Phtf2</i>	RIKEN cDNA 9330189K18 gene
-1.56	0.0347	5	<i>Ep400</i>	E1A binding protein p400
-1.55	0.0004	3	<i>A730042J05Rik</i>	RIKEN cDNA A730042J05 gene
-1.55	0.0012	3	<i>Kif21b</i>	Kinesin family member 21B
-1.55	0.0050	3	<i>Nts</i>	Neurotensin
-1.55	0.0077	3	<i>Arl6ip1</i>	ADP-ribosylation factor-like 6 interacting protein 1
-1.55	0.0182	4	<i>Extl2</i>	Exotoses-like 2
-1.54	0.0019	3	<i>5830417I10Rik</i>	RIKEN cDNA 5830417I10 gene
-1.54	0.0051	3	<i>Mgrn1</i>	Mahogunin, ring finger 1
-1.54	0.0270	3	<i>Ctss</i>	Cathepsin S
-1.54	0.0532	4	<i>Ptprz1</i>	Protein tyrosine phosphatase, receptor type Z, polypeptide 1
-1.53	0.0018	4	<i>2510009E07Rik</i>	RIKEN cDNA 2510009E07 gene
-1.53	0.0070	4	<i>Mt1</i>	Metallothionein 1
-1.52	0.0012	3	<i>1700030A21Rik</i>	Zinc finger, CSL-type containing 3
-1.52	0.0091	3	<i>Deadc1</i>	Deaminase domain containing 1
-1.51	0.0016	3	<i>Epm2aip1</i>	EPM2A (laforin) interacting protein 1
-1.51	0.0048	3	<i>BC026585</i>	cDNA sequence BC026585
-1.50	0.0256	4	<i>Pycs</i>	Aldehyde dehydrogenase 18 family, member A1
-1.50	0.0352	4	<i>Sqrdl</i>	Sulfide quinone reductase-like



Fold regulation	p-value	# of regions	Gene symbol	Gene name
-1.50	0.0436	3	<i>Prkcb1</i>	Acid phosphatase 1, soluble
-1.49	0.0223	3	<i>Zfp148</i>	Zinc finger protein 148
-1.49	0.0474	4	<i>Btrc</i>	Beta-transducin repeat containing protein
-1.48	0.0016	3	<i>Ndufv1</i>	NADH dehydrogenase (ubiquinone) flavoprotein 1
-1.48	0.0334	3	<i>Tcf1</i>	Transcription factor 1
-1.47	0.0111	3	<i>Bace2</i>	Beta-site APP-cleaving enzyme 2
-1.47	0.0245	3	<i>Aldoc</i>	Aldolase 3, C isoform
-1.44	0.0008	3	<i>Cox6c</i>	Cytochrome c oxidase, subunit VIc
-1.44	0.0306	3	<i>Bteb1</i>	RIKEN cDNA 2310051E17 gene
-1.44	0.1045	1	<i>Npy</i>	Neuropeptide Y
-1.43	0.0015	3	<i>Hrmt111</i>	Heterogeneous nuclear ribonucleoprotein methyltransferase-like 1
-1.43	0.0414	3	<i>C6.1A</i>	C6.1a protein
-1.42	0.0341	4	<i>Tac1</i>	Tachykinin 1
-1.41	0.0030	3	<i>Galnt10</i>	UDP-N-acetyl-alpha-D-galactosamine:polypeptide N-acetylgalactosaminyltransferase 10
-1.40	0.0011	4	<i>2410066E13Rik</i>	RIKEN cDNA 2410066E13 gene
-1.40	0.0048	4	<i>Mef2d</i>	Myocyte enhancer factor 2D
-1.40	0.0346	3	<i>Polm</i>	Polymerase (DNA directed), mu
-1.39	0.0117	3	<i>Igsf4c</i>	Immunoglobulin superfamily, member 4C
-1.39	0.0134	4	<i>8430420C20Rik</i>	RIKEN cDNA 8430420C20 gene
-1.39	0.0184	3	<i>Tcf19</i>	Transcription factor 19
-1.39	0.0290	3	<i>AI851716</i>	Expressed sequence AI851716
-1.39	0.0411	4	<i>Gpd2</i>	Glycerol phosphate dehydrogenase 2, mitochondrial
-1.39	0.0744	3	<i>Ssbp4</i>	Single stranded DNA binding protein 4
-1.38	0.0258	3	<i>Ehf</i>	Ets homologous factor

Fold regulation	p-value	# of regions	Gene symbol	Gene name
-1.37	0.0094	3	<i>Dusp18</i>	Dual specificity phosphatase 18
-1.37	0.0332	3	<i>Ube2m</i>	Ubiquitin-conjugating enzyme E2M (UBC12 homolog, yeast)
-1.36	0.0395	5	<i>Actb</i>	Actin, beta, cytoplasmic
-1.36	0.0368	3	<i>Mef2c</i>	Myocyte enhancer factor 2C
-1.36	0.0498	4	<i>Hkr2</i>	GLI-Kruppel family member HKR2
-1.35	0.0386	4	<i>1110015K06Rik</i>	RIKEN cDNA 1110015K06 gene
-1.35	0.0561	3	<i>Sepp1</i>	Selenoprotein P, plasma, 1
-1.34	0.0002	3	<i>Tpd52</i>	Tumor protein D52
-1.34	0.0245	3	<i>Rad21</i>	RAD21 homolog (S. pombe)
-1.34	0.0321	3	<i>AI481105</i>	Expressed sequence AI481105
-1.33	0.0192	4	<i>1110018D06Rik</i>	RIKEN cDNA 1110018D06 gene
-1.33	0.0561	3	<i>Cog3</i>	Component of oligomeric golgi complex 3
-1.32	0.0026	3	<i>Serpini1</i>	Serine (or cysteine) peptidase inhibitor, clade I, member 1
-1.32	0.0486	3	<i>Egfl7</i>	EGF-like domain 7
-1.31	0.0030	3	<i>ldh1</i>	Isocitrate dehydrogenase 1 (NADP+), soluble
-1.31	0.0087	3	<i>Aarsl</i>	Alanyl-tRNA synthetase like
-1.31	0.0238	3	<i>Fbxw8</i>	F-box and WD-40 domain protein 8
-1.31	0.0957	3	<i>Gprasp2</i>	G protein-coupled receptor associated sorting protein 2
-1.31	0.0994	3	<i>Gusb</i>	Glucuronidase, beta
-1.29	0.0005	3	<i>Wdr45l</i>	Wdr45 like
-1.29	0.0118	3	<i>Gas1</i>	Growth arrest specific 1
-1.29	0.0179	3	<i>Rarb</i>	Retinoic acid receptor, beta
-1.29	0.0643	3	<i>Ppt2</i>	Palmitoyl-protein thioesterase 2
-1.29	0.0049	3	<i>2900010J23Rik</i>	RIKEN cDNA 2900010J23 gene
-1.28	0.0379	3	<i>Nckap1</i>	NCK-associated protein 1
-1.28	0.0055	3	<i>Rnpep</i>	Arginyl aminopeptidase (aminopeptidase B)



Fold regulation	p-value	# of regions	Gene symbol	Gene name
-1.28	0.0141	3	<i>Ddx58</i>	DEAD (Asp-Glu-Ala-Asp) box polypeptide 58
-1.28	0.0144	3	<i>Adam10</i>	A disintegrin and metallopeptidase domain 10
-1.28	0.0207	3	<i>Sod2</i>	Superoxide dismutase 2, mitochondrial
-1.27	0.0383	3	<i>4933402J24Rik</i>	RIKEN cDNA 4933402J24 gene
-1.26	0.0098	3	<i>Ckmt1</i>	Creatine kinase, mitochondrial 1, ubiquitous
-1.26	0.0574	3	<i>Rpl27a</i>	Ribosomal protein L27a
-1.26	0.0665	3	<i>AI196514</i>	Expressed sequence AI196514
-1.25	0.0129	3	<i>Ubb</i>	Ubiquitin B
-1.24	0.0712	5	<i>Smo</i>	smoothened homolog (Drosophila)
-1.24	0.0024	3	<i>Max</i>	Max protein
-1.23	0.0606	3	<i>Zfp162</i>	Zinc finger protein 162
-1.22	0.0291	3	<i>Lu</i>	Lutheran blood group
-1.21	0.0115	3	<i>Tgfb1i4</i>	Transforming growth factor beta 1 induced transcript 4
-1.21	0.0749	4	<i>Ubc</i>	Ubiquitin C
-1.20	0.0237	3	<i>2310047M10Rik</i>	RIKEN cDNA 2310047M10 gene
-1.20	0.0258	3	<i>Mrps33</i>	Mitochondrial ribosomal protein S33
-1.20	0.0555	3	<i>Pros1</i>	Protein S (alpha)
-1.18	0.0463	3	<i>E430002G05Rik</i>	RIKEN cDNA E430002G05 gene
-1.18	0.0626	3	<i>Glul</i>	Glutamate-ammonia ligase
-1.17	0.0745	3	<i>Slc26a3</i>	Solute carrier family 26, member 3
-1.17	0.0840	4	<i>Sap18</i>	Sin3-associated polypeptide 18
-1.17	0.0041	3	<i>Calm1</i>	Calmodulin 1
-1.15	0.0269	3	<i>Nsg2</i>	Neuron specific gene family member 2
-1.15	0.0603	3	<i>Olfml3</i>	Olfactomedin-like 3

Fold regulation	p-value	# of regions	Gene symbol	Gene name
-1.15	0.0924	3	<i>Taf6l</i>	TAF6-like RNA polymerase II, p300/CBP-associated factor (PCAF)-associated factor
-1.14	0.0516	3	<i>Hap1</i>	Huntingtin-associated protein 1
-1.12	0.0263	3	<i>Abca2</i>	ATP-binding cassette, sub-family A (ABC1), member 2
1.09	0.0482	3	<i>Tgfb1i4</i>	Transforming growth factor beta 1 induced transcript 4
1.11	0.0585	3	<i>Rit2</i>	Ras-like without CAAX 2
1.13	0.0224	3	<i>Rpl17</i>	Ribosomal protein L17
1.14	0.0401	3	<i>Tde2</i>	Tumor differentially expressed 2
1.16	0.0851	3	<i>Atrx</i>	RIKEN cDNA 4833408C14 gene
1.20	0.0072	3	<i>Cpe</i>	Carboxypeptidase E
1.20	0.0503	3	<i>Canx</i>	Calnexin
1.20	0.0528	3	<i>Smn1</i>	Survival motor neuron 1
1.21	0.0074	3	<i>Rbbp7</i>	Retinoblastoma binding protein 7 DNA segment, Chr 2, Brigham & Women's Genetics 1356 expressed
1.21	0.0144	3	<i>D2Bwg1356e</i>	expressed
1.21	0.0394	3	<i>Dctn6</i>	Dynactin 6
1.21	0.0670	3	<i>Nap1l5</i>	Nucleosome assembly protein 1-like 5
1.22	0.0023	3	<i>Nme4</i>	Expressed in non-metastatic cells 4, protein
1.22	0.0453	3	<i>Rab10</i>	RIKEN cDNA 1700012B15 gene
1.22	0.0723	3	<i>D9Wsu20e</i>	Transmembrane protein 30A
1.23	0.0164	3	<i>BC051244</i>	CDNA sequence BC051244
1.24	0.0149	3	<i>9130413I22Rik</i>	Morf4 family associated protein 1
1.24	0.0218	3	<i>2700046G09Rik</i>	RIKEN cDNA 2700046G09 gene
1.24	0.0253	4	<i>Spnb2</i>	Spectrin beta 2
1.24	0.0639	3	<i>Golga7</i>	Golgi autoantigen, golgin subfamily a, 7
1.25	0.0768	3	<i>Pcoln3</i>	procollagen (type III) N-endopeptidase
1.25	0.0074	3	<i>Gpm6a</i>	Glycoprotein m6a



Fold regulation	p-value	# of regions	Gene symbol	Gene name
1.26	0.0288	3	<i>Qdpr</i>	Quinoid dihydropteridine reductase
1.26	0.0904	3	<i>Ndfip1</i>	Nedd4 family interacting protein 1
1.27	0.0406	5	<i>3830421F13Rik</i>	Forty-two-three domain containing 1
1.27	0.0027	3	<i>D19Ert144e</i>	CDK2-associated protein 2
1.27	0.0029	3	<i>Ap1s2</i>	Adaptor-related protein complex 1, sigma 2 subunit
1.27	0.0634	3	<i>Arhgap5</i>	Rho GTPase activating protein 5
1.28	0.0006	3	<i>Idh3a</i>	Isocitrate dehydrogenase 3 (NAD+) alpha
1.29	0.0288	3	<i>Snap91</i>	Synaptosomal-associated protein 91
1.29	0.0451	3	<i>Elovl5</i>	ELOVL family member 5, elongation of long chain fatty acids (yeast)
1.29	0.0775	3	<i>Luzp2</i>	Leucine zipper protein 2
1.31	0.0225	4	<i>Slc25a12</i>	RIKEN cDNA 5730410E19 gene
1.31	0.0874	3	<i>Syt11</i>	Synaptotagmin XI
1.32	0.0241	3	<i>Rps3a</i>	ribosomal protein S3a
1.33	0.0153	3	<i>Slc39a6</i>	Solute carrier family 39 (metal ion transporter), member 6
1.33	0.0268	4	<i>Peg3</i>	Paternally expressed 3
1.33	0.0404	4	<i>Cldn12</i>	Claudin 12
1.33	0.0154	5	<i>Ext2</i>	Exostoses 2
1.34	0.0253	4	<i>Zmynd11</i>	Zinc finger, MYND domain containing 11
1.35	0.0110	3	<i>Ncald</i>	Neurocalcin delta
1.35	0.0266	4	<i>Rab11a</i>	RAB11a, member RAS oncogene family
1.36	0.0020	4	<i>Raf1</i>	V-raf-1 leukemia viral oncogene 1
1.36	0.0118	3	<i>1300006C19Rik</i>	RIKEN cDNA 1300006C19 gene
1.36	0.0394	3	<i>Hspca</i>	Heat shock protein 1, alpha
1.37	0.0368	3	<i>Nap115</i>	Nucleosome assembly protein 1-like 5

Fold regulation	p-value	# of regions	Gene symbol	Gene name
1.37	0.0498	3	<i>Mbp</i>	Myelin basic protein
1.38	0.0411	3	<i>Slc36a4</i>	Solute carrier family 36 (proton/amino acid symporter), member 4
1.39	0.0012	3	<i>Stmn1</i>	Stathmin 1
1.39	0.0046	3	<i>Calm2</i>	Calmodulin 2
1.39	0.0266	3	<i>6330439K17Rik</i>	RIKEN cDNA 6330439K17 gene
1.39	0.0270	4	<i>Gnas</i>	GNAS complex locus
1.41	0.0085	3	<i>Clic4</i>	Chloride intracellular channel 4
1.41	0.0144	4	<i>Incenp</i>	Inner centromere protein
1.41	0.0177	4	<i>Ctso</i>	Cathepsin O
1.41	0.0189	5	<i>Gprasp1</i>	G protein-coupled receptor associated sorting protein 1
1.41	0.0291	3	<i>Wnt10b</i>	Wingless related MMTV integration site 10b
1.42	0.0053	4	<i>1700045I19Rik</i>	RIKEN cDNA 1700045I19 gene
1.42	0.0712	3	<i>Aak1</i>	AP2 associated kinase 1
1.43	0.0040	3	<i>Sfrs10</i>	Splicing factor, arginine/serine-rich 10
1.44	0.0284	4	<i>Mtss1</i>	Metastasis suppressor 1
1.45	0.0130	3	<i>Ywhaq</i>	Tyrosine 3-monooxygenase/tryptophan 5-monooxygenase activation protein, theta polypeptide
1.45	0.0424	4	<i>Suclg2</i>	Succinate-Coenzyme A ligase, GDP-forming, beta subunit
1.46	0.0002	3	<i>Ddx27</i>	DEAD (Asp-Glu-Ala-Asp) box polypeptide 27
1.46	0.0020	3	<i>Atp6ap2</i>	ATPase, H+ transporting, lysosomal accessory protein 2
1.46	0.0022	4	<i>Rtn1</i>	Reticulon 1
1.46	0.0584	4	<i>Ogfr1</i>	Opioid growth factor receptor-like 1



Fold regulation	p-value	# of regions	Gene symbol	Gene name
1.47	0.0267	5	<i>Wsb2</i>	WD repeat and SOCS box-containing 2
1.47	0.0017	3	<i>Kctd12</i>	Potassium channel tetramerisation domain containing 12
1.47	0.0018	3	<i>Hspa8</i>	Heat shock protein 8
1.48	0.0009	4	<i>Matr3</i>	Matrin 3
1.48	0.0018	3	<i>Nedd4l</i>	Neural precursor cell expressed, developmentally down-regulated gene 4-like
1.48	0.0031	3	<i>Mtpn</i>	Myotrophin
1.48	0.0112	3	<i>Hnrpk</i>	Heterogeneous nuclear ribonucleoprotein K
1.49	0.0014	4	<i>Rab25</i>	RAB25, member RAS oncogene family
1.50	0.0019	3	<i>Sdha</i>	Succinate dehydrogenase complex, subunit A, flavoprotein (Fp)
1.50	0.0077	4	<i>Prph1</i>	Peripherin 1
1.51	0.0056	4	<i>Elavl2</i>	ELAV (embryonic lethal, abnormal vision, Drosophila)-like 2 (Hu antigen B)
1.53	0.0005	3	<i>Dusp6</i>	Dual specificity phosphatase 6
1.53	0.0017	3	<i>Spag9</i>	Sperm associated antigen 9
1.53	0.0048	3	<i>Uhmk1</i>	U2AF homology motif (UHM) kinase 1
1.53	0.0105	4	<i>Amd1</i>	Regulator of G-protein signaling 12
1.54	0.0029	3	<i>Ppp3ca</i>	RIKEN cDNA 4930599N24 gene
1.54	0.0207	4	<i>Hadhb</i>	Hydroxyacyl-Coenzyme A dehydrogenase/3-ketoacyl-Coenzyme A thiolase/enoyl-Coenzyme A hydratase beta subunit
1.54	0.0534	4	<i>Ppia</i>	Peptidylprolyl isomerase A
1.56	0.0110	3	<i>Stmn2</i>	Stathmin-like 2

Fold regulation	p-value	# of regions	Gene symbol	Gene name
1.58	0.0014	3	<i>Sdccag33</i>	Serologically defined colon cancer antigen 33
1.58	0.0073	3	<i>Nudt4</i>	Nudix-type motif 4
1.58	0.0118	3	<i>Ddx3x</i>	DEAD/H box polypeptide 3, X-linked
1.59	0.0042	3	<i>Hbb-y</i>	Hemoglobin Y, beta-like embryonic chain
1.59	0.0175	5	<i>Pgm2l1</i>	Phosphoglucomutase 2-like 1
1.59	0.0018	3	<i>Clcn3</i>	RIKEN cDNA 9030622M22 gene
1.60	0.0154	4	<i>Foxp1</i>	Forkhead box P1
1.64	0.0022	4	<i>Slc36a2</i>	Solute carrier family 36 member 2
1.64	0.0055	3	<i>Rpa2</i>	Replication protein A2
1.66	0.0163	3	<i>Dpysl2</i>	Dihydropyrimidinase-like 2
1.68	0.0160	5	<i>Hmgb1</i>	High mobility group box 1
1.68	0.0038	4	<i>Vipr1</i>	Vasoactive intestinal peptide receptor 1
1.68	0.0110	4	<i>Rab20</i>	RAB20, member RAS oncogene family
1.68	0.0409	4	<i>Wsb1</i>	WD repeat and SOCS box-containing 1
1.74	0.0006	3	<i>Rnf11</i>	Ring finger protein 11
1.74	0.0210	6	<i>Hmgn3</i>	High mobility group nucleosomal binding domain 3
1.77	0.0026	4	<i>Egr1</i>	Early growth response 1
1.80	0.0484	2	<i>Avp</i>	Arginine vasopressin
1.87	0.0005	3	<i>Snap25</i>	Synaptosomal-associated protein 25
1.89	0.0670	4	<i>Loxl3</i>	Lysyl oxidase-like 3
2.08	0.0085	4	<i>Syt4</i>	Synaptotagmin IV
2.09	0.0110	3	<i>Slc12a3</i>	Solute carrier family 12, member 3
2.49	0.0123	3	<i>Atp9a</i>	ATPase, class II, type 9A
2.62	0.0051	4	<i>Unc84a</i>	Unc-84 homolog A
4.36	0.0029	7	<i>Rab6</i>	RAB6, member RAS oncogene



Supplementary table 2: Excerpt of transcripts identified on the Illumina mouse gene expression screening platform, with positive fold regulation values meaning an overexpression in HAB compared to LAB mice and negative values an overexpression of LAB compared to HAB mice. P-values are adjusted to multiple testing. Number of brain regions for significant regulation differences between HAB and LAB mice. Last column shows fold regulation of HAB vs. NAB mice. Data are presented as means.

HAB vs. LAB	p-value	# of regions	Gene symbol	Gene name	HAB vs. NAB
-14.15	8.35E-12	5	<i>Enpp5</i>	ectonucleotide pyrophosphatase/ phosphodiesterase 5	-5.05
-12.29	4.18E-35	5	<i>Ctsb</i>	cathepsin B	-13.61
-5.79	1.29E-32	5	<i>Sc4mol</i>	sterol-C4-methyl oxidase-like	-5.86
-5.74	3.13E-27	5	<i>Slco1c1</i>	solute carrier organic anion transporter family	-0.75
-5.37	1.67E-39	5	<i>B3galt6</i>	UDP-Gal:betaGal beta 1	-5.56
-4.09	2.48E-25	5	<i>2610511O17Rik</i>	RIKEN cDNA 2610511O17 gene	0.61
-4.06	1.83E-30	5	<i>Ccrn4l</i>	CCR4 carbon catabolite repression 4-like	-4.30
-3.93	1.44E-10	5	<i>Mela</i>	melanoma antigen	-0.81
-3.85	5.56E-26	5	<i>Kras2</i>	Kirsten rat sarcoma oncogene 2	-4.31
-3.75	9.28E-10	5	<i>9030612M13Rik</i>	RIKEN cDNA 9030612M13 gene	-2.13
-3.61	3.79E-19	5	<i>A430106J12Rik</i>	RIKEN cDNA A430106J12 gene	-1.25
-3.58	1.19E-09	5	<i>Kcnh1</i>	potassium voltage-gated channel 1	-2.59
-3.26	9.18E-29	5	<i>4933421G18Rik</i>	RIKEN cDNA 4933421G18 gene	-3.96
-2.97	1.12E-25	5	<i>Pygb</i>	brain glycogen phosphorylase	-3.07
-2.84	4.53E-20	5	<i>6330416L07Rik</i>	RIKEN cDNA 6330416L07 gene	-2.68
-2.71	1.19E-18	5	<i>Mipep</i>	mitochondrial intermediate peptidase	0.19
-2.68	3.51E-20	5	<i>Cntn2</i>	contactin 2	-1.09
-2.63	1.72E-12	5	<i>Mrps27</i>	mitochondrial rib. protein S27	-0.92

HAB vs. LAB	p-value	# of regions	Gene symbol	Gene name	HAB vs. NAB
-2.62	3.15E-11	5	<i>Pip5k2a</i>	phosphatidylinositol-4-phosphate 5-kinase	-1.03
-2.61	1.25E-11	5	<i>Glo1</i>	glyoxalase 1	-1.69
-2.50	4.42E-10	5	<i>Frs3</i>	fibroblast growth factor receptor substrate 3	-1.57
-2.47	2.85E-16	5	<i>Pop4</i>	processing of precursor 4	-0.14
-2.39	6.34E-28	5	<i>0610033H09Rik</i>	RIKEN cDNA 0610033H09 gene	-2.52
-2.35	3.25E-12	5	<i>Brf2</i>	BRF2	-2.03
-2.34	8.31E-12	5	<i>Slc25a18</i>	solute carrier family 25 member 18	-7.57
-2.30	4.90E-05	5	<i>A630042L21Rik</i>	RIKEN cDNA A630042L21 gene	-1.67
-2.23	2.33E-02	5	<i>4933427D14Rik</i>	RIKEN cDNA 4933427D14 gene	-0.24
-2.18	9.84E-17	5	<i>Dutp</i>	deoxyuridine triphosphatase	-0.79
-2.17	7.63E-22	5	<i>D330038K10Rik</i>	RIKEN cDNA D330038K10 gene	-2.31
-2.14	2.15E-17	5	<i>Hbb-b2</i>	hemoglobin	-2.56
-2.10	7.94E-14	5	<i>Myst2</i>	MYST histone acetyltransferase 2	-2.18
-2.08	3.53E-33	2	<i>Ghrh</i>	growth hormone releasing hormone	-2.45
-2.08	1.04E-25	5	<i>Arl8</i>	ADP-ribosylation factor-like 8	-2.16
-2.06	3.70E-23	5	<i>1200003M09Rik</i>	RIKEN cDNA 1200003M09 gene	-2.02
-2.04	1.83E-24	5	<i>2610040E16Rik</i>	RIKEN cDNA 2610040E16 gene	-2.09
-2.03	3.05E-14	5	<i>Slc25a17</i>	solute carrier family 25 member 17	-1.92
-1.98	1.34E-29	2	<i>1700008P20Rik</i>	RIKEN cDNA 1700008P20 gene	-1.71
-1.98	1.64E-04	5	<i>Fjx1</i>	four jointed box 1	-1.58
-1.97	2.35E-07	5	<i>2410129H14Rik</i>	RIKEN cDNA 2410129H14 gene	-1.80
-1.95	2.35E-07	5	<i>Drctnnb1a</i>	down-regulated by Ctnnb1	0.22



HAB vs. LAB	p-value	# of regions	Gene symbol	Gene name	HAB vs. NAB	HAB vs. LAB	p-value	# of regions	Gene symbol	Gene name	HAB vs. NAB
-1.93	1.06E-05	5	<i>Dok5</i>	downstream of tyrosine kinase 5	-0.24	-1.52	1.03E-04	4	<i>Bub3</i>	budding uninhibited by benzimidazoles 3 homolog	-1.32
-1.92	2.27E-14	5	<i>Rpp14</i>	ribonuclease P 14kDa subunit	-1.73	-1.52	1.80E-14	4	<i>Frmd3</i>	FERM domain containing 3	-1.63
-1.92	9.14E-08	5	<i>Rfng</i>	radical fringe gene homolog	-0.75	-1.52	6.74E-07	5	<i>F2r</i>	coagulation factor II	-1.25
-1.84	1.28E-16	5	<i>Me2</i>	malic enzyme 2	0.71	-1.52	1.94E-13	4	<i>Spag1</i>	sperm associated antigen 1	0.17
-1.83	2.11E-06	5	<i>Gukmi1</i>	guanylate kinase membrane-associated inverted 1	-1.42	-1.52	1.90E-13	5	<i>Vars2l</i>	valyl-tRNA synthetase 2-like	-1.29
-1.83	5.66E-05	5	<i>Baiap1</i>	BAI1-associated protein 1	-1.42	-1.51	9.95E-12	5	<i>1700009P03Rik</i>	RIKEN cDNA 1700009P03 gene	-0.25
-1.83	1.24E-12	5	<i>LOC381259</i>	similar to hypothetical protein FLJ33282	-1.83	-1.51	9.43E-07	5	<i>C1qb</i>	complement component 1	-1.26
-1.77	1.77E-17	5	<i>E130307J04Rik</i>	RIKEN cDNA E130307J04 gene	-1.61	-1.50	5.36E-11	5	<i>4930519N13Rik</i>	RIKEN cDNA 4930519N13 gene	-1.53
-1.76	2.40E-12	5	<i>Rpl30</i>	ribosomal protein L30	3.81	-1.49	1.64E-18	2	<i>Tmie</i>	transmembrane inner ear	-1.51
-1.76	4.63E-16	5	<i>Aldh4a1</i>	aldehyde dehydrogenase 4 family member 1	-1.62	-1.48	6.77E-05	2	<i>2810036L13Rik</i>	RIKEN cDNA 2810036L13 gene	-0.69
-1.75	1.62E-08	5	<i>2610524H06Rik</i>	RIKEN cDNA 2610524H06 gene	-0.68	-1.48	1.71E-02	3	<i>Dbt</i>	dihydrolipoamide branched chain transacylase E2	-0.24
-1.71	6.06E-13	5	<i>Pdk2</i>	pyruvate dehydrogenase kinase 2	-1.57	-1.47	5.15E-14	5	<i>9830001H06Rik</i>	RIKEN cDNA 9830001H06 gene	-1.53
-1.68	2.05E-14	4	<i>Pigl</i>	phosphatidylinositol glycan	-0.79	-1.47	8.11E-18	3	<i>Reck</i>	reversion-inducing-cysteine-rich protein with kazal motifs	0.19
-1.66	2.40E-10	3	<i>Nupr1</i>	nuclear protein 1	-0.93	-1.47	2.08E-05	4	<i>D430033N04Rik</i>	RIKEN cDNA D430033N04 gene	-1.20
-1.64	1.60E-09	5	<i>Myh9</i>	myosin heavy chain IX	-1.44	-1.47	1.50E-10	4	<i>C1qtnf5</i>	C1q and tumor necrosis factor related protein 5	-1.54
-1.63	9.36E-08	3	<i>Sepw1</i>	selenoprotein W	-0.74	-1.46	3.22E-08	5	<i>5430437P03Rik</i>	RIKEN cDNA 5430437P03 gene	-0.61
-1.62	5.08E-06	5	<i>Sv2a</i>	synaptic vesicle glycoprotein 2 a	-0.38	-1.45	6.10E-08	4	<i>4930455C21Rik</i>	RIKEN cDNA 4930455C21 gene	-1.34
-1.62	4.56E-03	4	<i>Omg</i>	oligodendrocyte myelin glycoprotein	0.02	-1.45	4.38E-08	1	<i>Zfp297b</i>	zinc finger protein 297B	-1.49
-1.61	1.28E-14	3	<i>Ube2i</i>	ubiquitin-conjugating enzyme E2I	-1.58	-1.45	1.83E-07	4	<i>2610319K07Rik</i>	RIKEN cDNA 2610319K07 gene	-1.19
-1.59	1.00E-12	5	<i>Aebp2</i>	AE binding protein 2	-0.26	-1.44	9.23E-06	5	<i>3200001K10Rik</i>	RIKEN cDNA 3200001K10 gene	-1.30
-1.58	1.45E-12	4	<i>Fads3</i>	fatty acid desaturase 3	-1.77	-1.44	3.23E-12	4	<i>Rrm1</i>	ribonucleotide reductase M1	-1.38
-1.57	3.63E-05	5	<i>9230117N10Rik</i>	RIKEN cDNA 9230117N10 gene	-1.57	-1.42	5.19E-04	5	<i>C1qg</i>	complement component 1	-0.75
-1.56	1.63E-06	5	<i>4432411E13Rik</i>	RIKEN cDNA 4432411E13 gene	-0.70	-1.42	1.07E-05	4	<i>Epb7.2</i>	erythrocyte protein band 7.2	-0.32



HAB vs. LAB	p-value	# of regions	Gene symbol	Gene name	HAB vs. NAB	HAB vs. LAB	p-value	# of regions	Gene symbol	Gene name	HAB vs. NAB
-1.42	3.63E-03	3	<i>Igf2r</i>	insulin-like growth factor 2 receptor	-0.86	-1.36	4.28E-02	2	<i>Nefh</i>	neurofilament	-0.68
-1.41	2.02E-08	3	<i>Hist3h2ba</i>	histone 3	-0.73	-1.36	1.21E-02	3	<i>Ski</i>	Sloan-Kettering viral oncogene homolog	-1.46
-1.41	1.25E-07	3	<i>Brp17</i>	brain protein 17	-1.38	-1.36	7.52E-06	3	<i>A430079E08</i>	hypothetical protein A430079E08	0.24
-1.41	2.45E-10	5	<i>Pik3cg</i>	phosphoinositide-3-kinase	-0.21	-1.36	1.88E-08	3	<i>A730017C20Rik</i>	RIKEN cDNA A730017C20 gene	-1.07
-1.41	1.85E-06	3	<i>Atpaf2</i>	ATP synthase mitochondrial F1 complex assembly factor 2	-1.17	-1.35	4.80E-10	2	<i>9130404D08Rik</i>	RIKEN cDNA 9130404D08 gene	0.20
-1.40	1.36E-13	2	<i>BC003993</i>	cDNA sequence BC003993	2.33	-1.35	2.84E-06	5	<i>Anxa6</i>	annexin A6	-1.20
-1.40	5.31E-05	2	<i>Kptn</i>	kaptin	-1.32	-1.35	4.10E-03	2	<i>Ttc4</i>	tetratricopeptide repeat domain 4	-0.72
-1.40	1.73E-03	2	<i>Arl10c</i>	ADP-ribosylation factor-like 10C	-1.24	-1.35	4.49E-08	2	<i>Usp49</i>	ubiquitin specific protease 49	-1.19
-1.40	8.25E-10	2	<i>Gtf3c1</i>	general transcription factor III C 1	-1.67	-1.35	1.25E-05	2	<i>1110054H05Rik</i>	RIKEN cDNA 1110054H05 gene	0.17
-1.39	5.21E-06	3	<i>2410012H22Rik</i>	RIKEN cDNA 2410012H22 gene	-0.69	-1.35	2.09E-03	3	<i>Wars2</i>	tryptophanyl tRNA synthetase 2	-0.68
-1.38	4.96E-05	3	<i>1200016B10Rik</i>	RIKEN cDNA 1200016B10 gene	-1.43	-1.34	2.13E-03	1	<i>Fjx1</i>	four jointed box 1	-0.14
-1.38	7.60E-02	1	<i>Sep3</i>	septin 3	-1.31	-1.34	1.45E-05	2	<i>Ssbp2</i>	single-stranded DNA binding protein 2	-1.30
-1.38	2.30E-02	4	<i>Peg3</i>	paternally expressed 3	-0.70	-1.34	1.08E-04	4	<i>4930471O16Rik</i>	RIKEN cDNA 4930471O16 gene	-0.62
-1.38	5.87E-18	3	<i>Nkiras1</i>	NFKB inhibitor interacting Ras-like protein 1 hypothetical	-1.39	-1.34	5.15E-06	2	<i>D130078K04Rik</i>	GRP1 BINDING PROTEIN GRSP1	-1.29
-1.38	5.85E-08	3	<i>6330583M11Rik</i>	Esterase/lipase/thioesterase family active site containing protein	-1.34	-1.33	4.70E-04	3	<i>1500041J02Rik</i>	RIKEN cDNA 1500041J02 gene	-0.23
-1.37	4.65E-04	1	<i>Cxcl12</i>	chemokine	0.21	-1.33	1.01E-03	2	<i>AW060207</i>	expressed sequence AW060207	0.12
-1.37	5.14E-13	2	<i>Pdzk2</i>	PDZ domain containing 2	-1.29	-1.33	6.00E-04	1	<i>6820402O20Rik</i>	RIKEN cDNA 6820402O20 gene	-1.50
-1.37	1.02E-03	3	<i>Peg3</i>	paternally expressed 3	-1.11	-1.32	1.85E-07	3	<i>1700064K09Rik</i>	RIKEN cDNA 1700064K09 gene	-0.22
-1.37	1.75E-04	3	<i>Cln2</i>	ceroid-lipofuscinosis 2	-1.26	-1.30	5.35E-03	1	<i>6030413G23Rik</i>	RIKEN cDNA 6030413G23 gene	-0.26
-1.36	1.14E-13	2	<i>Mftc</i>	mitochondrial folate transporter/carrier	0.60	1.30	3.95E-03	1	<i>Noxo1</i>	NADPH oxidase organizer 1	1.36
-1.36	1.37E-03	2	<i>Lpin2</i>	lipin 2	-1.18	1.30	7.48E-03	3	<i>Rasgrp1</i>	RAS guanyl releasing protein 1	0.70
-1.36	4.17E-03	1	<i>Dlk1</i>	delta-like 1 homolog	-0.70						
-1.36	2.22E-09	2	<i>Ogdh</i>	oxoglutarate dehydrogenase	-2.48						
-1.36	3.09E-14	3	<i>Phtf1</i>	putative homeodomain transcription factor 1	-1.41						



HAB vs. LAB	p-value	# of regions	Gene symbol	Gene name	HAB vs. NAB
1.30	3.65E-03	3	<i>Ppil1</i>	peptidylprolyl isomerase	1.14
1.30	5.49E-10	2	<i>Tnfrsf4</i>	tumor necrosis factor receptor superfamily	1.32
1.30	1.90E-04	1	<i>Scp2</i>	sterol carrier protein 2	1.14
1.30	3.11E-02	2	<i>Stim1</i>	stromal interaction molecule 1	1.17
1.31	2.49E-05	1	<i>Aass</i>	aminoadipate-semialdehyde synthase	1.35
1.31	1.39E-03	4	<i>Abcb4</i>	ATP-binding cassette	0.72
1.31	3.23E-02	3	<i>Egr3</i>	early growth response 3	-0.18
1.31	9.77E-07	3	<i>Gfpt2</i>	glutamine fructose-6-phosphate transaminase 2	1.12
1.31	7.92E-04	2	<i>Ltc4s</i>	leukotriene C4 synthase	1.30
1.32	2.47E-09	2	<i>Laptm4b</i>	lysosomal-associated protein transmembrane 4B	0.24
1.32	2.36E-02	2	<i>Plvap</i>	plasmalemma vesicle associated protein	0.65
1.32	2.59E-16	1	<i>2310012P17Rik</i>	RIKEN cDNA 2310012P17 gene	1.29
1.32	2.23E-10	1	<i>Ctsb</i>	cathepsin B	1.41
1.33	4.52E-12	2	<i>4933439J20Rik</i>	hypothetical XRCC1 N terminal domain containing protein	1.26
1.33	8.90E-10	3	<i>1810009N02Rik</i>	RIKEN cDNA 1810009N02 gene	-1.71
1.34	1.67E-03	4	<i>H2-Q2</i>	histocompatibility 2	1.35
1.34	3.94E-13	3	<i>4931440B09Rik</i>	RIKEN cDNA 4931440B09 gene	1.35
1.35	4.73E-07	3	<i>2410015N17Rik</i>	RIKEN cDNA 2410015N17 gene	-0.16
1.35	9.60E-02	2	<i>Timm10</i>	translocase of inner mitochondrial membrane 10 homolog	1.48
1.35	1.03E-07	1	<i>Mvp</i>	major vault protein	0.67
1.35	1.20E-05	3	<i>Dmwd</i>	dystrophia myotonica-containing WD repeat motif	0.91
1.38	1.26E-04	3	<i>Rbm9</i>	RNA binding motif protein 9	0.65

HAB vs. LAB	p-value	# of regions	Gene symbol	Gene name	HAB vs. NAB
1.38	3.38E-07	2	<i>Elmo3</i>	engulfment and cell motility 3	1.46
1.38	1.18E-02	4	<i>Rpo1-1</i>	RNA polymerase 1-1	0.81
1.38	3.40E-09	3	<i>Gfra1</i>	glial cell line derived neurotrophic factor family receptor alpha 1	0.82
1.38	2.49E-03	4	<i>Dnajc5</i>	DnaJ	1.45
1.39	2.35E-09	4	<i>Mopt</i>	protein containing single MORN motif in testis	-0.68
1.39	2.36E-10	5	<i>Tnfrsf13b</i>	tumor necrosis factor receptor superfamily	1.16
1.40	4.66E-05	4	<i>Mad2l1bp</i>	MAD2L1 binding protein	0.65
1.40	1.04E-08	4	<i>1810073G14Rik</i>	RIKEN cDNA 1810073G14 gene	1.14
1.40	7.17E-04	3	<i>Mag</i>	myelin-associated glycoprotein	1.30
1.41	1.87E-15	4	<i>Creb3</i>	cAMP responsive element binding protein 3	0.22
1.41	7.34E-05	1	<i>Zfp68</i>	zinc finger protein 68	-0.74
1.43	7.85E-07	5	<i>Slc35b1</i>	solute carrier family 35	1.16
1.43	1.61E-07	4	<i>2610528C06Rik</i>	RIKEN cDNA 2610528C06 gene	0.73
1.43	5.48E-05	3	<i>Alad</i>	aminolevulinate	0.29
1.44	2.43E-06	5	<i>Ercc1</i>	excision repair cross-complementing rodent repair deficiency	1.47
1.45	1.65E-10	4	<i>Ntsr2</i>	neurotensin receptor 2	1.55
1.45	2.31E-02	5	<i>2310007A19Rik</i>	RIKEN cDNA 2310007A19 gene	1.30
1.45	1.99E-05	4	<i>Laf4l</i>	lymphoid nuclear protein related to AF4-like	0.74
1.46	1.55E-06	4	<i>9330196J05Rik</i>	RIKEN cDNA 9330196J05 gene	0.17
1.46	1.94E-14	4	<i>Map1lc3a</i>	microtubule-associated protein 1 light chain 3 alpha	1.59
1.46	5.16E-09	5	<i>Bcl2a1b</i>	B-cell leukemia/lymphoma 2 related protein A1b	0.68
1.46	6.84E-08	3	<i>6720463L11Rik</i>	SPLICING FACTOR	-0.69



HAB vs. LAB	p-value	# of regions	Gene symbol	Gene name	HAB vs. NAB
1.47	5.07E-10	3	<i>Alg1</i>	asparagine-linked glycosylation 1 homolog	-0.18
1.48	4.44E-10	4	<i>Eml1</i>	echinoderm microtubule associated protein like 1	0.66
1.48	9.00E-08	4	<i>6330530A05Rik</i>	RIKEN cDNA 6330530A05 gene	0.72
1.48	1.41E-06	3	<i>G2-pending</i>	G2 protein	1.40
1.49	8.25E-07	5	<i>1110012N22Rik</i>	RIKEN cDNA 1110012N22 gene	1.14
1.49	5.53E-02	3	<i>Hbb-b1</i>	hemoglobin	0.86
1.49	1.44E-07	4	<i>Syt4</i>	synaptotagmin 4	-0.29
1.51	4.23E-06	4	<i>Rutbc2</i>	RUN and TBC1 domain containing 2	-0.25
1.51	7.46E-07	5	<i>Eppb9</i>	endothelial precursor protein B9	1.28
1.52	7.96E-10	2	<i>BC034099</i>	cDNA sequence BC034099	1.19
1.52	4.27E-14	2	<i>LOC226654</i>	similar to KAT protein	0.66
1.52	2.42E-19	4	<i>H2-T23</i>	histocompatibility 2	1.50
1.52	5.10E-12	5	<i>1110029E03Rik</i>	RIKEN cDNA 1110029E03 gene	-0.69
1.53	1.77E-04	3	<i>A530072M07Rik</i>	hypothetical protein	0.25
1.54	1.71E-09	5	<i>0610012D14Rik</i>	RIKEN cDNA 0610012D14 gene	1.58
1.54	8.46E-15	5	<i>LOC210245</i>	similar to WTAP protein	0.63
1.54	3.31E-06	5	<i>Cd59a</i>	CD59a antigen	1.44
1.55	1.76E-04	4	<i>5031425E22Rik</i>	RIKEN cDNA 5031425E22 gene	0.28
1.55	3.40E-10	5	<i>1700023O11Rik</i>	RIKEN cDNA 1700023O11 gene	0.28
1.55	3.26E-07	3	<i>2310036D22Rik</i>	RIKEN cDNA 2310036D22 gene	3.32
1.56	9.09E-17	5	<i>1300019C06Rik</i>	RIKEN cDNA 1300019C06 gene	1.65
1.56	5.76E-03	5	<i>Prkag2</i>	protein kinase	1.30
1.57	1.96E-09	5	<i>1110032N12Rik</i>	RIKEN cDNA 1110032N12 gene	-0.18

HAB vs. LAB	p-value	# of regions	Gene symbol	Gene name	HAB vs. NAB
1.57	1.36E-08	4	<i>Trim3</i>	tripartite motif protein 3	1.12
1.58	6.22E-05	2	<i>Wnt9a</i>	wingless-type MMTV integration site 9A	0.85
1.59	2.15E-15	4	<i>Elac1</i>	elaC homolog 1	-0.18
1.60	1.90E-11	5	<i>1700027N10Rik</i>	RIKEN cDNA 1700027N10 gene	1.20
1.60	6.26E-05	4	<i>Rps3a</i>	ribosomal protein S3a	-0.79
1.62	1.85E-08	4	<i>Slc1a2</i>	solute carrier family 1 member 2	1.57
1.62	3.48E-12	5	<i>Slc35b1</i>	solute carrier family 35 member b1	1.13
1.63	1.90E-07	3	<i>Sox5</i>	SRY-box containing gene 5	1.54
1.65	4.36E-10	5	<i>Zfp365</i>	zinc finger protein 365	1.64
1.65	3.95E-05	4	<i>Zfp318</i>	zinc finger protein 318	0.65
1.67	7.06E-09	4	<i>Twistnb</i>	TWIST neighbor	1.49
1.68	5.71E-21	5	<i>2700008N14Rik</i>	RIKEN cDNA 2700008N14 gene	1.86
1.69	4.22E-14	5	<i>1300010F03Rik</i>	RIKEN cDNA 1300010F03 gene	1.84
1.70	7.59E-12	4	<i>Chic1</i>	cysteine-rich hydrophobic domain 1	-1.14
1.71	1.50E-02	5	<i>Hba-a1</i>	hemoglobin alpha	0.90
1.72	1.36E-02	5	<i>Hbb-b1</i>	hemoglobin beta	1.08
1.77	2.08E-19	5	<i>Mpeg1</i>	macrophage expressed gene 1	1.81
1.80	1.03E-10	4	<i>Vti1b</i>	arginase type II	0.63
1.86	1.67E-11	5	<i>LOC384154</i>	similar to ribosomal protein L31	1.20
1.87	1.34E-06	5	<i>1700024K14Rik</i>	RIKEN cDNA 1700024K14 gene	0.87
1.89	2.19E-14	5	<i>Mpg</i>	N-methylpurine-DNA glycosylase	0.61
1.89	9.64E-10	4	<i>Gtpbp4</i>	GTP binding protein 4	1.87
1.89	1.37E-12	4	<i>Ddr1</i>	discoïdin domain receptor family	1.89



HAB vs. LAB	p-value	# of regions	Gene symbol	Gene name	HAB vs. NAB
1.91	9.30E-09	5	<i>Rapgef5</i>	Rap guanine nucleotide exchange factor 5	0.70
1.91	6.08E-04	4	<i>Ppfbp1</i>	PTPRF interacting protein	1.49
1.93	1.76E-14	5	<i>Dgkq</i>	diacylglycerol kinase theta	0.20
1.94	1.02E-10	5	<i>Tnnt1</i>	troponin T1	2.42
1.96	8.43E-15	5	<i>Add3</i>	adducin 3	-0.28
1.99	1.70E-18	5	<i>Ercc5</i>	excision repair cross-complementing rodent repair deficiency	1.99
1.99	4.51E-09	5	<i>Arhgef10</i>	Rho guanine nucleotide exchange factor	1.47
2.00	5.35E-10	5	<i>Rapgef5</i>	Rap guanine nucleotide exchange factor	0.75
2.03	5.24E-20	5	<i>1110032N12Rik</i>	RIKEN cDNA 1110032N12 gene	0.71
2.05	3.35E-19	5	<i>Hmgn3</i>	high mobility group nucleosomal binding domain 3	2.08
2.05	1.61E-06	5	<i>Rapgef5</i>	Rap guanine nucleotide exchange factor 5	0.86
2.06	3.66E-18	5	<i>Trim11</i>	tripartite motif protein 11	1.20
2.08	1.80E-13	5	<i>Sirt7</i>	sirtuin 7	0.29
2.08	6.89E-25	5	<i>Rtn4</i>	reticulon 4	2.09
2.08	7.65E-05	4	<i>Erdr1</i>	erythroid differentiation regulator 1	-0.48
2.12	1.51E-17	5	<i>Usp29</i>	ubiquitin specific protease 29	0.26
2.12	9.72E-16	5	<i>Ahcy</i>	S-adenosylhomocysteine hydrolase	2.18
2.14	3.38E-26	5	<i>Pdhb</i>	pyruvate dehydrogenase	-1.58
2.14	3.23E-10	5	<i>Cox6a2</i>	cytochrome c oxidase	1.23
2.15	2.31E-12	4	<i>Cxadr</i>	coxsackievirus and adenovirus receptor	0.30
2.16	2.87E-04	4	<i>Hspcb</i>	heat shock protein 1	0.63
2.18	4.78E-23	5	<i>Tpr</i>	translocated promoter region	2.15
2.21	2.10E-08	4	<i>Mef2c</i>	myocyte enhancer factor 2C	0.78
2.21	1.25E-14	5	<i>Dgkh</i>	diacylglycerol kinase eta	2.58

HAB vs. LAB	p-value	# of regions	Gene symbol	Gene name	HAB vs. NAB
2.21	6.97E-14	5	<i>Elov14</i>	elongation of very long chain fatty acids	1.32
2.22	1.20E-15	5	<i>Fstl5</i>	ollistatin-like 5	2.27
2.22	6.02E-05	5	<i>Ehd3</i>	EH-domain containing 3	0.82
2.23	8.50E-22	4	<i>H2-T9</i>	histocompatibility 2	2.39
2.26	5.26E-25	5	<i>2310034L04Rik</i>	RIKEN cDNA 2310034L04 gene	-0.27
2.27	2.66E-13	4	<i>Kcnj16</i>	potassium inwardly-rectifying channel	0.69
2.29	1.75E-14	5	<i>6430559E15Rik</i>	RIKEN cDNA 6430559E15 gene	0.17
2.30	3.83E-12	5	<i>Map4k3</i>	mitogen-activated protein kinase kinase kinase 3	0.15
2.31	3.74E-09	5	<i>Twistnb</i>	TWIST neighbor	1.86
2.34	3.12E-24	5	<i>Vars2l</i>	valyl-tRNA synthetase 2-like	2.38
2.38	1.97E-24	5	<i>1110015E22Rik</i>	RIKEN cDNA 1110015E22 gene	2.79
2.47	2.71E-22	5	<i>1600014C10Rik</i>	RIKEN cDNA 1600014C10 gene	-0.21
2.51	1.24E-18	5	<i>2410131K14Rik</i>	RIKEN cDNA 2410131K14 gene	1.84
2.55	1.80E-14	5	<i>Sdf4</i>	stromal cell derived factor 4	2.51
2.56	4.35E-17	5	<i>Pmp22</i>	peripheral myelin protein	1.34
2.57	4.15E-16	5	<i>Abca2</i>	ATP-binding cassette	0.63
2.60	5.51E-08	5	<i>Hbb-b1</i>	hemoglobin beta 1	2.23
2.61	2.03E-16	5	<i>Cars</i>	cysteinyl-tRNA synthetase	0.14
2.62	8.59E-20	5		16 days neonate cerebellum cDNA	0.15
2.73	7.58E-08	5	<i>Erdr1</i>	erythroid differentiation regulator 1	0.37
3.05	1.26E-11	5	<i>LOC380983</i>	similar to 60S ribosomal protein L15	3.09
3.07	1.59E-10	5	<i>Slc25a3</i>	solute carrier family 25 member 3	3.09
3.39	1.17E-21	5	<i>Rfng</i>	radical fringe gene homolog	0.71

ATGCTCGCCAGGA
TACGAGCGGTCCT



Supplementary tables

HAB vs. LAB	p-value	# of regions	Gene symbol	Gene name	HAB vs. NAB
3.46	3.35E-22	5	<i>Aldh3a2</i>	aldehyde dehydrogenase family 3	1.48
3.60	8.56E-26	5	<i>Gnaq</i>	guanine nucleotide binding protein	3.72
3.63	7.16E-12	5	<i>BC018472</i>	cDNA sequence BC018472	1.91
3.76	2.46E-13	5	<i>Satb1</i>	special AT-rich sequence binding protein 1	0.90
3.79	6.53E-29	5	<i>BC002216</i>	cDNA sequence BC002216	4.13
4.05	9.41E-13	5	<i>Hbb-b1</i>	hemoglobin	3.41
4.05	2.76E-42	5	<i>Stx3</i>	syntaxin 3	4.25
4.31	1.14E-13	5	<i>Msr2</i>	macrophage scavenger receptor 2	1.43

HAB vs. LAB	p-value	# of regions	Gene symbol	Gene name	HAB vs. NAB
4.34	5.47E-30	5	<i>BC003331</i>	cDNA sequence BC003331	5.10
4.54	4.05E-16	5	<i>Gig1</i>	glucocorticoid induced gene 1	1.56
4.75	5.85E-38	5	<i>H2-T17</i>	histocompatibility 2	5.03
5.23	4.68E-08	5	<i>2900019G14Rik</i>	RIKEN cDNA 2900019G14 gene	2.16
6.12	6.54E-12	5	<i>C330008L01Rik</i>	RIKEN cDNA C330008L01 gene	1.73
6.27	1.19E-24	5	<i>Grim19</i>	genes associated with retinoid-IFN-induced mortality 19	0.24
17.58	1.38E-17	5	<i>Hbb-b1</i>	Hemoglobin beta 1	14.41



Supplementary Table 3: Association between selected phenotypes and selected chromosomal loci. Distance (OF) refers to the total distance travelled in the open field, immobility time to the tail suspension test, percent time to the elevated plus-maze test and response to the level of corticosterone concentration increase in blood plasma after 15 minutes of restraint stress.

SNP	Phenotype	p-value
mCV23695025	distance (OF)	6.05E-01
mCV24784983	distance (OF)	5.86E-01
rs3677683	distance (OF)	5.63E-01
rs4137502	distance (OF)	5.60E-01
rs3707642	distance (OF)	5.99E-01
rs3683997	distance (OF)	4.25E-01
rs13475827	distance (OF)	3.62E-01
CEL-1_44668113	distance (OF)	7.98E-01
rs13475881	distance (OF)	6.71E-01
rs13475919	distance (OF)	6.38E-01
rs30238169	distance (OF)	4.68E-01
rs30238168	distance (OF)	4.68E-01
rs30237262	distance (OF)	4.68E-01
rs30236408	distance (OF)	4.68E-01
rs30242174	distance (OF)	4.68E-01
UT_1_89.100476	distance (OF)	4.88E-01
rs13476012	distance (OF)	4.07E-01
CEL-1_103251925	distance (OF)	3.73E-01
rs3685919	distance (OF)	2.99E-01
rs13476050	distance (OF)	2.76E-01
rs3699561	distance (OF)	9.81E-02
rs3672697	distance (OF)	7.17E-01
rs13476163	distance (OF)	7.17E-01
rs6393307	distance (OF)	7.75E-01
rs13476187	distance (OF)	7.06E-01

SNP	Phenotype	p-value
rs6157620	distance (OF)	2.87E-01
rs3667164	distance (OF)	6.90E-02
rs6240512	distance (OF)	5.84E-05
CZECH-2_15618849	distance (OF)	2.06E-07
rs13476366	distance (OF)	3.38E-07
rs4223189	distance (OF)	1.95E-01
rs3664661	distance (OF)	6.78E-01
CEL-2_73370728	distance (OF)	6.61E-01
rs13476639	distance (OF)	8.35E-01
rs6406705	distance (OF)	6.18E-01
rs13476666	distance (OF)	6.26E-01
rs13476689	distance (OF)	7.06E-01
rs13476723	distance (OF)	4.90E-01
cmfcsnpavp1	distance (OF)	4.99E-01
rs13476783	distance (OF)	4.97E-01
CEL-2_168586738	distance (OF)	1.53E-02
rs13477043	distance (OF)	5.72E-02
gnf03.030.222	distance (OF)	7.36E-02
rs6376008	distance (OF)	3.52E-01
rs6211610	distance (OF)	1.91E-02
rs13477268	distance (OF)	2.39E-01
rs4138887	distance (OF)	1.61E-01
CEL-3_120379605	distance (OF)	1.21E-01
rs13477379	distance (OF)	8.29E-02
rs3671119	distance (OF)	4.25E-01
rs3676039	distance (OF)	3.38E-01
rs6407142	distance (OF)	2.61E-01
gnf03.160.599	distance (OF)	7.21E-03
CEL-4_30653207	distance (OF)	3.92E-01
rs3708471	distance (OF)	5.85E-01
rs3023025	distance (OF)	4.56E-01

SNP	Phenotype	p-value
rs13478110	distance (OF)	8.48E-01
rs3714258	distance (OF)	8.41E-01
rs6341620	distance (OF)	1.12E-01
CEL-5_45872918	distance (OF)	1.75E-02
rs3664008	distance (OF)	1.10E-02
mCV23386455	distance (OF)	1.01E-02
rs3667334	distance (OF)	4.21E-03
rs13459087	distance (OF)	9.54E-03
rs3673049	distance (OF)	9.54E-03
rs3661241	distance (OF)	2.06E-02
rs13460000	distance (OF)	3.81E-02
rs13460001	distance (OF)	3.81E-02
rs13478433	distance (OF)	9.14E-03
rs13459186	distance (OF)	1.48E-02
rs13478483	distance (OF)	7.76E-02
rs13478518	distance (OF)	5.94E-02
rs13478520	distance (OF)	6.21E-02
rs36247439	distance (OF)	2.03E-01
rs33343556	distance (OF)	2.03E-01
rs36309698	distance (OF)	2.03E-01
rs37452785	distance (OF)	2.03E-01
mCV23695025	immobility time	7.88E-02
mCV24784983	immobility time	1.76E-02
rs3677683	immobility time	1.45E-02
rs4137502	immobility time	1.28E-02
rs3707642	immobility time	1.89E-02
rs3683997	immobility time	1.93E-02
rs13475827	immobility time	1.14E-01
CEL-1_44668113	immobility time	5.90E-01
rs13475881	immobility time	6.69E-02
rs13475919	immobility time	4.18E-01
rs30238169	immobility time	1.06E-01



SNP	Phenotype	p-value	SNP	Phenotype	p-value	SNP	Phenotype	p-value
rs30238168	immobility time	1.06E-01	gnf03.030.222	immobility time	3.21E-01	rs33343556	immobility time	8.67E-01
rs30237262	immobility time	1.06E-01	rs6376008	immobility time	2.75E-01	rs36309698	immobility time	8.67E-01
rs30236408	immobility time	1.06E-01	rs6211610	immobility time	5.94E-01	rs37452785	immobility time	8.67E-01
rs30242174	immobility time	1.06E-01	rs13477268	immobility time	2.64E-01	mCV23695025	percent time	5.81E-01
UT_1_89.100476	immobility time	8.20E-03	rs4138887	immobility time	2.22E-01	mCV24784983	percent time	4.13E-01
rs13476012	immobility time	3.93E-03	CEL-3_120379605	immobility time	2.46E-01	rs3677683	percent time	4.49E-01
CEL-1_103251925	immobility time	3.72E-03	rs13477379	immobility time	7.71E-01	rs4137502	percent time	3.72E-01
rs3685919	immobility time	1.04E-03	rs3671119	immobility time	7.01E-01	rs3707642	percent time	3.40E-01
rs13476050	immobility time	1.17E-03	rs3676039	immobility time	7.80E-01	rs3683997	percent time	3.32E-01
rs3699561	immobility time	5.66E-06	rs6407142	immobility time	3.94E-01	rs13475827	percent time	9.41E-02
rs3672697	immobility time	7.45E-08	gnf03.160.599	immobility time	9.32E-01	CEL-1_44668113	percent time	6.98E-02
rs13476163	immobility time	7.45E-08	CEL-4_30653207	immobility time	7.07E-01	rs13475881	percent time	3.19E-01
rs6393307	immobility time	3.77E-08	rs3708471	immobility time	5.89E-02	rs13475919	percent time	8.13E-01
rs13476187	immobility time	1.00E-07	rs3023025	immobility time	3.23E-01	rs30238169	percent time	7.90E-01
rs6157620	immobility time	1.04E-04	rs13478110	immobility time	9.04E-01	rs30238168	percent time	7.90E-01
rs3667164	immobility time	9.25E-04	rs3714258	immobility time	8.84E-01	rs30237262	percent time	7.90E-01
rs6240512	immobility time	1.76E-13	rs6341620	immobility time	4.77E-01	rs30236408	percent time	7.90E-01
CZECH-2_15618849	immobility time	1.42E-17	CEL-5_45872918	immobility time	2.75E-01	rs30242174	percent time	7.90E-01
rs13476366	immobility time	4.66E-19	rs3664008	immobility time	1.91E-01	UT_1_89.100476	percent time	7.88E-01
rs4223189	immobility time	3.40E-05	mCV23386455	immobility time	1.99E-01	rs13476012	percent time	3.86E-01
rs3664661	immobility time	2.15E-03	rs3667334	immobility time	1.38E-01	CEL-1_103251925	percent time	1.75E-01
CEL-2_73370728	immobility time	6.18E-03	rs13459087	immobility time	2.19E-01	rs3685919	percent time	2.83E-01
rs13476639	immobility time	1.78E-01	rs3673049	immobility time	2.19E-01	rs13476050	percent time	3.00E-01
rs6406705	immobility time	1.71E-01	rs3661241	immobility time	2.22E-01	rs3699561	percent time	2.50E-01
rs13476666	immobility time	3.11E-01	rs13460000	immobility time	2.32E-01	rs3672697	percent time	5.52E-01
rs13476689	immobility time	3.53E-01	rs13460001	immobility time	2.32E-01	rs13476163	percent time	5.52E-01
rs13476723	immobility time	6.47E-01	rs13478433	immobility time	1.31E-01	rs6393307	percent time	4.83E-01
cmcsnpvp1	immobility time	7.31E-01	rs13459186	immobility time	7.36E-02	rs13476187	percent time	5.48E-01
rs13476783	immobility time	8.21E-01	rs13478483	immobility time	4.98E-01	rs6157620	percent time	2.23E-01
CEL-2_168586738	immobility time	4.56E-02	rs13478518	immobility time	4.58E-01	rs3667164	percent time	1.65E-01
rs13477043	immobility time	3.25E-01	rs13478520	immobility time	3.18E-01	rs6240512	percent time	6.41E-04
			rs36247439	immobility time	8.67E-01			



SNP	Phenotype	p-value
CZECH-2_15618849	percent time	1.20E-03
rs13476366	percent time	3.73E-04
rs4223189	percent time	5.13E-01
rs3664661	percent time	2.03E-01
CEL-2_73370728	percent time	3.13E-01
rs13476639	percent time	9.96E-02
rs6406705	percent time	3.56E-02
rs13476666	percent time	2.16E-02
rs13476689	percent time	5.41E-02
rs13476723	percent time	5.65E-02
cmlicsnpvp1	percent time	1.84E-01
rs13476783	percent time	3.18E-01
CEL-2_168586738	percent time	2.89E-01
rs13477043	percent time	1.41E-05
gnf03.030.222	percent time	1.01E-05
rs6376008	percent time	8.12E-02
rs6211610	percent time	2.29E-02
rs13477268	percent time	1.30E-01
rs4138887	percent time	8.75E-02
CEL-3_120379605	percent time	9.00E-02
rs13477379	percent time	3.06E-02
rs3671119	percent time	4.09E-01
rs3676039	percent time	3.13E-01
rs6407142	percent time	2.03E-01
gnf03.160.599	percent time	2.06E-02
CEL-4_30653207	percent time	7.52E-01
rs3708471	percent time	2.41E-01
rs3023025	percent time	2.19E-01
rs13478110	percent time	5.05E-01
rs3714258	percent time	7.44E-01
rs6341620	percent time	2.28E-01

SNP	Phenotype	p-value
CEL-5_45872918	percent time	3.85E-02
rs3664008	percent time	2.63E-04
mCV23386455	percent time	1.24E-04
rs3667334	percent time	9.66E-07
rs13459087	percent time	2.06E-06
rs3673049	percent time	2.06E-06
rs3661241	percent time	7.94E-07
rs13460000	percent time	1.05E-06
rs13460001	percent time	1.05E-06
rs13478433	percent time	3.52E-07
rs13459186	percent time	2.44E-07
rs13478483	percent time	9.97E-08
rs13478518	percent time	2.04E-03
rs13478520	percent time	9.80E-04
rs36247439	percent time	6.98E-01
rs33343556	percent time	6.98E-01
rs36309698	percent time	6.98E-01
rs37452785	percent time	6.98E-01
mCV23695025	response	5.88E-01
mCV24784983	response	6.27E-01
rs3677683	response	5.63E-01
rs4137502	response	5.30E-01
rs3707642	response	4.82E-01
rs3683997	response	4.79E-01
rs13475827	response	3.62E-02
CEL-1_44668113	response	1.27E-01
rs13475881	response	3.63E-01
rs13475919	response	7.74E-02
rs30238169	response	7.97E-02
rs30238168	response	7.97E-02
rs30237262	response	7.97E-02
rs30236408	response	7.97E-02

SNP	Phenotype	p-value
rs30242174	response	7.97E-02
UT_1_89.100476	response	1.32E-01
rs13476012	response	3.63E-01
CEL-1_103251925	response	4.22E-01
rs3685919	response	5.43E-01
rs13476050	response	5.43E-01
rs3699561	response	5.02E-01
rs3672697	response	8.92E-01
rs13476163	response	8.92E-01
rs6393307	response	7.76E-01
rs13476187	response	8.38E-01
rs6157620	response	1.94E-01
rs3667164	response	1.26E-01
rs6240512	response	7.93E-01
CZECH-2_15618849	response	5.78E-01
rs13476366	response	3.28E-01
rs4223189	response	5.97E-01
rs3664661	response	1.08E-01
CEL-2_73370728	response	9.86E-02
rs13476639	response	2.49E-01
rs6406705	response	1.25E-01
rs13476666	response	1.33E-01
rs13476689	response	3.60E-01
rs13476723	response	2.53E-01
cmlicsnpvp1	response	9.82E-02
rs13476783	response	5.38E-02
CEL-2_168586738	response	9.89E-02
rs13477043	response	2.04E-07
gnf03.030.222	response	3.98E-07
rs6376008	response	7.35E-46
rs6211610	response	5.56E-23

ATGCTCGCCAGGA
TACGAGCGGTCCT



Supplementary tables

SNP	Phenotype	p-value
rs13477268	response	1.20E-50
rs4138887	response	2.31E-50
CEL-3_120379605	response	2.02E-34
rs13477379	response	1.64E-30
rs3671119	response	7.01E-28
rs3676039	response	4.13E-16
rs6407142	response	9.80E-10
gnf03.160.599	response	1.96E-03
CEL-4_30653207	response	9.84E-02
rs3708471	response	3.51E-01

SNP	Phenotype	p-value
rs3023025	response	5.49E-01
rs13478110	response	1.44E-01
rs3714258	response	1.47E-01
rs6341620	response	4.34E-01
CEL-5_45872918	response	4.68E-01
rs3664008	response	3.80E-01
mCV23386455	response	2.41E-01
rs3667334	response	2.38E-01
rs13459087	response	2.43E-01
rs3673049	response	2.43E-01
rs13460000	response	9.15E-02

SNP	Phenotype	p-value
rs3661241	response	6.70E-02
rs13460001	response	9.15E-02
rs13478433	response	1.57E-01
rs13459186	response	1.23E-01
rs13478483	response	6.09E-02
rs13478518	response	3.74E-01
rs13478520	response	4.88E-01
rs36247439	response	5.34E-01
rs33343556	response	5.34E-01
rs36309698	response	5.34E-01
rs37452785	response	5.34E-01



7. References

Alikhani-Koupaei, R., Fouladkou, F., Fustier, P., Cenni, B., Sharma, A. M., Deter, H. C., Frey, B. M. and Frey, F. J. (2007): Identification of polymorphisms in the human 11beta-hydroxysteroid dehydrogenase type 2 gene promoter: functional characterization and relevance for salt sensitivity. *FASEB J.* 21(13): p. 3618-28.

Altschuler, E. L. (2000): Plague as HIV vaccine adjuvant. *Med Hypotheses.* 54(6): p. 1003-4.

Ayi, K., Turrini, F., Piga, A. and Arese, P. (2004): Enhanced phagocytosis of ring-parasitized mutant erythrocytes: a common mechanism that may explain protection against falciparum malaria in sickle trait and beta-thalassemia trait. *Blood.* 104(10): p. 3364-71.

Barden, N., Harvey, M., Gagne, B., Shink, E., Tremblay, M., Raymond, C., Labbe, M., Villeneuve, A., Rochette, D., Bordeleau, L., Stadler, H., Holsboer, F. and Muller-Myhsok, B. (2006): Analysis of single nucleotide polymorphisms in genes in the chromosome 12Q24.31 region points to P2RX7 as a susceptibility gene to bipolar affective disorder. *Am J Med Genet B Neuropsychiatr Genet.* 141B(4): p. 374-82.

Baum, A. E., Akula, N., Cabanero, M., Cardona, I., Corona, W., Klemens, B., Schulze, T. G., Cichon, S., Rietschel, M., Nothen, M. M., Georgi, A., Schumacher, J., Schwarz, M., Abou Jamra, R., Hofels, S., Propping, P., Satagopan, J., Detera-Wadleigh, S. D., Hardy, J. and McMahon, F. J. (2008): A genome-wide association study implicates diacylglycerol kinase eta (DGKH) and several other genes in the etiology of bipolar disorder. *Mol Psychiatry.* 13(2): p. 197-207.

Beck, J. A., Lloyd, S., Hafezparast, M., Lennon-Pierce, M., Eppig, J. T., Festing, M. F. and Fisher, E. M. (2000): Genealogies of mouse inbred strains. *Nat Genet.* 24(1): p. 23-5.

Belknap, J. K., Richards, S. P., O'Toole, L. A., Helms, M. L. and Phillips, T. J. (1997): Short-term selective breeding as a tool for QTL mapping: ethanol preference drinking in mice. *Behav Genet.* 27(1): p. 55-66.

Beltramini, M., Di Pisa, C., Zambenedetti, P., Wittkowski, W., Mocchegiani, E., Musicco, M. and Zatta, P. (2004a): Zn and Cu alteration in connection with astrocyte metallothionein I/II overexpression in the mouse brain upon physical stress. *Glia.* 47(1): p. 30-4.

Beltramini, M., Zambenedetti, P., Wittkowski, W. and Zatta, P. (2004b): Effects of steroid hormones on the Zn, Cu and MTI/II levels in the mouse brain. *Brain Res.* 1013(1): p. 134-41.

Belzung, C. and Philippot, P. (2007): Anxiety from a phylogenetic perspective: is there a qualitative difference between human and animal anxiety? *Neural Plast.* 2007: p. 59676.

Bielsky, I. F., Hu, S. B., Szegda, K. L., Westphal, H. and Young, L. J. (2004): Profound impairment in social recognition and reduction in anxiety-like behavior in vasopressin V1a receptor knockout mice. *Neuropsychopharmacology.* 29(3): p. 483-93.

Bielsky, I. F., Hu, S. B., Ren, X., Terwilliger, E. F. and Young, L. J. (2005): The V1a vasopressin receptor is necessary and sufficient for normal social recognition: a gene replacement study. *Neuron.* 47(4): p. 503-13.



- Bilkei-Gorzo, A., Racz, I., Michel, K. and Zimmer, A. (2002): Diminished anxiety- and depression-related behaviors in mice with selective deletion of the Tac1 gene. *J Neurosci.* 22(22): p. 10046-52.
- Bishop, S. J., Duncan, J. and Lawrence, A. D. (2004): State anxiety modulation of the amygdala response to unattended threat-related stimuli. *J Neurosci.* 24(46): p. 10364-8.
- Bishop, S. J. (2008): Neural mechanisms underlying selective attention to threat. *Ann N Y Acad Sci.* 1129: p. 141-52.
- Bittner, A., Goodwin, R. D., Wittchen, H. U., Beesdo, K., Hofler, M. and Lieb, R. (2004): What characteristics of primary anxiety disorders predict subsequent major depressive disorder? *J Clin Psychiatry.* 65(5): p. 618-26, quiz 730.
- Bock, C. and Lengauer, T. (2008): Computational epigenetics. *Bioinformatics.* 24(1): p. 1-10.
- Bourin, M., Petit-Demouliere, B., Dhonnchadha, B. N. and Hascoet, M. (2007): Animal models of anxiety in mice. *Fundam Clin Pharmacol.* 21(6): p. 567-74.
- Bruins, J., Kovacs, G. L., Abbes, A. P., Burbach, J. P., van den Akker, E. L., Engel, H., Franken, A. A. and de Wied, D. (2006): Minor disturbances in central nervous system function in familial neurohypophysial diabetes insipidus. *Psychoneuroendocrinology.* 31(1): p. 80-91.
- Buckland, P. R., Hoogendoorn, B., Guy, C. A., Coleman, S. L., Smith, S. K., Buxbaum, J. D., Haroutunian, V. and O'Donovan, M. C. (2004): A high proportion of polymorphisms in the promoters of brain expressed genes influences transcriptional activity. *Biochim Biophys Acta.* 1690(3): p. 238-49.
- Bult, C. J., Eppig, J. T., Kadin, J. A., Richardson, J. E. and Blake, J. A. (2008): The Mouse Genome Database (MGD): mouse biology and model systems. *Nucleic Acids Res.* 36(Database issue): p. D724-8.
- Bunck, M. (2008): Behavioral phenotyping, gene expression profiles and cognitive aspects in a mouse model of trait anxiety. *Dissertation at the LMU München, Faculty of Biology.*
- Bunck, M., Czibere, L., Horvath, C., Graf, C., Murgatroyd, C., Muller-Myhsok, B., Gonik, M., Muigg, P., Singewald, N., Kessler, M. S., Frank, E., Bettecken, T., Deussing, J. M., Holsboer, F., Spengler, D. and Landgraf, R. (2009): A hypomorphic vasopressin allele prevents anxiety-related behavior. *PLoS ONE:* 4(4):e5129. Epub 2009 Apr 9.
- Cabreiro, F., Picot, C. R., Perichon, M., Castel, J., Friguet, B. and Petropoulos, I. (2008): Overexpression of mitochondrial methionine sulfoxide reductase B2 protects leukemia cells from oxidative stress-induced cell death and protein damage. *J Biol Chem.* 283(24): p. 16673-81.
- Caldji, C., Tannenbaum, B., Sharma, S., Francis, D., Plotsky, P. M. and Meaney, M. J. (1998): Maternal care during infancy regulates the development of neural systems mediating the expression of fearfulness in the rat. *Proc Natl Acad Sci U S A.* 95(9): p. 5335-40.



- Caldwell, H. K., Lee, H. J., Macbeth, A. H. and Young, W. S., 3rd (2008): Vasopressin: behavioral roles of an "original" neuropeptide. *Prog Neurobiol.* 84(1): p. 1-24.
- Carter, M. S. and Krause, J. E. (1990): Structure, expression, and some regulatory mechanisms of the rat preprotachykinin gene encoding substance P, neurokinin A, neuropeptide K, and neuropeptide gamma. *J Neurosci.* 10(7): p. 2203-14.
- Chakrabarty, A. and Roberts, M. R. (2007): Ets-2 and C/EBP-beta are important mediators of ovine trophoblast Kunitz domain protein-1 gene expression in trophoblast. *BMC Mol Biol.* 8: p. 14.
- Champagne, F. A. (2008): Epigenetic mechanisms and the transgenerational effects of maternal care. *Front Neuroendocrinol.* 29(3): p. 386-97.
- Chesler, E. J., Wilson, S. G., Lariviere, W. R., Rodriguez-Zas, S. L. and Mogil, J. S. (2002): Identification and ranking of genetic and laboratory environment factors influencing a behavioral trait, thermal nociception, via computational analysis of a large data archive. *Neurosci Biobehav Rev.* 26(8): p. 907-23.
- Chia, R., Achilli, F., Festing, M. F. and Fisher, E. M. (2005): The origins and uses of mouse outbred stocks. *Nat Genet.* 37(11): p. 1181-6.
- Christen, Y. (2000): Oxidative stress and Alzheimer disease. *Am J Clin Nutr.* 71(2): p. 621S-629S.
- Cipriano, C., Giacconi, R., Muzzioli, M., Gasparini, N., Orlando, F., Corradi, A., Cabassi, E. and Mocchegiani, E. (2003): Metallothionein (I+II) confers, via c-myc, immune plasticity in oldest mice: model of partial hepatectomy/liver regeneration. *Mech Ageing Dev.* 124(8-9): p. 877-86.
- Consortium, T. W. T. C. C. (2007): Genome-wide association study of 14,000 cases of seven common diseases and 3,000 shared controls. *Nature.* 447(7145): p. 661-78.
- Conti, L. H., Jirout, M., Breen, L., Vanella, J. J., Schork, N. J. and Printz, M. P. (2004): Identification of quantitative trait loci for anxiety and locomotion phenotypes in rat recombinant inbred strains. *Behav Genet.* 34(1): p. 93-103.
- Coplan, J. D. and Lydiard, R. B. (1998): Brain circuits in panic disorder. *Biol Psychiatry.* 44(12): p. 1264-76.
- Coulson, D. T., Brockbank, S., Quinn, J. G., Murphy, S., Ravid, R., Irvine, G. B. and Johnston, J. A. (2008): Identification of valid reference genes for the normalization of RT qPCR gene expression data in human brain tissue. *BMC Mol Biol.* 9: p. 46.
- Cryan, J. F. and Mombereau, C. (2004): In search of a depressed mouse: utility of models for studying depression-related behavior in genetically modified mice. *Mol Psychiatry.* 9(4): p. 326-57.
- Cryan, J. F. and Holmes, A. (2005): The ascent of mouse: advances in modelling human depression and anxiety. *Nat Rev Drug Discov.* 4(9): p. 775-90.
- Czeh, B., Fuchs, E. and Simon, M. (2006): NK1 receptor antagonists under investigation for the treatment of affective disorders. *Expert Opin Investig Drugs.* 15(5): p. 479-86.



- Darios, F. and Davletov, B. (2006): Omega-3 and omega-6 fatty acids stimulate cell membrane expansion by acting on syntaxin 3. *Nature*. 440(7085): p. 813-7.
- Delaval, K. and Feil, R. (2004): Epigenetic regulation of mammalian genomic imprinting. *Curr Opin Genet Dev*. 14(2): p. 188-95.
- Denes, A. S., Jekely, G., Steinmetz, P. R., Raible, F., Snyman, H., Prud'homme, B., Ferrier, D. E., Balavoine, G. and Arendt, D. (2007): Molecular architecture of annelid nerve cord supports common origin of nervous system centralization in bilateria. *Cell*. 129(2): p. 277-88.
- Deussing, J. M., Kuhne, C., Putz, B., Panhuysen, M., Breu, J., Stenzel-Poore, M. P., Holsboer, F. and Wurst, W. (2007): Expression profiling identifies the CRH/CRH-R1 system as a modulator of neurovascular gene activity. *J Cereb Blood Flow Metab*. 27(8): p. 1476-95.
- Dierick, H. A. and Greenspan, R. J. (2006): Molecular analysis of flies selected for aggressive behavior. *Nat Genet*. 38(9): p. 1023-31.
- Ditzen, C., Jastorff, A. M., Kessler, M. S., Bunck, M., Teplytska, L., Erhardt, A., Kromer, S. A., Varadarajulu, J., Targosz, B. S., Sayan-Ayata, E. F., Holsboer, F., Landgraf, R. and Turck, C. W. (2006): Protein biomarkers in a mouse model of extremes in trait anxiety. *Mol Cell Proteomics*. 5(10): p. 1914-20.
- Ditzen, C., Varadarajulu, J., Czibere, L., Gonik, M., Targosz, B.-S., Hamsch, B., Bettecken, T., Kessler, M. S., Frank, E., Bunck, M., Teplytska, L., Muller-Myhsok, B., Holsboer, F., Landgraf, R. and Turck, C. W. (2009): Proteomic genotyping in a mouse model of trait anxiety exposes disease-relevant pathways. *Mol Psychiatry*: Jan 13, [Epub ahead of print].
- Do, M. S., Jeong, H. S., Choi, B. H., Hunter, L., Langley, S., Pazmany, L. and Trayhurn, P. (2006): Inflammatory gene expression patterns revealed by DNA microarray analysis in TNF-alpha-treated SGBS human adipocytes. *Yonsei Med J*. 47(5): p. 729-36.
- Duarte, C. R., Schutz, B. and Zimmer, A. (2006): Incongruent pattern of neurokinin B expression in rat and mouse brains. *Cell Tissue Res*. 323(1): p. 43-51.
- Dudoit, S., Yang, Y. H., Callow, M. J. and Speed, T. P. (2002): Statistical methods for identifying differentially expressed genes in replicated cDNA microarray experiments. *Statistica Sinica*. 12(1): p. 111-139.
- Ebner, K., Rupniak, N. M., Saria, A. and Singewald, N. (2004): Substance P in the medial amygdala: emotional stress-sensitive release and modulation of anxiety-related behavior in rats. *Proc Natl Acad Sci U S A*. 101(12): p. 4280-5.
- Ebner, K. and Singewald, N. (2006): The role of substance P in stress and anxiety responses. *Amino Acids*. 31(3): p. 251-72.
- Egashira, N., Tanoue, A., Matsuda, T., Koushi, E., Harada, S., Takano, Y., Tsujimoto, G., Mishima, K., Iwasaki, K. and Fujiwara, M. (2007): Impaired social interaction and reduced anxiety-related behavior in vasopressin V1a receptor knockout mice. *Behav Brain Res*. 178(1): p. 123-7.
- Engel, J. D., Beug, H., LaVail, J. H., Zenke, M. W., Mayo, K., Leonard, M. W., Foley, K. P., Yang, Z., Kornhauser, J. M., Ko, L. J. and et al. (1992): cis and trans regulation of tissue-specific transcription. *J Cell Sci Suppl*. 16: p. 21-31.



- Erhardt, A., Lucae, S., Unschuld, P. G., Ising, M., Kern, N., Salyakina, D., Lieb, R., Uhr, M., Binder, E. B., Keck, M. E., Muller-Myhsok, B. and Holsboer, F. (2007): Association of polymorphisms in P2RX7 and CaMKKb with anxiety disorders. *J Affect Disord.* 101(1-3): p. 159-68.
- Erhardt, A., Czibere, L., Roeske, D., Lucae, S., Unschuld, P. G., Ripke, S., Specht, M., Kohli, M., Kloiber, S., Weber, P., Deussing, J. M., Ising, M., Heck, A., Zimmermann, P., Pfister, H., Lieb, R., Putz, B., Uhr, M., Hohoff, C., Domschke, K., Krakowitzky, P., Maier, W., Bandelow, B., Jacob, C., Deckert, J., Landgraf, R., Gonik, M., Bunck, M., Kessler, M. S., Frank, E., Schreiber, S., Strohmaier, J., Nothen, M., Cichon, S., Rietschel, M., Bettecken, T., Keck, M. E., Landgraf, R., Muller-Myhsok, B., Holsboer, F. and Binder, E. B. (submitted): Genomewide association study in panic disorder identifies transmembrane protein 132D (TMEM132D) as susceptibility gene for anxiety-related phenotypes: evidence from human and mice studies. *Mol Psychiatry.*
- Etkin, A. and Wager, T. D. (2007): Functional neuroimaging of anxiety: a meta-analysis of emotional processing in PTSD, social anxiety disorder, and specific phobia. *Am J Psychiatry.* 164(10): p. 1476-88.
- Felbor, U., Kessler, B., Mothes, W., Goebel, H. H., Ploegh, H. L., Bronson, R. T. and Olsen, B. R. (2002): Neuronal loss and brain atrophy in mice lacking cathepsins B and L. *Proc Natl Acad Sci U S A.* 99(12): p. 7883-8.
- Feuk, L., Marshall, C. R., Wintle, R. F. and Scherer, S. W. (2006): Structural variants: changing the landscape of chromosomes and design of disease studies. *Hum Mol Genet.* 15 Spec No 1: p. R57-66.
- Fields, R. L., House, S. B. and Gainer, H. (2003): Regulatory domains in the intergenic region of the oxytocin and vasopressin genes that control their hypothalamus-specific expression in vitro. *J Neurosci.* 23(21): p. 7801-9.
- File, S. E. (2001): Factors controlling measures of anxiety and responses to novelty in the mouse. *Behav Brain Res.* 125(1-2): p. 151-7.
- Flannelly, K. J., Koenig, H. G., Galek, K. and Ellison, C. G. (2007): Beliefs, mental health, and evolutionary threat assessment systems in the brain. *J Nerv Ment Dis.* 195(12): p. 996-1003.
- Fox, C., Merali, Z. and Harrison, C. (2006): Therapeutic and protective effect of environmental enrichment against psychogenic and neurogenic stress. *Behav Brain Res.* 175(1): p. 1-8.
- Francis, D. D. and Meaney, M. J. (1999): Maternal care and the development of stress responses. *Curr Opin Neurobiol.* 9(1): p. 128-34.
- Frank, E., Salchner, P., Aldag, J. M., Salome, N., Singewald, N., Landgraf, R. and Wigger, A. (2006): Genetic predisposition to anxiety-related behavior determines coping style, neuroendocrine responses, and neuronal activation during social defeat. *Behav Neurosci.* 120(1): p. 60-71.
- Frank, E. and Landgraf, R. (2008): The vasopressin system - from antidiuresis to psychopathology. *Eur J Pharmacol.* 583(2-3): p. 226-42.
- Green, J. E., Desai, K. V., Ye, Y., Kavanaugh, C., Calvo, A. and Huh, J. I. (2004): Application of gene expression profiling for validating models of human breast cancer. *Toxicol Pathol.* 32 Suppl 1: p. 84-9.



Gwee, P. C., Amemiya, C. T., Brenner, S. and Venkatesh, B. (2008): Sequence and organization of coelacanth neurohypophysial hormone genes: evolutionary history of the vertebrate neurohypophysial hormone gene locus. *BMC Evol Biol.* 8: p. 93.

Harrington, S. (2008): The role of sugar-sweetened beverage consumption in adolescent obesity: A review of the literature. *The Journal of School Nursing.* 24(1): p. 3-12.

Hasler, G., Fromm, S., Alvarez, R. P., Luckenbaugh, D. A., Drevets, W. C. and Grillon, C. (2007): Cerebral blood flow in immediate and sustained anxiety. *J Neurosci.* 27(23): p. 6313-9.

Hejjas, K., Szekely, A., Domotor, E., Halmi, Z., Balogh, G., Schilling, B., Sarosi, A., Faludi, G., Sasvari-Szekely, M. and Nemoda, Z. (2008): Association between depression and the Gln460Arg polymorphism of P2RX7 Gene: A dimensional approach. *Am J Med Genet B Neuropsychiatr Genet.*

Henderson, N. D., Turri, M. G., DeFries, J. C. and Flint, J. (2004): QTL analysis of multiple behavioral measures of anxiety in mice. *Behav Genet.* 34(3): p. 267-93.

Herman, J. P. and Cullinan, W. E. (1997): Neurocircuitry of stress: central control of the hypothalamo-pituitary-adrenocortical axis. *Trends Neurosci.* 20(2): p. 78-84.

Herman, J. P., Figueiredo, H., Mueller, N. K., Ulrich-Lai, Y., Ostrander, M. M., Choi, D. C. and Cullinan, W. E. (2003): Central mechanisms of stress integration: hierarchical circuitry controlling hypothalamo-pituitary-adrenocortical responsiveness. *Front Neuroendocrinol.* 24(3): p. 151-80.

Hettema, J. M., Prescott, C. A. and Kendler, K. S. (2004): Genetic and environmental sources of covariation between generalized anxiety disorder and neuroticism. *Am J Psychiatry.* 161(9): p. 1581-7.

Hettema, J. M., Prescott, C. A., Myers, J. M., Neale, M. C. and Kendler, K. S. (2005): The structure of genetic and environmental risk factors for anxiety disorders in men and women. *Arch Gen Psychiatry.* 62(2): p. 182-9.

Hitzemann, R., Malmanger, B., Belknap, J., Darakjian, P. and McWeeney, S. (2008): Short-term selective breeding for High and Low prepulse inhibition of the acoustic startle response; pharmacological characterization and QTL mapping in the selected lines. *Pharmacol Biochem Behav.*

Holland, N. D. (2003): Early central nervous system evolution: an era of skin brains? *Nat Rev Neurosci.* 4(8): p. 617-27.

Holmes, A., Wrenn, C. C., Harris, A. P., Thayer, K. E. and Crawley, J. N. (2002): Behavioral profiles of inbred strains on novel olfactory, spatial and emotional tests for reference memory in mice. *Genes Brain Behav.* 1(1): p. 55-69.

Holsboer, F. (2008): How can we realize the promise of personalized antidepressant medicines? *Nat Rev Neurosci.* 9(8): p. 638-46.

Hovatta, I., Tennant, R. S., Helton, R., Marr, R. A., Singer, O., Redwine, J. M., Ellison, J. A., Schadt, E. E., Verma, I. M., Lockhart, D. J. and Barlow, C. (2005): Glyoxalase 1 and glutathione reductase 1 regulate anxiety in mice. *Nature.* 438(7068): p. 662-6.



- Hovatta, I. and Barlow, C. (2008): Molecular genetics of anxiety in mice and men. *Ann Med.* 40(2): p. 92-109.
- Hubler, T. R. and Scammell, J. G. (2004): Intronic hormone response elements mediate regulation of FKBP5 by progestins and glucocorticoids. *Cell Stress Chaperones.* 9(3): p. 243-52.
- Jacobi, F., Wittchen, H. U., Holting, C., Hofler, M., Pfister, H., Muller, N. and Lieb, R. (2004): Prevalence, co-morbidity and correlates of mental disorders in the general population: results from the German Health Interview and Examination Survey (GHS). *Psychol Med.* 34(4): p. 597-611.
- Ji, C., Chen, Y., Centrella, M. and McCarthy, T. L. (1999): Activation of the insulin-like growth factor-binding protein-5 promoter in osteoblasts by cooperative E box, CCAAT enhancer-binding protein, and nuclear factor-1 deoxyribonucleic acid-binding sequences. *Endocrinology.* 140(10): p. 4564-72.
- Kavushansky, A. and Richter-Levin, G. (2006): Effects of stress and corticosterone on activity and plasticity in the amygdala. *J Neurosci Res.* 84(7): p. 1580-7.
- Kessler, M. S. (2007): The AVP deficit in LAB mice: physiological and behavioral effects. *Dissertation at the LMU München, Faculty of Biology.*
- Kessler, M. S., Murgatroyd, C., Bunck, M., Czibere, L., Frank, E., Jacob, W., Horvath, C., Muigg, P., Holsboer, F., Singewald, N., Spengler, D. and Landgraf, R. (2007): Diabetes insipidus and, partially, low anxiety-related behaviour are linked to a SNP-associated vasopressin deficit in LAB mice. *Eur J Neurosci.* 26(10): p. 2857-64.
- Kim, J. and Gorman, J. (2005): The psychobiology of anxiety. *Clinical Neuroscience Research.* 4(5-6): p. 335-347.
- Knerr, I., Gibson, K. M., Jakobs, C. and Pearl, P. L. (2008): Neuropsychiatric morbidity in adolescent and adult succinic semialdehyde dehydrogenase deficiency patients. *CNS Spectr.* 13(7): p. 598-605.
- Kraus, R. J., Shadley, L. and Mertz, J. E. (2001): Nuclear factor 1 family members mediate repression of the BK virus late promoter. *Virology.* 287(1): p. 89-104.
- Kromer, S. A., Kessler, M. S., Milfay, D., Birg, I. N., Bunck, M., Czibere, L., Panhuysen, M., Putz, B., Deussing, J. M., Holsboer, F., Landgraf, R. and Turck, C. W. (2005): Identification of glyoxalase-I as a protein marker in a mouse model of extremes in trait anxiety. *J Neurosci.* 25(17): p. 4375-84.
- Kuhla, B., Luth, H. J., Haferburg, D., Weick, M., Reichenbach, A., Arendt, T. and Munch, G. (2006): Pathological effects of glyoxalase I inhibition in SH-SY5Y neuroblastoma cells. *J Neurosci Res.* 83(8): p. 1591-600.
- Landgraf, R., Gerstberger, R., Montkowski, A., Probst, J. C., Wotjak, C. T., Holsboer, F. and Engelmann, M. (1995): V1 vasopressin receptor antisense oligodeoxynucleotide into septum reduces vasopressin binding, social discrimination abilities, and anxiety-related behavior in rats. *J Neurosci.* 15(6): p. 4250-8.
- Landgraf, R. (2001a): Neuropeptides and anxiety-related behavior. *Endocr J.* 48(5): p. 517-33.
- Landgraf, R. (2001b): Neuropeptides and anxiety. *Stress.* 4: p. 273-276.



- Landgraf, R. and Wigger, A. (2002): High vs low anxiety-related behavior rats: an animal model of extremes in trait anxiety. *Behav Genet.* 32(5): p. 301-14.
- Landgraf, R. and Neumann, I. D. (2004): Vasopressin and oxytocin release within the brain: a dynamic concept of multiple and variable modes of neuropeptide communication. *Front Neuroendocrinol.* 25(3-4): p. 150-76.
- Landgraf, R. and Holsboer, F. (2005): The involvement of neuropeptides in evolution, signaling, behavioral regulation and psychopathology: focus on vasopressin. *Drug Development Research.* 65: p. 185-90.
- Landgraf, R., Kessler, M. S., Bunck, M., Murgatroyd, C., Spengler, D., Zimbelmann, M., Nussbaumer, M., Czibere, L., Turck, C. W., Singewald, N., Rujescu, D. and Frank, E. (2007): Candidate genes of anxiety-related behavior in HAB/LAB rats and mice: focus on vasopressin and glyoxalase-I. *Neurosci Biobehav Rev.* 31(1): p. 89-102.
- Lang, P. J., Davis, M. and Ohman, A. (2000): Fear and anxiety: animal models and human cognitive psychophysiology. *J Affect Disord.* 61(3): p. 137-59.
- Levine, J., Cole, D. P., Chengappa, K. N. and Gershon, S. (2001): Anxiety disorders and major depression, together or apart. *Depress Anxiety.* 14(2): p. 94-104.
- Levine, M. and Tjian, R. (2003): Transcription regulation and animal diversity. *Nature.* 424(6945): p. 147-51.
- Lewin, B., *Genes VIII.* 2004, London: Pearson Education Ltd. 1027.
- Liebsch, G., Linthorst, A. C., Neumann, I. D., Reul, J. M., Holsboer, F. and Landgraf, R. (1998a): Behavioral, physiological, and neuroendocrine stress responses and differential sensitivity to diazepam in two Wistar rat lines selectively bred for high- and low-anxiety-related behavior. *Neuropsychopharmacology.* 19(5): p. 381-96.
- Liebsch, G., Montkowski, A., Holsboer, F. and Landgraf, R. (1998b): Behavioural profiles of two Wistar rat lines selectively bred for high or low anxiety-related behaviour. *Behav Brain Res.* 94(2): p. 301-10.
- Livak, K. J. and Schmittgen, T. D. (2001): Analysis of relative gene expression data using real-time quantitative PCR and the 2(-Delta Delta C(T)) Method. *Methods.* 25(4): p. 402-8.
- Lonnstedt, I. and Speed, T. P. (2002): Replicated microarray data. *Statistica Sinica*(12): p. 31-46.
- Lucae, S., Salyakina, D., Barden, N., Harvey, M., Gagne, B., Labbe, M., Binder, E. B., Uhr, M., Paez-Pereda, M., Sillaber, I., Ising, M., Bruckl, T., Lieb, R., Holsboer, F. and Muller-Myhsok, B. (2006): P2RX7, a gene coding for a purinergic ligand-gated ion channel, is associated with major depressive disorder. *Hum Mol Genet.* 15(16): p. 2438-45.
- Maccari, S., Darnaudery, M., Morley-Fletcher, S., Zuena, A. R., Cinque, C. and Van Reeth, O. (2003): Prenatal stress and long-term consequences: implications of glucocorticoid hormones. *Neurosci Biobehav Rev.* 27(1-2): p. 119-27.



- Majumder, S., Kutay, H., Datta, J., Summers, D., Jacob, S. T. and Ghoshal, K. (2006): Epigenetic regulation of metallothionein-i gene expression: differential regulation of methylated and unmethylated promoters by DNA methyltransferases and methyl CpG binding proteins. *J Cell Biochem.* 97(6): p. 1300-16.
- Marin-Garcia, P., Sanchez-Nogueiro, J., Gomez-Villafuertes, R., Leon, D. and Miras-Portugal, M. T. (2008): Synaptic terminals from mice midbrain exhibit functional P2X7 receptor. *Neuroscience.* 151(2): p. 361-73.
- Milad, M. R., Quirk, G. J., Pitman, R. K., Orr, S. P., Fischl, B. and Rauch, S. L. (2007): A role for the human dorsal anterior cingulate cortex in fear expression. *Biol Psychiatry.* 62(10): p. 1191-4.
- Milad, M. R. and Rauch, S. L. (2007): The role of the orbitofrontal cortex in anxiety disorders. *Ann N Y Acad Sci.* 1121: p. 546-61.
- Mill, J. and Petronis, A. (2007): Molecular studies of major depressive disorder: the epigenetic perspective. *Mol Psychiatry.* 12(9): p. 799-814.
- Mlynarik, M., Zelena, D., Bagdy, G., Makara, G. B. and Jezova, D. (2007): Signs of attenuated depression-like behavior in vasopressin deficient Brattleboro rats. *Horm Behav.* 51(3): p. 395-405.
- Mobbs, D., Petrovic, P., Marchant, J. L., Hassabis, D., Weiskopf, N., Seymour, B., Dolan, R. J. and Frith, C. D. (2007): When fear is near: threat imminence elicits prefrontal-periaqueductal gray shifts in humans. *Science.* 317(5841): p. 1079-83.
- Muller, M. B., Preil, J., Renner, U., Zimmermann, S., Kresse, A. E., Stalla, G. K., Keck, M. E., Holsboer, F. and Wurst, W. (2001): Expression of CRHR1 and CRHR2 in mouse pituitary and adrenal gland: implications for HPA system regulation. *Endocrinology.* 142(9): p. 4150-3.
- Murgatroyd, C., Wigger, A., Frank, E., Singewald, N., Bunck, M., Holsboer, F., Landgraf, R. and Spengler, D. (2004): Impaired repression at a vasopressin promoter polymorphism underlies overexpression of vasopressin in a rat model of trait anxiety. *J Neurosci.* 24(35): p. 7762-70.
- Nagase, T., Kikuno, R. and Ohara, O. (2001): Prediction of the coding sequences of unidentified human genes. XXII. The complete sequences of 50 new cDNA clones which code for large proteins. *DNA Res.* 8(6): p. 319-27.
- Nomoto, H., Yonezawa, T., Itoh, K., Ono, K., Yamamoto, K., Oohashi, T., Shiraga, F., Ohtsuki, H. and Ninomiya, Y. (2003): Molecular cloning of a novel transmembrane protein MOLT expressed by mature oligodendrocytes. *J Biochem.* 134(2): p. 231-8.
- Nygaard, A. B., Jorgensen, C. B., Cirera, S. and Fredholm, M. (2007): Selection of reference genes for gene expression studies in pig tissues using SYBR green qPCR. *BMC Mol Biol.* 8: p. 67.
- Ohman, A. (2005): The role of the amygdala in human fear: automatic detection of threat. *Psychoneuroendocrinology.* 30(10): p. 953-8.
- Okajima, K., Korotchkina, L. G., Prasad, C., Rugar, T., Phillips, J. A., 3rd, Ficicioglu, C., Hertecant, J., Patel, M. S. and Kerr, D. S. (2008): Mutations of the E1beta subunit gene (PDHB) in four families with pyruvate dehydrogenase deficiency. *Mol Genet Metab.* 93(4): p. 371-80.



- Otsuka, M. and Yoshioka, K. (1993): Neurotransmitter functions of mammalian tachykinins. *Physiol Rev.* 73(2): p. 229-308.
- Page, N. M. (2004): Hemokinins and endokinins. *Cell Mol Life Sci.* 61(13): p. 1652-63.
- Palkovits, M. (1973): Isolated removal of hypothalamic or other brain nuclei of the rat. *Brain Res.* 59: p. 449-50.
- Palmer, A. A., Verbitsky, M., Suresh, R., Kamens, H. M., Reed, C. L., Li, N., Burkhart-Kasch, S., McKinnon, C. S., Belknap, J. K., Gilliam, T. C. and Phillips, T. J. (2005): Gene expression differences in mice divergently selected for methamphetamine sensitivity. *Mamm Genome.* 16(5): p. 291-305.
- Paxinos, G. and Franklin, K., *The mouse brain in stereotaxic coordinates.* 2nd ed. 2001, San Diego, San Francisco, New York, Boston, London, Sydney, Tokyo: Academic Press.
- Peters, L. L., Robledo, R. F., Bult, C. J., Churchill, G. A., Paigen, B. J. and Svenson, K. L. (2007): The mouse as a model for human biology: a resource guide for complex trait analysis. *Nat Rev Genet.* 8(1): p. 58-69.
- Ponder, C. A., Kliethermes, C. L., Drew, M. R., Muller, J., Das, K., Risbrough, V. B., Crabbe, J. C., Gilliam, T. C. and Palmer, A. A. (2007): Selection for contextual fear conditioning affects anxiety-like behaviors and gene expression. *Genes Brain Behav.* 6(8): p. 736-49.
- Quinn, J. P., Fiskerstrand, C. E., Gerrard, L., MacKenzie, A. and Payne, C. M. (2000): Molecular models to analyse preprotachykinin-A expression and function. *Neuropeptides.* 34(5): p. 292-302.
- Raison, C. L. and Miller, A. H. (2003): When not enough is too much: the role of insufficient glucocorticoid signaling in the pathophysiology of stress-related disorders. *Am J Psychiatry.* 160(9): p. 1554-65.
- Ramos, A., Pereira, E., Martins, G. C., Wehrmeister, T. D. and Izidio, G. S. (2008): Integrating the open field, elevated plus maze and light/dark box to assess different types of emotional behaviors in one single trial. *Behav Brain Res.* 193(2): p. 277-88.
- Rosen, J. B. and Schulkin, J. (1998): From normal fear to pathological anxiety. *Psychol Rev.* 105(2): p. 325-50.
- Rozen, S. and Skaletsky, H. (2000): Primer3 on the WWW for general users and for biologist programmers. *Methods Mol Biol.* 132: p. 365-86.
- Rybakin, V., Stumpf, M., Schulze, A., Majoul, I. V., Noegel, A. A. and Hasse, A. (2004): Coronin 7, the mammalian POD-1 homologue, localizes to the Golgi apparatus. *FEBS Lett.* 573(1-3): p. 161-7.
- Rybakin, V., Gounko, N. V., Spate, K., Honing, S., Majoul, I. V., Duden, R. and Noegel, A. A. (2006): Crn7 interacts with AP-1 and is required for the maintenance of Golgi morphology and protein export from the Golgi. *J Biol Chem.* 281(41): p. 31070-8.



Sakai, H., Tanaka, Y., Tanaka, M., Ban, N., Yamada, K., Matsumura, Y., Watanabe, D., Sasaki, M., Kita, T. and Inagaki, N. (2007): ABCA2 deficiency results in abnormal sphingolipid metabolism in mouse brain. *J Biol Chem.* 282(27): p. 19692-9.

Salvamoser, J. (2008): Einfluss von exogenem AVP auf LAB und CD1-Mäuse, sowie die Charakterisierung der Replikation einer Mauszucht für Angstextreme. *Diploma-thesis at the LMU München, Faculty of Biology.*

Saria, A. (1999): The tachykinin NK1 receptor in the brain: pharmacology and putative functions. *Eur J Pharmacol.* 375(1-3): p. 51-60.

Scalera, G. and Tarozzi, G. (2001): Sapid solutions and food intake in repeated dehydration and rehydration periods in rats. *Exp Physiol.* 86(4): p. 489-98.

Schadt, E. E., Lamb, J., Yang, X., Zhu, J., Edwards, S., Guhathakurta, D., Sieberts, S. K., Monks, S., Reitman, M., Zhang, C., Lum, P. Y., Leonardson, A., Thieringer, R., Metzger, J. M., Yang, L., Castle, J., Zhu, H., Kash, S. F., Drake, T. A., Sachs, A. and Lusk, A. J. (2005): An integrative genomics approach to infer causal associations between gene expression and disease. *Nat Genet.* 37(7): p. 710-7.

Schormair, B., Kemlink, D., Roeske, D., Eckstein, G., Xiong, L., Lichtner, P., Ripke, S., Trenkwalder, C., Zimprich, A., Stiasny-Kolster, K., Oertel, W., Bachmann, C. G., Paulus, W., Höggl, B., Frauscher, B., Gschliesser, V., Poewe, W., Peglau, I., Vodicka, P., Vavrova, J., Sonka, K., Nevsimalova, S., Montplaisir, J., Turecki, G., Rouleau, G., Gieger, C., Illig, T., Wichmann, H. E., Holsboer, F., Müller-Myhsok, B., Meitinger, T. and Winkelmann, J. (2008): PTPRD (protein tyrosine phosphatase receptor type delta) is associated with restless legs syndrome. *Nat Genet.* 40(8): p. 946-8.

Scott, L. V. and Dinan, T. G. (2002): Vasopressin as a target for antidepressant development: an assessment of the available evidence. *J Affect Disord.* 72(2): p. 113-24.

Severini, C., Improta, G., Falconieri-Ersamer, G., Salvadori, S. and Ersamer, V. (2002): The tachykinin peptide family. *Pharmacol Rev.* 54(2): p. 285-322.

Shabalina, S. A., Ogurtsov, A. Y. and Spiridonov, N. A. (2006): A periodic pattern of mRNA secondary structure created by the genetic code. *Nucleic Acids Res.* 34(8): p. 2428-37.

Simon, N. G., Guillon, C., Fabio, K., Heindel, N. D., Lu, S. F., Miller, M., Ferris, C. F., Brownstein, M. J., Garripa, C. and Koppel, G. A. (2008): Vasopressin antagonists as anxiolytics and antidepressants: recent developments. *Recent Patents CNS Drug Discov.* 3(2): p. 77-93.

Simonian, N. A. and Hyman, B. T. (1993): Functional alterations in Alzheimer's disease: diminution of cytochrome oxidase in the hippocampal formation. *J Neuropathol Exp Neurol.* 52(6): p. 580-5.

Skolnick, P. (1999): Antidepressants for the new millennium. *Eur J Pharmacol.* 375(1-3): p. 31-40.

Smoller, J. W., Finn, C. and White, C. (2000): The genetics of anxiety disorders: An overview. *Psychiatric Annals.* 30(12): p. 745-753.



- Smyth, G. K. (2004): Linear models and empirical bayes methods for assessing differential expression in microarray experiments. *Stat Appl Genet Mol Biol.* 3: p. Article3.
- Sorci, G., Riuzzi, F., Agneletti, A. L., Marchetti, C., Donato, R. (2003): S100B inhibits myogenic differentiation and myotube formation in a RAGE-independent manner. *Mol Cell Biol.* 23(14): p. 4870-4881.
- Stahl, S., Reinders, Y., Asan, E., Mothes, W., Conzelmann, E., Sickmann, A. and Felbor, U. (2007): Proteomic analysis of cathepsin B- and L-deficient mouse brain lysosomes. *Biochim Biophys Acta.* 1774(10): p. 1237-46.
- Stern, C. A., Carobrez, A. P. and Bertoglio, L. J. (2008): Aversive learning as a mechanism for lack of repeated anxiolytic-like effect in the elevated plus-maze. *Pharmacol Biochem Behav.*
- Straube, T., Mentzel, H. J. and Miltner, W. H. (2007): Waiting for spiders: brain activation during anticipatory anxiety in spider phobics. *Neuroimage.* 37(4): p. 1427-36.
- Strohle, A. and Holsboer, F. (2003): Stress responsive neurohormones in depression and anxiety. *Pharmacopsychiatry.* 36 Suppl 3: p. S207-14.
- Thornalley, P. J. (2006): Unease on the role of glyoxalase 1 in high-anxiety-related behaviour. *Trends Mol Med.* 12(5): p. 195-9.
- Touma, C., Bunck, M., Glasl, L., Nussbaumer, M., Palme, R., Stein, H., Wolferstatter, M., Zeh, R., Zimbelmann, M., Holsboer, F. and Landgraf, R. (2008): Mice selected for high versus low stress reactivity: A new animal model for affective disorders. *Psychoneuroendocrinology.*
- Tsigos, C. and Chrousos, G. P. (2002): Hypothalamic-pituitary-adrenal axis, neuroendocrine factors and stress. *J Psychosom Res.* 53(4): p. 865-71.
- Turri, M. G., Talbot, C. J., Radcliffe, R. A., Wehner, J. M. and Flint, J. (1999): High-resolution mapping of quantitative trait loci for emotionality in selected strains of mice. *Mamm Genome.* 10(11): p. 1098-101.
- Turri, M. G., DeFries, J. C., Henderson, N. D. and Flint, J. (2004): Multivariate analysis of quantitative trait loci influencing variation in anxiety-related behavior in laboratory mice. *Mamm Genome.* 15(2): p. 69-76.
- Ungar, D. and Hughson, F. M. (2003): SNARE protein structure and function. *Annu Rev Cell Dev Biol.* 19: p. 493-517.
- Valdar, W., Solberg, L. C., Gauguier, D., Burnett, S., Klenerman, P., Cookson, W. O., Taylor, M. S., Rawlins, J. N., Mott, R. and Flint, J. (2006): Genome-wide genetic association of complex traits in heterogeneous stock mice. *Nat Genet.* 38(8): p. 879-87.
- Visser, W. F., van Roermund, C. W., Waterham, H. R. and Wanders, R. J. (2002): Identification of human PMP34 as a peroxisomal ATP transporter. *Biochem Biophys Res Commun.* 299(3): p. 494-7.



- Vorbrod, A. W., Dobrogowska, D. H., Meeker, H. C. and Carp, R. I. (2006): Quantitative immunogold study of increased expression of metallothionein-I/II in the brain perivascular areas of diabetic scrapie-infected mice. *J Mol Histol.* 37(3-4): p. 143-51.
- Wang, Q., Li, M., Wang, Y., Zhang, Y., Jin, S., Xie, G., Liu, Z., Wang, S., Zhang, H., Shen, L. and Ge, H. (2008): RNA interference targeting CML66, a novel tumor antigen, inhibits proliferation, invasion and metastasis of HeLa cells. *Cancer Lett.* 269(1): p. 127-38.
- Weaver, I. C., Meaney, M. J. and Szyf, M. (2006): Maternal care effects on the hippocampal transcriptome and anxiety-mediated behaviors in the offspring that are reversible in adulthood. *Proc Natl Acad Sci U S A.* 103(9): p. 3480-5.
- West, K. L., Castellini, M. A., Duncan, M. K. and Bustin, M. (2004): Chromosomal proteins HMGN3a and HMGN3b regulate the expression of glycine transporter 1. *Mol Cell Biol.* 24(9): p. 3747-56.
- Wigger, A., Loerscher, P., Weissenbacher, P., Holsboer, F. and Landgraf, R. (2001): Cross-fostering and cross-breeding of HAB and LAB rats: a genetic rat model of anxiety. *Behav Genet.* 31(4): p. 371-82.
- Wigger, A., Sanchez, M. M., Mathys, K. C., Ebner, K., Frank, E., Liu, D., Kresse, A., Neumann, I. D., Holsboer, F., Plotsky, P. M. and Landgraf, R. (2004): Alterations in central neuropeptide expression, release, and receptor binding in rats bred for high anxiety: critical role of vasopressin. *Neuropsychopharmacology.* 29(1): p. 1-14.
- Wilhelm, C. J., Reeves, J. M., Phillips, T. J. and Mitchell, S. H. (2007): Mouse lines selected for alcohol consumption differ on certain measures of impulsivity. *Alcohol Clin Exp Res.* 31(11): p. 1839-45.
- Wilkins, J. F. and Haig, D. (2003a): Inbreeding, maternal care and genomic imprinting. *J Theor Biol.* 221(4): p. 559-64.
- Wilkins, J. F. and Haig, D. (2003b): What good is genomic imprinting: the function of parent-specific gene expression. *Nat Rev Genet.* 4(5): p. 359-68.
- Williams, K. (1997): Interactions of polyamines with ion channels. *Biochem J.* 325 (Pt 2): p. 289-97.
- Williams, P. (2007): Quorum sensing, communication and cross-kingdom signalling in the bacterial world. *Microbiology.* 153(Pt 12): p. 3923-38.
- Winkelmann, J., Schormair, B., Lichtner, P., Ripke, S., Xiong, L., Jalilzadeh, S., Fulda, S., Putz, B., Eckstein, G., Hauk, S., Trenkwalder, C., Zimprich, A., Stiasny-Kolster, K., Oertel, W., Bachmann, C. G., Paulus, W., Peglau, I., Eisensehr, I., Montplaisir, J., Turecki, G., Rouleau, G., Gieger, C., Illig, T., Wichmann, H. E., Holsboer, F., Muller-Myhsok, B. and Meitinger, T. (2007): Genome-wide association study of restless legs syndrome identifies common variants in three genomic regions. *Nat Genet.* 39(8): p. 1000-6.
- Winkelmann, J., Lichtner, P., Schormair, B., Uhr, M., Hauk, S., Stiasny-Kolster, K., Trenkwalder, C., Paulus, W., Peglau, I., Eisensehr, I., Illig, T., Wichmann, H. E., Pfister, H., Golic, J., Bettecken, T., Putz, B., Holsboer, F., Meitinger, T. and Muller-Myhsok, B. (2008): Variants in the neuronal nitric oxide synthase (nNOS, NOS1) gene are associated with restless legs syndrome. *Mov Disord.* 23(3): p. 350-8.



Wotjak, C. T., Ludwig, M. and Landgraf, R. (1994): Vasopressin facilitates its own release within the rat supraoptic nucleus in vivo. *Neuroreport*. 5(10): p. 1181-4.

Yang, Y. H., Dudoit, S., Luu, P., Lin, D. M., Peng, V., Ngai, J. and Speed, T. P. (2002): Normalization for cDNA microarray data: a robust composite method addressing single and multiple slide systematic variation. *Nucleic Acids Res.* 30(4): p. e15.

Yauk, C. L. and Berndt, M. L. (2007): Review of the literature examining the correlation among DNA microarray technologies. *Environ Mol Mutagen.* 48(5): p. 380-94.

Yvert, G., Brem, R. B., Whittle, J., Akey, J. M., Foss, E., Smith, E. N., Mackelprang, R. and Kruglyak, L. (2003): Trans-acting regulatory variation in *Saccharomyces cerevisiae* and the role of transcription factors. *Nat Genet.* 35(1): p. 57-64.

Zafra, F. and Gimenez, C. (2008): Glycine transporters and synaptic function. *IUBMB Life*.

Zurmuehlen, R. (2007): Untersuchungen zum Zusammenhang von Emotionalität und kognitiver Fähigkeit in einem Mausmodell für Angsterkrankung. *Diplomathesis at the LMU, Faculty of Biology*.



7. Acknowledgements

First of all, I want to express my gratitude to Prof. Rainer Landgraf, the supervisor of my doctoral thesis, for the opportunity to work on these fascinating topics in his research group. I pay tribute to him for the helpful guidance, his support, his faith in my abilities and for giving me the opportunity to develop and pursue own ideas.

I would also like to thank Prof. Thomas Cremer for his readiness to invest his time in the second evaluation of my thesis.

Furthermore I would like to mention our institute's head, Prof Florian Holsboer, who always assured the financial support for these projects. Parts of the projects were funded by the "Bundesministerium für Bildung und Forschung". I also thank Dr. Dietmar Spengler, Dr. Thomas Bettecken, Dr. Jan Deussing, Dr. Elisabeth Binder, Dr. Marcus Ising, PD Dr. Bertram Müller-Myhsok, PD Dr. Gabriele Rieder, Prof. Christoph Turck, Dr. Carsten Wotjak and Dr. Theo Rein for the meritorious, fruitful discussions and cooperations.

I would like to highlight the names of those people especially, whose help and knowledge were always available to me, whenever I needed. Therefore I'm deeply indebted to my colleagues and – in part – meanwhile friends Dr. Chris Murgatroyd, Claudia Kühne, Cornelia Graf and Dr. Mirjam Bunck, whose professional support and advice saved my work (and life) so often. Special thanks also go to Peter Weber, Dr. Benno Pütz and Dr. Mariya Gonik for their vital support in the evaluation of all the high-throughput data, as without them, I'd probably sit in a room filled with calculations on paper that I'd have to light to find the way out again.

And to give all those helpful hands a name, who made my work speed up many times, I say thank you to: Katja Zeiner, Andrea Steiner, Charlotte Horvath, Laura Baur-Jaronowski, Dr. Elisabeth Frank, Dr. Melanie Keßler, Josephine Salvamoser, Jennifer Prigl and Nafees Ahmad. Further to: Anke Hoffmann, Maria Lebar, Bernica Kubat, Julia Bär, Lisa Halbsgut, Nariné Mousissian, Maria Roßbauer, Nikola Müller, Martina Schifferer, Jan-Michael Heinzmann, Daniela Harbich, Michael Specht, Tobias Wiedemann, Yvonne Wegerich, Yonghe Wu, Helena Kronsbein, Yi-Chun Yen and Ursula Genning.

I would also like to point out the helping hands of our technicians Marina Zimbelmann and Markus Nußbaumer. Without them, our lab would have already drowned years ago!

Our work would also be harder - if not impossible - without the caring help of our animal facility led by Albin Varga, the technical service and of course the IT section.

Many small but powerful hints and ideas were contributed by: Dr. Amalia Tsolakidou, Alana Knapman, Carola Hetzel, Christiane Rewerts, Claudia Liebl, Dr. Alexandra Wigger, Dr. Angelika Erhardt, Dr. Anja Siegmund, Dr. Guiseppina Maccarone, Dr. Jeeva Daravarajulu, Dr. Kornelia Kamprath, Dr. Markus Panhuysen, Dr. Mathias Schmidt, Dr. Jürgen Zschokke, Dr. Melanie Scheibel, Dr. Chadi Touma, Dr. Boris Hamsch, Dr. Peter Lichtner, Dr. Karin Ganea, Hélène Savignac, Dr. Christoph Thöringer, Dr. Corinna Storch, Dr. Dr. Susanne Lucae, Evelyn Weiß, Gabriella Czepek, Hendrik Stein, Jadranka Doric, Jelena Golic, Julia Baier, Julianna Ranzmeyer, Larysa Teplytska, Lisa Glasl, Michael Wolferstätter, Michaela Filiou, Nicole Zimmermann, Ramona Zeh, Regina Knapp, Dr. Martin Kohli, Jan Schülke, Sabine Damast, Stephanie Siegl, Susann Sauer, Tanja Holjevac and Yvonne Grübler.

Insbesondere bedanke ich mich bei meinen Freunden, die mich über all die Jahre tatkräftig unterstützten (besonderer Dank an Susa!), mich von der Arbeit auch ablenkten und freue mich auch neue Freunde über die Arbeit gefunden haben, die mir auch in Zukunft hoffentlich erhalten bleiben. Danke Miri, Jenny und Nele!

Valamint utoljára, de nem utolso sorban szüleimnek és öcsémnek köszönöm az örökké tartó támogatást és köszönöm, hogy velem vagytok!



9. Curriculum vitae

Name: Ludwig Czibere
DOB: 13/05/1979
POB: Budapest, Hungary
Address: Paul-Ehrlich-Weg 26, 80999 Munich, Germany
Email: ludwig@czibere.de
Nationality: German, Hungarian

Educational Qualifications:

Since 2005 Ph.D. student at the Ludwig Maximilians University, Faculty of Biology
Thesis title: Assessing the complex nature of behavior: Sequence-based and transcriptomic analyses in a mouse model of extremes in trait anxiety

1999-2005 Diploma-student in biology, Ludwig Maximilians University, Munich, Germany
Primary subject: neurobiology; secondary subjects: human biology, genetics, pharmacology and toxicology;
Diploma thesis (2004/2005): Gene expression profiling in a mouse model of trait anxiety, Max Planck Institute of Psychiatry, Department of Behavioral Neuroendocrinology, Munich, Germany

1989-1998 High School Louise-Schroeder-Gymnasium, Munich, Germany

Employment History:

Since 2005 Ph.D. student at the Max Planck Institute of Psychiatry, Department of Behavioral Neuroendocrinology, Munich, Germany

2001-2005 Assistant in a bacteriological laboratory, Labor Dr. Becker, Dr. Olgemöller, Munich, Germany

03/-05/2003 Internship at QIMR, Queensland Institute of Medical Research Genetic Epidemiology, Brisbane, Australia

08/-10/2000 Assistant at GSF Research Centre for Environment and Health, Neuherberg, Germany
Expositional Chambers (EPOKA)

Awards:

2005: Invited talk at the 24th Symposium of the Consortium for Neuropsychopharmacology and Pharmacopsychiatry (AGNP), Munich

Munich, September 30th 2008



10. List of publications and other contributions

Krömer S. A., Keßler M. S., Milfay D., Birg I. N., Bunck M., **Czibere L.**, Panhuysen M., Pütz B., Deussing J. M., Holsboer F., Landgraf R. and Turck C. W. (2005): Identification of glyoxalase-I as a protein marker in a mouse model of extremes in trait anxiety. *J Neurosci* 25:4375-4384.

Landgraf R., Keßler M. S., Bunck M., Murgatroyd C., Spengler D., Zimbelmann M., Nußbaumer M., **Czibere L.**, Turck C. W., Singewald N., Rujescu D. and Frank E. (2007): Candidate genes of anxiety-related behavior in HAB/LAB rats and mice: focus on vasopressin and glyoxalase-I. *Neurosci Biobehav Rev* 31:89-102.

Keßler M. S., Murgatroyd C., Bunck M., **Czibere L.**, Frank E., Jacob W., Horvath C., Muigg P., Holsboer F., Singewald N., Spengler D. and Landgraf R. (2007): Diabetes insipidus and, partially, low anxiety-related behaviour are linked to a SNP associated vasopressin deficit in LAB mice. *Eur J Neurosci* 26:2857-2864. #

Ditzen C.*, Varadarajulu J.*, **Czibere L.***, Gonik M., Targosz B.-S., Hamsch B., Bettecken T., Kessler M. S., Frank E., Bunck M., Teplytska L., Müller-Myhsok B., Holsboer F., Landgraf R. and Turck C. W. (2009): Proteomic genotyping in a mouse model of trait anxiety exposes disease-relevant pathways. *Mol Psychiatry*: Jan 13, [Epub ahead of print]. #

* Authors contributed equally

Bunck M.*, **Czibere L.***, Horvath C., Graf C., Frank E., Keßler M. S., Murgatroyd C., Müller-Myhsok B., Gonik M., Weber P., Pütz B., Muigg P., Panhuysen M., Singewald N., Bettecken T., Deussing J. M., Holsboer F., Spengler D. and Landgraf R. (2009): A hypomorphic vasopressin allele prevents anxiety-related behavior. *PLoS ONE*: 4(4):e5129. Epub 2009 Apr 9. #

* Authors contributed equally

Hamsch B., **Czibere L.**, Landgraf R. and Touma C. (2009): Genetic transmission of behavior and its neuroendocrine correlates. In: Pfaff D., Arnold A. P., Etgen A. M., Fahrbach S. E. and Rubin R. T. (Eds.): *Hormones, Brain and Behavior* 2nd ed., Elsevier Science, San Diego, CA, USA pp.

Erhardt A., **Czibere L.**, Roeske D., Lucae S., Unschuld P. G., Ripke S., Specht M., Kohli M., Kloiber S., Weber P., Deussing J. M., Ising M., Heck A., Zimmermann P., Pfister H., Lieb R., Pütz B., Uhr M., Hohoff C., Domschke K., Krakowitzky P., Maier W., Bandelow B., Jacob C., Deckert J., Landgraf R., Gonik M., Bunck M., Keßler M. S., Frank E., Schreiber S., Strohmaier J., Nothen M., Cichon S., Rietschel M., Bettecken T., Keck M. E., Landgraf R., Müller-Myhsok B., Holsboer F. and Binder E. B. (submitted): Genomewide association study in panic disorder identifies transmembrane protein 132D (TMEM132D) as susceptibility gene for anxiety-related phenotypes: evidence from human and mice studies. *Mol Psychiatry*. #

Czibere L., Baur-Jaronowski L. A., Zeiner K., Bunck M., Prigl J., Weber P., Pütz B., Graf C., Kühne C., Panhuysen M., Holsboer F., Deussing J. M. and Landgraf R. (in preparation): Profiling anxiety: A comprehensive gene expression study in mice bred for extremes in trait anxiety.

Czibere L., Gonik M., Frank E., Keßler M. S., Bunck M., Nußbaumer M., Müller-Myhsok B., Bettecken T. and Landgraf R. (in preparation): Genes of anxiety: freely segregating alleles in an F2-panel based on mice bred for extremes in trait anxiety reveal their association with behavior.

.

parts of this thesis were published in these articles.



11. Declaration / Erklärung

Hiermit versichere ich, dass ich die vorliegende Arbeit selbstständig und nur mit den angegebenen Quellen und Hilfsmitteln angefertigt habe. Alle Ausführungen, die wörtlich oder sinngemäß übernommen wurden, sind als solche gekennzeichnet. Auch habe ich nicht anderweitig versucht, eine Dissertation einzureichen oder mich der Doktorprüfung zu unterziehen.

München, 30. September 2008

Ludwig Czibere